

University of *Ljubljana*
Veterinary faculty



Maša Mavri

**CHARACTERIZATION OF TRAFFICKING AND SIGNALING
PROPERTIES OF HERPESVIRUS ENCODED G PROTEIN-
COUPLED RECEPTORS**

Doctoral dissertation

Ljubljana, 2023

University of *Ljubljana*
Veterinary faculty



UDK 577.2:576.314:577.354:612.014(043.3)

Maša Mavri, DVM

**CHARACTERIZATION OF TRAFFICKING AND SIGNALING
PROPERTIES OF HERPESVIRUS ENCODED G PROTEIN-
COUPLED RECEPTORS**

Doctoral dissertation

**KARAKTERIZACIJA ZNOTRAJCELIČNEGA PROMETA IN
SIGNALIZIRANJA S HERPESVIRUSNIMI S PROTEINOM G
SKLOPLJENIMI RECEPTORJI**

Doktorska disertacija

Ljubljana, 2023

Maša Mavri

Characterization of trafficking and signaling properties of herpesvirus encoded G protein-coupled receptors

The research was carried out at the Institute of Preclinical Sciences of the Veterinary Faculty, University of Ljubljana, at the Department of Biomedical Sciences of the Faculty of Health and Medical Sciences, University of Copenhagen, at the Institute of Cell Biology of the Faculty of Medicine, University of Ljubljana, the Department of Molecular and Biomedical Sciences at the Jožef Stefan Institute, and at the Institute of Immunology and Immunotherapy, College of Medical and Dental Sciences, University of Birmingham.

Date of public defence:

Supervisor: **Assoc. Prof. Valentina Kubale Dvojmoč,**

University of Ljubljana, Veterinary Faculty, Institute of Preclinical Sciences

Co-supervisor: **Assist. Prof. Katja Spiess,**

University of Copenhagen, Faculty of Health and Medical Sciences,
Department of Biomedical Sciences, Copenhagen, Denmark

Current address: Department of Virus and Microbiological Special
Diagnostics, Statens Serum Institut, Copenhagen, Denmark

The expert committee for evaluation and defence:

President: **Prof. Gregor Majdič,** University of Ljubljana, University rectorate

Member: **Prof. Mojca Kržan,** University of Ljubljana, Medical faculty

Member: **Sr. Res. Assoc. Mateja Manček Keber,** National Institute of Chemistry

I declare that the doctoral dissertation is the result of my own research work, that the results are correctly stated and that I have not violated the copyrights and intellectual property of others. I declare that the electronic copy is identical to the printed copy.

ABSTRACT

Keywords: molecular biology; cell membrane; herpesvirus 4, human; herpesvirus 1, suid; receptors, G-protein coupled; protein transport – physiology; signal transduction; endocytosis; caveolins; clathrin; dynamins

The objective of this study was to characterize and compare the molecular and biological properties of BILF1 encoded by the human Epstein-Barr virus (EBV) and BILF1 orthologues encoded by three porcine lymphotropic herpesviruses (PLHV1-3). The localization, constitutive internalization, and signaling, as well as the immunoregulatory role of PLHV1-3 BILFs, were determined and compared to the previously studied molecular properties of EBV-BILF1. Via cell based enzyme-linked immunosorbent assay (ELISA) and fluorescence microscopy, the conserved cell surface expression was confirmed. Moreover, for the first time, detailed endocytic pathways were described in this study of all four BILFs by antibody-feeding and a novel real-time internalization assay in live cells. Dominant negative mutants (DNMs) and chemical inhibitors confirmed clathrin-mediated endocytosis as a mechanism for BILF1 internalization. This mechanism was β -arrestin-independent as was confirmed by bioluminescence resonance energy transfer assay (BRET2) and bioinformatics analysis. Furthermore, caveolin seems to be involved in BILF1 trafficking. Investigating downstream signaling events mediated by the BILF1 receptors, $G\alpha_i$ dependent constitutive BILF1 activity but differential activation of downstream transcription factors were shown by luciferase assay. There was no activation of extracellular signal-regulated kinase (ERK) 1/2 by the BILF1 receptors. The immunoevasive properties of PLHV1-3 BILFs were confirmed, as shown for EBV-BILF1 by flow cytometry and supported by a new method based on fluorescence microscopy. Moreover, downregulation of major histocompatibility complex (MHC-I) was conserved for all BILFs in human embryonic kidney (HEK-293) cells but not in porcine kidney 15 (PK-15) cells. Finally, the association of PLHV1-BILF1 expression with the development of post-transplant lymphoproliferative disease (PTLD) was determined via RT-qPCR showing specific expression of only PLHV1-BILF1 after the disease onset. These results represent a first step toward establishing a PLHV1-associated porcine PTLD model, not only to study the pathological aspects of EBV-mediated disease but also to test BILF1 as a potential drug target relevant for the treatment of EBV-associated PTLD in humans.

IZVLEČEK

Ključne besede: molekularna biologija; celična membran; človeški herpesvirus 4; prašičji herpesvirus; receptor, sklopljen z G-proteinom; protein transport – fiziologija; prenos signalov; endocitoza; kaveolin; klatrin; dynamin

Cilj disertacije sta opredelitev in primerjava molekularnih in bioloških lastnosti ortologov BILF1, kodiranih v treh prašičjih limfotropnih herpesvirusih (PLHV1-3) in humanem virusu Epstein-Barr (EBV). Proučevali smo lokalizacijo, konstitutivno internalizacijo, konstitutivno aktivnost in imunoregulatorno vlogo receptorjev PLHV1-3 BILF1 in te lastnosti primerjali z receptorjem EBV-BILF1. V raziskavi smo prvič opisali lastnosti endocitoze za vse štiri našete receptorje BILF1. Z encimsko-immunskim testom (ELISA) in fluorescenčno mikroskopijo smo potrdili ohranjeno lokalizacijo na celični površini. Konstitutivno internalizacijo smo dokazali s pristopom, ki obravnava od temperature odvisno endocitozo receptorjev v različnih časovnih intervalih (iz angl. antibody-feeding), in z novim testom internalizacije v realnem času. Z dominantno negativno mutanto (DNM) in kemičnim zaviralcem smo pokazali vključenost klatrinske poti pri internalizaciji receptorjev BILF1. Z analizo bioluminiscenčnega prenosa (BRET2) in bioinformacijskim pristopom smo potrdili, da mehanizem ni odvisen od arestina β . Dodatno smo potrdili tudi vključenost kaveolina pri internalizaciji receptorjev BILF1. Z luciferaznim testom smo dokazali ohranjenost konstitutivnega znotrajceličnega prenosa signala, odvisnega od $G\alpha_i$, ter različno aktivacijo znotrajceličnih transkripcijskih faktorjev. S prenosom western nismo potrdili aktivacije zunajcelično signalno regulirane kinaze (ERK1/2). Sposobnost receptorjev BILF1 za izmikanje imunskemu sistemu smo potrdili s pretočno citometrijo in metodo fluorescenčne mikroskopije. Pokazali smo, da je sposobnost zniževanja površinske izraženosti molekul poglobitnega histokompatibilnostnega kompleksa (MHC-I) ohranjena za vse receptorje BILF1 v humanih embrionalnih ledvičnih celicah (HEK-293), ne pa tudi v prašičjih ledvičnih celicah (PK-15). Z metodo RT-qPCR smo dokazali povečano izraženost receptorjev PLHV1-BILF1 po razvoju post-transplantacijske limfoproliferativne bolezni (PTLD). Pridobljeni rezultati so prvi korak k vzpostavitvi s PLHV1 okuženega prašičjega modela za bolezen PTLD, ki bi v prihodnje omogočal raziskavo patoloških vidikov bolezni, povezanih z EBV, in raziskavo receptorjev BILF1 kot potencialne tarče za zdravljenje humane oblike bolezni PTLD.

TABLE OF CONTENTS

ABSTRACT	4
IZVLEČEK	5
TABLE OF CONTENTS	6
LIST OF TABLES	12
LIST OF ABBREVIATIONS AND SYMBOLS	13
1 INTRODUCTION	19
1.1 RESEARCH OBJECTIVES	20
1.2 RESEARCH HYPOTHESIS	20
2 LITERATURE REVIEW	21
2.1 G PROTEIN-COUPLED RECEPTORS	21
2.2 GAMMAHERPESVIRUSES AND THEIR VIRAL G PROTEIN-COUPLED RECEPTORS	22
2.2.1 Gammaherpesviruses	23
2.2.1.1 Epstein-Barr virus.....	26
2.2.1.2 Porcine lymphotropic herpesviruses 1, 2 and 3	28
2.2.2 Viral G protein-coupled receptors.....	29
2.2.2.1 BILF1	33
2.3 GPCR RECEPTOR FUNCTION	36
2.3.1 G protein mediated signaling.....	36
2.3.2 G protein independent signaling.....	37
2.3.3 Receptor endocytosis.....	38
2.3.3.1 Clathrin-Mediated Pathway	41
2.3.3.2 Caveolae-mediated endocytosis	42
2.3.3.3 Endocytosis mediated by lipid rafts	44
2.4 CLINICAL RELEVANCE	45
2.4.1 Clinical models	46
2.4.2 Potential use of vGPCRs for pharmacological intervention	47
3 MATERIALS AND METHODS	49
3.1 STANDARD MOLECULAR BIOLOGY METHODS	49
3.1.1 Receptor construct design.....	49
3.1.2 Restriction enzyme molecular cloning	50
3.1.2.1 Polymerase chain reaction	51
3.1.2.2 Digestion	52
3.1.2.3 Electrophoresis, DNA extraction and purification from agarose gel	52
3.1.2.4 Ligation	53
3.1.3 Transformation of chemically competent <i>E.coli</i> cells.....	53
3.1.4 cDNA purification	54
3.1.5 Spectrophotometric cDNA quantitation	54
3.1.6 Verification of receptor construct sequences.....	54
3.2 CELL CULTURE AND TRANSFECTION	55
3.2.1 Cell lines.....	55
3.2.2 Working with <i>in vitro</i> systems – cell cultures	55
3.2.3 Methods for transient transfection of cell lines	56
3.2.3.1 Lipofectamine transfection	57
3.2.3.2 FuGENE transfection	58

3.3 METHODS TO EVALUATE RECEPTOR EXPRESSION LEVEL	59
3.3.1 Cell-based Enzyme-linked immunosorbent assay	59
3.3.2 Microscopy experiments	60
3.4 ANALYSIS OF RECEPTOR ENDOCYTOSIS	61
3.4.1 Antibody-uptake internalization assay	61
3.4.1.1 Time-course cell-based ELISA internalization assay	62
3.4.1.2 Microscopy-based internalization assay	62
3.4.2 The effect of protein depletion on clathrin- and caveolae-mediated endocytosis of BILF1 receptors	63
3.4.3 Fluorescence-based resonance energy transfer based real-time internalization assay	64
3.5 CO-LOCALIZATION STUDIES FOR DETERMINING RECEPTOR INTRACELLULAR TRAFFICKING	66
3.6 PROTEIN – PROTEIN INTERACTIONS	67
3.6.1 Bioluminescence resonance energy transfer	67
3.6.2 Informational spectrum method	68
3.7 METHODS FOR DETECTION OF SECOND MESSENGER PROTEINS	69
3.7.1 Western blot	69
3.7.2 Luciferase assay	70
3.8 METHODS TO ANALYSE THE IMMUNOEVASIVE ROLE OF RECEPTORS ..	71
3.8.1 Flow cytometry analysis	71
3.8.2 Microscopy-based approach observing MHC-I downregulation	72
3.9 HOMOLOGY MODELLING OF MHC-I MOLECULES	72
3.10 ANALYSIS OF SAMPLE MATERIAL FROM PTLD DISEASED PIGS	73
3.10.1 Sample material from PTLD diseased pigs	73
3.10.2 Sequencing of PLHV infected pig samples and competitive alignment ...	73
3.10.3 Real-time polymerase chain reaction	75
3.11 DATA ANALYSIS AND NORMALISATION OF CURVES	76
4 RESULTS	77
4.1 BILF1 RECEPTOR LOCALIZATION	77
4.2 CHARACTERIZATION OF BILF1-MEDIATED TRAFFICKING AND ENDOCYTOTIC PATHWAYS	78
4.2.1 Constitutive internalization properties of BILF1 receptors	78
4.2.2 Effect of dominant negative mutant Dyn K44A on BILF1 mediated endocytosis	83
4.2.3 Effect of chemical inhibitor Pitstop2 on clathrin-mediated endocytosis of BILF1 receptors	86
4.2.4 The involvement of β -arrestin 1 and 2 in clathrin-mediated BILF1 endocytosis	87
4.2.5 Effect of dominant negative mutant Cav S80E on BILF1 endocytosis and expression	91
4.2.6 Visualization of the intracellular localization and trafficking of BILF1 receptors after endocytosis	93
4.2.7 Analysis of BILF1 receptor interaction with Rab7 and the estimation of receptor recycling	94
4.3 SIGNALING	98
4.3.1 MAPK signaling	98
4.3.2 Evaluation of G protein-mediated constitutive signaling	99

4.3.2.1 Activation of CRE reporter gene by BILF1 receptors as a result of constitutive G α_i signaling.....	99
4.3.2.2 Activation of NF- κ B and NFAT transcription factors in CRISPR/Cas9 engineered HEK-293A cells relies on the BILF1 mediated G α_i signaling.....	101
4.4 BIOLOGICAL ROLE OF BILF1 RECEPTORS	106
4.4.1 Comparison of immunoevasive properties for BILF1 receptors.....	106
4.4.2 Expression of PLHV1 and PLHV1-BILF1 in samples from PTLD diseased pigs	110
5 DISCUSSION.....	112
5.1 CONSTITUTIVE ENDOCYTOSIS AND TRAFFICKING.....	113
5.2 CONSTITUTIVE SIGNALING.....	118
5.3 BIOLOGICAL ROLE FOR BILF1 RECEPTORS.....	121
6 CONCLUSIONS	126
7 SUMMARY	128
8 POVZETEK.....	132
9 ACKNOWLEDGEMENTS.....	143
10 LITERATURE	145
11 APPENDIXES	174

LIST OF FIGURES

Figure 1:	Schematic structure of a G protein-coupled receptor (GPCR), alternatively named a seven transmembrane receptor (7 TM-R).	
Slika 1:	Shematski prikaz strukture receptorja, sklopljenega s proteinom G, imenovanega tudi 7-transmembranski receptor (7 TM-R).....	22
Figure 2:	Herpesvirus exploited and encoded GPCRs.	
Slika 2:	GPCR-ji, uravnavani in izraženi s strani herpesvirusov.....	23
Figure 3:	Identified and proposed properties of Epstein-Barr-encoded BILF1 (EBV-BILF1).	
Slika 3:	Znane in predlagane lastnosti receptorja BILF1, kodiranega v virusu Epstein-Barr (EBV-BILF1).....	34
Figure 4:	EBV-BILF1 cryo-EM structure in complex with $G\alpha_i$ protein.	
Slika 4:	Krio-EM struktura EBV-BILF1 v kompleksu s proteinom $G\alpha_i$	35
Figure 5:	Schematic overview of endocytic pathways.	
Slika 5:	Shematski prikaz endocitotskih poti.	39
Figure 6:	Pigs represent a potential model to study EBV mediated pathology and test the utility of BILF1 as a pharmacological target.	
Slika 6:	Prašiči so potencialen model za raziskavo EBV in njegovih patoloških posledic in za testiranje receptorja BILF1 kot potencialne tarče za zdravila.....	46
Figure 7:	Basic principle of chemical transfection using cationic lipids.	
Slika 7:	Osnovne značilnosti kemične transfekcije s kationskimi lipidi.	57
Figure 8:	Essential proteins of clathrin and caveolae mediated endocytosis affected by dominant negative mutants (Dyn K44A, Cav S80E) and chemical inhibitor (Pitstop2).	
Slika 8:	Ključni proteini endocitoze, posredovane s klatrinom in kaveolinom, na katere vplivajo dominantno negativne mutante (Dyn K44A, Cav S80E) in kemični inhibitor (Pitstop2).....	64
Figure 9:	Principle of FRET-based real-time internalization method.	
Slika 9:	Način delovanja metode internalizacije v realnem času, ki temelji na metodi FRET.....	65
Figure 10:	Principle of BRET method.	
Slika 10:	Način delovanja metode BRET.	67
Figure 11:	The aim of the thesis and presentation of the four main topics studied.	
Slika 11:	Namen doktorske disertacije s predstavljenimi štirimi glavnimi področji opravljenih raziskav.....	76

Figure 12:	Cellular localization of the BILF1 receptors.	
Slika 12:	Celična lokalizacija receptorjev BILF1.....	78
Figure 13:	Constitutive internalization of BILF1 receptors studied by antibody feeding approach.	
Slika 13:	Konstitutivna internalizacija receptorjev BILF1, proučevana s pristopom, ki obravnava od temperature odvisno endocitozo receptorjev v različnih časovnih intervalih (iz angl. "antibody feeding" approach).....	80
Figure 14:	Constitutive internalization of BILF1 receptors studied by FRET-based real-time internalization assay.	
Slika 14:	Konstitutivna internalizacija receptorjev BILF1, proučevana s testom internalizacije v realnem času, ki temelji na tehnologiji FRET.	82
Figure 15:	Kinetic parameters of BILF1 receptor constitutive internalization.	
Slika 15:	Kinetični parametri konstitutivne internalizacije receptorjev BILF1.....	83
Figure 16:	Effect of dominant negative mutant Dyn K44A on BILF1-mediated endocytosis.	
Slika 16:	Vpliv dominantno negativne mutante Dyn K44A na endocitozo receptorjev BILF1.....	85
Figure 17:	Effect of chemical inhibitor Pitstop2 on BILF1-mediated endocytosis.	
Slika 17:	Vpliv kemičnega inhibitorja Pitstop2 na endocitozo receptorjev BILF1.....	86
Figure 18:	The involvement of β -arrestin in BILF1-mediated endocytosis.	
Slika 18:	Vloga arestina β pri endocitozi receptorjev BILF1.....	87
Figure 19:	Non-specific interaction of β -arrestin 2 and 17aa-membrane insert with BILF1 receptors.	
Slika 19:	Nespecifična interakcija arestina β in membranskega vključka 17aa z receptorji BILF1.....	88
Figure 20:	Effect of dominant negative mutant Cav S80E on BILF1 endocytosis.	
Slika 20:	Vpliv dominantno negativne mutante Cav S80E na endocitozo receptorjev BILF1.....	92
Figure 21:	BILF1 receptor co-localization with markers of intracellular organelles.	
Slika 21:	Kolokalizacija receptorjev BILF1 z označevalci znotrajceličnih organel.	94
Figure 22:	Specific interaction of BILF1 receptors with Rab7 protein and the estimation of BILF1 receptor intracellular pool.	
Slika 22:	Specifična interakcija receptorjev BILF1 s proteini Rab7 in ocena znotrajcelične lokalizacije receptorjev BILF1.....	96
Figure 23:	The principle of determining intracellular pool of BILF1 receptors.	

Slika 23:	Način določanja količine znotrajceličnih receptorjev BILF1.	97
Figure 24:	Measurement of ERK1/2 MAPK signaling pathway activation by the BILF1 receptors.	
Slika 24:	Meritev aktivacije znotrajceličnega prenosa signala ERK1/2 MAPK, pogojene z receptorjem BILF1.	98
Figure 25:	Schematic representation of CRE signaling pathways in the presence of forskolin and chimeric G protein.	
Slika 25:	Shematski prikaz signalne poti CRE, v prisotnosti forskolina in himernega proteina G.....	100
Figure 26:	G α _i dependent CRE activity of BILF1 receptors.	
Slika 26:	CRE-aktivacija receptorjev BILF1, odvisna od G α _i	101
Figure 27:	NF- κ B activity of BILF1 receptors.	
Slika 27:	NF- κ B-aktivnost receptorjev BILF1.....	102
Figure 28:	NFAT activity of BILF1 receptors.	
Slika 28:	NFAT-aktivnost receptorjev BILF1.	103
Figure 29:	Comparison of viability and BILF1 expression in pan KO HEK-293A and parental HEK-293A cell line.	
Slika 29:	Primerjava preživetvene sposobnosti in izražanja receptorjev BILF1 v celičnih linijah "pan KO HEK-293A" in "parental HEK-293A".	104
Figure 30:	NFAT activity of BILF1 receptors with additional co-transfection of G α _q and G α ₁₁ .	
Slika 30:	NFAT-aktivnost receptorjev BILF1, kotransfeciranih s proteinoma G α _q in G α ₁₁	105
Figure 31:	Homology model of human HLA-I and porcine SLA-I molecules.	
Slika 31:	Primerjava med humano molekulo HLA-I in prašičjo molekulo SLA-I.	107
Figure 32:	MHC-I downregulation studied by flow cytometry.	
Slika 32:	Meritve zniževanja površinske izraženosti molekul MHC-I z uporabo pretočne citometrije.	108
Figure 33:	MHC-I downregulation studied by microscopy approach.	
Slika 33:	Meritve zniževanja površinske izraženosti molekul MHC-I z uporabo mikroskopije.	109
Figure 34:	PLHV1 infection and PLHV1-BILF1 expression in PTLD diseased pigs.	
Slika 34:	Infekcija s PLHV1 in izražanje PLHV1-BILF1 v vzorcih tkiv prašičev, ki so razvili PTLD.....	111

LIST OF TABLES

Table 1:	Representatives of Herpesvirus family.	
Tabela 1:	Predstavniki družine herpesvirusov.....	25
Table 2:	EBV latent genes and their function.	
Tabela 2:	Latentni geni, kodirani v genomu EBV, in njihova funkcija.	28
Table 3:	Examples of viral GPCRs from different herpesvirus families (β and γ) and their endocytic and signaling characteristics.	
Tabela 3:	Primeri virusnih GPCR-jev, kodiranih v različnih družinah herpesvirusov (β in γ) ter njihove značilnosti endocitoze in znotrajceličnega prenosa signala.	30
Table 4:	Different constructs of BILF1 receptors used in different methodological approaches.	
Tabela 4:	Različni konstrukti receptorjev BILF1, uporabljeni pri različnih metodoloških pristopih.....	50
Table 5:	PCR protocol used in our study.	
Tabela 5:	Protokol PCR, uporabljen v naši raziskavi.....	51
Table 6:	The affinity of β 2 adrenergic receptor (β 2AR) and BILF1 receptors for β -arrestin2 interaction.	
Tabela 6:	Afiniteta adrenergičnega receptorja β 2 (β 2AR) in receptorjev BILF1 za vezavo z arestinom β	89
Table 7:	The affinity of β 2 adrenergic receptor (β 2AR) and BILF1 receptors to interact with AP2.	
Tabela 7:	Afiniteta adrenergičnega receptorja β 2 (β 2AR) in receptorjev BILF1 za vezavo z AP2.	89
Table 8:	Predicted eukaryotic linear motifs (ELM) of BILF1 receptors.	
Tabela 8:	Predvideni motivi ELM (iz angl. eukaryotic linear motifs) receptorjev BILF1.....	90
Table 9:	The affinity of epidermal growth factor receptor (EGF-R) and BILF1 receptors to interact with caveolin-1.	
Tabela 9:	Afiniteta receptorja za epidermalni rastni faktor (EGF-R) in receptorjev BILF1 za interakcijo s kaveolinom-1.....	91

LIST OF ABBREVIATIONS AND SYMBOLS

AC	adenylate cyclase
Akt	protein kinase b
AIHV-1	alcelaphine herpesvirus 1
ApanLCV1	Ateles paniscus lymphocryptovirus 1
APC	Allophycocyanine
AP1	Adaptins
AP2	adaptor protein 2
ARH	autosomal recessive hypercholesterolemia protein
ATCC	American Type Culture Collection
AtHV3	<i>Ateline herpesvirus 3</i>
ATP	adenosine triphosphate
AUC	area under curve
BAR domain	Bin/amphiphysin/Rvs domain
BL	Burkitt's lymphoma
BLHV	bovine lymphotropic gammaherpesvirus
BoHV1	<i>Bovine herpesvirus 1</i>
BoHV2	<i>Bovine herpesvirus 2</i>
BoHV4	<i>Bovine herpesvirus 4</i>
BoHV5	<i>Bovine herpesvirus 5</i>
BoHV6	<i>Bovine herpesvirus 6</i>
BRET	bioluminescence resonance energy transfer
BSA	bovine serum albumin
CaHV1	<i>Canid herpesvirus 1</i>
CalHV3	<i>Callitrichine herpesvirus 3</i>
cAMP	cyclic adenosine monophosphate
Cav	caveolin
cDNA	complementary deoxyribonucleic acid
CMV	Cytomegalovirus
COS-7 cells	African green monkey kidney SV40 transformed fibroblasts
CO ₂	carbon dioxide

CRE	cyclic AMP-responsive elements
Cryo-EM	cryo-electron microscopy
Ct	cycle threshold
DMEM	Dulbecco's modified Eagle's medium
DNA	deoxyribonucleic acid
DNM	dominant negative mutant
dsDNA	double stranded DNA
DTT	dithiothreitol
E genes	early genes
EBV	Epstein-Barr virus
ECACC	European Collection of Authenticated Cell Cultures
ECL	extracellular loop
EDTA	ethylenediaminetetraacetic acid
EE	early endosomes
EGF-R	epidermal growth factor receptor
EHD	Eps15 homology domain
EHV1	Equine herpesvirus 1
EHV2	Equine herpesvirus 2
EHV3	Equine herpesvirus 3
EHV4	Equine herpesvirus 4
EHV5	Equine herpesvirus 5
ELISA	Enzyme-linked immunosorbent assay
EIHV1	<i>Elephantid herpesvirus 1</i>
EM	electron microscopy
EpatLCV1	<i>Erythrocebus patas lymphocryptovirus 1</i>
Eps15	EGFR pathway substrate 15
ER	endoplasmatic reticulum
ERK	extracellular signal-regulated kinase
FCHO	FCH domain only
FDA	U.S. Food and Drug Administration
FRET	fluorescence resonance energy transfer
FSC-A	forward scatter-area

FSC-H	forward scatter-height
GaHV1	<i>Gallid herpesvirus 1</i>
GaHV2	<i>Gallid herpesvirus 2</i>
GaHV3	<i>Gallid herpesvirus 3</i>
gDNA	genomic DNA
GDP	guanosine diphosphate
GEF	guanine nucleotide exchange factor
gER	granulated endoplasmatic reticulum
GFP	green fluorescence protein
GgorLCV1	<i>Gorilla gorilla lymphocryptovirus 1</i>
GgorLCV2	<i>Gorilla gorilla lymphocryptovirus 2</i>
GLP-1 R	glucagon like peptide 1 receptor
GLP-2 R	glucagon like peptide 2 receptor
GPCR	G protein-coupled receptor
GPI	glycosylphosphatidylinositol
G protein	guanine nucleotide binding protein
GRK	GPCR kinase
GSK3	glycogen synthase kinase 3
GTP	guanosine triphosphate
h	hour
HCMV	human cytomegalovirus
HEK-293 cells	human embryonic kidney 293 cells
HHV1	<i>human herpesvirus 1</i>
HHV2	<i>human herpesvirus 2</i>
HHV3	<i>human herpesvirus 3</i>
HHV4	<i>human herpesvirus 4</i>
HHV5	<i>human herpesvirus 5</i>
HHV6	<i>human herpesvirus 6</i>
HHV7	<i>human herpesvirus 7</i>
HHV8	<i>human herpesvirus 8</i>
HIF1 α	hypoxia inducible factor 1 α
HLA	human leukocyte antigen

HSCT	hematopoietic stem cell transplantation
HVS	Herpesvirus Saimiri
ICL	intracellular loop
IE genes	immediate early genes
IP ₃	inositol 1,4,5 triphosphate
IS	informational spectrum
JAK2	janus kinase 2
JNK	c-jun N-terminal kinase
kb	kilo-base
KO	knock out
KSHV	Kaposi's sarcoma-associated herpesvirus
LAMP	lysosomal-associated membrane protein 1
LB	Luria-Bertani
LE	late endosomes
LEF	lymphocyte enhancing factor
L genes	late genes
LCV	<i>Lymphocryptovirus</i>
LYN	tyrosine-protein kinase
LYSO	lysosome
MAPK	mitogen-activated protein kinases
MAPKK	mitogen-activated protein kinase kinase
MAPKKK	mitogen-activated protein kinase kinase kinase
McHV4	<i>Macacine herpesvirus 4</i>
McHV5	<i>Macacine herpesvirus 5</i>
MEM	minimum essential medium
MfasLCV1	<i>Macaca fascicularis lymphocryptovirus 1</i>
MHC-I	major histocompatibility complex I
min	minute
miRNA	micro RNA
MuHV1	<i>Murid herpesvirus 1</i>
MuHV4	<i>Murid herpesvirus 4</i>
MV68	Murine herpesvirus 68

M6P	mannose-6-phosphate receptor
NFAT	nuclear factor of activated T cells
NF- κ B	nuclear factor κ -B
NHP	non-human primate
ORF74	open reading frame 74
OvHV-2	ovine herpesvirus 2
PbadLCV1	<i>Piliocolobus badius lymphocryptovirus 1</i>
PBS	phosphate-buffered saline
PCR	polymerase chain reaction
PI3Ky	phosphatoinositide-3-kinase- γ polypeptide
PK-15 cells	porcine kidney 15 cells
PLC	phospholipase C
PLC- β	phospholipase C- β
PKA	protein kinase A
PKC	protein kinase C
PKR	RNA-dependent protein kinase
PLHV 1-3	Porcine lymphotropic herpesvirus 1, 2 and 3
Ppit LCV1	<i>Pithecia pithecia lymphocryptovirus 1</i>
PpygLCV1	<i>Pongo pygmaeus lymphocryptovirus 1</i>
PpygLCV2	<i>Pongo pygmaeus lymphocryptovirus 2</i>
PsHV1	<i>Psittacid herpesvirus 1</i>
PtdIns(4,5)P ₂	phosphatidylinositol-4,5-bisphosphate
PTLD	post-transplant lymphoproliferative disease
PtroLCV1	<i>Pan troglodytes lymphocryptovirus 1</i>
RAC1	ras-related C3 botulinum toxin substrate 1
RE	recycling endosomes
RhLCV	Rhesus lymphocryptovirus
RLuc	<i>Renilla luciferase</i>
RNA	ribonucleic acid
RT	room temperature
RT-qPCR	real-time quantitative polymerase chain reaction
s	second

SaHV2	<i>Samairiine herpesvirus 2</i>
SAPK	stress-activated protein kinase
SBD	sequencing by synthesis
siRNA	small interfering RNA
SEM	standard error of mean
shRNA	short hairpin RNA
S/N	signal to noise ratio
SNX9	sorting nexin 9
SOC	superoptimal broth medium with catabolite repression
SOT	solid organ transplantation
SRF	serum response factor
ssDNA	single stranded DNA
SsynLCV1	<i>Symphalangus syndactylus lymphocryptovirus 1</i>
SsynLCV2	<i>Symphalangus syndactylus lymphocryptovirus 2</i>
STAT3	signal transducer and activator of transcription 3
SuHV-1	<i>Suid herpesvirus 1</i>
SuHV-3	<i>Suid herpesvirus 3</i>
SuHV-4	<i>Suid herpesvirus 4</i>
SuHV-5	<i>Suid herpesvirus 5</i>
TBE	tris/borate/EDTA buffer
TCF	T-cell factor
TI	thymic irradiation
TM	transmembrane
TMB	3,3'-5,5'-tetramethyl benzidine substrate
UK	United Kingdom
USA	United States of America
UV	ultraviolet
vGPCR	viral G protein-coupled receptor
WGA	wheat germ agglutinin
YFP	yellow fluorescent protein
3D	three-dimensional
7 TM-R	seven transmembrane receptors

1 INTRODUCTION

Viral G protein-coupled receptors (vGPCRs) are seven-transmembrane receptors (7 TM-R) encoded by several herpesviruses that share structural hallmarks with endogenous G protein-coupled receptors (GPCRs), a large group of mammalian receptors critically involved in physiological, immunological, and metabolic processes and generally recognized as important drug targets. vGPCRs are thought to have been acquired from the host through years of co-evolution and have been modified by viruses to promote their survival and infectivity. One such receptor is BILF1 encoded by Epstein-Barr virus (EBV; γ -herpesvirus; genus *Lymphocryptoviruses*), known for its immunomodulatory and oncogenic properties. Although EBV-BILF1 is the most extensively studied BILF1 receptor to date, other herpesviruses including primate lymphocryptoviruses and three porcine lymphotropic herpesviruses (PLHV1-3 γ -herpesviruses; genus *Macaviruses*) also encode this vGPCR. In general, complex GPCR signaling exhibits diverse functions *in vivo* and is closely associated with receptor endocytosis, which plays an important role in trafficking of various extracellular and transmembrane molecules from the cell surface to its interior to enable cellular communication with extracellular environment, maintain cellular homeostasis, and transduce signals. Previous studies on EBV-BILF1 linked its constitutive, $G\alpha_i$ -dependent signaling with the oncogenic potential of the receptor. Importantly, BILF1 is the first vGPCR shown to downregulate MHC-I molecules at the surface of infected cells and, therefore, potentially contributes to the immune evasion of the virus. This strategy presumably relies on constitutive endocytosis of the receptor/MHC-I complex and subsequent degradation in lysosomes. Given the important role of vGPCRs in viral pathogenesis and their general similarity with GPCRs, BILF1 and other vGPCRs have recently been implicated as potential drug targets for the treatment of viral diseases. However, a critical step toward confirming BILF1 as a drug target requires a pharmacological characterization and validation. Moreover, the characterization of BILF1 receptors encoded by PLHV1-3 is of great importance due to the high seroprevalence of these viruses in pig population worldwide. Furthermore, their structural similarity with EBV-BILF1 indicates the important biological functions for BILF1 receptors. Importantly, previous studies have

reported the development of PLHV1-associated post-transplant lymphoproliferative disease (PTLD) in naturally PLHV1 infected pigs, where the disease resembled the EBV-mediated PTLD in humans, thereby proposing a novel model to study EBV-mediated disease. The characterization of the BILF1 receptors on a cellular and molecular level would provide the basis for establishing this novel *in vivo* model, to study EBV pathology associated with PTLD and to demonstrate the potential of BILF1 as an anti-viral drug target.

1.1 RESEARCH OBJECTIVES

The aim of the thesis is to characterize the pharmacological properties of BILF1 receptors encoded by three porcine PLHVs and compare them to well-described EBV-BILF1. BILF1 receptors were examined from the perspective of their localization, signaling, trafficking, and immunoevasive properties as well as their RNA expression level in samples of PTLD diseased pigs. In a wider perspective, an in-depth characterization of BILF1 receptors at the cellular and molecular levels is required to provide the foundation to establish the novel *in vivo* model and to demonstrate the potential of BILF1 as an antiviral drug target.

1.2 RESEARCH HYPOTHESIS

The research aimed to test the following hypotheses:

HYPOTHESIS 1: The BILF1 receptor family undergoes constitutive endocytosis by employing multiple pathways.

HYPOTHESIS 2: Internalization of the BILF1 receptor family is independent of the cell type.

HYPOTHESIS 3: The constitutive signaling properties of BILF1 depend on G proteins.

HYPOTHESIS 4: The immune evasion strategy of PLHV1 corresponds to that of EBV.

2 LITERATURE REVIEW

2.1 G PROTEIN-COUPLED RECEPTORS

G protein-coupled receptors (GPCRs), are a large group of transmembrane proteins that transduce extracellular signals across the cell membrane and are involved in key physiological responses (Alberts et al., 2015). They are recognized as drug targets for approximately 34% of all FDA-approved drugs importantly contributing to the treatment of a variety of diseases (Hauser et al., 2017). Their significant structure crosses the membrane by seven α -helical domains (TMs) (thereby also named seven transmembrane receptors), connected by three extracellular (ECL) and three intracellular loops (ICL) terminating extracellularly with an amino-terminal segment (N-terminus) and intracellularly with a carboxy-terminal (C-terminus) segment (Yang et al., 2021) (Figure 1). Based on their sequence and structural similarity, GPCRs are divided into five subfamilies: rhodopsin-like (class A), secretin (class B), glutamate (class C), adhesion and frizzled/taste (class F) (Fredriksson et al., 2003). GPCRs are activated by diverse stimuli from endogenous metabolites, neurotransmitters, cytokines, and hormones to environmental stimulants such as ions, odours, and light. Recent advances in cryo-electron microscopy (cryo-EM) provided new insights into structure-based molecular mechanisms and deepened the understanding of the complex signal transductions of GPCRs (Choy et al., 2021, García-Nafría and Tate, 2021, Tsutsumi et al., 2021). This will enable the discovery of new ligands as drugs and will aid work with uncharacterized orphan GPCRs.

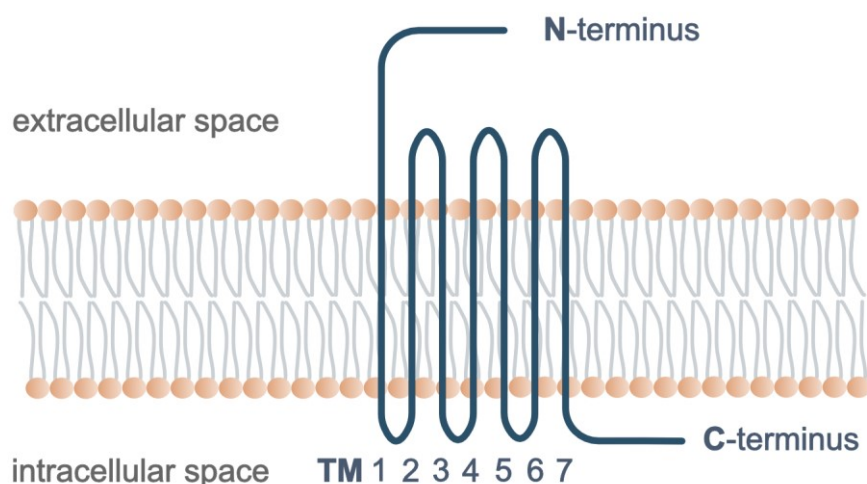


Figure 1: Schematic structure of a G protein-coupled receptor (GPCR), alternatively named a seven transmembrane receptor (7 TM-R).

Slika 1: Shematski prikaz strukture receptorja, sklopljenega s proteinom G, imenovanega tudi 7-transmembranski receptor (7 TM-R).

TM(trans-membrane domain), N-terminus (amino-terminal segment), C-terminus (carboxy-terminal segment).

2.2 GAMMAHERPESVIRUSES AND THEIR VIRAL G PROTEIN-COUPLED RECEPTORS

Over the years of co-evolution with their host, herpesviruses have evolved different mechanisms to effectively persist and replicate in their hosts. Figure 2 shows three viral mechanisms leading to molecular mimicry in infected cells. Viruses can encode viral ligands, for example, chemokines that can either activate (agonist) or deactivate (partial agonist/antagonist) host-encoded GPCRs. Furthermore, they can induce the expression of host cellular proteins, as exemplified by EBV, which induces the expression of GPR183 (also named EBI2; EBV induced gene 2) upon infection (Birkenbach et al., 1993). Finally, they express vGPCRs that were initially adapted from their hosts (Brunovskis and Kung, 1995, Rosenkilde, 2005, Rosenkilde et al., 2008, van Senten et al., 2020, Rosenkilde et al., 2022). The expression of vGPCRs in the host upon infection, can serve the virus in different ways: promoting viral dissemination, cellular transformation, immune evasion, tissue targeting, or by triggering proinflammatory responses (Rosenkilde et al., 2008, Vischer et al., 2014). The following sections cover the basics of gammaherpesvirus classification, infection,

and replication and describe four gammaherpesviruses that encode vGPCRs that are the focus of this dissertation.

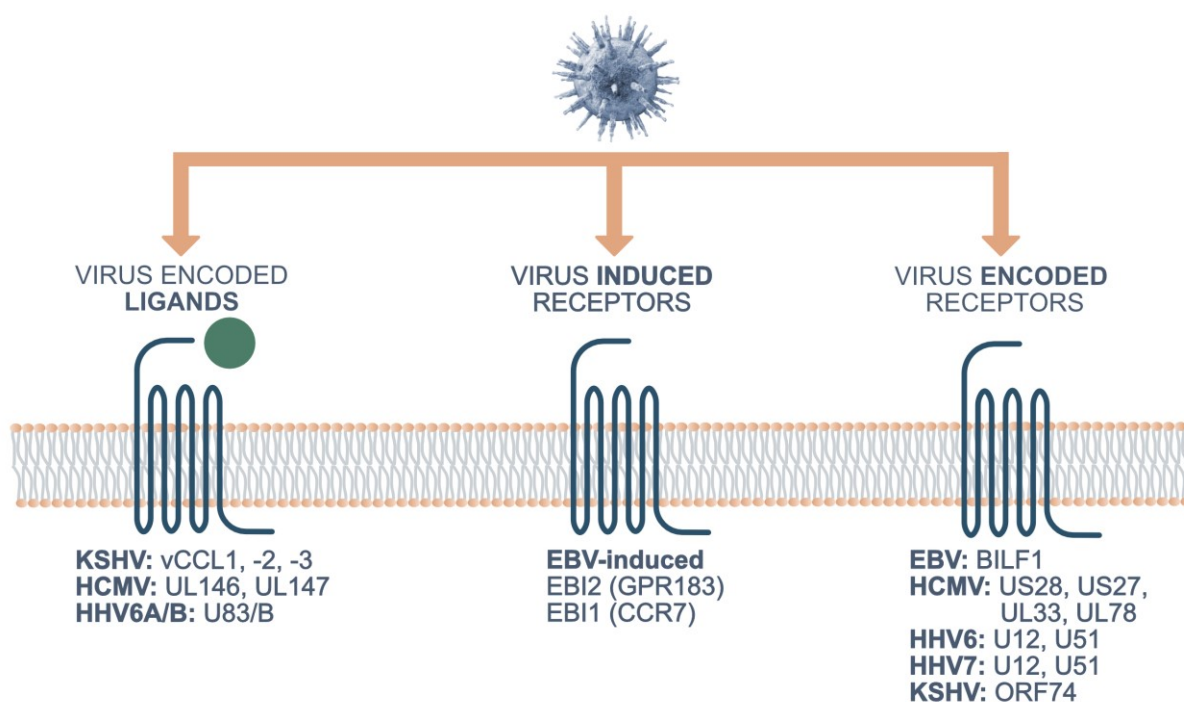


Figure 2: Herpesvirus exploited and encoded GPCRs.

Slika 2: GPCR-ji, uravnavani in izraženi s strani herpesvirusov.

2.2.1 Gammaherpesviruses

The herpesvirus family (*herpesviridae*) consists of three subfamilies: alphaherpesviruses (*Alphaherpesvirinae*), betaherpesviruses (*Betaherpesvirinae*) and gammaherpesviruses (*Gammaherpesvirinae*). The most prominent representatives of each subfamily are listed in Table 1. The gammaherpesvirus subfamily is further divided into *Lymphocryptovirus* (LCV), *Macavirus*, *Rhadinovirus*, and *Percavirus* (Davison, 2010). In general, gammaherpesviruses are widespread DNA viruses with the genome composed with a specific bipartite life cycle, switching between active lytic replication and silent latent replication (Babcock et al., 1998). Herpesviruses are usually transmitted directly by aerosol or via mucosal contact and are mainly transmitted between individuals (i.e., horizontal transmission) or from a mother to her offspring (i.e., vertical transmission) (Whitley, 1996). After primary, usually asymptomatic infection, they invade susceptible cells and initiate active replication

during the lytic cycle. The host immune system normally responds to the infection, preventing severe life-threatening consequences. However, during evolution, herpesviruses have adapted to the host immune response with different mechanisms, by i) developing immunoevasive strategies; ii) expressing only a limited number of viral genes, and iii) integrating into the host genome. This allows herpesviruses to survive undetected and persist effectively in the infected host for a lifetime through latent infection (Arvin et al., 2007). Although viral activity during latency is minimal, the development of several malignancies during this cycle has been described, with PTLN and Burkitt's lymphoma (BL) associated with EBV as examples (Drouet, 2019). Herpesviruses can occasionally reactivate and re-enter the lytic cycle spreading within and between hosts. In immunocompetent hosts (immunosuppressed patients or young children), reactivation can lead to the progression of severe pathology.

The 200 nm virion of herpesviruses consists of the icosahedral nucleocapsid containing linear double-stranded 125–240 kb linear DNA, the tegument, and the envelope. Several glycoproteins in the envelope are involved in initial binding and endocytosis upon infection. The herpesvirus genome encodes 100 to 200 proteins, involved in viral entry, DNA replication (e.g., DNA polymerase), immunoevasion, spread between cells, and pathogenesis (Arvin et al., 2007). Regulatory proteins include vGPCRs, proteins that have been adopted by hosts during decades of evolution and benefit the virus.

Table 1: Representatives of Herpesvirus family (adapted from (Davison, 2010)).

Tabela 1: Predstavniki družine herpesvirusov (povzeto po (Davison, 2010)).

Taxon name	Common name	Acronym
Subfamily <i>Alphaherpesvirinae</i>		
Genus <i>Iltovirus</i>	<i>Gallid herpesvirus 1</i>	Infectious laryngotracheitis virus GaHV1
	<i>Psittacid herpesvirus 1</i>	Pacheco's disease virus PsHV1
Genus <i>Mardivirus</i>	<i>Gallid herpesvirus 2</i>	Marek's disease virus type 1 GaHV2
	<i>Gallid herpesvirus 3</i>	Marek's disease virus type 2 GaHV3
Genus <i>Simplexvirus</i>	<i>Bovine herpesvirus 2</i>	Bovine mammillitis virus BoHV2
	<i>Human herpesvirus 1</i>	Herpes simplex virus type 1 HHV1
	<i>Human herpesvirus 2</i>	Herpes simplex virus type 2 HHV2
Genus <i>Varicellovirus</i>	<i>Bovine herpesvirus 1</i>	Infectious bovine rhinotracheitis virus BoHV1
	<i>Bovine herpesvirus 5</i>	Bovine encephalitis herpesvirus BoHV5
	<i>Canid herpesvirus 1</i>	Canine herpesvirus CaHV1
	<i>Equid herpesvirus 1</i>	Equine abortion virus EHV1
	<i>Equid herpesvirus 3</i>	Equine coital exanthema virus EHV3
	<i>Equid herpesvirus 4</i>	Equine rhinopneumonitis virus EHV4
	<i>Human herpesvirus 3</i>	Varicella-zoster virus HHV3
	<i>Suid herpesvirus 1</i>	Pseudorabies virus SuHV1
Subfamily <i>Betaherpesvirinae</i>		
Genus <i>Cytomegalovirus</i>	<i>Human herpesvirus 5</i>	Human cytomegalovirus (HCMV) HHV5
Genus <i>Muromegalovirus</i>	<i>Murid herpesvirus 1</i>	Murine cytomegalovirus MuHV1
Genus <i>Roseolovirus</i>	<i>Human herpesvirus 6</i>	Human herpesvirus 6 HHV6
	<i>Human herpesvirus 7</i>	Human herpesvirus 7 HHV7

Taxon name	Common name	Acronym	
Subfamily <i>Gammaherpesvirinae</i>			
Genus <i>Callitrichine herpesvirus 3</i> <i>Lymphocryptovirus</i>	Marmoset lymphocryptovirus	CalHV3	
<i>Human herpesvirus 4</i>	Epstein-Barr virus	HHV4	
<i>Macacine herpesvirus 4</i>	Rhesus lymphocryptovirus	McHV4	
Genus <i>Macavirus</i>	<i>Alcelaphine herpesvirus 1</i>	Wildebeest-associated malignant catarrhal fever virus	AlHV1
	<i>Bovine herpesvirus 6</i>	Bovine lymphotropic herpesvirus	BoHV6
	<i>Ovine herpesvirus 2</i>	Sheep-associated malignant catarrhal fever virus	OvHV2
	<i>Suid herpesvirus 3</i>	Porcine lymphotropic herpesvirus 1	PLHV1/ SuHV3
	<i>Suid herpesvirus 4</i>	Porcine lymphotropic herpesvirus 2	PLHV2/ SuHV4
	<i>Suid herpesvirus 5</i>	Porcine lymphotropic herpesvirus 3	PLHV3/ SuHV5
Genus <i>Percavirus</i>	<i>Equid herpesvirus 2</i>	Equine herpesvirus 2	EHV2
	<i>Equid herpesvirus 5</i>	Equine herpesvirus 5	EHV5
Genus <i>Rhadinovirus</i>	<i>Ateline herpesvirus 3</i>	Herpesvirus ateles	AtHV3
	<i>Bovine herpesvirus 4</i>	Bovine herpesvirus 4	BoHV4
	<i>Human herpesvirus 8</i>	Human herpesvirus 8	HHV8
	<i>Maccacine herpesvirus 5</i>	Rhesus rhadinovirus	McHV5
	<i>Murid herpesvirus 4</i>	Murine herpesvirus 68	MuHV4 / MV68
	<i>Samairine herpesvirus 2</i>	Herpesvirus saimiri	SaHV2

2.2.1.1 Epstein-Barr virus

EBV (or human herpesvirus 4; HHV4), is a *lymphocryptovirus*, present in approximately 95% of the world's adult population (Andrei et al., 2019). It is an oncovirus that annually affects approximately 50,000 patients worldwide and is most

commonly associated with classical Hodgkin's lymphoma, nasopharyngeal carcinoma, Burkitt's lymphoma and gastric cancer (Bass et al., 2014, de Martel et al., 2020). In addition, EBV infection has been recognised as a driving factor for the development of PTLD in patients with immunocompromised solid organ (SOT) and hematopoietic stem cell transplant (HSCT). PTLD is a major complication occurring after transplantation, resulting in the development of diverse types of tumours with a high risk of fatal outcome (Chang et al., 1978, Dierickx and Habermann, 2018, Naik et al., 2018). EBV's linear, double-stranded 172 kb DNA genome encodes approximately 100 proteins (Johannsen et al., 2004). Consistent with other gammaherpesvirus family members, EBV can switch between active lytic replication and silent latent replication. Following primary, usually asymptomatic infection, EBV establishes immediate lifelong latent infection in memory B cells (Kanda, 2018). Four latency programs (0, I, II, III) (Table 2) are defined with restricted number of specific subset of proteins involved and are recognized in different EBV-associated malignancies (Arfelt et al., 2015).

In contrast, the lytic replication cycle occurs during primary infection and reactivation. This phase is also characterized by a regulated gene expression profile with immediate (IE), early (E), and late (L) lytic genes encoding lytic proteins (Tsurumi et al., 2005, Murata, 2018). IE gene expression initiates lytic replication and behaves as transactivation for the E and L genes. BZLF1 is an IE gene important for the initiation of lytic replication. E genes have an important role in i) viral replication with DNA polymerase (BALF5), ii) metabolism and iii) inhibition of antigen processing, with the immunoevasive proteins, such as BNLF2a, BGLF5 and BILF1 proteins, interfering with MHC-I presentation (Zuo et al., 2009, Zuo et al., 2011, Quinn et al., 2014). Finally, the late lytic cycle proteins have a more structural role, assembling envelope glycoproteins or new virions and playing an immunoregulatory role (Quinn et al., 2014, Murata, 2018).

Table 2: EBV latent genes and their function (adapted from (Arfelt et al., 2015, Kanda, 2018)).
Tabela 2: Latentni geni, kodirani v genomu EBV, in njihova funkcija (povzeto po (Arfelt et al., 2015, Kanda, 2018)).

Latency program	Latent gene	Function
0	No gene expression	
I, II, III	EBNA-1	Regulation of genes, replication, viral genome maintenance through regulation of viral promoters
II, III	LMP1	Mimics CD40 signal, promoting B-cell growth, transformation, and survival
II, III	LMP2A	Mimics B-cell receptor signaling, provides survival and anti-differentiation signals to B-cells
II, III	LMP2B	Modulates LMP2A activation
III	EBNA-2	Initiates the transcription of viral and cellular genes, induces B-cell transformation
III	EBNA-LP	Initiates the transcription of viral and cellular genes, induces B-cell transformation
III	EBNA-3A	Contributes to the transcription of viral and cellular genes, induces B-cell transformation
III	EBNA-3B	Tumour suppressor
III	EBNA-3C	Contributes to the transcription of viral and cellular genes, induces B-cell transformation

2.2.1.2 Porcine lymphotropic herpesviruses 1, 2 and 3

Three porcine gammaherpesviruses, PLHV 1, 2 and 3 (also named SuHV-3, SuHV-4 and SuHV-5) are classified in the genus *Macavirus* and are closely related to the alcelaphine herpesvirus 1 (AIHV-1), ovine herpesvirus 2 (OvHV-2) and bovine lymphotropic gammaherpesvirus (BLHV) as well as human EBV (Ehlers et al., 1999). PLHV1 and PLHV2 have an 85–98% amino acid identity to each other. Therefore, PLHV1 and PLHV2 are thought to be derived from closely related virus species, rather than two different strains of the same species. PLHV3, in contrast, has a lower amino acid identity (49–89%) compared to PLHV1 and PLHV2 (Chmielewicz et al., 2003). The prevalence of PLHV1, 2, and 3 in the domestic and wild pig population is 29–80%,

11–41%, and 5–65%, respectively (Meng, 2012). Furthermore, several studies have reported the co-infection with all three PLHVs in domestic pigs (Ehlers et al., 1999, Chmielewicz et al., 2003, McMahon et al., 2006, Meng, 2012).

After primary infection which usually occurs horizontally or vertically, PLHVs cause persistent latent infection of B cells, comparable to EBV (Tucker et al., 2003, Mueller et al., 2005, Hartline et al., 2018). To date, PLHV1-3 have not been shown to have pathogenic potential, so their relevance for the swine industry appears low despite high prevalence. However, undergoing experimental HSCT, miniature swine naturally infected with PLHV1 developed PTLD closely resembling the morphological and histological characteristics of EBV-associated PTLD in humans (Huang et al., 2001, Goltz et al., 2002, Cho et al., 2004, Dor et al., 2004, Doucette et al., 2007).

2.2.2 Viral G protein-coupled receptors

Representatives of vGPCRs include US28 encoded by human cytomegalovirus (HCMV, betaherpesvirus) (Chee et al., 1990, Kledal et al., 1998), ORF74 encoded by human Kaposi's sarcoma-associated herpesvirus (KSHV, gammaherpesvirus) (Chang et al., 1994, Rosenkilde et al., 1999) and equine herpesvirus 2 (EHV2, gammaherpesvirus) (Rosenkilde et al., 2005), and BILF1 encoded by 21 gammaherpesviruses including human EBV (Baer et al., 1984, Beisser et al., 2001, Paulsen et al., 2005), non-human primate lymphocryptoviruses (old world primate LCVs and new world primate LCVs) (Spiess et al., 2015a), PLHV 1, 2, and 3 (Chmielewicz et al., 2003, Lindner et al., 2007), Alcelaphine herpesvirus 1 (AIHV1) (Ensser et al., 1997), ovine herpesvirus 2 (OvHV2) (Meier-Trummer et al., 2009) and EHV2 (Telford et al., 1995). ORF74 and US28 are structural GPCR homologs of endogenous chemokine receptors with high affinity for both virally encoded and endogenous chemokines, activating downstream signaling pathways (Rosenkilde et al., 2008, Vischer et al., 2014). In contrast, EBV-BILF1 is classified as an "orphan" vGPCR for which no ligand has yet been identified and is described in more detail in Section 2.2.2.1. Importantly, these vGPCRs were linked to tumorigenesis as oncogenes (ORF74 and BILF1) or oncomodulators (US28) and to angiogenesis (ORF74 and US28) through

ligand-induced (ORF74 and US28) or ligand-independent (i.e., constitutive) signaling (ORF74, US28, and BILF1) (Vischer et al., 2014, Rosenkilde et al., 2022). Representatives of betaherpesvirus and gammaherpesvirus encoded vGPCRs and their endocytic and signaling properties are described in Table 3.

Table 3: Examples of viral GPCRs from different herpesvirus families (β and γ) and their endocytic and signaling characteristics (adapted from (Mavri et al., 2020)).

Tabela 3: Primeri virusnih GPCR-jev, kodiranih v različnih družinah herpesvirusov (β in γ) ter njihove značilnosti endocitoze in znotrajceličnega prenosa signala (povzeto po (Mavri et al., 2020)).

Virus	Receptor	Endocytic Pathway	Signaling Pathways
Subfamily <i>Betaherpesvirinae</i>			
Human cytomegalovirus (CMV)	US27	-	-
	US28	β -arrestin independent clathrin-mediated, partly through lipid rafts	Constitutive NF κ B, NFAT, CREB, PLC, SRF, STAT3, TCF/LEF, Ligand induced PLC, MAPK G α_q , G $\alpha_{i/o}$, G $\alpha_{12/13}$
	UL33	-	Constitutive SRC, CREB G α_q , G α_i , G α_s
Human herpesvirus 6	UL78	-	-
	U12	-	-
Human herpesvirus 7	U51	-	-
	U12	-	-
Mouse cytomegalovirus	U51	-	-
	M33	-	Constitutive PLC, NF κ B, CREB G α_s
Rat cytomegalovirus	M78	-	-
	R33	-	Constitutive PLC, NF κ B G α_q , G α_i

Virus	Receptor	Endocytic Pathway	Signaling Pathways
Subfamily <i>Gammaherpesvirinae</i>			
Human herpesvirus 8 (HHV8 or Kaposi's sarcoma virus (KSHV))	ORF74	β -arrestin independent clathrin-mediated constitutive endocytosis, β -arrestin dependent clathrin-mediated ligand dependent endocytosis	Constitutive and ligand induced RAC1, PLC, PKC, AKT, JNK-SAPK, LYN-SRC, GSK3, JAK2-STAT3, HIF1 α , PI3K γ , calcineurin G α_q , G α_i , G $\alpha_{12/13}$
Ateles herpesvirus (AtHV)	ORF74	-	-
MouseHV68	ORF74	-	not constitutively active PLC, MAPK, Akt, NF κ B G α_i
Equine HV2 (EHV2)	E1	-	-
	E6	-	-
	ORF74	-	G α_i
Herpesvirus Saimiri (HVS)	ECRF3	-	-
Human Epstein-Barr virus (EBV)	BILF1	-	Constitutive NF κ B, NFAT, CREB G α_i
Rhesus lymphocryptovirus (RhLCV)	BILF1	-	Constitutive NF κ B G α_i
Callitrichine herpesvirus 3 (CalHv3)	BILF1	-	Constitutive NF κ B, NFAT G α_i
<i>Pan troglodytes</i> lymphocryptovirus 1 (PtroLCV1)	BILF1	-	Constitutive NF κ B G α_i

Virus	Receptor	Endocytic Pathway	Signaling Pathways
Subfamily <i>Gammaherpesvirinae</i>			
<i>Gorilla gorilla</i> lymphocryptovirus 1 (GgorLCV1)	BILF1	-	-
<i>Gorilla gorilla</i> lymphocryptovirus 2 (GgorLCV2)	BILF1	-	-
<i>Pongo pygmaeus</i> lymphocryptovirus 1 (PpygLCV1)	BILF1	-	Constitutive NFκB Gα _i
<i>Pongo pygmaeus</i> lymphocryptovirus 2 (PpygLCV2)	BILF1	-	-
<i>Symphalangus syndactylus</i> lymphocryptovirus 1 (SsynLCV1)	BILF1	-	Constitutive NFκB, NFAT Gα _i
<i>Symphalangus syndactylus</i> lymphocryptovirus 2 (SsynLCV2)	BILF1	-	-
<i>Macaca fascicularis</i> lymphocryptovirus 1 (MfasLCV1)	BILF1	-	-
<i>Erythrocebus patas</i> lymphocryptovirus 1 (EpatLCV1)	BILF1	-	-
<i>Ptilocolobus badius</i> lymphocryptovirus 1 (PbadLCV1)	BILF1	-	-
<i>Ateles paniscus</i> lymphocryptovirus 1 (ApanLCV1)	BILF1	-	-
<i>Pithecia pithecia</i> lymphocryptovirus 1 (Ppit LCV1)	BILF1	-	-
Porcine lymphotropic herpesvirus 1, 2 and 3 (PLHV1-3)	BILF1	-	-

protein kinase B (Akt), cAMP responsive element binding protein (CREB), glycogen synthase kinase 3 (GSK3), hypoxia inducible factor 1α (HIF1α), Janus kinase 2 (JAK2), c-jun N-terminal kinase (JNK), lymphocyte enhancing factor (LEF), tyrosine-protein kinase (LYN), mitogen-activated protein kinase (MAPK), nuclear factor of activated T-cells (NFAT), Nuclear factor kappa B (NF-κB), phosphatoinositide-3-kinase-γ polypeptide (PI3Kγ), protein kinase C (PKC), phospholipase C (PLC), Ras-related C3 botulinum toxin substrate 1 (RAC1), stress-activated protein kinase (SAPK), serum response factor (SRF), signal transducer and activator of transcription 3 (STAT3), T-cell factor (TCF).

2.2.2.1 BILF1

Among the BILF1 receptor family, EBV-BILF1 has been the most intensively studied receptor (Figure 3). EBV-BILF1 is primarily expressed in the late stage of lytic cycle, with marked progressive activity throughout the cycle (Quinn et al., 2014); however, its expression during latency has also been observed in Burkitt's lymphoma samples (Tierney et al., 2015). EBV-BILF1 expression is mainly restricted to the cellular surface, with additional intracellular accumulation (Spiess et al., 2015a). An oncogenic function of EBV-BILF1, demonstrated by *in vitro* cellular transformation and *in vivo* tumour formation, was linked to the receptor's ability to constitutively activate G α_i protein at the plasma membrane (Beisser et al., 2005, Paulsen et al., 2005, Lyngaa et al., 2010). Moreover, investigations of downstream signaling of EBV-BILF1 showed constitutively signaling and activation of nuclear factor κ -B (NF- κ B) and nuclear factor of activated T cells (NFAT) transcription factors, and inhibition of forskolin-induced transcription of cyclic AMP-responsive elements (CRE) (Beisser et al., 2005, Paulsen et al., 2005, Spiess et al., 2015a). Furthermore, in Burkitt's lymphoma B cells and COS-7 cells, EBV-BILF1 downregulates phosphorylation of double-stranded RNA-dependent protein kinase (PKR) (Beisser et al., 2005) an interferon-inducible enzyme important for host anti-viral defence mechanism. As phosphorylation of PKR results in cessation of protein synthesis and apoptosis of infected cells, this mechanism allows the virus to evade the host response and spread more easily (Kaufman, 1999). Another immune-avoidance strategy mediated by BILF1 is the receptor's ability to downregulate MHC-I molecules at the surface of infected cells and thereby prevent the recognition by CD8+ T lymphocytes (Zuo et al., 2009, Zuo et al., 2011, Griffin et al., 2013). This function has previously been linked to the ability of this receptor to constitutively internalize (Zuo et al., 2009, Spiess et al., 2015a). Presumably, EBV-BILF1 interferes with MHC-I endocytic and exocytotic pathways, which results in increased degradation in lysosomes and decreased presentation of newly synthesized MHC-I molecules at the cell surface (Zuo et al., 2011). For EBV-BILF1, a cryo-EM structure has been reported previously, showing marked differences in comparison with class A GPCRs (Tsutsumi et al., 2021) (Figure 4). Unlike other vGPCRs or chemokine-binding GPCRs, the ECL2 of EBV-BILF1 forms a lid on top of the receptor, which together with ECL3 blocks the

typical binding pocket and prevents the access of extracellular ligands. A highly conserved ECL2 sequence among BILF1 receptor family implies similar feature for all BILF1 receptors (Spiess et al., 2015a). The structure has been proposed to act as a “self-agonist”; however, major mutational changes in ECL2 did not prevent constitutive $G\alpha_i$ signaling (Tsutsumi et al., 2021).

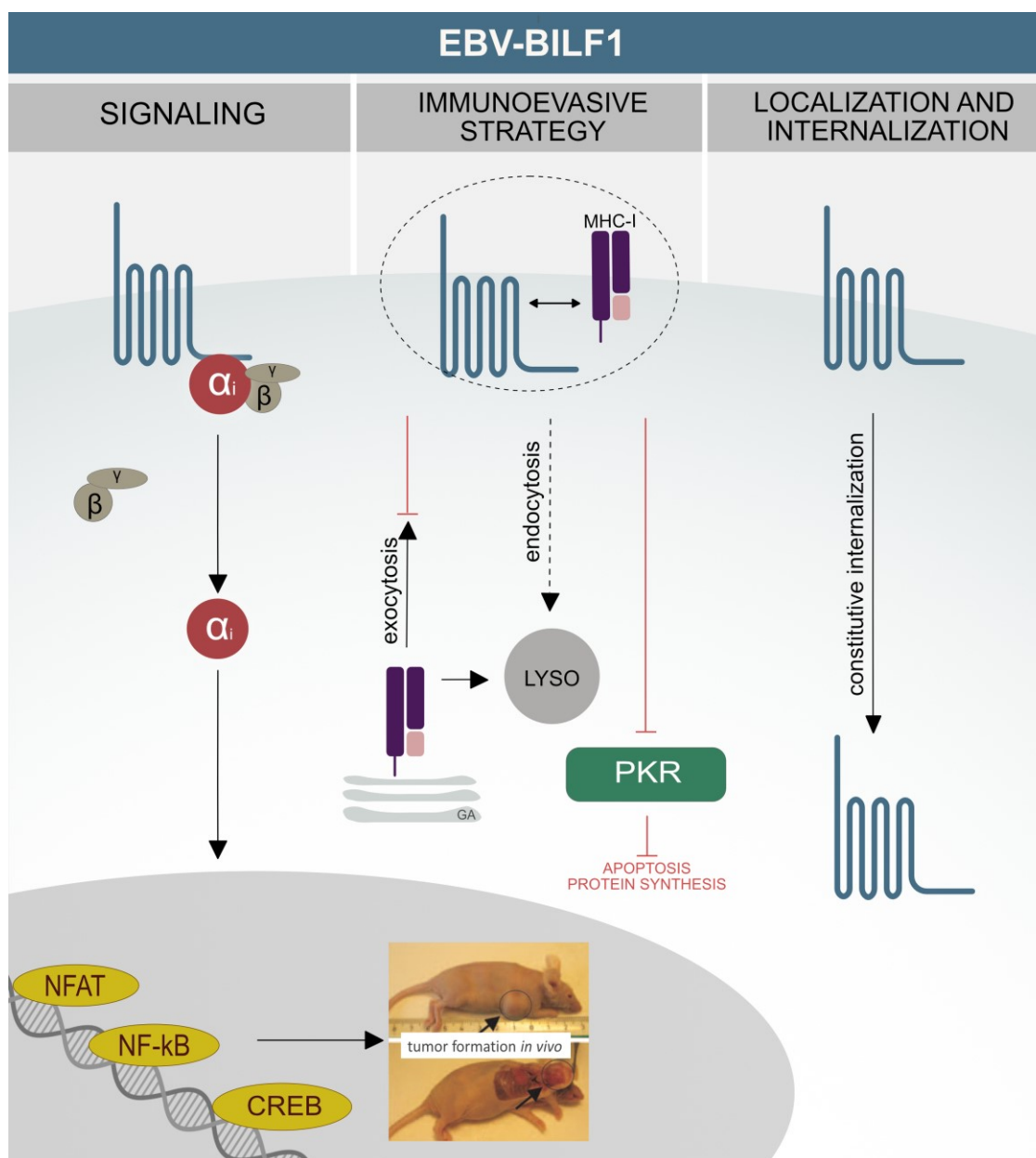


Figure 3: Identified and proposed properties of Epstein-Barr-encoded BILF1 (EBV-BILF1).

Slika 3: Znale in predlagane lastnosti receptorja BILF1, kodiranega v virusu Epstein-Barr (EBV-BILF1).

LYSO (lysosome), PKR (RNA-dependent protein kinase), MHC-I (major histocompatibility complex class I), NFAT (nuclear factor of activated T cells), NF- κ B (nuclear factor κ -B). Black arrows indicate the activated pathways; red lines and red text indicate blocked pathways. Dashed lines and arrows indicate proposed properties and pathways.

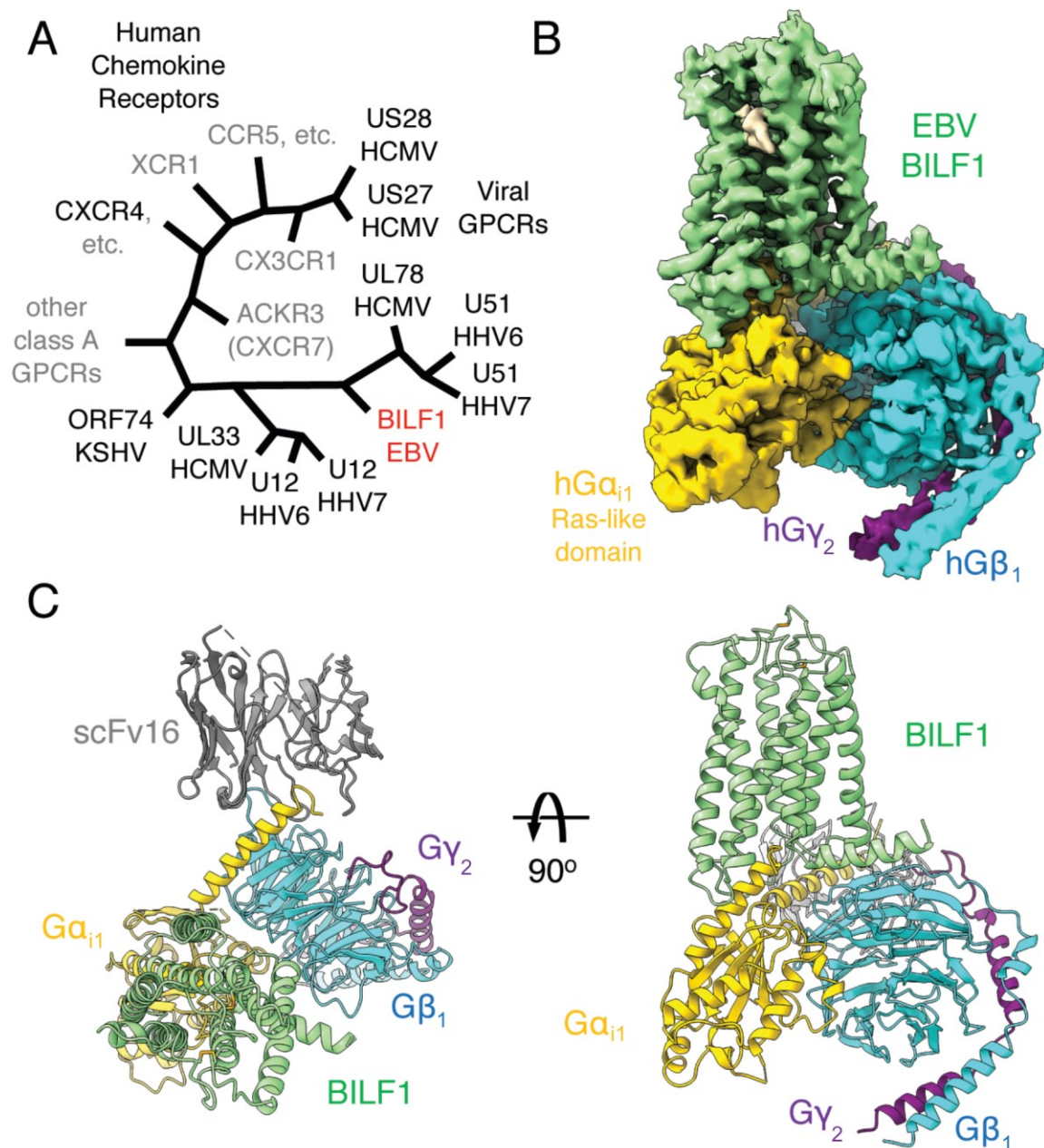


Figure 4: EBV-BILF1 cryo-EM structure in complex with $G\alpha_i$ protein (adapted from (Tsutsumi et al., 2021)).

Slika 4: Krio-EM struktura EBV-BILF1 v kompleksu s proteinom $G\alpha_i$ (povzeto po (Tsutsumi et al., 2021)).

A) Phylogenetic representation of relationship between BILF1 and other herpesvirus encoded vGPCRs and human chemokine receptors. B) 3D reconstruction of full-length EBV-BILF1 in complex with $G\alpha_1G\beta_1\gamma_2$ and the complex stabilizing antibody scFv16. C) A representation of the EBV-BILF1 in complex with $G\alpha_1G\beta_1\gamma_2$ and scFv16 from top (left) and side (right).

2.3 GPCR RECEPTOR FUNCTION

2.3.1 G protein mediated signaling

As the name implies, signal transduction mediated by GPCRs usually occurs through association with G proteins. Heterotrimeric G proteins consist of three subunits: alpha, beta, and gamma. Upon GPCR activation mediated by ligand binding or constitutive activation (without ligand binding), $G\alpha$ subunit exchanges guanosine diphosphate (GDP) with guanosine triphosphate (GTP) leading to conformational change, consequently resulting in dissociation of $G\alpha$ from $G\beta\gamma$ subunit in cytosol, where both subunits can mediate different downstream signaling pathways (Hilger et al., 2018). Based on their structure and function, the $G\alpha$ subunit is further divided into four families: $G\alpha_s$ (olf and s), $G\alpha_i$ (1, oA, t1, g, z, i2, oB, t2, i3), $G\alpha_q$ (q, 11, 14, 15, 16) and $G\alpha_{12}$ (12 and 13). $G\alpha_s$ (s=stimulation) can be found in different cell types, whereas $G\alpha_{olf}$ is only expressed in olfactory sensory neurons. Activated $G\alpha_s$ binds to and activates adenylate cyclase (AC), an enzyme important for synthesis of cyclic AMP (cAMP) from adenosine triphosphate (ATP). In the majority of cells, cAMP activates cAMP-dependant protein kinase (PKA), which further phosphorylates serine and threonine residues on intracellular signal proteins and effector proteins, regulating their activity (Alberts et al., 2015). The cAMP effect is cell-type-dependent due to diverse target proteins within the different cell types. The $G\alpha_i$ (i=inhibition) family is the largest and most diverse group of $G\alpha$ proteins and can be found in all cell types. It inhibits AC and therefore diminishes cAMP production in the cell. Members of the $G\alpha_q$ family can be found in all cell types, $G\alpha_{14}$ is specifically located in kidneys, lungs, and liver, whereas $G\alpha_{15/16}$ are located in hematopoietic cells ($G\alpha_{15}$ is equivalent from mice). $G\alpha_q$ activates plasma membrane-bound phospholipase C- β (PLC β), which cleaves phosphatidylinositol-4,5-bisphosphate (PI(4,5)P2) into two products: inositol 1,4,5, triphosphat (IP₃) in diacylglycerol. A water-soluble IP₃ is released from plasma membrane into the cytosol. At the membrane of the endoplasmic reticulum (ER), it binds to IP₃ receptors (IP₃-gated Ca²⁺ release channels) resulting in a rapid increase in Ca²⁺ concentration in cytosol, which results in signalization through Ca²⁺ sensitive proteins. Diacylglycerol, in contrast, is a membrane-bound protein and exerts different

signaling pathways. Its most important role is the activation of protein kinase C (PKC), which is translocated to the plasma membrane after IP₃ induced Ca²⁺ increase and is further activated by Ca²⁺, diacylglycerol, and phosphatidylserine. PKC phosphorylates various target proteins; therefore, its activation results in various cell-type-based responses. Gα₁₂ and Gα₁₃ can be found in different cell types, where they remodel actin cytoskeleton by activating a guanine nucleotide exchange factor (GEF), which further activates a monomeric GTP-ase proteins of Rho family (Quilliam et al., 2002). Gβγ subunits exert several different signaling pathways on their own, with PLC- and ion channel activation and later described ERK signaling pathway as examples (Tang and Gilman, 1991, Inglese et al., 1995, Brock et al., 2003). Tight regulation of receptor signaling is necessary to maintain physiological responses within the cell. Therefore, the control of receptor signaling termination is equally important as receptor activation and can be achieved by three general processes: receptor desensitization, sequestration, and downregulation. Desensitization is a fast response initiated by GPCR kinases (GRKs) phosphorylating serine and threonine residues on activated receptors. In the next step, a protein called β-arrestin is recruited from the cytoplasm to the phosphorylated receptor, resulting in the inhibition of G protein-mediated signaling. Sequestration (also termed receptor internalization) is initiated by GRK-mediated phosphorylation and subsequent β-arrestin binding, and usually leads to clathrin-mediated endocytosis. However, the role of β-arrestins in internalization varies depending on receptor, ligand, and cell type; therefore, both β-arrestin-dependent and β-arrestin-independent internalization has been reported for GPCRs. GPCR downregulation results in the loss of cell surface-expressed receptors and regulates availability of receptor for ligand binding. It involves lysosomal degradation of internalized receptors or recycling back to the cell surface (Luttrell and Lefkowitz, 2002).

2.3.2 G protein independent signaling

In recent years, β-arrestins have been assigned a new important role. In addition to their aforementioned ability to terminate G protein-mediated signaling of GPCRs and their role in GPCR endocytosis, β-arrestins can act as GPCR signal transducers

(Irannejad et al., 2015). It has been shown that β -arrestins can bind Src family tyrosine kinases and serve as scaffolds for some mitogen-activated protein kinase module (MAP kinase) (Grundmann and Kostenis, 2017). MAP kinases are serine/threonine kinases involved in the regulation of cell growth, cell division and differentiation, and apoptosis. Three components mediate different responses in signaling cascade. The MAP kinase (MAPK also named Erk) is the kinase that is most downstream. The next upstream kinase that phosphorylates MAPK and thereby activates MAPK is MAP kinase kinase (MAPKK also termed Mek). Further upstream is MAP kinase kinase kinase (MAPKKK also known as Raf), which is directly activated by Ras, a monomeric GTP-ase located at the cytosolic face of the plasma membrane (Roskoski, 2012). Based on preferred signaling outcome, the term “GPCR biased signaling” was introduced (Smith et al., 2018). It describes the situation in which one receptor favours the activation of one specific signaling pathway (e.g., G protein signaling pathway or β -arrestin signaling pathways) over another.

2.3.3 Receptor endocytosis

To maintain cellular homeostasis, a cell communicates with and responds to the extracellular environment by sorting the material at the plasma membrane (Hanyaloglu and von Zastrow, 2008). Cells use various endocytic mechanisms to uptake receptor-ligand complexes, growth factors, nutrients, cell debris, extracellular matrix, bacteria, and viruses (Sigismund et al., 2012, Joseph and Liu, 2020). It is also importantly linked with the initial entry of several herpesviruses into the cell (for example EBV, KSHV, HCMV, and varicella zoster virus) (Sobhy, 2017). Furthermore, as described in the previous chapter, receptor endocytosis, which involves receptor internalization, regulates receptor signaling at the plasma membrane and controls the availability of the receptors for further ligand-induced or constitutive activity (Hanyaloglu and von Zastrow, 2008, Barbieri et al., 2016).

Depending on the sorted material, endocytosis can be further divided into two distinct processes, pinocytosis, and phagocytosis (Figure 5). With pinocytosis, cells uptake small particles and fluids. Phagocytosis occurs in phagocytes, which are cells

specialized for large particles uptake (> 500 nm) such as cell debris and microorganisms. Pinocytosis covers macro- and micropinocytosis, mechanisms that differ in size of vesicles formed at the membrane. Macropinosomes are heterologous, large endocytic vesicles (200–500 nm), whereas micropinosomes include specified small vesicles (60–50 nm) further described as clathrin-coated vesicles (clathrin-mediated endocytosis), caveolae (caveolae-mediated endocytosis), or non-coated vesicles, depending on the type of protein involved in vesicle formation (Sigismund et al., 2012, Weeratunga et al., 2020).

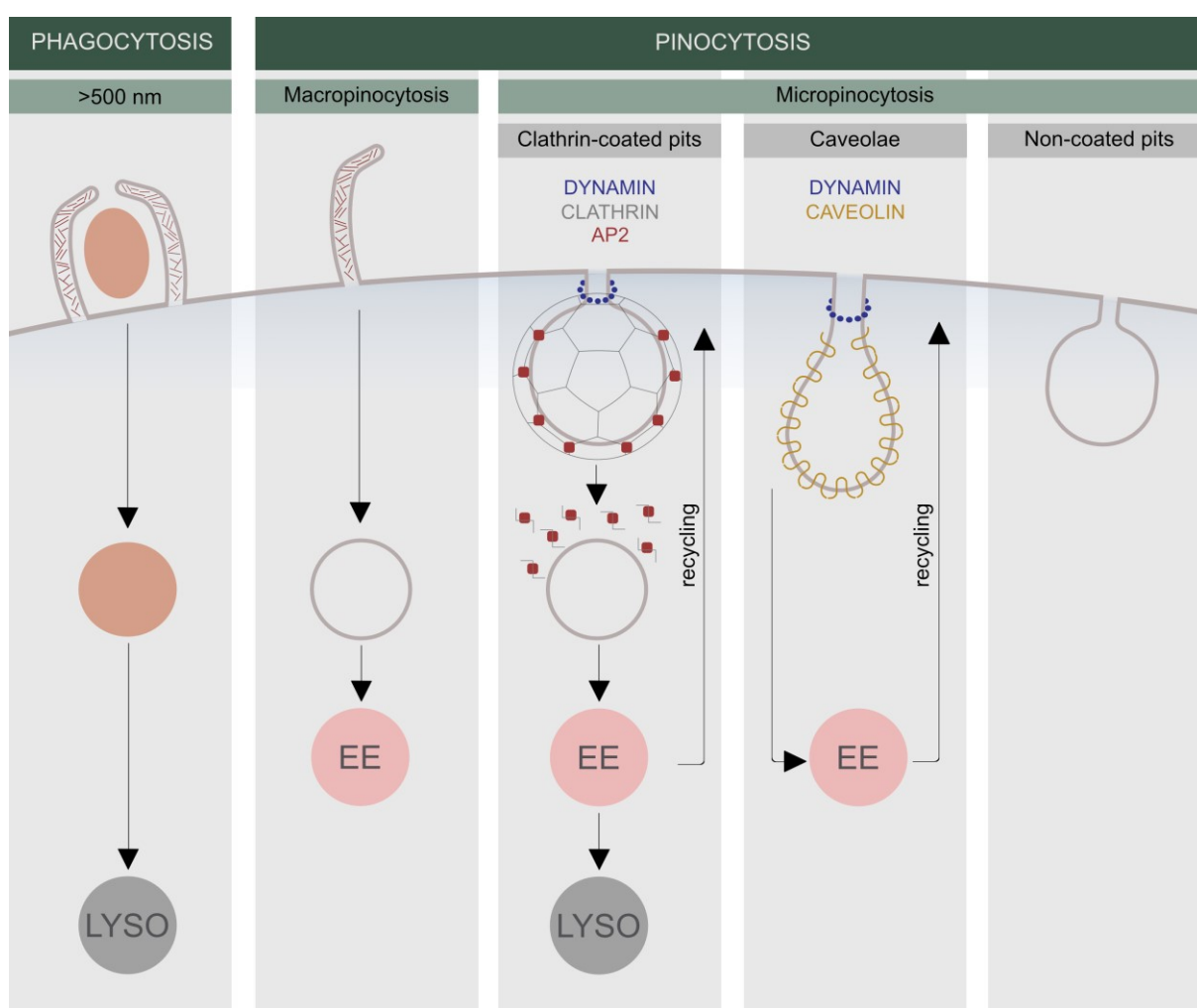


Figure 5: Schematic overview of endocytic pathways (adapted from (Mavri et al., 2020)).

Slika 5: Shematski prikaz endocitotskih poti (povzeto po (Mavri et al., 2020)).

LYSO (lysosomes), EE (early endosomes), AP2 (adaptor protein 2). Black arrows indicate trafficking pathways.

Cargo sorting begins in the cytoplasm, after endocytic vesicles fuse with early endosomes, a pleomorphic compartment consisting of tubular and vacuolar domains rich in Rab5, a regulator of early endosome content and endosome fusion (Sönnichsen et al., 2000). Cargo from different endocytic pathways including clathrin-mediated and caveolae-mediated pathways is gathered in early endosomes and can be further sorted for recycling or lysosomal degradation. The lysosomal degradation pathway is a process of vesicle maturation that begins in the peripheral cytoplasm with late endosomes and ends in a perinuclear compartment with formation of lysosomes. Late endosomes are 250–10000 nm large round-to-oval-shaped vesicles, with membrane-bound lysosomal proteins (e.g., LAMP1). Moving towards cell interior, the late endosomes fuse with each other and eventually fuse with lysosomes where the cargo finally degrades into micromolecules that can be further used by the cell to build new structures. Lysosomes contain more than 40 different hydrolytic enzymes with their optimum activity in acid pH present in lysosomes. Their synthesis takes place in the granulated endoplasmatic reticulum (gER) and are transferred to the lysosomes based on the mannose-6-phosphate marker. In the trans-golgi network, mannose-6-phosphate is recognized by mannose-6-phosphate receptors (M6P), which are proteins important for sorting the lysosomal material and bind to adaptins (AP1), which further participate in clathrin coat formation. Clathrin-coated vesicles are further fused with late endosomes where the enzymes separate from M6P based on acid pH (Jovic et al., 2010, Huotari and Helenius, 2011, Alberts et al., 2015).

Another possible fate for internalized cargo is that it is recycled back to plasma membrane. In fact, the plasma membrane is actively changing its composition with the equivalent of 50–180% of its surface area being cycled every hour (Huotari and Helenius, 2011). Recycling can occur directly from early endosomes or in a slow recycling pathway through recycling endosomes located in the perinuclear region (O'Sullivan and Lindsay, 2020, Weeratunga et al., 2020). Through this mechanism, cells regulate and maintain the plasma membrane protein and lipid composition and regulate cellular responses to the extracellular environment (McNally and Cullen, 2018). Based on the type of proteins involved, GPCR internalization is further divided into few distinct pathways already mentioned above. Below, the clathrin-mediated

pathway, the caveolae-mediated pathway, and raft-dependent pathways will be described.

2.3.3.1 Clathrin-Mediated Pathway

Clathrin-mediated endocytosis is the most extensively studied endocytic pathway, occurring in all mammalian cells, and is used by many GPCRs, including vGPCRs for internalization (Wolfe and Trejo, 2007). As mentioned previously, in many cases, this occurs after initial G protein activation and subsequent desensitization by β -arrestins. During clathrin-mediated endocytosis, five distinct stages are described: coat nucleation, cargo selection, coat assembly, scission, and un-coating (McMahon and Boucrot, 2011).

Recently, a novel model for the initiation of clathrin-mediated endocytosis has been proposed. At the plasma membrane, initial nucleation is thought to be associated with the formation of a putative nucleation module, a plasma membrane area rich in PtdIns(4,5)P₂ to which the clathrin is recruited (Janetzko et al., 2022). It includes EGFR pathway substrate 15 (Eps15), FCH domain-only proteins (FCHO) and intersectins (Stimpson et al., 2009, Henne et al., 2010). These proteins recruit adaptor protein 2 (AP2), which further mediates cargo selection together with other adaptor proteins (Henne et al., 2010). AP2, with its ability to bind many important factors of the clathrin-mediated endocytosis, plays an important role in the formation of the clathrin envelope. At the plasma membrane, AP2 binds to PtdIns(4,5)P₂, which triggers AP2 activation (Jackson et al., 2010, Kelly et al., 2014, Kadlecova et al., 2017). AP2 also mediates the cargo selection by binding two types of specific C-terminal domain motifs on transmembrane proteins (including GPCRs and vGPCRs): μ 2 subunit recognizes the YXX Φ motif (Ohno et al., 1995), whereas α/σ 2 hemicomplex (Chaudhuri et al., 2007, Doray et al., 2007) and presumably β 2 subunit (Rapoport et al., 1998) recognize the [DE]XXXL[LI] motif. Two other internalization signals direct membrane proteins to clathrin-coated pits: the FXNPXY motif, which is recognized by the accessory proteins Dab1 and autosomal recessive hypercholesterolemia protein (ARH) (Hawryluk et al., 2006, Maurer and Cooper, 2006) and polyubiquitination, which is recognized by epsin

and Eps15 (Polo et al., 2002, Hawryluk et al., 2006, Traub and Lukacs, 2007). In addition, AP2 can direct cargo indirectly by binding to other accessory proteins, for example, by binding with $\beta 2$ subunit to the RxR motif of β -arrestin (Laporte et al., 1999, Laporte et al., 2000, Luttrell and Lefkowitz, 2002). After cargo selection, clathrin coat assembly begins on the cytosolic surface of the plasma membrane with the recruitment of clathrin from the cytosol by AP2. Clathrin, also named triskelion based on its recognizable structure, consists of three clathrin heavy chains and three clathrin light chains (Mettlen et al., 2018). Clathrin is bound to the membrane by its direct interaction with specific motifs in the linker region of the AP2 β -subunit (Owen et al., 2000). Additionally, β -arrestin binds to the N-terminus of the clathrin heavy chain through LIELD or LIEFE sequence (Goodman et al., 1996, Krupnick et al., 1997). After clathrin polymerisation, a lattice structure forms at the edge of the vesicle, stabilizing the membrane curvature (Kumari et al., 2010, Kaksonen and Roux, 2018). Clathrin polymerization has been assumed to be efficient for membrane curving, but evidence has been found for curvature effectors that drive membrane invagination formation, with Bin/amphiphysin/Rvs (BAR) domain-containing proteins being the most prominent representatives (McMahon and Gallop, 2005). BAR domain-containing proteins are also critically involved in the vesicle neck formation and the recruitment of a GTP-ase dynamin (Kosaka and Ikeda, 1983). Amphiphysin, endophilin, and sorting nexin 9 (SNX9) are BAR representatives that bind dynamin, which polymerizes around the vesicle neck and induces GTP hydrolysis resulting in vesicle fission (Hinshaw and Schmid, 1995, Sweitzer and Hinshaw, 1998). Released in the cytoplasm, a newly formed vesicle loses its clathrin coat under the influence of the cytosolic chaperone heat shock cognate 70 (HSC70) and auxilin (Schlossman et al., 1984, Ungewickell et al., 1995). The vesicles with cargo fuse with early endosomes and continue the recycling or degradation pathway, whereas released clathrin monomers are available for a new cycle of vesicle formation.

2.3.3.2 Caveolae-mediated endocytosis

The caveolae, originally named "little-caves", were first discovered nearly 70 years ago (Palade, 1953, Yamada, 1955). Since their discovery, these 60–80 nm wide membrane

pits have been assigned many different roles in different tissue cells. Caveolae exhibit tissue specific roles and expression. They are covering approximately 50% of the cellular surface in adipocytes and smooth muscle and participate in fatty acid transport (Liu and Pilch, 2016, Matthaeus et al., 2020) and have a mechanoprotective role in skeletal muscle (Sinha et al., 2011, Lo et al., 2015, Dewulf et al., 2019), zebrafish notochord (Garcia et al., 2017, Lim et al., 2017) and adipocytes. They regulate the regeneration of liver tissue and lead to mechanosensation in migrating cells (Hetmanski et al., 2019). In contrast to their high expression in some cell types, the caveolae are undetectable in others (Zhuang et al., 2011). Recently, the ability of caveolae to respond to oxidative stress and UV exposure by activating downstream signaling pathways have been described (Jung et al., 2018, McMahon et al., 2019). In general, caveolae formation occurs in plasma membrane areas rich in cholesterol and sphingomyelin (Roy et al., 1999, Prior et al., 2001). Therefore, they are often described as a subtype of lipid rafts rich in protein caveolin. Many proteins are involved in caveolar formation, with caveolins (CAV-1, CAV-2, and CAV-3), cavins (cavin 1–4) and syndapin (also named pacsin) as the core structural component (Parton et al., 2021). Three caveolin genes are recognized in mammals: CAV1, CAV2, and CAV3. Caveolins are cholesterol-binding integral membrane proteins with a specific hairpin structure, showing cell type specific expression pattern, with caveolin-1 and caveolin-2 expressed in non-muscle cells, and caveolin-3 expressed specifically in muscle cells. In contrast to caveolin-1 and -3, caveolin-2 is not essential for caveolar formation (Parton, 2018). Caveolin-1 synthesis occurs in ER, where it forms oligomers (Monier et al., 1995). Caveolin oligomers continue to traffic to the Golgi complex, where they bind to cholesterol, directing the protein towards the plasma membrane (Hayer et al., 2010). Cavin-1 is a membrane, lipid-binding protein that stabilizes the caveolar formation by binding to PtdIns(4,5)P2 and phosphatidylserine in the caveolae-rich domains (Hill et al., 2008, Kovtun et al., 2014, Kovtun et al., 2015). As caveolins and cavins shape the bulb of caveolae, another protein, Eps15 homology domain (EHD) protein, shapes the neck of caveolae (Morén et al., 2012, Ariotti et al., 2015, Yeow et al., 2017). The F-BAR domain-containing protein syndapin has recently been assigned the membrane deformation role, as well as a role in the recruitment of dynamin, a protein that mediates vesicle scission, and is therefore recognized as one of the main

caveolae-forming proteins (Hansen et al., 2011, Senju et al., 2011, Seemann et al., 2017). After pinching off the plasma membrane, caveolae fuses with early endosomes and recycle back to plasma membrane (Pelkmans et al., 2004). However, in the absence of cavin or cholesterol disruption, caveolae undergo degradation pathway in lysosomes. Compared to clathrin-mediated endocytosis, caveolae-mediated endocytosis is slower (Shvets et al., 2015). Although not exclusively, several GPCRs have been shown to utilize caveolae for endocytosis (Chini and Parenti, 2004). $\Phi X \Phi X X X X \Phi$ or $\Phi X X X X \Phi X X \Phi$ motifs are recognized on GPCRs as binding regions for caveolin (Couet et al., 1997a); however, unlike in clathrin-mediated endocytosis, interaction with caveolin does not necessarily lead to endocytosis of the receptor (Chini and Parenti, 2004). In light of recent studies that show the importance of caveolae in regulating plasma membrane tension and signaling, the aspect of endocytosis mediated by caveolae is considered to be a secondary mechanism (Parton et al., 2020). Therefore, the role and mechanism of caveolae in GPCR endocytosis remain poorly understood.

2.3.3.3 Endocytosis mediated by lipid rafts

The plasma membrane is organized into two distinct regions: ordered and non-ordered. Lipid rafts represent the mobile, heterogeneous, ordered regions of 10–200 nm in size. They differ from the non-ordered regions by the abundance of cholesterol, sphingolipids, glycosylphosphatidylinositol (GPI-anchored protein), and glycosphingolipid. In recent years, difficulties in studying lipid rafts due to their instability and heterogeneity raised many questions on their existence, role, and regulation. However, they evidently play an important role in different levels of cellular physiology (Sezgin et al., 2017).

Lipid rafts have also been recognized as the plasma membrane areas used for endocytosis by different molecules and ligands. Endocytosis through lipid rafts relies on specific proteins, such as caveolin (caveolae-mediated endocytosis is described in Section 2.3.3.2) or is caveolae-independent. Upon their activation, various immune receptors translocate and internalize through lipid rafts based on the abundance of

signaling molecules in the rafts (Razani et al., 1999, Sproul et al., 2000, Beck-García et al., 2015). Furthermore, bacterial toxins (Shiga toxin and Cholera toxin) and viruses including novel SARS-CoV-2, polyoma virus and simian virus 40 virus, bind specific lipids in rafts to initiate cell entry (Teissier and Pécheur, 2007, Ewers and Helenius, 2011, Fecchi et al., 2020). Several GPCRs, such as glucagon like peptide 2 (GLP-2) (Estall et al., 2004) and US28 (Droese et al., 2004) have been described using the endocytosis through lipid rafts as one of their endocytic mechanisms.

2.4 CLINICAL RELEVANCE

Although EBV was discovered nearly 60 years ago, no antiviral drug or vaccine exists against it (Epstein et al., 1964, Cohen, 2018, Andrei et al., 2019). Many promising antiviral agents that showed effective inhibitory properties against EBV replication *in vitro* failed in clinical trials (Coen et al., 2013, Coen et al., 2014, Keith et al., 2018). In part, this is explained by the lack of suitable animal models to study the complexity of EBV pathogenesis and drug efficacy, as EBV is strictly host specific (Munz, 2017). EBV evades host immunity by using multiple strategies, one of which is the expression of the immunomodulatory BILF1 receptor. In EBV-associated PTLD, the organ recipients are immunosuppressed to prevent graft rejection (Naik et al., 2018). The degree of immunosuppression holds an important risk factor for the disease development and is tightly linked with the ability of EBV-positive B-cells to expand uncontrollably (Martinez and Krams, 2017). When EBV-specific cytotoxic T-cells are reconstituted in a donor and injected into the recipient, the development of EBV-associated PTLD was prevented, suggesting this as a successful treatment approach against EBV (Papadopoulos et al., 1994, Heslop et al., 2010). Considering the ability of EBV-BILF1 to downregulate MHC-I expression and therefore reduce the recognition of infected cells by CD8+ T cells, suppressing BILF1 function may restore immune recognition and therefore the elimination of EBV-positive cells. However, a critical step in confirming BILF1 as a drug target requires an in-depth receptor characterization and validation in a reliable *in vivo* animal model (Figure 6).

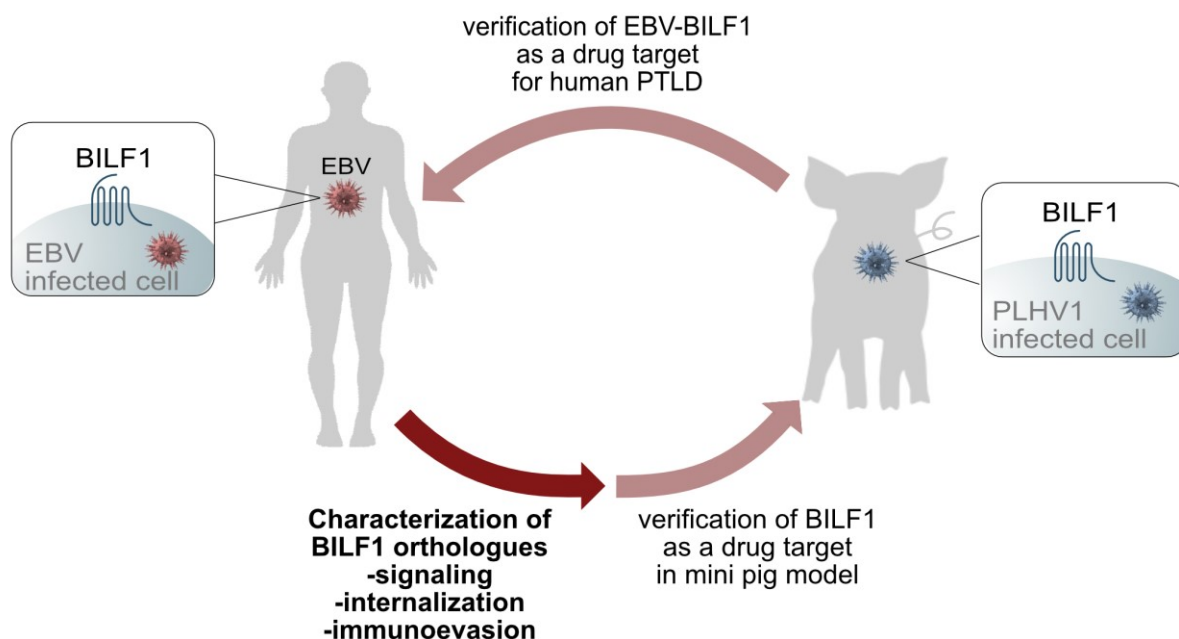


Figure 6: Pigs represent a potential model to study EBV mediated pathology and test the utility of BILF1 as a pharmacological target.

Slika 6: Prašiči so potencialen model za raziskavo EBV in njegovih patoloških posledic in za testiranje receptorja BILF1 kot potencialne tarče za zdravila.

PTLD (post-transplant lymphoproliferative disease), EBV (Epstein-Barr virus), PLHV1 (Porcine lymphotropic herpesvirus 1).

2.4.1 Clinical models

Several animal models exist to mimic the pathological, physiological, and immunological properties of EBV-mediated diseases in humans. However, due to the strict host tropism of EBV, an ideal preclinical animal model is still not available (Munz, 2017).

Early rodent models used mice infected with murine gammaherpesvirus 68 (MuHV68; genus Rhadinovirus), which exhibited the acute infectious mononucleosis (Tripp et al., 1997), and B-cell lymphoproliferative disease (normally associated with EBV-infection) but failed to display oncogenic properties of the virus (Sunil-Chandra et al., 1994, Tarakanova et al., 2005). Currently the most promising rodent models are based on humanized mice engrafted with human cells or tissues lacking both B and T cells (Mosier et al., 1988, Fujiwara and Nakamura, 2020). The development of EBV-associated lymphoproliferative disease or lymphoma (Islas-Ohlmayer et al., 2004,

Yajima et al., 2008, Strowig et al., 2009, Fujiwara et al., 2015) and the development of primary EBV infection (Sato et al., 2011, Chijioke et al., 2013) can be studied in immunodeficient mouse strains (NOG and NSG) reconstituted with human stem cells. However, direct translation from these models is challenging due to differences in immunological, physiological, and genetic characteristics, and especially in cancer development (Duran-Struuck et al., 2019). Large animal models could be more useful due to their greater similarity to humans in terms of anatomy, physiology, genetics, and immune response (Duran-Struuck et al., 2019). Although non-human primate (NHP) models infected with lymphocryptovirus homologous to EBV are permissive for primary infection (Moghaddam et al., 1997) and develop PTLD-like disease as well as other B-cell lymphomas (Feichtinger et al., 1992, Schmidtke et al., 2002), strict regulations, ethical considerations and economic constraints have prevented their widespread use. An alternative model for studying PTLD was proposed after the observation that the disease develops in PLHV1-infected miniature pigs subjected to experimental immunosuppression during SOT or HSCT (Huang et al., 2001, Dor et al., 2004). In addition to clinical, histological, and pathological similarities between human and porcine PTLD disease, PTLD in pigs was caused by either primary infection or reactivation of the γ -herpesvirus PLHV1, which is widespread in the porcine population (Huang et al., 2001, Goltz et al., 2002, Doucette et al., 2007). Furthermore, two other *Macaviruses*, PLHV2 and PLHV3 show sequence similarity of conserved genes (including BILF1) to EBV as well as B-cell tropism, as observed for EBV (Ehlers et al., 1999, Ulrich et al., 1999, Chmielewicz et al., 2003). The link between PLHV1 and PTLD in experimentally immune suppressed miniature pigs indicates the suitability of this preclinical model to study EBV-mediated lymphoproliferative disease (Huang et al., 2001, Cho et al., 2004, Dor et al., 2004).

2.4.2 Potential use of vGPCRs for pharmacological intervention

Given their similarity to GPCRs and their role in viral pathogenesis, vGPCRs, including BILF1, have recently been attracting attention as potential drug targets for the treatment of viral diseases (Spiess et al., 2015b, Krishna et al., 2017, Spiess et al., 2017, Fares et al., 2019, De Groof et al., 2021, Tsutsumi et al., 2021). A first example

is US28, which has been used as a target for immunotoxin-mediated destruction of HCMV-infected cells.

HCMV-US28 binds the chemokine CX₃CL1, which was fused to the cytotoxic domain of *Pseudomonas Exotoxin A* leading to the design of a novel fusion toxin protein (FTP). Furthermore, HCMV-US28 is known for its fast, constitutive endocytosis. By modifying CX₃CL1 for selective binding to US28 and not to the endogenous chemokine receptor CX₃CR1, US28 delivered the toxin by endocytosis into the cells where it was released from CX₃CL by proteolytic cleavage, further resulting in cell death (Spiess et al., 2015b, Krishna et al., 2017). The advantage of this new strategy of killing HCMV-infected cells is its high selectivity as it only kills the virus-infected cells expressing US28 at the cell surface. This also applies to other potential vGPCRs as pharmacological targets, as their expression is only observed in virus-infected cells (Spiess et al., 2016). Although EBV-BILF1 remains an orphan receptor, its structure was recently solved using cryo-EM. The study revealed the lack of common ligand-binding sites usually occurring in endogenous GPCRs (Tsutsumi et al., 2021) and therefore revealed the reasons for the challenges in determining the ligands for this receptor. Although challenging, BILF1 remains a prime target for EBV inhibition based on its role in transformation, immune suppression, and viral pathogenesis. Pigs infected with PLHV1 could be a useful preclinical model not only to study EBV-associated PTLN disease but also to test the drugability of BILF1. However, an important step towards these aims is the pharmacological characterization of BILF1 receptors.

3 MATERIALS AND METHODS

The following sections describe the methodological approaches used in this thesis. A short introduction to the methods and a detailed description of procedures cover nine main topics: i) standard molecular biology methods, ii) cell cultures and different transfection methods; methods to evaluate iii) receptor expression, iv) receptor endocytosis, v) receptor trafficking, vi) protein-protein interactions, vii) receptor-mediated second messenger activation, viii) receptor-mediated immunoevasive mechanisms, and ix) analysis of tissue samples. For detailed lists of antibodies, chemicals, cell lines and constructs used, see Appendix I.

3.1 STANDARD MOLECULAR BIOLOGY METHODS

3.1.1 Receptor construct design

All the experiments described in this section were used to study BILF1 receptors encoded by EBV, PLHV1, PLHV2, and PLHV3. To allow the detection of receptors by the described methods, different tags were required fused to the N- or C-terminus of these receptors; they are described in Table 4. Additionally, human β -arrestin 2 (β arr2) N-terminally tagged with GFP2 (GFP2/ β arr2) was purchased at PerkinElmer BioSignal, Inc. (Montreal, ON, Canada). The membrane-inserted GFP2-tagged construct (GFP2-17aa) was kindly provided by Dr Rasmus Jørgensen (7TM Pharma A/S, Hørsholm, Denmark) and described previously (Svendson et al., 2009, Mandić et al., 2014). Dominant negative mutant (DNM) constructs of caveolin-1 (Cav S80E) and dynamin (Dyn K44A) were kindly provided by Prof. J.E. Pessin (Department of Physiology and Biophysics, University of Iowa, Iowa, USA) and Prof. M.G. Caron (Duke University Medical Center, N.C., USA), respectively, and were described previously (Kubale et al., 2007). $G\alpha_{\Delta 6qj4myr}$ recombinant G protein was kindly provided by Evi Kostenis (Institute for Pharmaceutical Biology, University of Bonn, Germany) (Conklin and Kostenis, 1999).

Table 4: Different constructs of BILF1 receptors used in different methodological approaches.
Tabela 4: Različni konstrukti receptorjev BILF1, uporabljeni pri različnih metodoloških pristopih.

Receptor construct name	Vector backbone and tag	Method	Source
flag-EBV-BILF1 flag-PLHV1-BILF1 flag-PLHV2-BILF1 flag-PLHV3-BILF1	pcDNA3.1+ with N-terminal FLAG tag	ELISA, microscopy experiments, antibody uptake internalization assay, co-localization assay, western blot, luciferase assay, flow cytometry, microscopy to determine MHC-I downregulation	Obtained from Bernhard Ehlers and Thomas Kledal (from the archive in Mette M Rosenkilde's laboratory)
SNAPtag-EBV-BILF1* SNAPtag-PLHV1-BILF1 SNAPtag -PLHV2-BILF1 SNAPtag -PLHV3-BILF1	pcDNA5/FRT/T O-FLAG-SNAP with N-terminal FLAG and SNAP tag	FRET-based real- time internalization assay	Purchased at GenScript (Piscataway, NJ)
EBV-BILF1-RLuc8 PLHV1-BILF1-RLuc8 PLHV2-BILF1-RLuc8 PLHV3-BILF1-RLuc8	pcDNA3.1+ with N-terminal FLAG tag and C-terminal RLuc8 tag	BRET2 assay	Purchased at GenScript (Piscataway, NJ)

* This construct was prepared in the laboratory using the protocol described in Section 3.1.2.

3.1.2 Restriction enzyme molecular cloning

Subcloning is a commonly used laboratory technique, allowing researchers to move a cDNA, promotor, selectable markers or other cDNA elements from a plasmid of origin into a new plasmid. This enables the use of a desirable cDNA in a variety of applications. For this study, cDNA of EBV-BILF1 receptors was subcloned from pcDNA3.1+ vector into a pcDNA5/FRT/TO-FLAG-SNAP vector in order to tag the receptors with a SNAP tag, a tag used in a novel FRET-based real-time internalization assay.

3.1.2.1 Polymerase chain reaction

Polymerase chain reaction (PCR) is a widely used technique that produces new copies of specific DNA segment. Denaturated DNA serves as a template from which known DNA sequences (primers) align and initiate the synthesis of new complementary DNA strand (Zhu et al., 2020). When performing molecular cloning, a high yield of quality DNA insert is required. During the PCR run, the DNA undergoes three specific cycles: i) denaturation at high temperature causes the separation of double-stranded DNA (dsDNA) into two single-stranded DNA (ssDNA) molecules ii) primer annealing at temperatures around 50–60 °C allows the specific nucleotides (primer pairs) to align to the ssDNA, iii) elongation at increasing temperature and in the presence of DNA polymerase allows the synthesis of DNA. The exact protocol used in our study is shown in Table 5.

The PCR mastermix consisted of 1 µL of 0.5 µg/µL DNA template, 0.4 µL of Pfu DNA polymerase, 5 µL of Pfu DNA polymerase 10 × Buffer with MgSO₄, dNTP mix (10 mM each), 5 µL (5 pmol/µL) upstream primer (5'TAAGCAACGCGTCTCTCCACCATGGCCCC3'), 5 µL (5 pmol/µL) of downstream primer (5'TGCTGCCTCGAGTCAGGTGGACTGGCTAGG3') and nuclease-free water to a final volume of 50 µL.

Table 5: PCR protocol used in our study.
Tabela 5: Protokol PCR, uporabljen v naši raziskavi.

Step	Temperature	Time	Number of cycles
Initial denaturation	95 °C	1–2 min	1 cycle
Denaturation	95 °C	0.5–1 min	25–35 cycles
Annealing	42–65 °C	30 sec	
Extension	72–74 °C	2–4 min	
Final extension	72–74 °C	5 min	1 cycle
Soak	4 °C	Indefinite	1 cycle

3.1.2.2 Digestion

Restriction digestion for both donor and recipient plasmids were performed after the PCR reaction. Restriction endonucleases recognize short DNA sequences and cleave the backbone on both sites. High amounts of both plasmid and recipient DNA were used to ensure sufficient yields in the next step. For EBV-BILF1, 40 μ L of PCR product, 1 μ L of XhoI restriction enzyme (New England Biolabs), 1 μ L of MluI restriction enzyme (New England Biolabs), 1 μ L DpnI and 2 μ L of appropriate buffer (New England Biolabs) were used for digestion. The mixture was incubated at 37 °C for 30 min and the digestion was deactivated at 80 °C.

3.1.2.3 Electrophoresis, DNA extraction and purification from agarose gel

To separate the insert from the backbone in the digestion mixture, gel-electrophoresis was performed. The principle of the method is based on the tendency of DNA molecules to migrate in the electrical field from negative potential to positive potential. In the agarose gel matrix, shorter DNA fragments migrate more quickly than longer ones, allowing the separation and visualization of size-specific fragments and their subsequent isolation and purification.

20 μ L of digestion mixture mixed with 2 μ L of loading buffer was loaded on a 1% agarose gel with nucleic acid gel stain GelRed[®]. The electrophoresis was run for approximately 40 min at 100 V in 0.5 \times TBE. cDNA fragments were visualized under the UV light. The fragments recognized as the insert based on their size, were cut from the gel, and purified using NucleoSpin Gel and a PCR Clean-up Mini kit (Macherey-Nagel GmbH & Co. KG). The kit is designed to solubilize the gel and bind the cDNA on the silica membrane of NucleoSpin column. Washing the membrane with high salt and ethanol prevents isolation of contaminants. cDNA is finally eluted under low salt conditions.

3.1.2.4 Ligation

To ligate DNA fragment with the compatible overhanging sequences, the ligation step with T4 DNA ligase enzyme was performed, in which the enzyme restored the backbone resulting in a circular DNA after connecting 3'-hydroxyl-group of one DNA fragment with the 5'-phosphate group of the other DNA fragment. 1 μ L of T4 DNA Ligase, 4 μ L of ligase 10 \times buffer, 14 μ L of the insert and 1–2 μ L of the vector backbone were used. The mixture was incubated at 4 $^{\circ}$ C overnight and then transformed into competent *Escherichia coli* cells.

3.1.3 Transformation of chemically competent *E.coli* cells

Transformation is a process in which the “competent cells” uptake plasmid cDNA from the extracellular environment. Using this method, recombinant plasmid vectors were replicated into chemically competent *E. coli* Top10' cells (Invitrogen) or *E. coli* XL1 Blue strain. 1 μ L of recombinant vector cDNA was added to 25 μ L of competent cells and the mixture was incubated for 30 min at 4 $^{\circ}$ C. Cells were exposed to heat shock at 42 $^{\circ}$ C for 90 s and immediately placed on ice for 2 min. 250 μ L of superoptimal broth medium with catabolite repression (SOC medium) was added and incubated on a shaker for 1 h at 37 $^{\circ}$ C at 220 rpm. After the incubation, 25 μ L of the cells were plated on Luria-Bertani (LB) agar plates containing 100 μ g/ml of ampicillin (Sigma-Aldrich) and the plates were incubated overnight at 37 $^{\circ}$ C. Several well-separated colonies were carefully picked out with an inoculation loop and separately inoculated into a 50 mL tube containing fresh, autoclaved LB medium containing 100 μ g/mL ampicillin. Cells were then incubated in a shaker overnight (maximum 18h) at 37 $^{\circ}$ C and 220 rpm. Subsequently, 250 μ L of the overnight culture was inoculated in 250 mL of fresh LB medium containing 100 μ g/mL ampicillin and incubated overnight at 37 $^{\circ}$ C and 220 rpm. The next day, culture was centrifuged for 15 min at 4 $^{\circ}$ C at 5000 rpm. Supernatant was discharged and the pellet was used to purify DNA.

3.1.4 cDNA purification

A bacterial pellet acquired from the transformation of *E. coli*, was further used to extract and purify cDNA. The commercially available HiSpeed Plamid Maxi kit (Qiagen) was used according to the manufacturer's protocol. First, the pellet was lysed with alkaline buffer and neutralized with neutralization buffer containing acetate. The precipitated proteins and genomic DNA (gDNA) were separated via an anion exchange purification column, while the supernatant containing cDNA was isolated and further purified with buffers and isopropanol. Finally, purified cDNA was washed from the membrane with sterilized H₂O.

3.1.5 Spectrophotometric cDNA quantitation

After purification, the cDNA concentration was evaluated by spectrophotometer NanoPhotometer® (Implen, Germany) or Ultrospec 3000 UV/visible spectrophotometer (Amersham Pharmacia Biotech, United Kingdom). The cDNA concentration was determined spectrophotometrically, by measuring the absorbance at 260 nm, further multiplying this value with 50 µg/mL and the dilution factor. Ratio between the absorbance at 260/280 nm indicates cDNA purity where the ratio at ~1.8 indicates good cDNA purity.

3.1.6 Verification of receptor construct sequences

All constructs were sequenced using Eurofins Genomics GATC services acquiring forward and reverse nucleotide sequences of the receptor constructs. Nucleotide sequences were aligned using Geneious software (Biomatters, New Zealand).

3.2 CELL CULTURE AND TRANSFECTION

3.2.1 Cell lines

For this study, two types of epithelial cells were used: human embryonic kidney 293 (HEK-293) and porcine kidney (PK-15) cells, which were obtained from European Collection of Authenticated Cell Cultures (ECACC) or American Type Culture Collection (ATCC), respectively. HEK-293 cells are commonly used in research as a tool for recombinant protein expression. Based on the aim of the thesis, to compare BILF1 receptors from human and porcine gammaherpesviruses, a comparable porcine epithelial cell line PK-15 was included. Moreover, specific signaling properties and the β -arrestin requirement in receptor internalization were studied in CRISPR/Cas9 modified HEK-293A pan knock-out (KO) cells ($\Delta G\alpha_{s/olf/q/11/12/13/z}$), CRISPR/Cas9 modified β -arrestin-1/2 knock out ($\Delta\beta$ -arr1/2 KO) HEK-293A cells, respectively and in a control HEK-293A parental cell line. HEK-293A cell line is a subclone of HEK-293 cells with flat morphology that facilitate the initial production, amplification and titering of replication-incompetent adenovirus. These cells are commonly used for CRISPR/Cas9-mediated gene editing. These cells were kindly provided by Asuka Inoue (Tohoku University, Japan).

3.2.2 Working with *in vitro* systems – cell cultures

HEK-293 and all HEK-293A cells (kindly provided by Asuka Inoue) were cultured in Dulbecco's modified Eagle's medium (DMEM; Invitrogen) at 37 °C and 5% CO₂ in a humidified atmosphere. PK-15 cells were cultured in minimum essential medium (MEM; Invitrogen) at 37 °C and 5% CO₂ in a humidified atmosphere. DMEM and MEM were supplemented with 10% heat inactivated foetal bovine serum (FBS) and 180 units/ml penicillin and 45 μ g/ml streptomycin. When cells reached approximately 80% confluence, the medium was removed and cells were washed with PBS (without Ca²⁺ and Mg²⁺), detached with Trypsin-EDTA solution (Sigma) and re-cultured in fresh medium.

Cell viability assay Celltiter glo[®] was performed to check and compare the viability of different cell lines. The assay was performed according to the manufacturer's instructions. Cells were seeded at 35,000 cells/well and transfected the next day. 24 h after transfection, plates were incubated at room temperature (RT) for approximately 30 min. 100 µL of CellTiter Glo[®] reagent was added to each well. Plates were incubated for 12 min on a shaker before the luminescence was measured on EnVision Multilabel Plate Reader (PerkinElmer).

3.2.3 Methods for transient transfection of cell lines

Transfection is a term used to describe the process in which foreign genetic material (DNA, RNA, siRNA, shRNA, or miRNA) is introduced into eukaryotic cells. Transfection can be stable, meaning that it provides long-term protein expression when the DNA is integrated into the host genome, or it can be transient, where the DNA is not integrated in the genome and provides only transient protein expression. In general, transfection is widely used and is a powerful tool to study gene function in various cell types. Nowadays, there are many different strategies based on chemical, biological, or physical principles. The use of a specific method depends on the application required, the equipment available (e.g., cell type and facility) and experience of the user. Chemical transfection is the most widely used method, due to its reproducibility, simplicity, adaptability, efficiency at all scales, and cost-effectiveness (Fus-Kujawa et al., 2021).

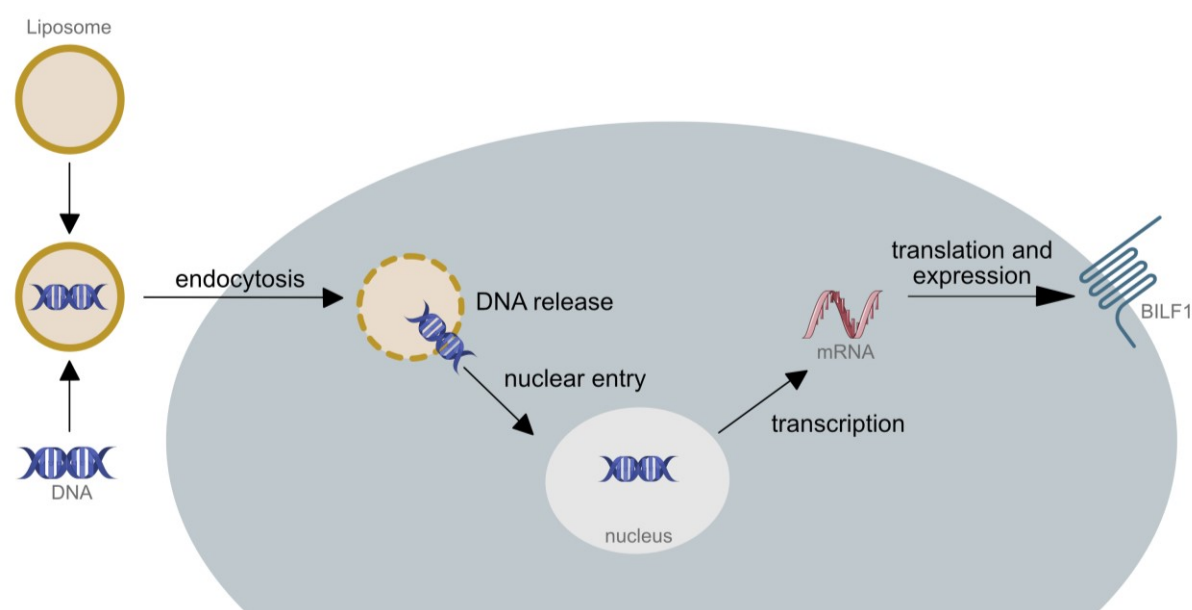


Figure 7: Basic principle of chemical transfection using cationic lipids.
Slika 7: Osnovne značilnosti kemične transfekcije s kationskimi lipidi.

The basic principle of chemical transfection is based on the use of a positively charged carrier that transports the negatively charged genetic material across the negatively charged plasma membrane by endocytosis or phagocytosis (Figure 7). The choice of chemical transfection depends on the application, cost, and efficiency for a given cell type. For our studies, cationic lipids were used to deliver DNA into the abovementioned cells. Different commercially available kits were used, depending on the assay or cell type.

3.2.3.1 Lipofectamine transfection

Lipofectamine™ (Invitrogen) transfection is widely used lipid-based transfection and offers many different reagent versions. In this study, Lipofectamine™ 2000 (used for cell-based ELISA, luciferase-based transcription factor assay and FRET-based real-time internalization assay) and Lipofectamine™ LTX reagent (used for BRET) were used. The procedures used for both reagents are identical. The described amounts of the reagents apply to the 96-well plate setup. For other plate well format setup conditions, the amounts were adjusted accordingly. For each transfection, two 1.5 mL Eppendorf tubes were prepared. In the first tube, 0.6 µL/well of Lipofectamine™

reagent (the total amount was calculated based on the number of transfected wells) was gently added and mixed with 50 μ L of Opti-MEM; in the second one, cDNA was diluted in 50 μ L reduced serum medium (Opti-MEM, Gibco). The ratio between Lipofectamine™ reagent and cDNA was 3:1. When using Lipofectamine™ LTX (BRET assay), PLUS™ reagent was additionally added to the Eppendorf tube containing cDNA in the same amount, in order to enhance transfection efficiency. After 5 min incubation, the cDNA mixture was added to the Lipofectamine mixture. During 15 min incubation at RT, the culture medium in wells was replaced with 100 μ L of Opti-MEM and afterwards, 100 μ L of transfection mixture was added to the cells. After 5 h of transfection, Opti-MEM was replaced with 200 μ L culture medium without penicillin and streptomycin. For the immunocytochemistry experiments, higher levels of the observed and previously published (Jacobsen et al., 2009) cytotoxicity induced with Lipofectamine™ 2000 transfection had to be avoided. The cytotoxicity occurs, because of the requirement for low serum concentrations and presumably toxic components in lipid complex.

3.2.3.2 *FuGENE transfection*

Although Lipofectamine™ 2000 transfection reagent proved very efficient for some of the experiments, in microscopy experiments, where cells are grown on glass slides and handling needs to be precise and delicate, Fugene 6® (Promega, USA) was used for HEK-293 cells or FuGENE® HD transfection reagent (Promega, USA) for PK-15 cells. This transfection method does not require reduced serum medium during the transfection, therefore, allowing minimum handling with the cells at this critical step. The reagents were used according to the manufacturer's instructions. For microscopy experiments, transfection was performed in a 24-well plate format. Fugene 6® or FuGENE® HD reagent was allowed to reach RT before use. For each transfection, a minimum of 100 μ L transfection mixture was prepared. For FuGene6 transfection, 0.6 μ L/well of Fugene® reagent was added gently, without touching the edges of the tube, to 20 μ L/well Opti-MEM and the mixture was incubated for 5 min at RT. Afterwards, 0.2 μ g/well cDNA (ratio Fugene/DNA 3:1) was added, and the mixture was incubated for additional 15 min. 20 μ L/well of transfection mixture was added directly to the cells

in the normal culture medium. For FugeneHD, 0.3 µg/well cDNA was diluted directly in Opti-MEM (the amount was adjusted to the final volume of 50 µL/well) and mixed afterwards. 0.9 µL/well of FugeneHD reagent (Fugene/DNA 3:1 ratio) was gently added to the tube, and the mixture was incubated for 5–15 min at RT. 50 µL/well of transfection mixture was added directly to the cells in the normal culture medium. Cells were used for microscopy experiments after 48 h.

3.3 METHODS TO EVALUATE RECEPTOR EXPRESSION LEVEL

3.3.1 Cell-based Enzyme-linked immunosorbent assay

Cell-based ELISA assay is a useful method for the quantitative determination of receptor expression in cells. The principle is based on the detection of the protein by a specific primary antibody. Primary antibodies against the FLAG tag, which was fused to the N-terminus of the receptor were used, as specific antibodies against BILF1 receptors are lacking. Primary antibodies are recognized by secondary antibodies conjugated with an enzyme horseradish peroxidase. The enzyme reacts with a horseradish peroxidase and yields a blue colour reaction. The reaction is terminated by sulfuric acid and the colorimetric detection method is used for quantification.

In this study, the cell surface expression of FLAG-tagged BILF1 receptor constructs was studied in transiently transfected HEK-293 and PK-15 cells. Cells were seeded in a density of 1×10^5 cells/well in a 96-well plate pre-coated with 100 µL/well Poly-D-lysine and after 24 h transiently transfected with various concentrations of receptor DNA (0, 1, 2, 5, 10, 25, 35, 50 ng) using Lipofectamine™ 2000. After 48 h, cells were washed with 200 µL/well of PBS/CaCl₂ and subsequently fixed with 150 µL/well of 3.7% paraformaldehyde in PBS/CaCl₂ (pH 7.3) for 10 min at 4 °C. After washing three times in 200 µL/well PBS/CaCl₂ on a shaker for 5 min, cells were incubated with 150 µL/well blocking buffer [PBS/CaCl₂, 1% bovine serum albumin (BSA)] for 30 min at RT. Cells were subsequently incubated with 100 µL/well primary mouse M1 anti-FLAG antibody (Sigma-Aldrich) at 2 µg/mL in 1% BSA/PBS/CaCl₂ for 1 h at RT. Following three washing steps in 200 µL/well PBS/CaCl₂, cells were incubated with 100 µL/well

secondary rabbit anti-mouse horseradish peroxidase-conjugated IgG antibody (Sigma-Aldrich) at 1:1000 in PBS/CaCl₂ for 1 h at RT. After the secondary antibodies were washed with 200 µL/well PBS/CaCl₂, the peroxidase activity was determined by adding 75 µL/well 3,3'-5,5'-tetramethyl benzidine substrate (TMB) (Sigma-Aldrich) in the dark. The reaction was terminated by addition of 75 µL/well 0.5 N H₂SO₄ and absorbance was measured at 450 nm using the FlexStation3[®] Benchtop Multi-Mode Microplate Reader (Molecular devices). Each BILF1 receptor as well as the controls were tested at least in three biological replicates.

3.3.2 Microscopy experiments

Laser scanning confocal microscopy is the gold standard in research, allowing the detection of fluorescence emission of specimen treated with fluorescent dyes, after the localized laser excitation of the field. It allows a wide range of studies on live and fixed cells, describing three-dimensional structures, protein localization and co-localization, dynamic cellular processes, and single molecule diffusion (Bayguinov et al., 2018).

Microscopy experiments were performed on HEK-293 and PK-15 cells to determine the surface and intracellular distribution of our FLAG-tagged receptor constructs. All the handling was performed gently, to ensure optimal cell morphology. 80,000 cells/well were seeded on fibronectin coated (350 µL/well; 10 µg/mL in PBS) coverslips in 24-well plates. The next day cells were transiently transfected using FuGene6 (HEK-293) or FugeneHD (PK-15). After 48 h, cells were washed with PBS/CaCl₂ and fixed in 500 µL/well with 4% paraformaldehyde for 10 min on ice and additional 10 min at RT. Following three washing steps, the non-specific background staining was reduced with 500 µL/well of 10% donkey serum in PBS/CaCl₂ for 20 min. To specifically label the receptor residing on the cell surface, incubation with 250 µL/well of the primary M1 anti-FLAG antibody (2 µg/mL) (Sigma-Aldrich) in 1% donkey serum/PBS/CaCl₂ for 1 h at RT was performed. When observing the cellular distribution of receptors, membrane permeabilization using 500 µL/well of 0.02% saponin in 1% donkey serum/PBS/CaCl₂ was performed prior to primary antibody incubation. After washing with 500 µL/well PBS/CaCl₂ for three times, cells were incubated with 250 µL/well secondary donkey

anti-mouse Alexa Fluor 594 antibody (Jackson ImmunoResearch) at 1:100 in PBS for 1 h at RT. During the last 10 min of the incubation, 20 μ L of wheat germ agglutinin (WGA) conjugated to Alexa488 (Invitrogen) was added to the cells as a membrane marker (5 μ g/mL). Cells were additionally washed and incubated with PBS/CaCl₂ containing Hoechst 33342 stain (Invitrogen) (1 μ g/mL) and samples were mounted with 8 μ L of Fluorescence mounting medium (Dako) and sealed with nail polish on a glass slide. Cells were examined with Plan-Apochromat \times 63 oil immersion objective on fluorescence microscope LSM700 (Zeiss). BILF1 receptors, plasma membrane and nuclei were visualized by using excitation lasers at 555 nm (Diode, 10 mV), 488 nm (Diode, 10 mW) and 405 nm (Diode, 5 mW), respectively. The data were collected at resolution of 1440 \times 1440 pixels with four-fold averaging. 0.3 μ m optical sections were taken on a z-axis and a representative section was used as representative image.

3.4 ANALYSIS OF RECEPTOR ENDOCYTOSIS

3.4.1 Antibody-uptake internalization assay

To determine the internalization properties of BILF1 receptors, two separate assays were performed, both based on the principle of antibody uptake over time. Using the time-course cell-based ELISA assay, the amount of surface expressed receptors was quantified over time. Microscopy can be used to visualize surface expressed and internalized receptors, at different time points after induction of the internalization. Few basic principles are common for both assays. First, incubation with the primary mouse M1 anti-FLAG antibody was performed at 4 °C to prevent receptor internalization during the labelling step. Second, the primary antibodies were added in saturation to ensure the labelling of all receptors residing at the cell surface. Third, after 1 h of incubation with the primary antibodies, the medium in the wells is replaced with fresh, pre-warmed medium and cells are subsequently incubated at 37 °C for various time points (t = 0, 15, 30, 60 min). This allows the receptors to internalize, so that the previously labelled receptors can be followed in the cell. Finally, secondary antibodies are used to allow the quantification or visualization of receptors.

3.4.1.1 Time-course cell-based ELISA internalization assay

HEK-293 cells transiently transfected with Lipofectamine 2000 were seeded in 24-well plates, previously coated with 200 $\mu\text{L}/\text{well}$ poly-D-lysine at a density 2×10^5 cells/well. The following day, cells were incubated with 220 $\mu\text{L}/\text{well}$ of the primary M1 anti-FLAG antibody (2 $\mu\text{g}/\text{mL}$) (Sigma-Aldrich) in cold DMEM at 4 $^{\circ}\text{C}$ for 1 h. Following three washes in 500 $\mu\text{L}/\text{well}$ of cold DMEM, cells were either immediately fixed ($t = 0$) with 250 $\mu\text{L}/\text{well}$ of 3.7% paraformaldehyde or incubated at different time points ($t = 5, 10, 20, 30, 60$ min) in 500 $\mu\text{L}/\text{well}$ pre-warmed DMEM media (37 $^{\circ}\text{C}$) to induce the internalization and then fixed. The procedure then followed the standard cell-based ELISA protocol described in Section 3.3.1. The experiment was performed at least three times in triplicate.

3.4.1.2 Microscopy-based internalization assay

80,000 HEK-293 and PK-15 cells/well were seeded on fibronectin-coated 12 mm round coverslips in 24-well plates and transfected the next day using Fugene[®] 6 (HEK-293) or FuGENE[®] HD (PK-15). 24 h after transfection, 250 $\mu\text{L}/\text{well}$ primary mouse M1 anti-FLAG antibody (2 $\mu\text{g}/\text{mL}$) was added to the cells for 1 h at 4 $^{\circ}\text{C}$. Cells were immediately fixed with 500 $\mu\text{L}/\text{well}$ of 3.7% paraformaldehyde for 20 min at 4 $^{\circ}\text{C}$ ($t = 0$) or incubated in 500 $\mu\text{L}/\text{well}$ pre-warmed DMEM at 37 $^{\circ}\text{C}$ for 15 or 30 min ($t = 15, 30$) to induce internalization and then fixed. After three washing steps with 500 $\mu\text{L}/\text{well}$ PBS/ CaCl_2 , cells were blocked in 500 $\mu\text{L}/\text{well}$ 10% donkey serum in PBS/ CaCl_2 for 20 min at RT. In the next step, with the plasma membrane intact, the receptors located at the cell surface of fixed cells were labelled with 250 $\mu\text{L}/\text{well}$ secondary donkey anti-mouse Alexa Fluor 488-conjugated antibody (Jackson ImmunoResearch) at 1:500 for 1 h, at RT. After membrane permeabilization step with 500 $\mu\text{L}/\text{well}$ 0.2% Saponin (Sigma) for 20 min, an additional incubation with 250 $\mu\text{L}/\text{well}$ donkey anti-mouse Alexa 594 antibody (Jackson ImmunoResearch) at a ratio 1:500 was performed to specifically label the internalized receptors. Following two washing steps, cells were incubated with 500 $\mu\text{L}/\text{well}$ PBS containing Hoechst 33342 stain (Invitrogen) (1 $\mu\text{g}/\text{mL}$). Before imaging on a fluorescence microscope (Zeiss, LSM700), cells were mounted with 8 μL

of fluorescence mounting medium (Dako) and sealed to glass slide with nail polish. Cells were examined by Plan-Apochromat × 63 oil immersion objective on fluorescence microscope LSM700 (Zeiss). Excitation lasers at 555 nm (Diode, 10 mV), 488 nm (Diode, 10 mW) and 405 nm (Diode, 5 mW) were used to visualize internalized BILF1 receptors, BILF1 receptors at the cell surface and cell nuclei, respectively. The data were collected at resolution of 1440 × 1440 pixels with four-fold averaging. 0.3 µm optical sections were taken on a z-axis and representative images were used for presentation.

3.4.2 The effect of protein depletion on clathrin- and caveolae-mediated endocytosis of BILF1 receptors

To elucidate the detailed pathways involved in BILF1-mediated endocytosis, DNM and a chemical inhibitor were additionally applied to the FRET-based real-time internalization assay that is described in detail in Section 3.4.3. Dyn K44A is a dynamin-1 DNM, which is a selective inhibitor of both clathrin- and caveolae-mediated endocytosis (Figure 8). The mutant is defective in GTP binding and hydrolysis, preventing the scission of newly formed endocytic vesicles at the membrane (Damke et al., 1994, Kubale et al., 2007). Cav S80E is a DNM of caveolin-1 localizing to the ER, disrupting the formation of caveolae at the membrane (Schlegel et al., 2001, Kubale et al., 2007). Chemical inhibitor Pitstop2, blocks the clathrin-mediated endocytosis by disrupting the interaction between clathrin and the adaptor protein amphiphysin (von Kleist et al., 2011) (Figure 8). HEK-293 cells expressing the SNAP-tagged constructs of BILF1 receptors were co-transfected with Dyn K44A and Cav S80E constructs or treated with chemical inhibitor Pitstop 2. By performing the FRET-based real-time internalization assay, constitutive BILF1 mediated internalization over a period of 88 min was measured.

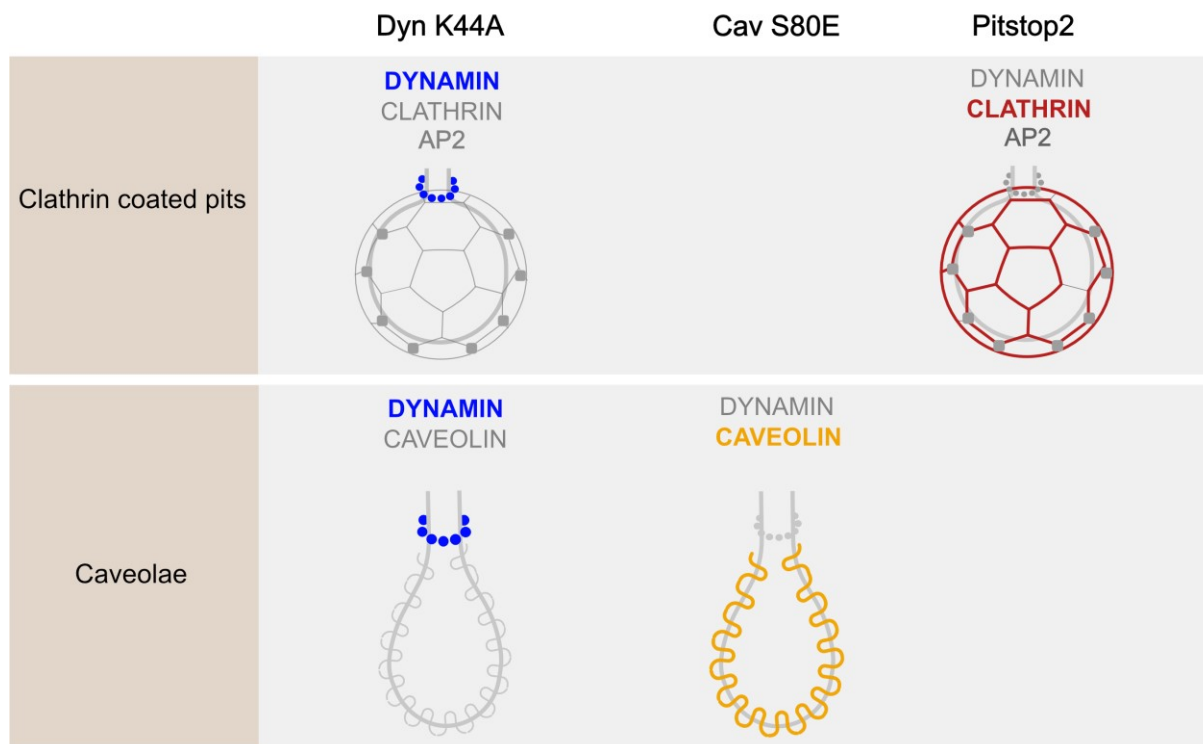


Figure 8: Essential proteins of clathrin and caveolae mediated endocytosis affected by dominant negative mutants (Dyn K44A, Cav S80E) and chemical inhibitor (Pitstop2).

Slika 8: Ključni proteini endocitoze, posredovane s klatrinom in kaveolinom, na katere vplivajo dominantno negativne mutante (Dyn K44A, Cav S80E) in kemični inhibitor (Pitstop2).

Coloured structures and text represent the proteins targeted by the mutants and inhibitors.

3.4.3 Fluorescence-based resonance energy transfer based real-time internalization assay

The novel FRET-based real-time internalization assay allows the monitoring of protein internalization in living cells. At the N-terminus, the studied receptor is fused to a SNAP-tag which is an O⁶-guanine nucleotide alkyltransferase derivative that can covalently react with fluorescently conjugated benzyl guanine substrates. The FRET principle is based on energy transfer from excited donor to the acceptor (Figure 9). In this case, a cell impermeable SNAP-Lumi4Tb is an energy donor covalently bound to the SNAP-label of the receptor. Fluorescein added to the solution acts as an energy acceptor. When the receptor is located on the cell surface, the donor is excited, and the energy is transferred to the acceptor occurs as both are in close proximity. At the same time, the donor emission is quenched, resulting in a low donor/acceptor ratio. During receptor internalization, the signal from the donor increases and the

donor/acceptor ratio increases, showing that the amount of the receptor on the cell surface decreases (Foster and Bräuner-Osborne, 2018).

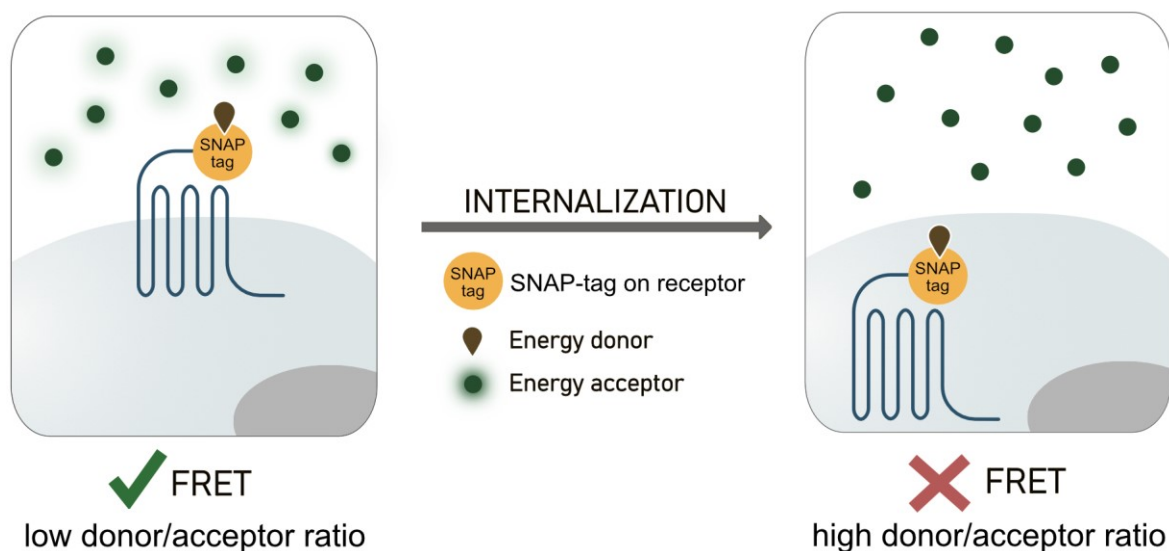


Figure 9: Principle of FRET-based real-time internalization method.

Slika 9: Način delovanja metode internalizacije v realnem času, ki temelji na metodi FRET.

HEK-293A cells (parental) or HEK-293A $\Delta\beta$ -arr1/2 KO cells were transiently transfected with Lipofectamine™ 2000 to express SNAP-EBV-BILF1, SNAP-PLHV1-BILF1, SNAP-PLHV2-BILF1, SNAP-PLHV3-BILF1, or SNAP-FRT empty vector. To determine specific internalization pathways, DNMs of dynamin (Dyn K44A) or caveolin-1 (Cav S80E) were co-transfected into parental cells at various concentrations. Cells mixed with the transfection mixture were seeded in Poly-D-lysine (Sigma-Aldrich) pre-coated 384-well plates at density 16,000 cells/well. After 24 h, the transfection medium was replaced with fresh growth medium. The next day, cells were incubated for 1 h with 10 μ L/well of 100 nmol/L cell impermeable Tag-Lite SNAP-Lumi4Tb (donor; Cisbio) in Opti-MEM at 4 °C to prevent internalization during labelling. Afterwards, cells were washed 4 times using 30 μ L/well of HBSS supplemented with 1 mmol/L CaCl₂, 1 mmol/L MgCl₂ and 20 mmol/L HEPES, pH 7.4 (internalization buffer). After the last wash, 20 μ L/well (50 μ mol/L) of pre-warmed fluorescein-O'-acetic acid (acceptor; Sigma-Aldrich) was added to the cells. Internalization was measured every 4 min for a total 90 min at 37 °C in the PerkinElmer™ EnVision 2104 Multilabel Reader using a 340 nm excitation filter. Emission was detected by 520 nm (acceptor) and 615 nm

(donor) emission filters. Results are presented as the ratio of donor-to-acceptor emission (615/520 nm). Experiments were performed at least in three biological replicates and three times. The area under the curve (AUC) data, normalized to each BILF1 receptor was used for statistical analysis. Receptor expression was presented relative to each BILF1 receptor using raw donor emission data.

3.5 CO-LOCALIZATION STUDIES FOR DETERMINING RECEPTOR INTRACELLULAR TRAFFICKING

The first part of the assay was performed as described above (Section 3.4.1.2). Specific antibodies against endogenous intracellular markers of early endosomes (CD71), recycling endosomes (Rab8) and lysosomes (LAMP1) were used. Primary antibodies used to label BILF1 receptors were either mouse M2 anti-FLAG antibody (used when studying co-localization with Rab8) or rabbit M2 anti-FLAG antibody (used when studying co-localization with CD-71 and LAMP). After blocking the cells with 500 μ L/well 10% BSA in PBS/CaCl₂ for 20 min at RT, cells were additionally incubated with 250 μ L/well of mouse anti-CD71 antibodies (Santa Cruz), mouse anti-LAMP1 antibodies (DSHB) or rabbit anti-Rab8 antibodies (Cell Signaling) at a concentration of 1:100 for 1 h to label early endosomes, late endosomes, and recycling endosomes, respectively. For visualization, cells were incubated with a mixture of 250 μ L/well of secondary Alexa Fluor 488 (green) antibodies (against primary anti-FLAG antibody) and Alexa Fluor 594 (red) antibodies (labelling primary antibody against intracellular markers) at 1:100 in PBS/CaCl₂ for 1 h at RT (goat anti-mouse Alexa Fluor 488 (BILF1)/goat anti-rabbit Alexa Fluor 594 (Rab8) or goat anti-rabbit Alexa Fluor 488 (BILF1)/goat anti-mouse Alexa Fluor 594 (CD71 or LAMP1)). Cells were additionally incubated with 500 μ L/well PBS/CaCl₂ containing Hoechst 33342 stain (Invitrogen) (1 μ g/mL) and samples were mounted with 8 μ L of fluorescent mounting medium (Dako) and sealed with nail polish before imaging with a fluorescence microscope (Zeiss, LSM700).

3.6 PROTEIN – PROTEIN INTERACTIONS

3.6.1 Bioluminescence resonance energy transfer

The basic principle of BRET allows the quantitative assessment of protein-protein interactions and conformational changes of proteins in living cells. The energy transfer occurs when energy is transferred from the bioluminescent donor to the fluorescent acceptor by resonance energy transfer when they are in close proximity (10–100 Å) (Kobayashi et al., 2019) (Figure 10).

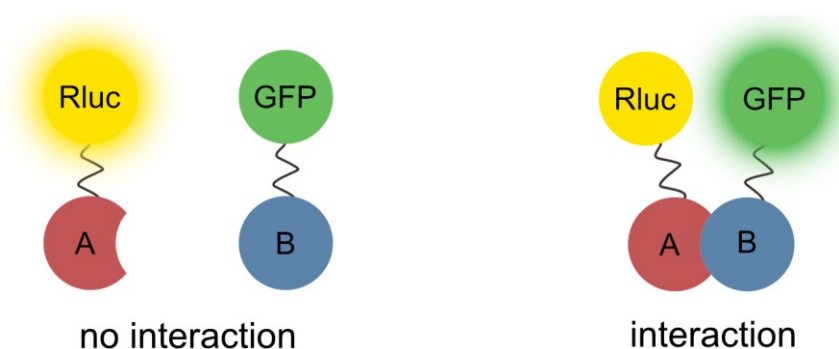


Figure 10: Principle of BRET method.

Slika 10: Način delovanja metode BRET.

Rluc (*Renilla luciferase*), GFP (green fluorescent protein), protein A (A), protein B (B).

In our system, *Renilla luciferase 8* (RLuc8) at the C-terminus of the receptor was used as the donor and a green fluorescence protein 2 (GFP2) fused to β -arr2 was used as acceptor. Coelenterazine 400A/DeepBlueC™ served as a substrate for RLuc8, resulting in the emission peak at 395 nm. When GFP2 is in close proximity with RLuc8, energy transfer to the GFP2 occurs, resulting in the emission at 510 nm. BRET2 is a variant of BRET using the substrate coelenterazine instead of its analogue DeepBlueC and GFP2 instead of YFP. The advantage of BRET2 is a larger Stokes shift (115 nm), which results in lower background noise due to the more separated RLuc8 and GFP2 emission. BRET2 experiments were performed as previously described (Drinovec et al., 2012, Kubale et al., 2016). HEK-293 cells were transiently co-transfected with constant amounts of the RLuc8-tagged BILF1 receptor constructs and increasing amounts of the GFP2-tagged β -arr2 or 17aa using Lipofectamine LTX reagent. 48 h

after transfection, 180 μ l of resuspended cells at density \sim 1.1 million cells/mL were distributed in 96-well microplates (white Optiplate; Packard BioScience, Meriden, CT, USA). 10 μ L of 100 μ M coelenterazine 400A (Biotium, San Francisco, USA) was added to each well using an injector. Sequential measurement of emission at 410 nm (RLuc8 luminescence signal) and 515 nm (emission of light from excited GFP2) was performed using a TriStar LB 942 microplate reader (Berthold Technologies, Bad Wildbad, Germany). Results were presented as ratios (515/410; BRET2 signal) and expressed in milliBRET units (mBU); BRET ratio \times 1000. The expression levels of RLuc8- and GFP2-tagged constructs were assessed for each experiment by total luminescence and fluorescence (measured in black plates, using excitation filter at 380 nm and an emission filter at 515 nm. Determinations were performed in triplicates.

3.6.2 Informational spectrum method

The principle of the informational spectrum method (ISM) describes the biological activity of a protein based on its physico-chemical property described by each amino acid. An obtained numerical sequence represents the primary structure of a protein and is further subjected to a Fourier transformation. This provides the informational spectrum (IS) with frequencies and amplitudes and corresponds to the distribution of structural motifs responsible for a particular protein function. Common biological properties of two or more proteins can be detected and determined by a cross-spectrum for two proteins or consensus informational spectrum for two or more proteins. By measuring a signal to noise ratio (S/N), the similarity for common frequency components can be measured for the sequences analysed (Veljkovic et al., 2008, Veljkovic et al., 2009, Veljkovic et al., 2011). Endogenous GPCRs and vGPCRs share similar signaling networks. The data on interactions between receptor and endogenous protein are commonly used for determining specific signaling pathways (Mei and Zhu, 2015, Zhang et al., 2016). Previously, it was demonstrated that proteins involved in similar signaling networks share common information and this information is represented by the IS frequencies (Patterson et al., 2022). The ISM method was performed by collaboration partners Sanja Glišić and Milan Senčanski from Center for

Multidisciplinary Research, Institute of Nuclear Sciences VINCA, University of Belgrade, Belgrade, Serbia.

3.7 METHODS FOR DETECTION OF SECOND MESSENGER PROTEINS

3.7.1 Western blot

Western blot is a widely used method, which allows the separation of proteins and detection of their quantity and molecular weight. It includes several critical steps: sample preparation by which the cells are lysed and non-protein components of the cells are removed; electrophoresis, which separates the proteins based on their molecular weight; transfer from gel to a membrane where the proteins are immobilized; detection by specific antibodies; image acquisition of labelled proteins; analysis and quantification (Meftahi et al., 2021).

HEK-293 cells were seeded one the day prior to transfection in 6-well plate at a density of 600,000 cells/well. The cells were transfected with 1.5 µg DNA/well using FuGene HD. 24 h after transfection, cells were starved using serum-free media and incubated for additional 24 h. The plates were placed on ice and the following steps were performed at 4 °C. The cells were washed once with cold PBS. 200 µl Ripa Lysis Buffer (Milipore) containing Complete Mini protease inhibitor cocktail (Roche) and Phosphatase Inhibitor Cocktail 3 were added for 30 min. Afterwards, cells were scraped loose and transferred to a cold 1.5 mL Eppendorf tube and kept on ice or stored at -20 °C. Samples were sonicated for 1–5 s and centrifuged for 10 min at 10,000 rpm at 4 °C. Supernatant was transferred to a new Eppendorf tube, and protein concentration was determined using an albumin standard curve. Sample buffer and 1M DL-dithiothreitol (DTT) were added to the samples after measuring the protein concentration. Immediately prior to loading, samples were heated at 92 °C for 5 min and returned to ice. 20 µL of the samples were loaded onto a 4–15% Criterion™ TGX™ Precast Midi Protein Gel (BIO-RAD) and run with 10 × Tris/Glycerin/SDS running buffer (BIO-RAD) at 100 V for 10 min and 300 V for additional 25 min. A PVDF membrane (BIO-RAD) was activated in 100% EtOH for 10 s and placed on top of filter paper

soaked with Transfer Buffer (BIO-RAD). The gel and additional wet filter paper was added on top and air bubbles were removed before the blot was run for 7 min. The membrane was blocked in appropriate amounts of Odyssey blocking buffer (Licor) for 30 min and incubated with primary antibodies against phosphorylated ERK (pERK (Phospho-p44/42 MAPK (Erk1/2) (Thr202/Tyr204)) or total ERK (tERK (p44/42 MAPK (Erk1/2)) (Cell signaling) diluted 1:1000 in Tris Buffered Saline (TBS) containing 0.1% Tween20 (1 × TBST) supplemented with 5% BSA at 4 °C overnight. The membrane was washed (3 × 10 min, TBST) and incubated with secondary goat anti-rabbit IgG 800CW antibody (1:5000 in 1 × TBST with 5% BSA) for 1 h, at RT. After washing (3 × 10 min, TBST), the membrane was dried on paper towels and wrapped in aluminium foil to protect it from light. Images of the membrane were acquired using the Odyssey Fc Imaging System (LI-COR). Images were quantified using Image Studio™ (LI-COR).

3.7.2 Luciferase assay

Luciferase assay determines the changes in expression of a target gene using a firefly luciferase as a reporter protein. When the protein of interest activates the expression of a target gene, the luciferase is produced. Upon addition of the substrate, the reaction results in light emission. The expression level of luciferase reflects the activation induced by the receptor construct in question (Mathiasen et al., 2020).

Receptor signaling was determined using a trans-reporting luciferase assay on HEK-293 cells or on CRISPR/Cas9 genetically engineered HEK-293A cells depleted of different G proteins (pan KO HEK-293A cells) and on parental HEK-293A cells. Cells were seeded in poly-D-lysine coated white 96-well plate at 35,000 cells/well. The next day, the cells were transiently transfected with receptor construct at 0, 5, 10, 20, 30, 40, 50 ng/well concentrations and co-transfected with transcription the reporter plasmids CRE-Luc, NFAT-Luc or NF- κ B-Luc at 30 ng/well using Lipofectamine™ 2000. Additional co-transfection with 30 ng/well $G\alpha_{\Delta 6qi4myr}$, which is recognized by GPCRs as a $G\alpha_i$ protein but elicits $G\alpha_q$ -dependent signaling (Kostenis et al., 2005), was performed in CRE and co-transfection with $G\alpha_q$ or $G\alpha_{11}$ was performed in NFAT luciferase assay. After 24 h, cells were washed with PBS and incubated for 30 min with a mixture of

SteadyLite (50 µL/well, PerkinElmer) and PBS (50 µL/well). The plate was read on an EnVision Multilable Plate Reader (PerkinElmer) using the luciferase program. The experiment was performed three times in three biological replicates.

3.8 METHODS TO ANALYSE THE IMMUNOEVASIVE ROLE OF RECEPTORS

3.8.1 Flow cytometry analysis

Flow cytometry is a widely used method that allows the analysis at the single cell level. In this system, cell suspension is passed through a fluid stream through detectors, measuring the physical or chemical properties of the cell. Fluorophores can be added to the cells in the form of antibodies or dyes or can be expressed on the cellular molecules. Lasers in the instrument are used to excite the fluorophores at specific wavelengths, resulting in light emission and detection by detectors that provide quantitative information about each cell.

Flow cytometry was used here to measure and compare the fluorescence intensity of MHC-I molecules on the surface of BILF1 transfected and non-transfected cells as controls. HEK-293 cells were seeded in a 6-well plate and transfected using FuGeneHD reagent. 48 h after transfection, cells were washed, trypsinized, and re-suspended in 10 ml PBS. 5×10^5 cells/sample in 100 µL were transferred to a tube and stained using 5 µL/100 µL APC-labelled anti human HLA-A,B,C (W6/32) antibody (Biolegend). Receptors were detected using 1 µL/100 µL anti-FLAG FITC conjugated antibodies (Genscript) and 5 µL/100 µL isotype controls were used to differentiate non-specific background signal from specific antibody signals. After 1 h of staining, samples were washed and finally re-suspended in 200 µL of PBS. Samples were analysed on a BD FACSCanto™ II instrument equipped with 488 nm and 633 nm lasers using FITC (530/30) and APC (660/20) filters. Data were analysed using Kaluza software. First, singlets were gated using FSC-H (height) and FSC-A (area) detector parameters. On the selected population of single cells, the FITC-positive cells and FITC-negative cells were selected, and the amount of transfected cells was determined. For both populations, the geometric mean of APC-A was determined, which represents the

MHC-I expression. The measurements were performed at the Institute of Josef Stefan, Ljubljana, Slovenia and the Institute of Immunology and Immunotherapy, University of Birmingham, Birmingham, United Kingdom.

3.8.2 Microscopy-based approach observing MHC-I downregulation

To specifically determine the expression of MHC-I molecules on the surface of BILF1 transfected and non-transfected cells and to avoid the low transfection efficiency observed for PLHV1-3 BILFs, a new microscopy-based method was applied, allowing the study of MHC-I downregulation on a single cell. Cells were seeded, transfected, and fixed as described above (Section 3.3.2). Non-specific background staining was reduced with 500 μ L/well of 10% BSA in PBS/CaCl₂ for 20 min. Cells were incubated with 250 μ L/well primary rabbit anti-FLAG antibody (Sigma-Aldrich) at a concentration of 2 μ g/mL and mouse anti human HLA-A, B, C class I antibody (1:100) in HEK-293 cells (Santa Cruz) or mouse anti-pig SLA class I antibody (1:100) for PK-15 cells (R&D systems) for 1 h, at RT. Following three washes with 500 μ L/well PBS/CaCl₂, cells were incubated with 250 μ L/well of secondary goat anti-rabbit Alexa Fluor 647 antibody and goat anti-mouse Alexa Fluor 555 antibody at a ratio of 1:500 in PBS for 1 h, at RT. For the last 10 min of the incubation, 20 μ L WGA conjugated to Alexa488 (Invitrogen) was added to the cells as a membrane marker (5 μ g/mL). Following two washing steps, cells were incubated with 500 μ L/well PBS containing Hoechst 33342 stain (Invitrogen) (1 μ g/mL). Before imaging on a fluorescence microscope (LSM700), cells were mounted with 8 μ L of Fluorescence mounting medium (Dako). Equivalent numbers of transfected and non-transfected cells were blindly selected and the intensity of 555 channel (MHC-I) was measured using FIJI software.

3.9 HOMOLOGY MODELLING OF MHC-I MOLECULES

To compare the sequences of human and porcine MHC-I molecules, two entries from the protein data bank were compared: 3BO8 (human) (<https://www.rcsb.org/structure/3bo8>) and 5NPZ (porcine) (<https://www.rcsb.org/structure/5NPZ>).

3.10 ANALYSIS OF SAMPLE MATERIAL FROM PTLD DISEASED PIGS

Previous studies by Huang et al. showed the development of PTLD in pigs which mimics the clinical phenotype of human PTLD (Huang et al., 2001). This led to a proposal of a porcine model to study this disease. To determine the involvement of PLHV viruses and BILF1 receptors in this disease, viral and BILF1 expression was determined in the samples from these PTLD diseased animals using Illumina sequencing and real-time polymerase chain reaction (RT-qPCR) approaches, respectively.

3.10.1 Sample material from PTLD diseased pigs

Porcine tissue samples were used to investigate the expression levels of PLHV1-3 BILF1 during the PTLD development. They were obtained from *in vivo* experiments described in previously published studies (Huang et al., 2001, Cho et al., 2004, Cho et al., 2007, Matar et al., 2015). The animals were derived from an MHC-defined miniature swine herd (Massachusetts General Hospital). Two days prior to cytokine-mobilized peripheral blood cell transplantation, all animals received 1000cGy thymic irradiation (TI) and 0.05 mg/kg pCD3-CRM9 (Huang et al., 1999). One day before transplantation, oral administration cyclosporine (Neoral) started at a dose of 15 mg/kg and continued for 30–60 days (or until death). Samples were either collected at the time of the transplantation and after the onset of PTLD disease (n = 3), or only after disease onset (n = 2). As a control, a sample from a pig without signs of disease was used.

3.10.2 Sequencing of PLHV infected pig samples and competitive alignment

To determine PLHV1-3 infection in porcine PTLD sample material, sequencing followed by competitive alignment was performed. Library preparation is the first step in next generation sequencing technology. First, fragmentation of DNA or RNA sample material and subsequent attachment of universal adapters to each end of the studied

template allows the recognition of sequences by covalently bound oligonucleotides located in the flow cell complementary to the adaptors. After the amplification of the fragments, the adaptors are ligated to each end of the fragment. Synthetic adaptors consist of read 1 or read 2 sequencing primer binding sites, which allows paired end sequencing of the region of interest, index 1 or index 2 or adaptor bar codes, and P5 or P7 adaptor oligonucleotides that are homologous to the oligonucleotides on the surface of the flow cell. The successful ligation of the DNA or RNA fragment with the adaptors allows on surface template amplification followed by sequencing by synthesis (SBD). SBD is a method that detects each nucleotide incorporated at X–Y coordinate based on the emission spectra emitted from each of four fluorescently labelled nucleotides in real time (Levy and Boone, 2019, McCombie et al., 2019).

For our study, the DNA extracted from PTLD diseased pigs (n = 4) described above was used to prepare sequencing libraries. Sequencing libraries were prepared using the NEBNext Ultra II DNA Library Prep Kit for Illumina (New England Biolabs), according to the manufacturer's instructions. Subsequently, libraries were multiplexed and sequenced using a 300-cycle mid-output kit (2×150 paired-end mode) on a NextSeq 550 device (Illumina Technologies).

Sequence-read datasets obtained with Illumina sequencing were quality and adapter trimmed using TrimGalore (https://www.bioinformatics.babraham.ac.uk/projects/trim_galore/) prior to competitive alignment. FASTA files containing the *Sus scrofa* (Sscrofa11.1) genome and partial genome sequences for PLHV1 (NC_038264.1), PLHV2 (NC_038265.1), and PLHV3 (AY170316) were merged to acquire a hybrid reference genome and use for competitive alignment. Sequence read datasets from Illumina sequencing were aligned against the hybrid genome using bbmap (<https://sourceforge.net/projects/bbmap/>) with `minid=0.9` and `ambiguous=random` before post-processing with SAMtools (Li et al., 2009) and BEDtools (Quinlan and Hall, 2010). Coverage plots were generated using the R 4.0 bioconductor packages Gviz (Hahne and Ivanek, 2016) and GenomicFeatures (Lawrence et al., 2013). Sequencing was performed by collaboration partner Daniel P. Depledge from University School of Medicine, Department of Medicine, New York, USA.

3.10.3 Real-time polymerase chain reaction

RT-qPCR was used to confirm the expression of PLHV1-3 BILF1 receptors in porcine samples. Customized TaqMan[®] gene expression assay probes (Thermo Fischer Scientific), designed for the specific detection of PLHV1-BILF1 ensured the specificity of the assay. The general principle of the method relies on the use of TaqMan[®] probe labelled with FAM[™] dye and two unlabelled oligonucleotide primers. The probe consists of fluorescent reporter FAM[™] at the 5' terminal end and non-fluorescent quencher at the 3' terminal end. When in close proximity, the quencher silences the excitation and fluorescence from the FAM reporter. During the extension cycle, the nuclease activity of Taq polymerase cleaves the FAM reporter from the rest of the probe, resulting in an increased fluorescent signal specific to the amount of DNA or RNA being examined.

To perform RT-qPCR, QIAzol[®] lysis reagent (Qiagen) was used to extract RNA from 5 porcine samples. Furthermore, cDNA was prepared from 500 ng RNA using Superscript III reverse transcriptase (Thermo Fischer Scientific). RT-qPCR was performed on 96-well using TaqMan[®] Fast Advanced Master mix (2 ×) (Thermo Fischer Scientific) and customized TaqMan[®] gene expression assay probes (Thermo Fischer Scientific), designed for specific detection of PLHV1-BILF1 (fwd primer: 5'TCTGATACTCACTGTTGCTAACTTTGTT3', rev primer: 5'ACTTATAGCTTGGCGACACTTGAA3', probe: 5'FAM-ACCTTCAAAGCTCAAAGTAGT-MGB3'), PLHV2-BILF1 (fwd primer: 5'GCTGTTGCTAACTTTCTTAGTTTTGGA3', rev primer: 5'ACTTATACCTTGGCGACACTTGAAG3', probe: 5'FAM-CCTTCAAAGCTCAATACAGC-MGB3'), PLHV3-BILF1 (fwd primer: 5'GTCTTTTGGCAGTTGTTGCTAATCT3', rev primer: 5'ACTTGTAGCCTGGCGACATT3', probe: 5'FAM-CAAGTGCAGCATAATTC-MGB3') and a reference gene RPL4 (Nygard et al., 2007) (assay identification number: Ss03374063_g1). Assay was performed on a QuantStudio 6 Flex Real-Time PCR system (Thermo Fisher Scientific) using a standard protocol, and Ct (cycle threshold) values were acquired using QuantStudio Real-Time PCR software. The relative fold change of cDNA levels in comparison to a reference gene (RPL4) was presented using the $2^{\Delta Ct}$ calculation.

3.11 DATA ANALYSIS AND NORMALISATION OF CURVES

Data were analysed using Graph Pad Prism (8.3.0), Kaluza analysis software, or FIJI software and are reported as mean \pm SEM (standard error of the mean). For all microscopy experiments, images were visualized using an LSM700 microscope and ZEN blue software. Statistical analysis was performed with Graph Pad Prism. ANOVA or Student t-test were chosen based on data distribution. Specifics of statistical tests are described in the figure legends. P value < 0.05 was considered statistically significant.

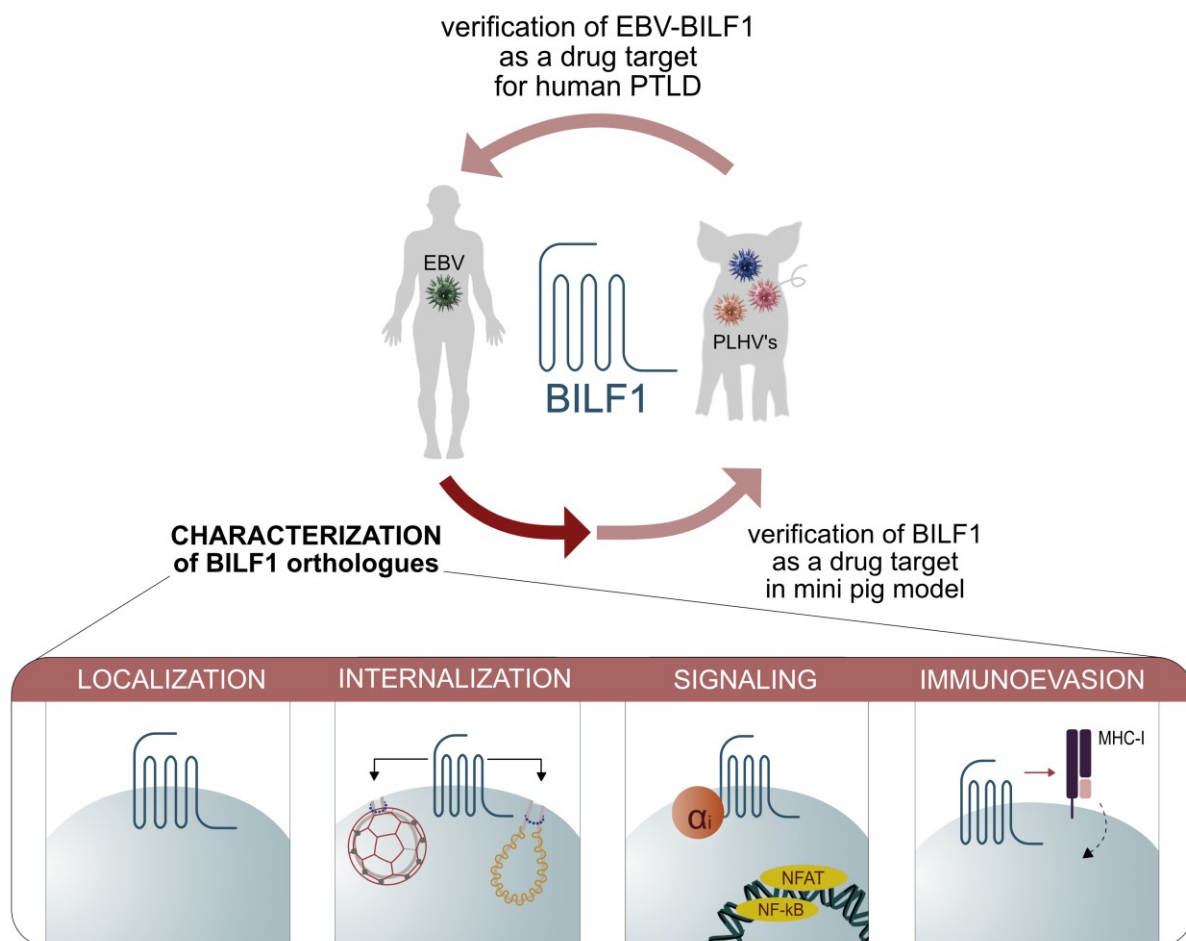


Figure 11: The aim of the thesis and presentation of the four main topics studied.

Slika 11: Namen doktorske disertacije s predstavljenimi štirimi glavnimi področji opravljenih raziskav.

4 RESULTS

4.1 BILF1 RECEPTOR LOCALIZATION

Previous studies on different cell lines (e.g., HEK-293 and human melanoma (MJS) cells) have reported high cell surface expression of EBV-BILF1 (Paulsen et al., 2005, Zuo et al., 2009). Therefore, a comparison of the cellular localization between EBV and PLHV1-3 encoded BILF1 receptors was performed in human HEK-293 cells and in a porcine PK-15 cells. For this purpose, the receptors were N-terminally tagged with a FLAG tag.

Cell-based ELISA was used to quantify the cell surface expression levels of the BILF1 receptors (Figure 12A, B). Increasing concentrations of BILF1 receptor DNA transfected in both HEK-293 (Figure 12A) and PK-15 (Figure 12B) cells resulted in increased expression of all BILF1 receptors on non-permeabilized cells, confirming conserved cell surface expression in a dose-dependent manner. PLHV1-BILF1, PLHV2-BILF1, and PLHV3-BILF1 showed 58%, 78%, and 83% lower expression, respectively compared to EBV-BILF1 (normalized as 100%) in HEK-293 cells. In PK-15 cells, higher receptor DNA concentrations were needed to obtain similar cell surface expression levels as in HEK-293 cells. Again comparing the surface expression to EBV-BILF1 (100%), the expression of PLHV1-BILF1, PLHV2-BILF1, and PLHV3-BILF1 was 44%, 27%, and 78% lower, respectively and therefore showed a lower expression differences between receptors (Figure 12B).

Furthermore, the cellular distribution of the BILF1 receptors in both HEK-293 and PK-15 cells was determined using fluorescence microscopy. The cell surface expression of the receptors shown by cell-based ELISA was confirmed by co-localization between plasma membrane marker WGA and the receptors. As shown in Figure 12C, D, EBV-BILF1 and PLHV1-3 BILF1 receptors showed co-localization with WGA at the plasma membrane, confirming the predominant cell surface expression for all BILF1 receptors in both HEK-293 (Figure 12C) and PK-15 (Figure 12D) cells.

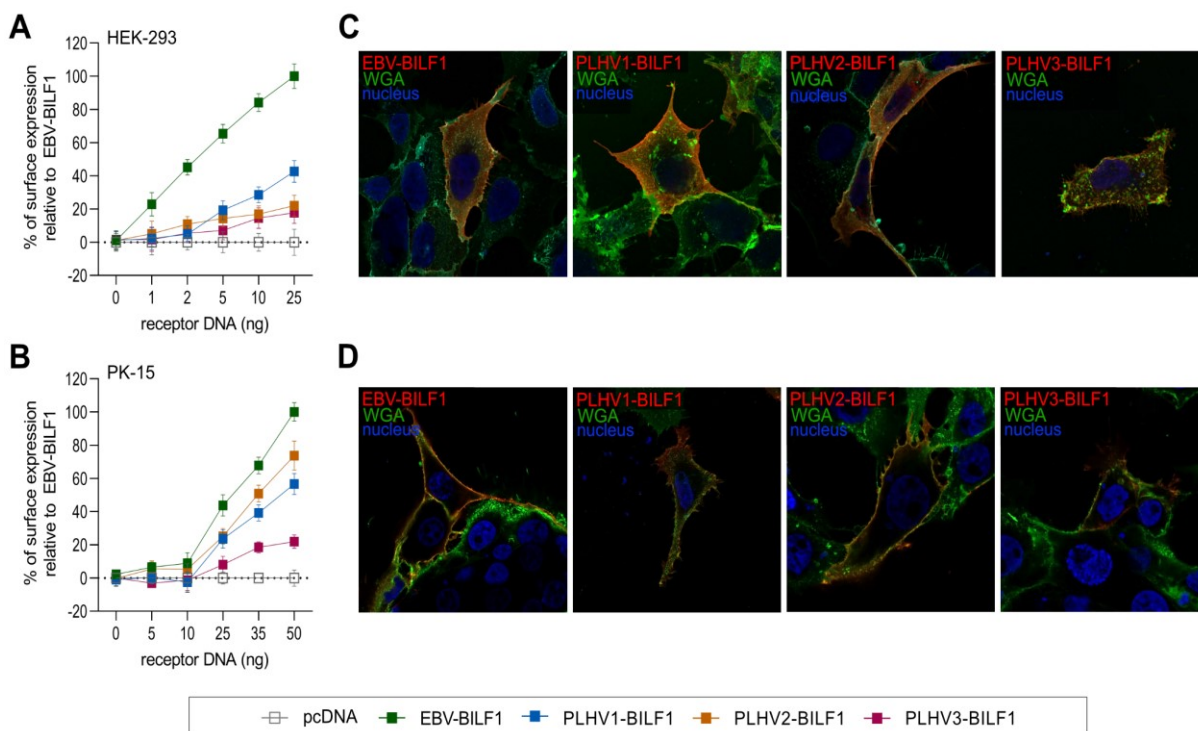


Figure 12: Cellular localization of the BILF1 receptors.

Slika 12: Celična lokalizacija receptorjev BILF1.

Graphs represent surface expression of BILF1 receptors in A) HEK-293 and B) PK-15 cells transfected with increasing BILF1 DNA concentrations and detected using cell-based ELISA. (Values are mean \pm SEM; n = 3). C) and D) show representative microscopy images of C) HEK-293- and D) PK-15 cells.

4.2 CHARACTERIZATION OF BILF1-MEDIATED TRAFFICKING AND ENDOCYTOTIC PATHWAYS

4.2.1 Constitutive internalization properties of BILF1 receptors

As described previously, no ligand that would bind to and activate EBV-BILF1 is known; however, a constitutive activity and internalization of the receptor in HEK-293 cells has been described (Paulsen et al., 2005, Spiess et al., 2015a). Different methods are available to study receptor internalization. Initially, a well-established antibody-feeding based method (Figure 13) was employed (Fraile-Ramos et al., 2003, Arancibia-Cárcamo et al., 2006, Jacobsen et al., 2017) to i) show the decline of BILF1 surface expression over time (Figure 13A) and ii) to visualize cellular localization pattern of the receptors over time (Figure 13B, C). Using cell-based ELISA antibody feeding approach in HEK-293 cells, changes in BILF1 receptor surface expression were

quantified after inducing the internalization with a temperature shift (the principal is described in materials and methods, Section 3.4.1). As controls, an empty vector and CXCR4 receptor were included. A chemokine receptor CXCR4 internalizes either constitutively or in a ligand-dependent manner. A comparable constitutive internalization for EBV-BILF1, PLHV1-BILF1, and PLHV2-BILF1 was observed, with an approximately 20% decrease of labelled receptor expression at the cell surface after 30 min. This was comparable with the constitutive internalization rate of CXCR4 (Figure 13A), in contrast to CXCL12-induced CXCR4 internalization, where ~25% of surface expressed receptors were internalized after 30 min. In the same period, only 8% of the PLHV3-BILF1 receptor internalized, showing a slower internalization dynamic for this BILF1 receptor (Figure 13A). Furthermore, a microscopy approach was used to visualize the receptor localization after inducing receptor internalization ($t = 30$ min) in both HEK-293 (Figure 13B) and PK-15 (Figure 13C) cells. To control the initial cell surface localization of the receptors in these experiments, one sample replicate was fixed prior receptor internalization ($t = 0$). At this time point, receptor surface expression comparable to the one described for the microscopy expression studies (Section 4.1) was observed. After exposing the cells to 37 °C and thereby initiating the internalization, all BILF1 receptors showed a comparable distribution within the cell, where fractions of the BILF1 receptors were located at the perinuclear endocytic vesicular site (red) in both HEK-293 (Figure 13B) and PK-15 cells (Figure 13C). However, the majority of the receptors were still expressed at the cell surface (green), which supported the observation from cell-based ELISA antibody feeding experiments.

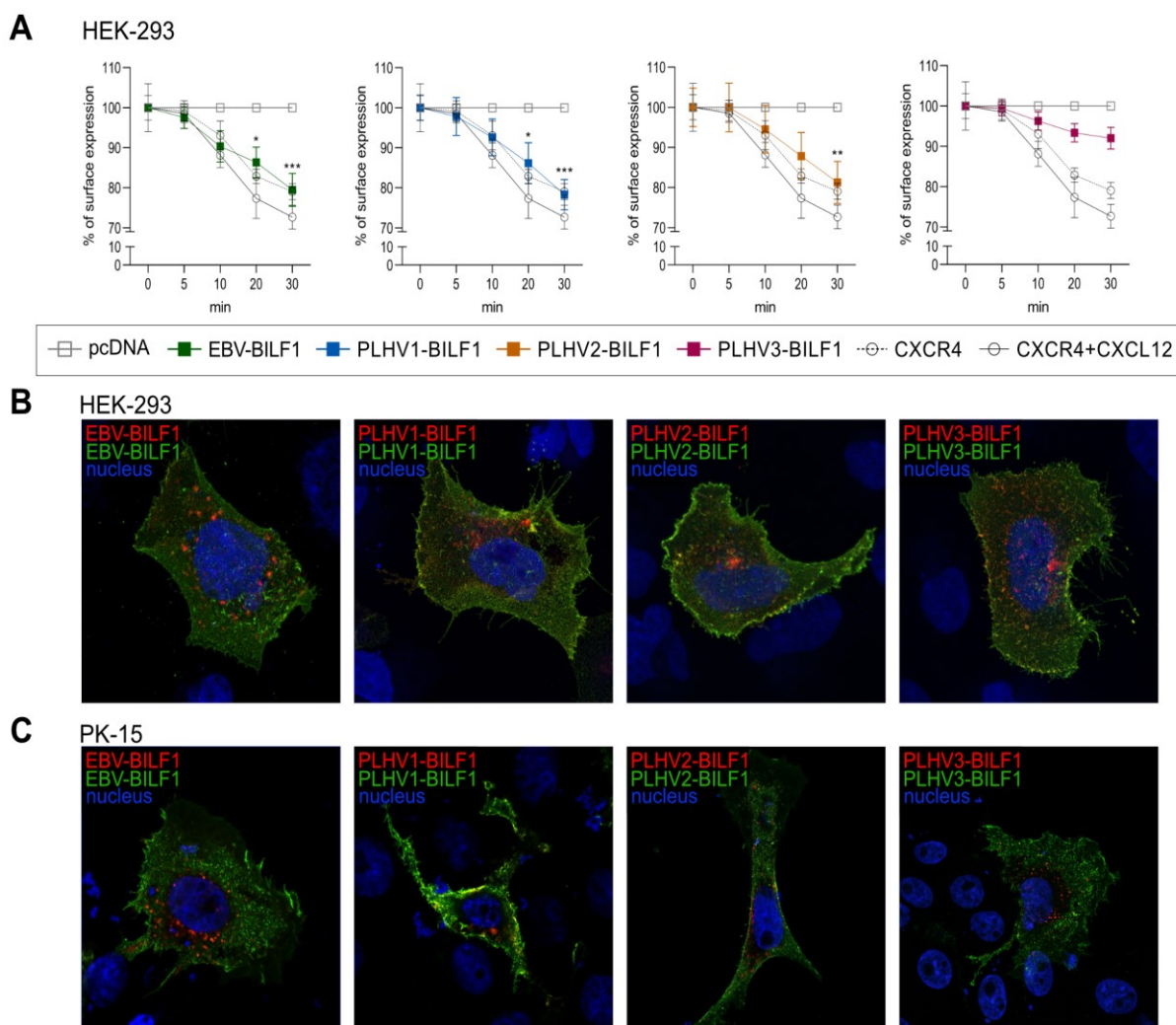


Figure 13: Constitutive internalization of BILF1 receptors studied by antibody feeding approach.
Slika 13: Konstitutivna internalizacija receptorjev BILF1, proučevana s pristopom, ki obravnava od temperature odvisno endocitozo receptorjev v različnih časovnih intervalih (iz angl. “antibody feeding” approach).

A) The decline of receptor surface expression over time was measured with an antibody-feeding ELISA approach. A positive control GPCR CXCR4 was additionally activated with 10 μ M CXCL12. Values are means \pm SEM, (n = 3). Statistics were performed by 2-way ANOVA using GraphPad Prism. * P < 0.05; ** P < 0.01; *** P < 0.001. B) (HEK-293 cells) and C) (PK-15 cells) show representative microscopy pictures of an antibody-feeding microscopy study, after 30 min of BILF1 internalization. Receptors expressed at the cell surface are labelled with green (Alexa488) antibody and internalized receptors are labelled with red (Alexa594) antibody. Hoechst 33342 was used to stain the nucleus (blue). Images were taken with 63 \times oil immersion plan-apochromat objective on LSM700 (Zeiss).

A novel FRET-based real-time internalization assay was used as a second approach, with the advantage of measuring receptor internalization dynamics at 37 $^{\circ}$ C in living cells. The curves shown on Figure 14 represent the donor emission/acceptor emission ratio measured and calculated every 4 min for 88 min total. First, two experiments were

performed in parallel with different temperature conditions during the SNAP-Lumi4Tb donor labelling step. Donor labelling performed at 4 °C (experiment A) prevented the receptor internalization and recycling during this step; therefore, only surface expressed receptors were labelled with the donor molecule. In the second experiment (experiment B), donor labelling at 37 °C allowed receptor cycling into the cell, which resulted in labelling of all BILF1 receptors. Cells from both experiments were then washed, and receptor internalization was measured in the presence of acceptor molecules. In the experiment A, the internalization during the measurement at 37 °C increased, corresponding to the constitutive internalization of all the labelled receptors, previously restrained at the cell surface by the 4 °C incubation. In contrast, the internalization from the experiment B resulted in a small internalization curve because the internalization/recycling of labelled receptors had reached the equilibrium prior the measurement.

The level of receptor internalization was quantified and compared by measuring the area under curve (AUC) for each BILF1 receptor (Sundqvist et al., 2020), using the internalization curves from experiment A (donor labelling performed at 4 °C) (Figure 15). As shown in Figure 15, PLHV1-3-BILF1, showed 28%, 35% and 80% lower AUC, respectively compared to the control EBV-BILF1 (100%) in HEK-293A cells and 53%, 64%, and 101% lower AUC, respectively, compared to EBV-BILF1 (100%) in PK-15 cells. Furthermore, calculating half-time ($t_{1/2}$) for BILF1 receptors we demonstrated the fastest constitutive internalization for EBV-BILF1 in HEK-293A (20 min) and PK-15 cells (17 min). PLHV1 and PLHV2-BILF1 showed slower constitutive internalization in HEK-293A cells with half-times of 37 min and 45 min compared to PK-15 cells for which the half-time reached 23 min and 25 min. In contrast, PLHV3 showed faster constitutive internalization in HEK-293A cells (20 min) compared to PK-15 cells (38 min). However, it is noteworthy that PLHV3-BILF1 constitutive internalization was very low in both cell lines and thus complicated data interpretation.

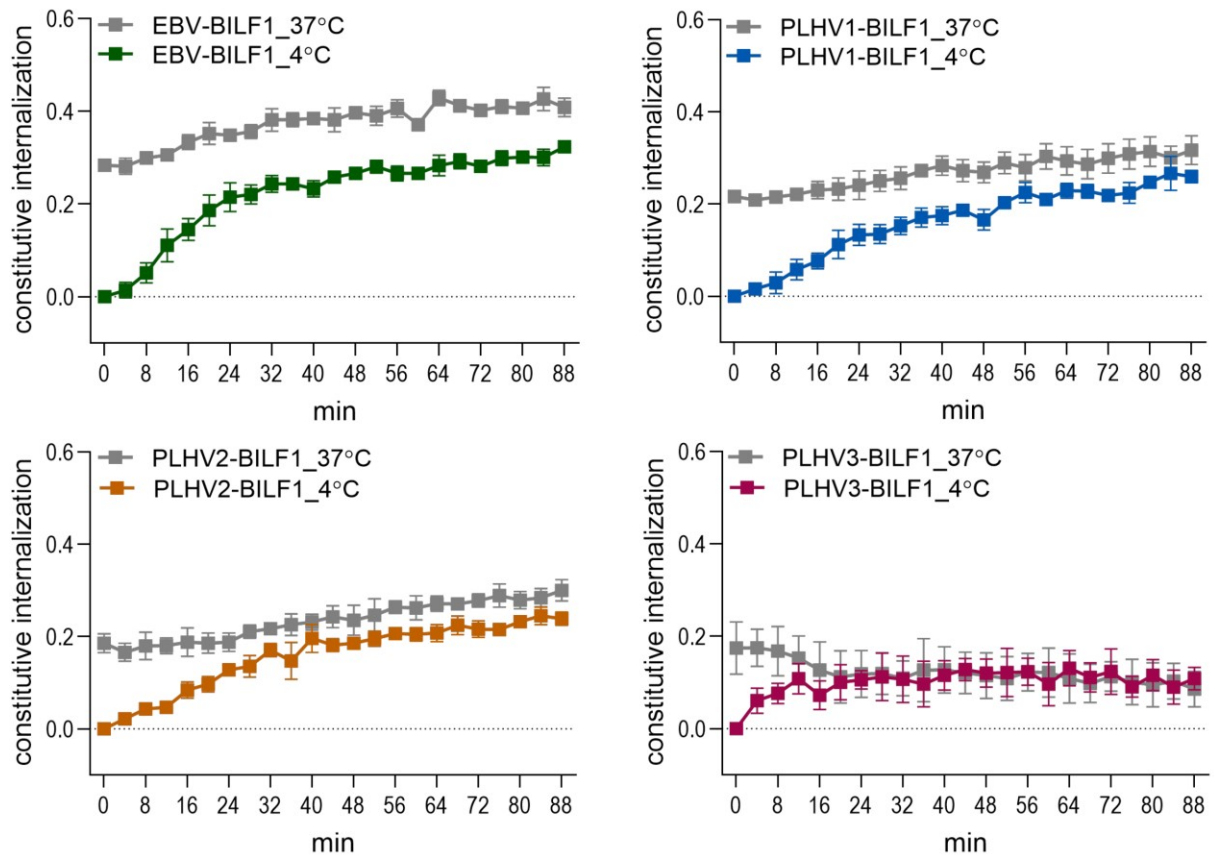


Figure 14: Constitutive internalization of BILF1 receptors studied by FRET-based real-time internalization assay.

Slika 14: Konstitutivna internalizacija receptorjev BILF1, proučevana s testom internalizacije v realnem času, ki temelji na tehnologiji FRET.

SNAP-tagged BILF1 receptors were expressed in HEK-293A cells. Labelling with Snap-Lumi4Tb donor was performed at 4 °C (coloured curves) and 37 °C (grey curves) and the internalization was measured at 37 °C in living cells. Graphs represent means \pm SEM, (n = 3).

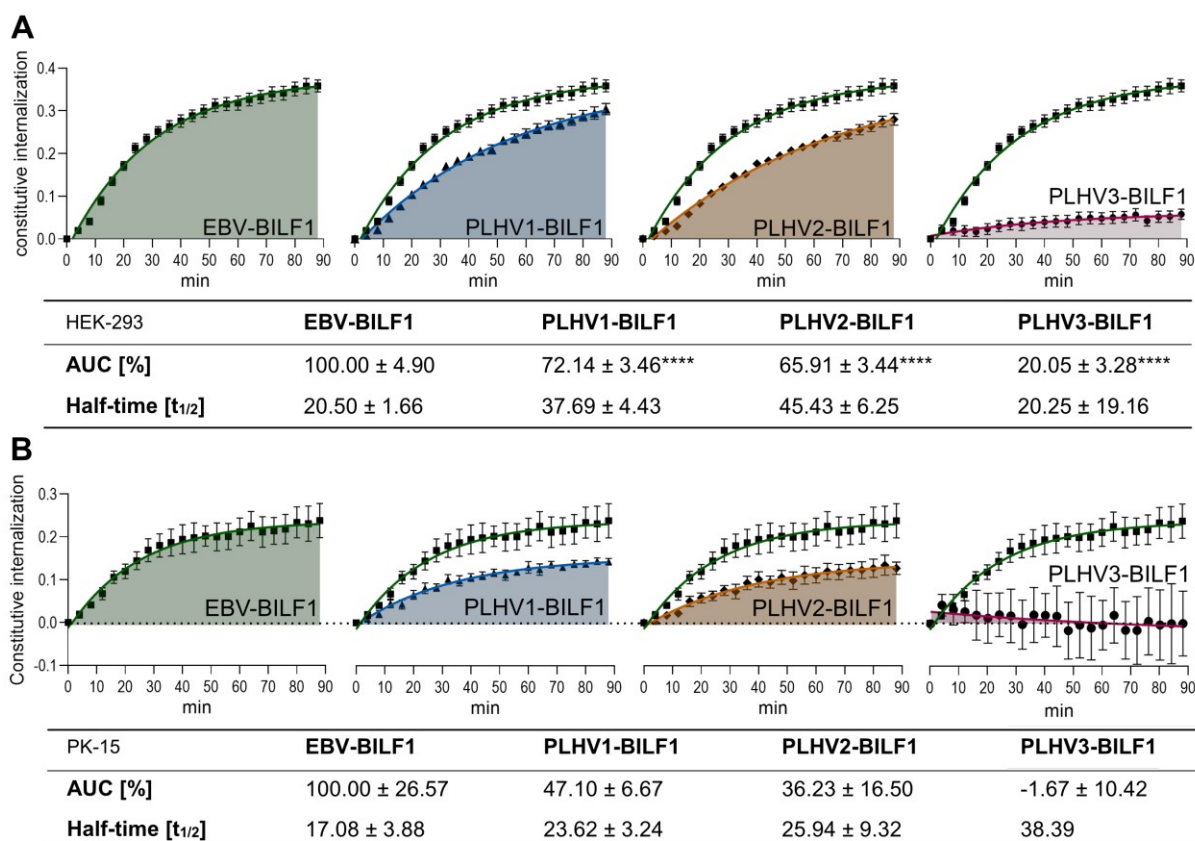


Figure 15: Kinetic parameters of BILF1 receptor constitutive internalization.

Slika 15: Kinetični parametri konstitutivne internalizacije receptorjev BILF1.

SNAP-EBV-BILF1 (■; green), SNAP-PLHV1-BILF1 (▲; blue), SNAP-PLHV2-BILF1 (◆; orange) and SNAP-PLHV3-BILF1 (●; purple) were expressed in A) HEK-293A and B) PK-15 cells. Internalization data was fitted using non-linear regression curves. AUC values and half-time ($t_{1/2}$) were determined by one-phase association analysis. Data are shown as mean ± SEM, (n = 3). Statistical differences were determined with Dunnett's multiple comparisons one-way ANOVA test. **** $P < 0.0001$.

4.2.2 Effect of dominant negative mutant Dyn K44A on BILF1 mediated endocytosis

HEK-293A cells expressing SNAP-tagged BILF1 receptors were additionally co-transfected with increasing concentrations of the Dyn K44A (3, 7 and 11 ng/well). As controls, an empty vector FRT (grey curve) and cells only expressing SNAP-tagged BILF1 receptors (0 ng/well of Dyn K44A; coloured curve) were used. The constitutive internalization of the BILF1 receptors decreased in the presence of Dyn K44A (Figure 16A). The AUC was used to quantify and compare the internalization of BILF1 receptors affected by the different concentrations of Dyn K44A (Figure 16B). Results were normalized to each BILF1 receptor in the absence of Dyn K44A (designated as 100%). For all BILF1 receptors, the addition of 11 ng Dyn K44A showed the highest

effect on the receptor internalization, with a decrease in AUC for 69% (EBV-BILF1), 60% (PLHV1-BILF1), 72% (PLHV2-BILF1) and 40% (PLHV3-BILF1) (Figure 16B). The internalization of EBV-BILF1 and PLHV2-BILF1 decreased significantly in response to 3 and 7 ng Dyn K44A, with 53–57% (3 ng Dyn K44A) and 33–42% (7 ng Dyn K44A) lower AUC. PLHV1-BILF1, in contrast, showed only moderate response to the addition of 3 and 7 ng Dyn K44A. As shown on Figure 16A, B, PLHV3-BILF1 internalization was very low; therefore, it was difficult to investigate the AUC for this receptor. Moreover, as shown in Figure 16C, cell surface expression of BILF1 receptors increased in the presence of Dyn K44A in a dose-dependent manner, demonstrating that the Dyn K44A dependent inhibition resulted in retention of the EBV, PLHV1 and PLHV2 BILF1 receptors at the cell surface. In contrast, PLHV3-BILF1 did not show any difference in receptor expression when co-transfected with Dyn K44A. Taken together, these results showed the importance of dynamin-1 for the endocytic trafficking of four BILF1 receptors.

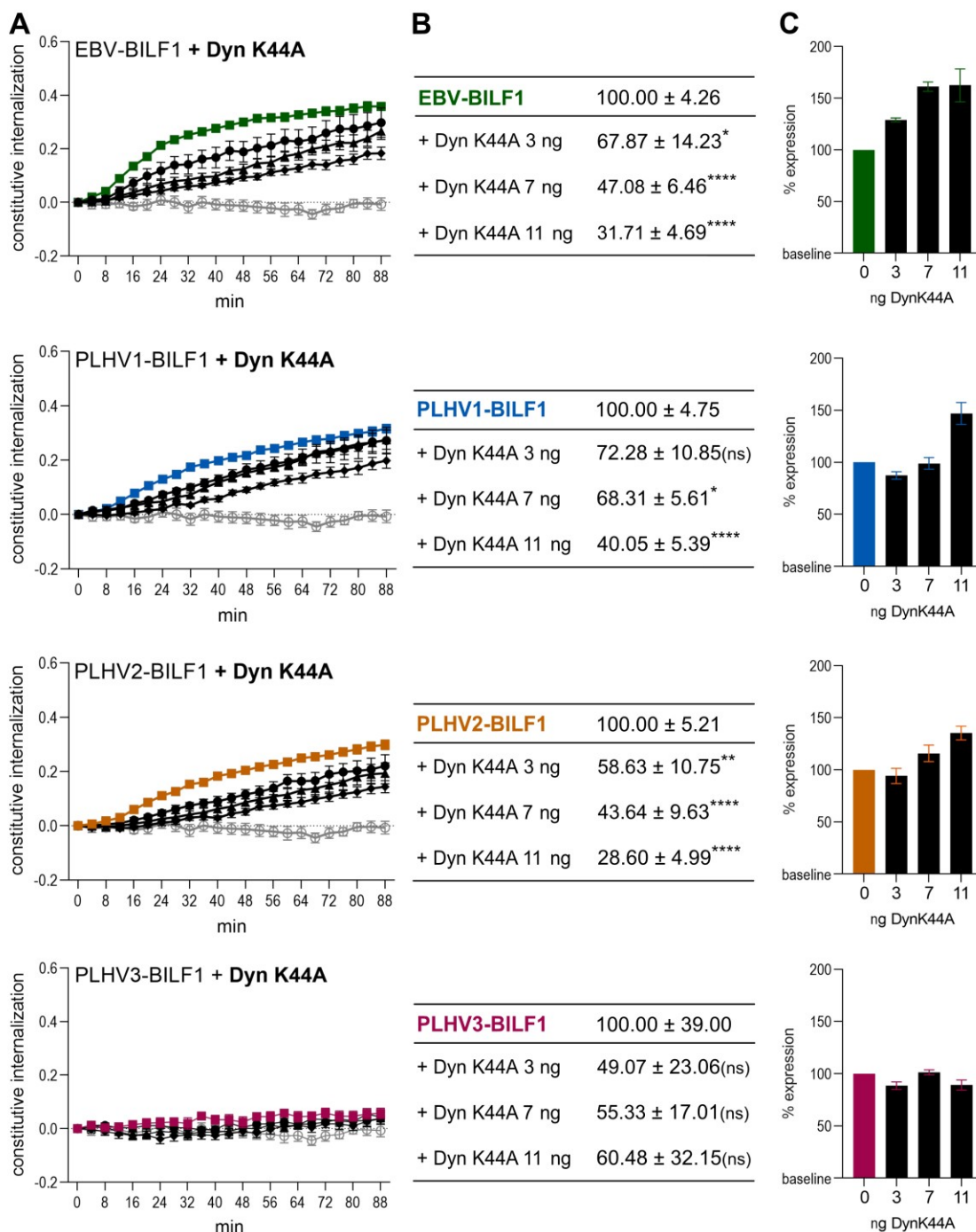


Figure 16: Effect of dominant negative mutant Dyn K44A on BILF1-mediated endocytosis.

Slika 16: Vpliv dominantno negativne mutante Dyn K44A na endocitozo receptorjev BILF1.

A) In HEK-293A cells, SNAP-tagged BILF1 receptors (coloured) and empty vector (grey) were co-transfected with different concentrations of Dyn K44A DNM (—●— 3ng; —▲— 7ng; —◆— 11ng). FRET was measured at 37 °C every 4 min for total of 88 min. Curves represent the ratio between donor and acceptor. B) The area under curve (AUC) parameter was calculated for each curve on Figure 16A and was normalized to each BILF1 AUC in the absence of Dyn K44A (0ng). Data are shown as mean ± SEM, (n = 3). Statistical differences were determined with Dunnett's multiple comparisons two-way ANOVA test. **P* < 0.05, ***P* < 0.01, *****P* < 0.0001. C) The BILF1 receptor surface expression in cell co-transfected with Dyn K44A construct is normalized to BILF1 receptor expression in cells without Dyn K44A expression.

4.2.3 Effect of chemical inhibitor Pitstop2 on clathrin-mediated endocytosis of BILF1 receptors

As a next step, clathrin-mediated endocytosis was blocked by using the chemical inhibitor Pitstop2 (Figure 17). The effect after treatment with Pitstop2 on EBV-BILF1-, PLHV1-BILF1-, and PLHV2-BILF1-mediated internalization was ~49–58%, comparing the AUC in the presence and absence of the inhibitor. PLHV3-BILF1 showed a milder only 20% effect of Pitstop2.

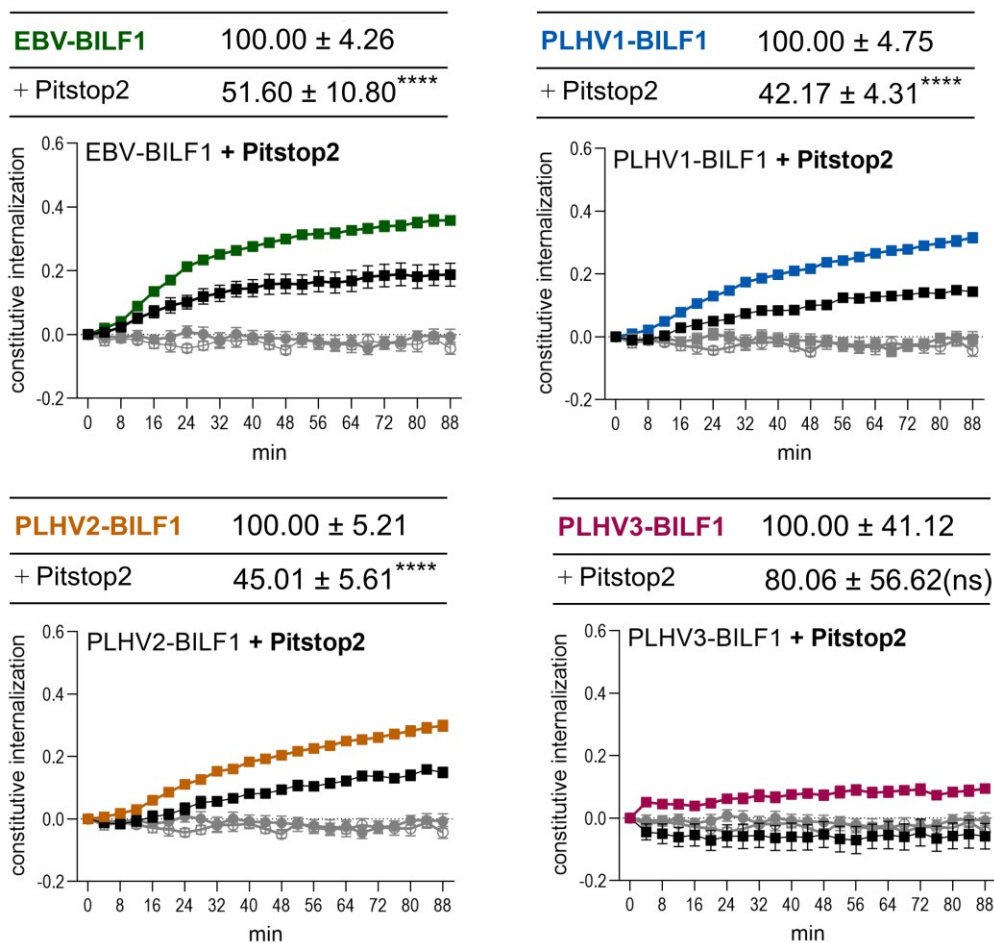


Figure 17: Effect of chemical inhibitor Pitstop2 on BILF1-mediated endocytosis.

Slika 17: Vpliv kemičnega inhibitorja Pitstop2 na endocitozo receptorjev BILF1.

SNAP-tagged BILF1 receptors (coloured) and empty vector (grey) were expressed in HEK-293A cells. Donor labelling with SnapLumi4-Tb was performed at 4 °C, preventing any internalization prior to the measurement. Prior to internalization measurement, 10 µL of 5 µM Pitstop2 or internalization buffer (control) was added to the cells. FRET was measured at 37 °C every 4 min for total of 88 min. Graph curves represent the ratios between donor and acceptor. Tables above graphs show area under curve (AUC) parameter, which was calculated for each curve on graphs and was normalized to each BILF1 AUC in the absence of Pitstop2 (control). Data are shown as mean ± SEM, (n = 3). Statistical differences were determined by Dunnett's multiple comparisons two-way ANOVA test. *****P* < 0.0001.

4.2.4 The involvement of β -arrestin 1 and 2 in clathrin-mediated BILF1 endocytosis

Studies on HCMV-US28 showed the ability of the receptor to mediate endocytosis through clathrin pits independently of β -arrestin (Fraile-Ramos et al., 2003). Therefore, BILF1-mediated internalization was investigated in CRISPR/Cas9-modified $\Delta\beta$ -arr1/2 KO HEK-293A cells and was compared to the internalization in HEK-293A cells (parental). As shown in Figure 18, all BILF1 receptors showed β -arrestin-independent internalization (outlined by both curves overlapping). EBV-BILF1 endocytosis appeared to be increased in $\Delta\beta$ -arr1/2 KO cells, but this was not significant.

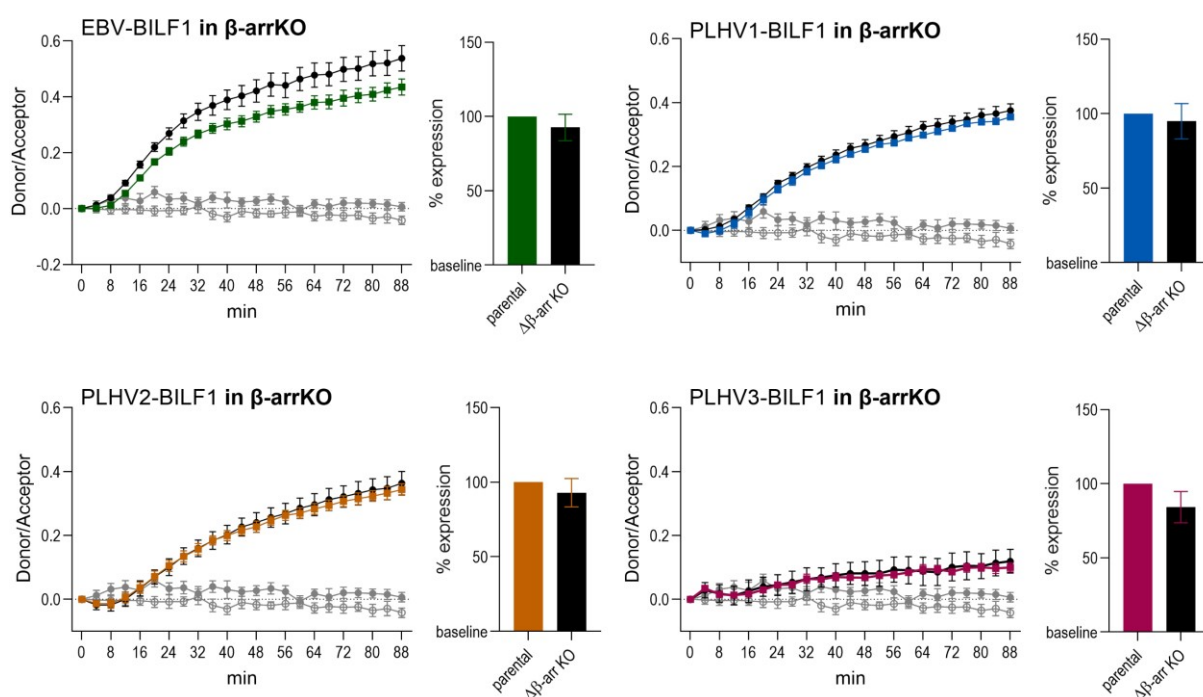


Figure 18: The involvement of β -arrestin in BILF1-mediated endocytosis.

Slika 18: Vloga arestina β pri endocitozi receptorjev BILF1.

SNAP-tagged BILF1 receptor constructs were expressed in β -arrestin 1/2 knock out HEK-293A cells ($\Delta\beta$ -arr1/2 KO) and parental HEK-293A cells (parental). FRET was measured at 37 °C every 4 min for a total of 88 min. Curves represent the ratios between donor and acceptor. Bar diagrams represent BILF1 receptor surface expression in $\Delta\beta$ -arr1/2 KO normalized to receptor expression in parental cells. Results are presented as mean \pm SEM, (n = 3).

The findings were supported using BRET2 recruitment experiments to further exclude the ability of the BILF1 receptors to recruit β -arrestin 2 (Figure 19). A so-called “bystander” BRET was observed, meaning that only random interactions between the

receptor and β -arr2 occurred. These results were comparable with the control experiments, looking at the recruitment of BILF1 receptors and a membrane insert GFP²-17aa. Similar BRET2 saturation experiments had been performed previously to confirm the interaction between β arr2 and human glucagon like peptide 1 (GLP-1R) (Jorgensen et al., 2011). The unspecific interactions between the BILF1 receptors and β -arr2 supported the observed finding that they do not require this adaptor protein for endocytosis.

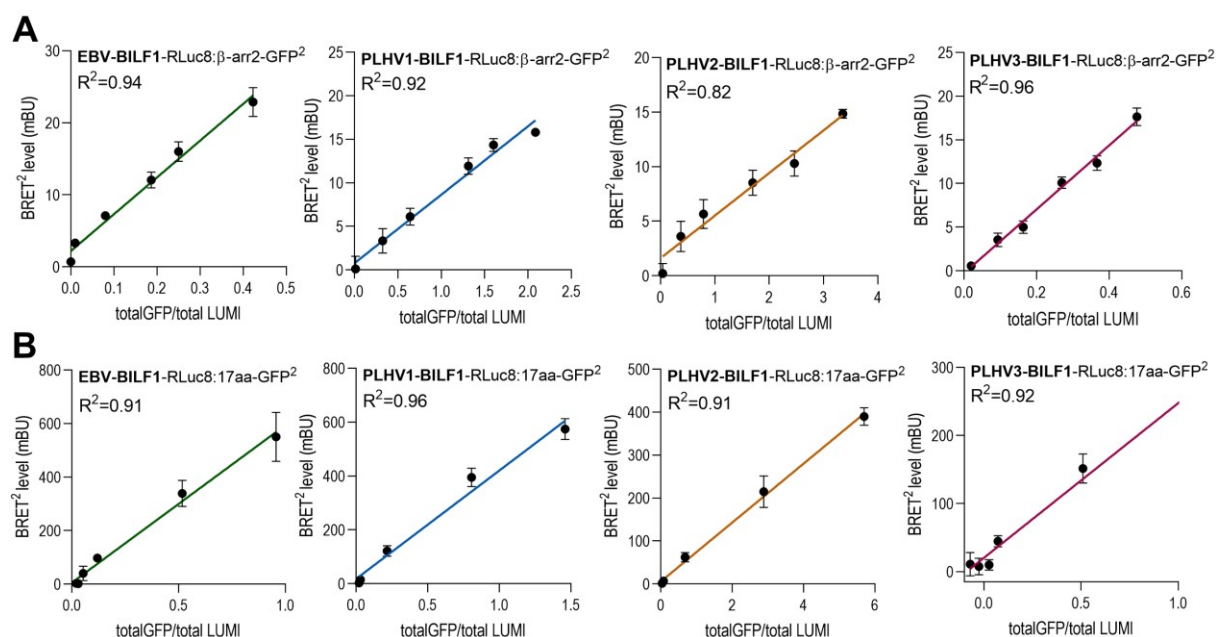


Figure 19: Non-specific interaction of β -arrestin 2 and 17aa-membrane insert with BILF1 receptors.

Slika 19: Nespecifična interakcija arestina β in membranskega vključka 17aa z receptorji BILF1. BILF1 receptor constructs with a C-terminal tag RLuc8 were expressed in HEK-293 cells together with increasing concentrations of A) β -arrestin 2-GFP² or B) GFP²-17aa construct. Graphs represent BRET2 values plotted as a function of the GFP₂/RLuc8 ratio. Results are presented as mean \pm SEM, (n = 3) and are fitted using non-linear regression equation.

Based on the fact that BILF1 crystal structure revealed marked differences between BILF1 and other GPCRs that recruit β -arrestin to mediate internalization (Tsutsumi et al., 2021), an investigation predicting if the BILF1 sequence motifs interact with β -arr2 was performed. For this purpose, the ISM method was applied, which investigates potential protein-protein interactions and analyses the structure-function relationship between different proteins (Table 6). First, informational spectrum (IS) frequency is a common informational characteristic of GPCRs and vGPCRs and represents the common information from proteins taking part in similar signaling networks. Here, this

common characteristic was represented by IS frequency F(0.216). Furthermore, the interaction affinity was shown by signal-to-noise ratio (S/N) at the IS frequency for the interaction with β arr2. Lower S/N ratio represents lower interaction affinity and *vice versa*. Comparing the interactions of β arr2 with β 2AR, a well-known β arrestin-binding GPCR, BILF1 receptors showed lower S/N ratios and therefore lower interaction affinity for β arr2, which again support the results from RT internalization assay and BRET2, showing that BILF1 receptors do not recruit β -arrestin for internalization.

Table 6: The affinity of β 2 adrenergic receptor (β 2AR) and BILF1 receptors for β -arrestin2 interaction.

Protein partners	S/N ratio at F(0.216) ¹
β 2AR: β -arr2	14.475
EBV-BILF1: β -arr2	4.95
PLHV1-BILF1: β -arr2	0.23
PLHV2-BILF1: β -arr2	0.23
PLHV3-BILF1: β -arr2	3.47

Tabela 6: Afiniteta adrenergičnega receptorja β 2 (β 2AR) in receptorjev BILF1 za vezavo z arestinom β .

¹ A lower S/N ratio indicates lower interaction affinity.

At the same characteristic frequency F (0.216), high interaction affinity (high S/N ratio) between all BILF1 receptors and AP2 was shown, which further supports the involvement of clathrin-mediated pathways in BILF1 receptor endocytosis (Table 7).

Table 7: The affinity of β 2 adrenergic receptor (β 2AR) and BILF1 receptors to interact with AP2.
Tabela 7: Afiniteta adrenergičnega receptorja β 2 (β 2AR) in receptorjev BILF1 za vezavo z AP2.

Protein partners	S/N ratio at F(0.216) ¹
β 2AR: AP2	6.48
EBV-BILF1: AP2	9.42
PLHV1-BILF1: AP2	12.42
PLHV2-BILF1: AP2	13.12

¹ A lower S/N ratio indicates lower interaction affinity.

Supporting the interaction with AP2, eukaryotic linear motifs (ELMs) were investigated for BILF1 receptors using ELM resource database (Kumar et al., 2022). ELMs are conserved amino acid patterns of proteins involved in the regulation of specific biological role of the receptor. Consistent with the data presented, a YXX Φ motif known for its interaction with AP2 complex of clathrin-coated vesicles was observed for all BILF1 receptors (Table 8).

Table 8: Predicted eukaryotic linear motifs (ELM) of BILF1 receptors (adapted from (Mavri et al., 2020)).

Tabela 8: Predvideni motivi ELM (iz angl. eukaryotic linear motifs) receptorjev BILF1 (povzeto po (Mavri et al., 2020)).

Receptor	ELM Name	Matched Sequence	Elm Description	Cell Compartment
EBV-BILF1	TRG ENDOCYTIC2	YSAF at position 32–35 [A]	Tyrosine-based sorting signal responsible for the interaction with μ 2 subunit of AP2 complex	plasma membrane, clathrin-coated endocytic vesicle, cytosol
PLHV1-BILF1	TRG ENDOCYTIC2	YTTL at position 179–182 [A]	Tyrosine-based sorting signal responsible for the interaction with mu subunit of AP2 complex	plasma membrane, clathrin-coated endocytic vesicle, cytosol
PLHV2-BILF1	TRG ENDOCYTIC2	YAVL at position 159–162 [A]	Tyrosine-based sorting signal responsible for the interaction with mu subunit of AP2 complex	plasma membrane, clathrin-coated endocytic vesicle, cytosol
PLHV3-BILF1	TRG ENDOCYTIC2	YAAL at position 194–197 [A]	Tyrosine-based sorting signal responsible for the interaction with mu subunit of AP2 complex	plasma membrane, clathrin-coated endocytic vesicle, cytosol

4.2.5 Effect of dominant negative mutant Cav S80E on BILF1 endocytosis and expression

Next, a DNM of caveolin-1, Cav S80E was used at increasing concentrations (3, 5, and 7 ng) to study the involvement of caveolin-1 in BILF1 mediated internalization (Figure 20). Cav S80E showed the comparable effect on EBV-BILF1 and PLHV1-BILF1 internalization, with 62–68% lower AUC after the addition of 7 ng Cav S80E (Figure 20 B). For PLHV2-BILF1, the co-transfection with 7 ng Cav S80E resulted in ~53% lower AUC. Again, low internalization of PLHV3-BILF1 complicated the interpretation of the results (Figure 20B). Importantly, as shown on Figure 20C, the BILF1 receptor expression declined after the addition of higher Cav S80E concentrations.

Table 9: The affinity of epidermal growth factor receptor (EGF-R) and BILF1 receptors to interact with caveolin-1.

Tabela 9: Afiniteta receptorja za epidermalni rastni faktor (EGF-R) in receptorjev BILF1 za interakcijo s kaveolinom-1.

Protein partners	S/N ratio at F(0.357)¹
EGF-R: caveolin-1	15.29 ²
EBV-BILF1: caveolin-1	17.46
PLHV1-BILF1: caveolin-1	12.86
PLHV2-BILF1: caveolin-1	15.61

¹ A lower S/N ratio indicates lower interaction affinity.

² S/N ration for EGF-R was previously published in (Couet et al., 1997b) and was used as a positive control.

Furthermore, applying the ISM method, we showed high S/N ratio at frequency F(0.357) indicating high interaction between all BILF1 receptors and caveolin-1. This additionally confirms the involvement of caveolin-1 in BILF1 receptor trafficking (Table 9).

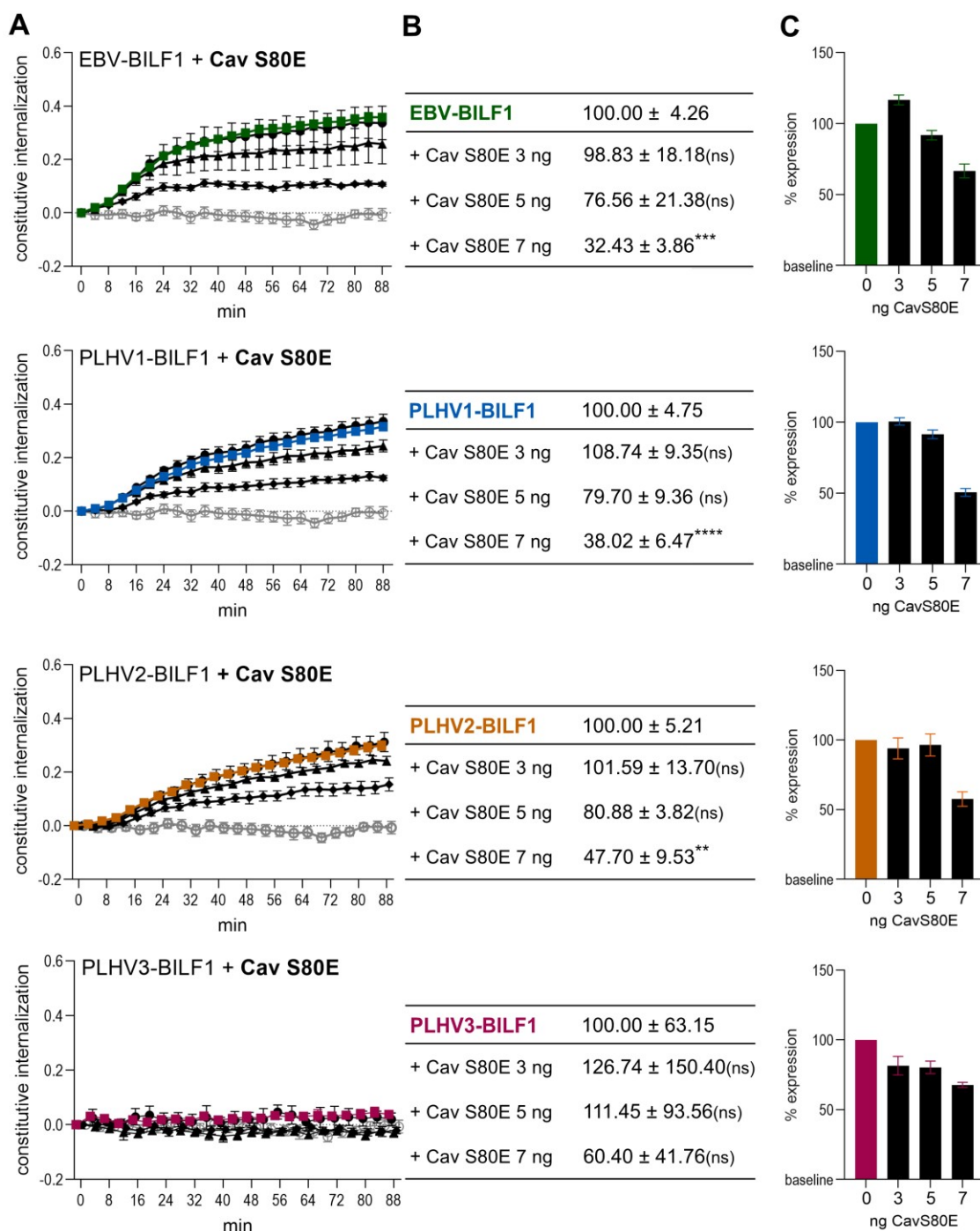


Figure 20: Effect of dominant negative mutant Cav S80E on BILF1 endocytosis.

Slika 20: Vpliv dominantno negativne mutante Cav S80E na endocitozo receptorjev BILF1.

A) SNAP-tagged BILF1 receptors (coloured) and empty vector (grey) were expressed in HEK-293A cells together with different concentrations of Cav S80E DNM construct (●-3ng; ▲-5ng; ◆-7ng). FRET was measured at 37 °C every 4 min for a total of 88 min. Graphs represent ratios between donor and acceptor. B) The area under curve (AUC) parameter was calculated for each curve on Figure 20A and was normalized to AUC of each BILF1 in the absence of Cav S80E (0ng). Results are presented as mean ± SEM, (n = 3). Statistical differences were determined with Dunnett's multiple comparison two-way ANOVA test. ***P* < 0.01, *** *P* < 0.001, *****P* < 0.0001. C) BILF1 receptor surface expression in cells co-transfected with Cav S80E is presented normalized to BILF1 receptor expression in cells without DNM.

4.2.6 Visualization of the intracellular localization and trafficking of BILF1 receptors after endocytosis

The fate of the BILF1 receptors after the internalization from the cell surface had not been studied. Therefore, here the receptors were tracked intracellularly to distinguish their fate following either of two different pathways: i) degradative pathway (i.e., degradation in lysosomes) and ii) recycling pathway (i.e., sorting in recycling endosomes). For this purpose, antibodies against intracellular membrane markers differentiating between three compartments were used: early endosomes (transferrin receptor or CD71 marker), lysosomes (LAMP1 marker) and recycling endosomes (Rab8 marker) (Figure 21). A microscopy-based antibody-feeding assay was performed to allow the labelled receptor to internalize constitutively for 15 or 30 min and to determine the co-localization with the above-mentioned markers (Figure 21A). To quantify the co-localization between two proteins, the cells expressing the receptor were manually selected and the fluorescence intensity from red and green channels, representing receptor and marker, respectively were measured. Finally, Pearson's correlation coefficient for images above the threshold was calculated. Values from -1 to 0 indicate negative correlation or non-significant correlation, whereas +1 indicates strong correlation (Figure 21B). After 30 min of internalization, co-localization was shown for the BILF1 receptors with early endosome marker CD71, showing values of 0.449 (EBV-BILF1), 0.230 (PLHV1-BILF1), 0.342 (PLHV2-BILF1), and 0.205 (PLHV3-BILF1). Only PLHV2-BILF1 and PLHV3-BILF1 showed co-localization with LAMP1 a lysosome marker, whereas EBV-BILF1 and PLHV1-BILF1 showed no co-localization with LAMP1, having negative correlation values of -0.55 and -0.131, respectively. None of the BILF1 receptors co-localized with Rab8, a marker of the recycling pathway, as negative correlation values were observed for all of them.

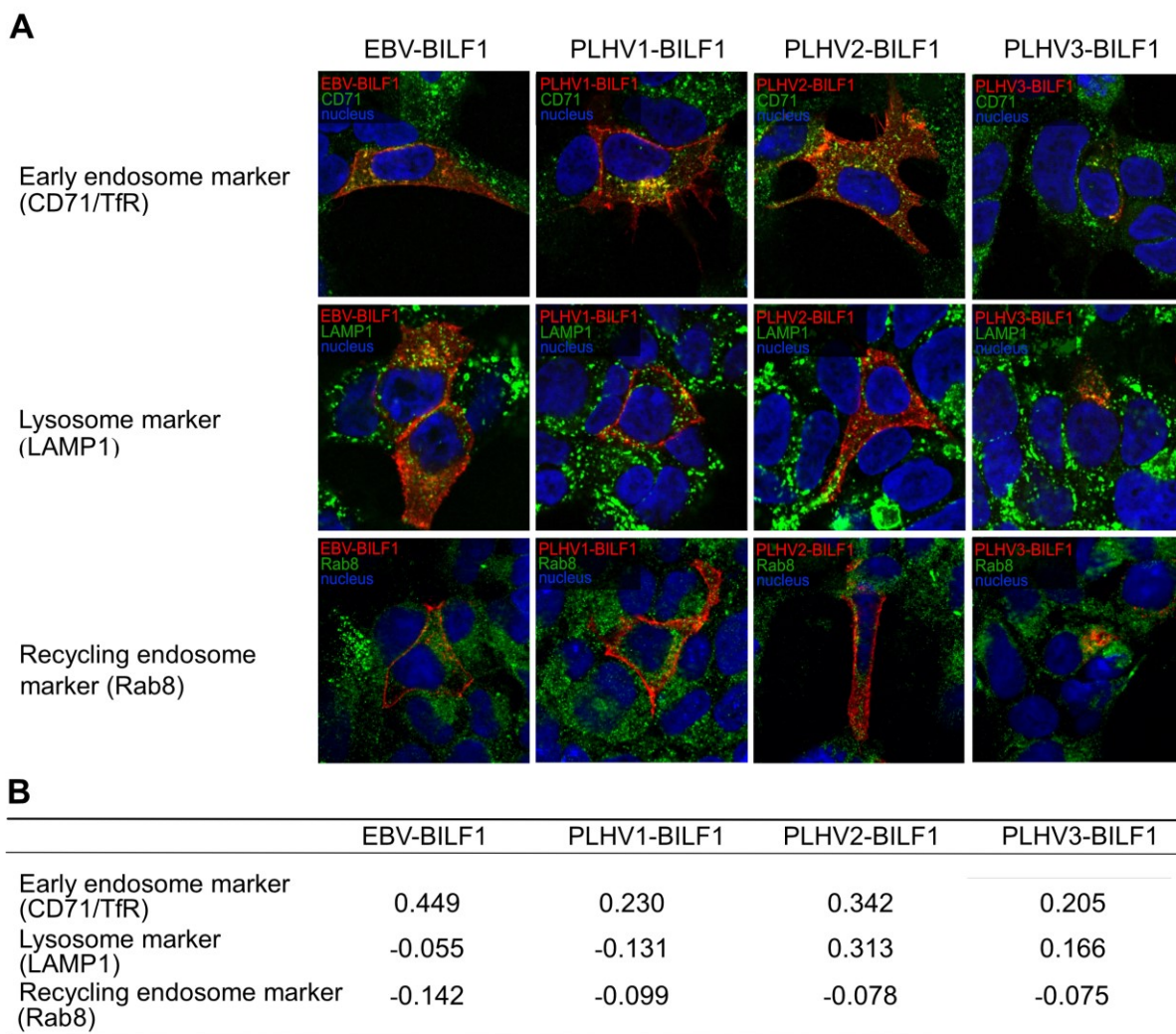


Figure 21: BILF1 receptor co-localization with markers of intracellular organelles.

Slika 21: Kolokalizacija receptorjev BILF1 z označevalci znotrajceličnih organel.

A) Representative pictures of antibody-feeding internalization experiment, expressing FLAG-tagged BILF1 receptors in HEK-293 cells. BILF1 receptors were visualized with Alexa Fluor 555 (red) secondary antibodies. Endogenous intracellular markers of early endosomes (CD71/TfR), lysosomes (LAMP1), or recycling endosomes (Rab8) were visualized with Alexa Fluor 488 (green) antibodies. B) Co-localization was quantified calculating Pearson's correlation coefficient for image above threshold, where -1 shows negative correlation, 0 shows no correlation, and 1 shows strong correlation.

4.2.7 Analysis of BILF1 receptor interaction with Rab7 and the estimation of receptor recycling

To further supplement the microscopy data in the previous section, investigating the co-localization with lysosomes, we performed a BRET1 saturation assay observing the interaction between marker for late endosomes/lysosomes (Rab7) and BILF1 receptors (Modica and Lefrancois, 2020). As the low surface expression of PLHV3-

BILF1 complicated the experiment, Figure 22A represent the data from EBV-BILF1, PLHV1-BILF1 and PLHV2-BILF1. In order to follow the fate of the receptors after constitutive internalization, HEK-293 cells were co-transfected with constant concentration of BILF1 receptor cDNA and various concentrations of Rab7 cDNA as described previously (Modica et al., 2017). For all BILF1 receptors, a hyperbolic saturation curve indicated the constitutive interaction between the receptor and Rab7 with BRET50 values of 0.028–0.172 (Figure 22A). This indicates that at least a fraction of BILF1 receptors gets degraded in lysosomes.

Furthermore, receptor recycling was verified by calculating the difference between the amount of receptors labelled at 4 °C and 37 °C (Figure 23). In more detail, when labelling SNAP-tagged BILF1 receptors with donor molecules at 4 °C, the internalization and recycling is prevented. This results in the labelling of surface expressed receptors only. In contrast, labelling the receptors at 37 °C allows normal receptor cycling and results in the labelling of all BILF1 receptors in the cell (designated at 100%). Measuring the donor values from both experiments, the difference corresponds to the amount of receptors located intracellularly (intracellular pool) and subsequently recycling to the plasma membrane. The observed intracellular pool of receptors corresponded to 65% (EBV-BILF1), 60% (PLHV1-BILF1), 58% (PLHV2-BILF1), and 65% (PLHV3-BILF1) (Figure 22B), which represents the receptors that recycle back to plasma membrane.

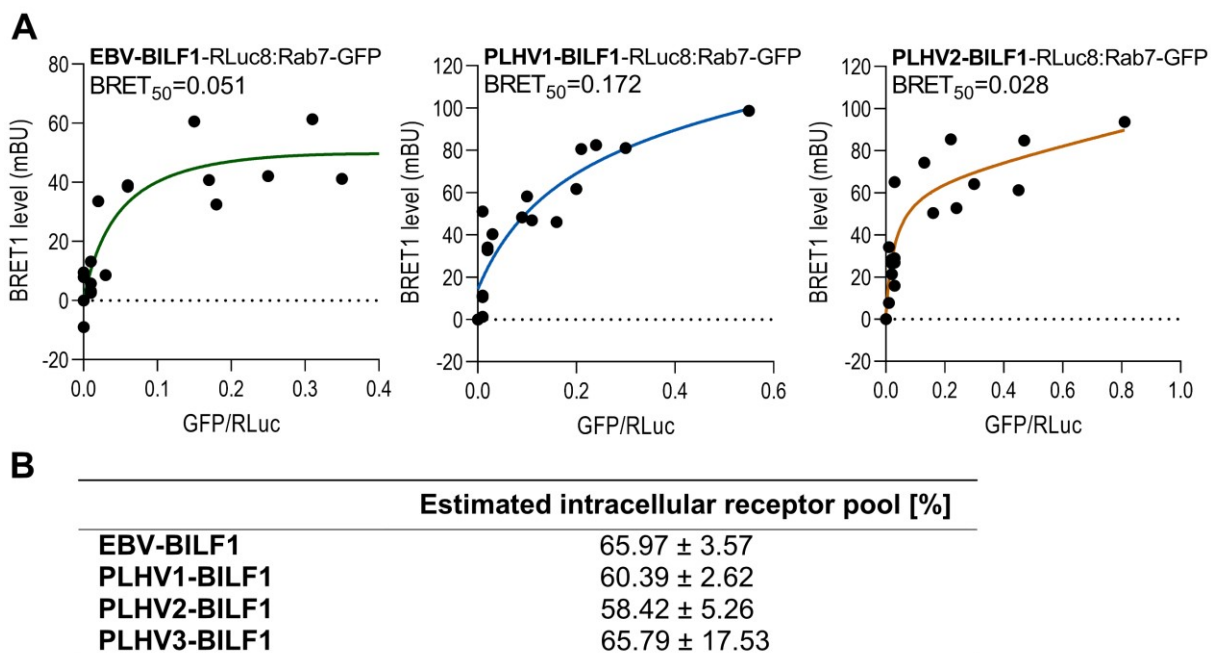


Figure 22: Specific interaction of BILF1 receptors with Rab7 protein and the estimation of BILF1 receptor intracellular pool.

Slika 22: Specifična interakcija receptorjev BILF1 s proteini Rab7 in ocena znotrajcelične lokalizacije receptorjev BILF1.

A) RLuc8-BILF1 receptors were expressed in HEK-293 cells together with various concentrations of Rab7-EGFP protein. BRET1 values are plotted as a function of the ratio between the total GFP (fluorescence) and total RLuc8 (luminescence) signal. $BRET_{50}$ values indicate the relative affinity of the acceptor for the donor molecules (Rab7-GFP) and represent the acceptor/donor ratio at 50% of the maximal BRET ratio. Non-linear regression equation was used to evaluate the results using Graph Pad Prism. Results are shown as triplicate values from at least three independent experiments. B) Table represents the estimated intracellular pool, calculated as presented on Figure 23.

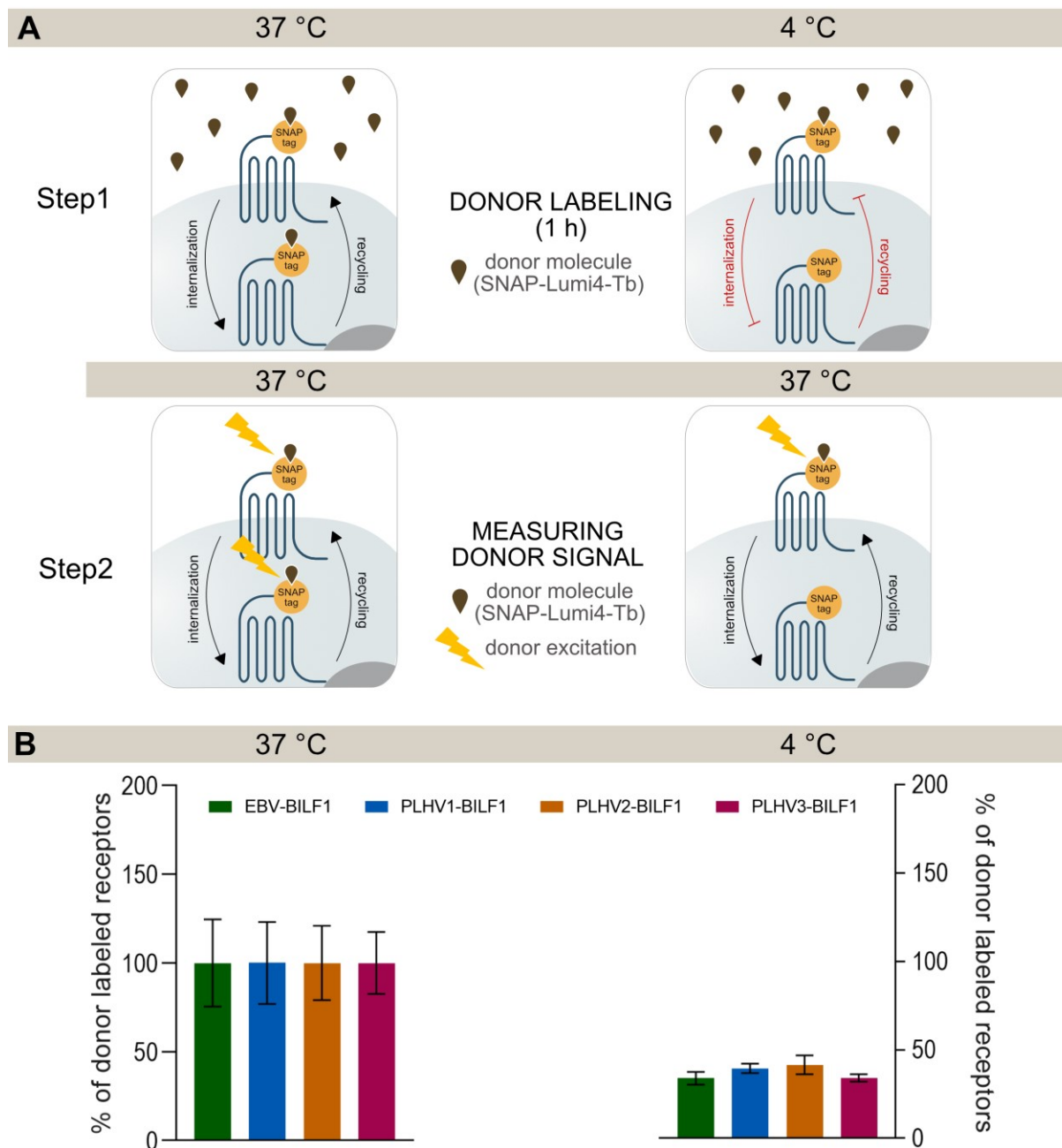


Figure 23: The principle of determining intracellular pool of BILF1 receptors.

Slika 23: Način določanja količine znotrajceličnih receptorjev BILF1.

A) A Donor molecule is added to SNAP-tag BILF1-expressing cells for 1 h. The unbound donor was then washed with an assay buffer. Labelling with donor was performed at 37 °C which allowed normal internalization and recycling and at 4 °C which prevented internalization and recycling. The total donor signal measured corresponded to the amount of the donor-labelled receptors. B) Graphs represent the difference in donor signal between the two conditions. The difference accounts for the estimated number of receptors trafficking to the plasma membrane.

4.3 SIGNALING

4.3.1 MAPK signaling

To determine a potential G protein-independent pathway for BILF1 receptors, the potential activation of MAP kinase pathways by BILF1 receptors was further investigated. The activation of MAP kinase ERK1/2 (also named p44/42 MAPK) was evaluated with the Western blot method, using antibodies against phosphorylated ERK and total ERK. The phosphorylation of ERK1/2 occurs at the tyrosine 204/187 residues (Tyr204/187) and threonine 202/185 (Thr202/185) residues. Therefore, two different antibodies were used to be able to quantify ERK1/2 protein expression and to calculate the ratio between the phosphorylated ERK1/2 protein and total ERK1/2 protein (pERK/tERK).

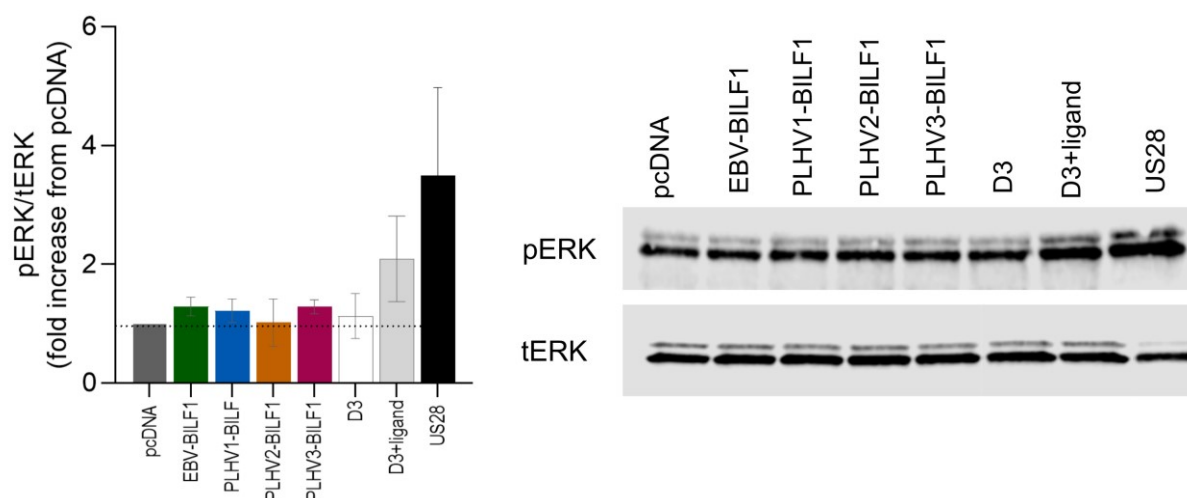


Figure 24: Measurement of ERK1/2 MAPK signaling pathway activation by the BILF1 receptors.
Slika 24: Meritev aktivacije znotrajceličnega prenosa signala ERK1/2 MAPK, pogojene z receptorjem BILF1.

Western blot analysis measuring ERK1/2 MAPK activation. The graph represents the ratio between phosphorylated ERK and total ERK (pERK/tERK) for BILF1 receptors, D3, and US28 normalized to pcDNA (designated as 1). On the right, representative Western blot figure shows bands for pERK and tERK.

To be able to control the protein loads in different lanes of the gel and, therefore, to quantify ERK expression, a loading control the endogenous Glyceraldehyde 3-phosphate dehydrogenase (GAPDH) protein was included. The graph on Figure 24

represent the pERK/tERK ratio of BILF1 receptors as well as the dopamine 3 (D3) and US28 receptors as positive controls. Ratios for all receptors are normalized to pcDNA (designated as 1). As seen on Figure 24, BILF1 receptors did not show the activation of ERK1/2, compared to US28 and D3 receptors previously shown to activate this signaling pathway.

4.3.2 Evaluation of G protein-mediated constitutive signaling

The activation of intracellular signaling pathways by GPCRs often affect gene transcription. To determine receptor-specific constitutive activity and the ability to stimulate downstream gene transcription, a luciferase reporter assay was used to study the activation of three cellular transcription factors: CREB, NFAT and NF- κ B. It is a cumulative assay, measuring the amount of gene product over time (Carter and Shieh, 2015).

The experiment requires the use of constructs in which the regulatory region of a transcription factor is fused with the firefly luciferase DNA-coding sequence. When a GPCR (i.e., BILF1 receptor) activates endogenous signaling pathways and upregulates the transcription factor, it results in luciferase expression. The addition of the reagent facilitates the enzymatic reaction and thus the quantification of firefly luciferase expression in mammalian cells (Carter and Shieh, 2015).

4.3.2.1 Activation of CRE reporter gene by BILF1 receptors as a result of constitutive $G\alpha_i$ signaling.

First, the activation of CRE transcription factor was determined in HEK-293 cells. These cells are commonly used for studying GPCR-signaling properties. This transcription factor is activated upon receptor activity through $G\alpha_s$ protein (stimulating CRE activity) and is inactivated by receptor activity through $G\alpha_i$ protein (inhibiting CRE activity). This allowed the study of the BILF1 receptor's activity at the plasma membrane. Given a previously determined $G\alpha_i$ dependent constitutive activity of EBV-BILF1, we hypothesized that porcine BILF1 receptors similarly constitutively signal

through $G\alpha_i$. Forskolin, which induces the formation of cAMP was used to test the ability of BILF1 receptors to decrease the cAMP in a gene dose dependent manner (Figure 25A).

PLHV1-3 BILFs showed a conserved ability to inhibit forskolin-induced CRE transcription factor activity. PLHV1-BILF1 and PLHV3-BILF1 showed approximately 60% of maximal EBV-BILF1-mediated decrease and PLHV2-BILF1 showed a moderate (30%) response (Figure 26A).

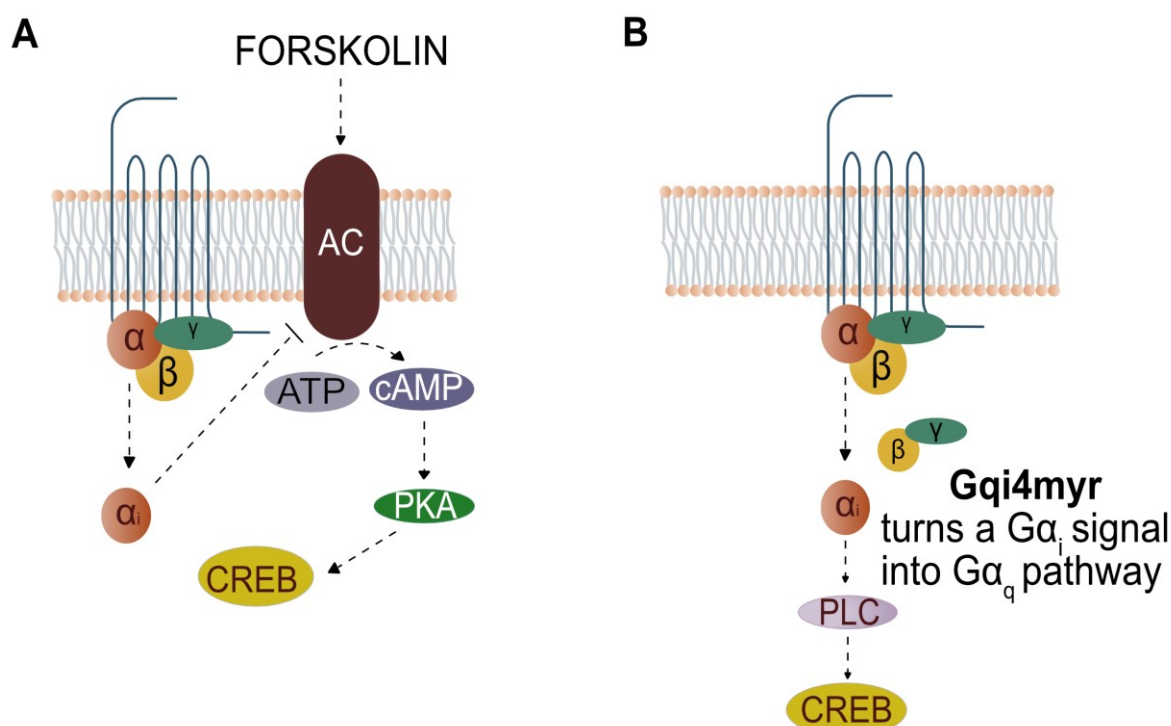


Figure 25: Schematic representation of CRE signaling pathways in the presence of forskolin and chimeric G protein.

Slika 25: Shematski prikaz signalne poti CRE, v prisotnosti forskolina in himernega proteina G.
(A) Forskolin induces cyclic AMP formation and enables the observation of its decrease mediated by receptors. (B) Chimeric G protein $G\alpha_{\Delta 6qi4myr}$ is recognized by receptor as a $G\alpha_i$, but functions as a $G\alpha_q$ subunit, resulting in increased activity of phospholipase C (PLC) and hence CRE activity.

Additionally, BILF1 expressing HEK-293 cells were co-transfected with a chimeric G protein $G\alpha_{\Delta 6qi4myr}$, which turns $G\alpha_i$ - into $G\alpha_q$ signaling, activating phospholipase C (PLC) (Figure 25B). Hereby, the activation of CRE activity observed for all BILF1 receptors confirmed the results above. Compared to EBV-BILF1 (normalized as 100%), PLHV1-BILF1 and PLHV2-BILF1 showed comparable gene-dose dependant increase, reaching maximum of 100% and 120% respectively, whereas PLHV3-BILF1

showed a lower only 46% increase in CRE activity (Figure 26B). These results showed that constitutive $G\alpha_i$ signaling is conserved for the PLHV1-3 BILF1 receptors and is similar to the previously reported EBV-BILF1 mediated $G\alpha_i$ signaling.

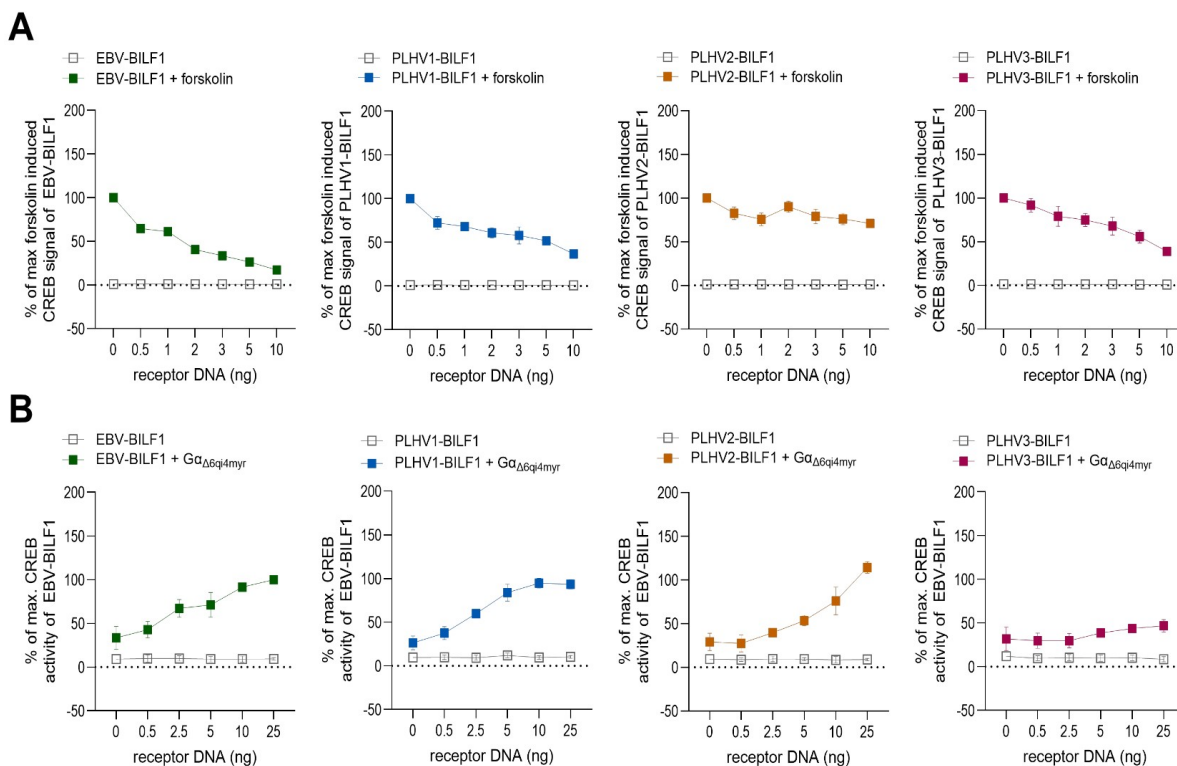


Figure 26: $G\alpha_i$ dependent CRE activity of BILF1 receptors.

Slika 26: CRE-aktivacija receptorjev BILF1, odvisna od $G\alpha_i$.

A) HEK-293A or B) HEK-293 cells were co-transfected with increasing concentrations of BILF1 receptors and 30 ng/well of CRE cis-reporter plasmid. A) 5 h, before BILF1-mediated CRE activity was measured, HEK-293A cells were stimulated with 10 μ M of forskolin. B) BILF1-expressing HEK-293 cells were co-transfected with 30 ng/well of $G\alpha_{\Delta 6q4myr}$ plasmid. CRE activity was measured 24 h after transfection. Values are means \pm SEM, (n = 3).

4.3.2.2 Activation of NF- κ B and NFAT transcription factors in CRISPR/Cas9 engineered HEK-293A cells relies on the BILF1 mediated $G\alpha_i$ signaling

Activation of the transcription factors NF- κ B and NFAT was previously shown by EBV-BILF1 (Beisser et al., 2005, Zuo et al., 2011, Griffin et al., 2013, Spiess et al., 2015a). Our first goal was to determine if PLHV1-3 BILF1 activate NF- κ B and NFAT. Second, to examine which specific G proteins are involved, the transcription factor activation was studied in CRISPR/Cas9-engineered HEK-293A cell depleted of various G proteins ($\Delta Gs/olf/q/11/12/13/z=pan$ KO cells) and in parental HEK-293A cells

(expressing full repertoire of G proteins). In Figure 27 and Figure 28, the NF- κ B or NFAT activity of PLHV1-3 BILF1 receptors are shown relative to the maximal activity of EBV-BILF1 in parental cells (normalized to 100%). The confirmed activation of both pathways observed for EBV-BILF1 was in line with previously published data (Beisser et al., 2005, Spiess et al., 2015a). In parental cells, PLHV1- and PLHV2-BILF1 showed ~120% and ~210% NF- κ B activity, respectively (Figure 27). However, PLHV1-BILF1 could only activate NFAT with 30% and PLHV2-BILF1 showed no NFAT activity (Figure 28). In contrast, PLHV3-BILF1 did not activate NF- κ B (Figure 27), although it showed high, EBV-like NFAT activity (~140%) in parental HEK-293A cells (Figure 28). In summary, NF- κ B activity is conserved for EBV- PLHV1- and PLHV2-BILF1, whereas only EBV- and PLHV3-BILF1 activated the NFAT transcription factor.

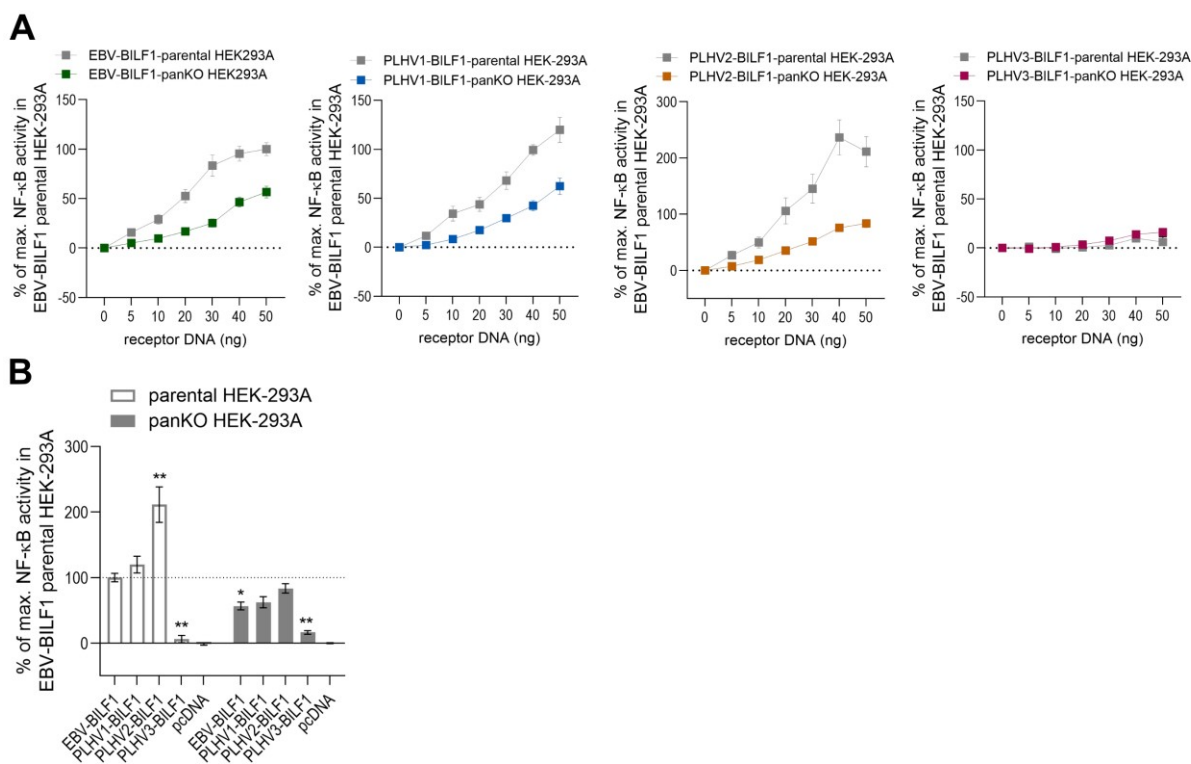


Figure 27: NF- κ B activity of BILF1 receptors.

Slika 27: NF- κ B-aktivnost receptorjev BILF1.

NF- κ B activity was measured in parental HEK-293A cells (grey curves in A and empty bars in B) and HEK-293A cells depleted of various G proteins (Δ Gas/olf/q/11/12/13/z) with CRISPR/Cas9 technology (pan KO HEK-293A cells) (coloured curves in A and full bars in B). A) Graphs represent the receptor gene dose dependent NF- κ B activity relative to the maximal activity of EBV-BILF1 in parental cells. B) Activity of the highest (50 ng/well) concentrations of BILF1 receptor DNA is compared in parental and pan KO cells, showing significant and non-significant differences. Values are means \pm SEM, (n = 3). Statistical analysis was performed using Šídák's multiple comparison two-way ANOVA test. * P < 0.05; ** P < 0.0001.

To further determine if the activation of NF- κ B and NFAT transcription factors depends on $G\alpha_i$ signaling, we used cells expressing only the $G\alpha_i$ protein, referred to as pan KO cells ($\Delta G_{s/olf/q/11/12/13/z}$). As a first step, two control experiments were performed in parallel to the signaling assays, comparing the receptor expression and cell viability in HEK-293A pan KO cells and parental HEK-293A cells (Figure 29). Receptor gene dose dependant expression in both cell lines corresponded to the results obtained from the ELISA using HEK-293 cells shown in Figure 12A. However, approximately 20% lower expression was observed for all BILF1 receptors in pan KO cells. The cell viability remained comparable in both cell lines after the transfection with up to 50 ng/well, which was a maximum concentration used in the experiments.

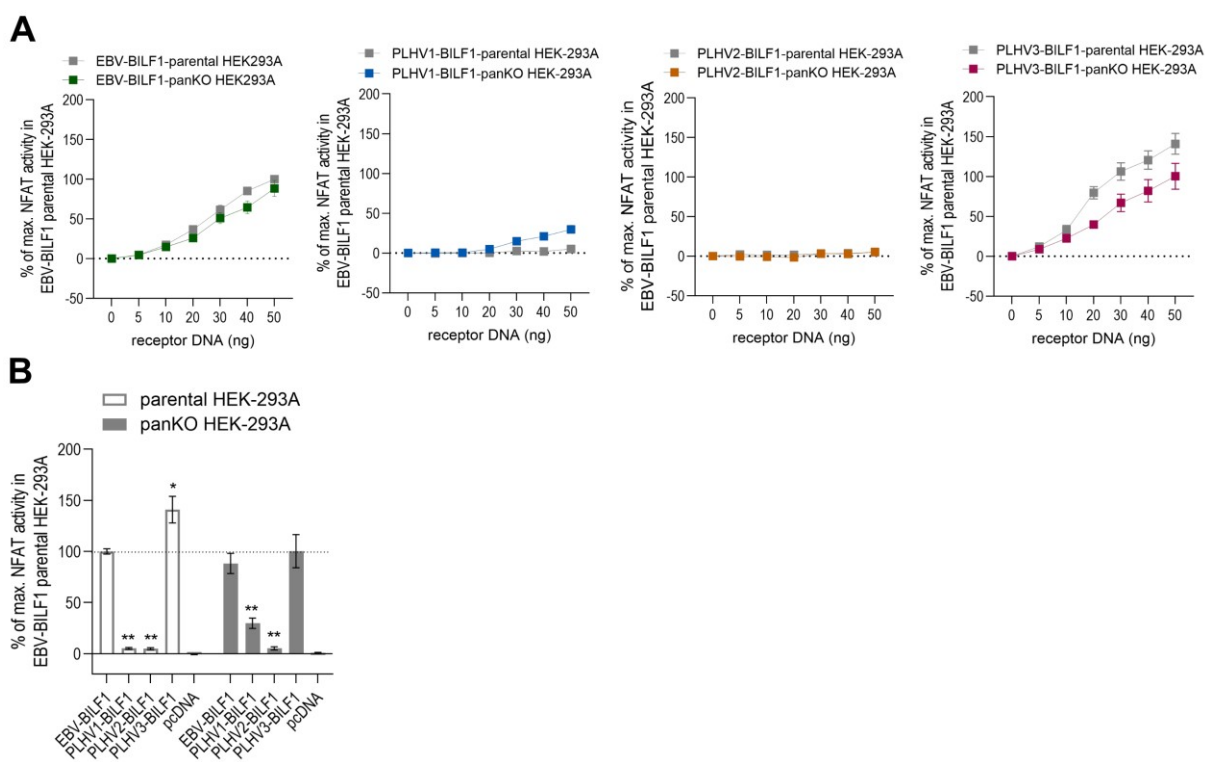


Figure 28: NFAT activity of BILF1 receptors.

Slika 28: NFAT-aktivnost receptorjev BILF1.

NFAT activity was measured in parental HEK-293A cells (grey curves in A and empty bars in B) and HEK-293A cells depleted of various G proteins ($\Delta G_{s/olf/q/11/12/13/z}$) by CRISPR/Cas9 technology (pan KO HEK-293A cells) (coloured curves in A and full bars in B). A) Graphs represent the receptor gene dose dependent NFAT activity relative to the maximal activity of EBV-BILF1 in parental cells. B) The activity of the highest (50 ng/well) concentrations of BILF1 receptor DNA is compared in parental and pan KO cells, showing significant and non-significant differences. Values are means \pm SEM, (n = 3). Statistical analysis was performed: Dunnett's multiple comparison two-way ANOVA test. * $P < 0.01$, ** $P < 0.0001$.

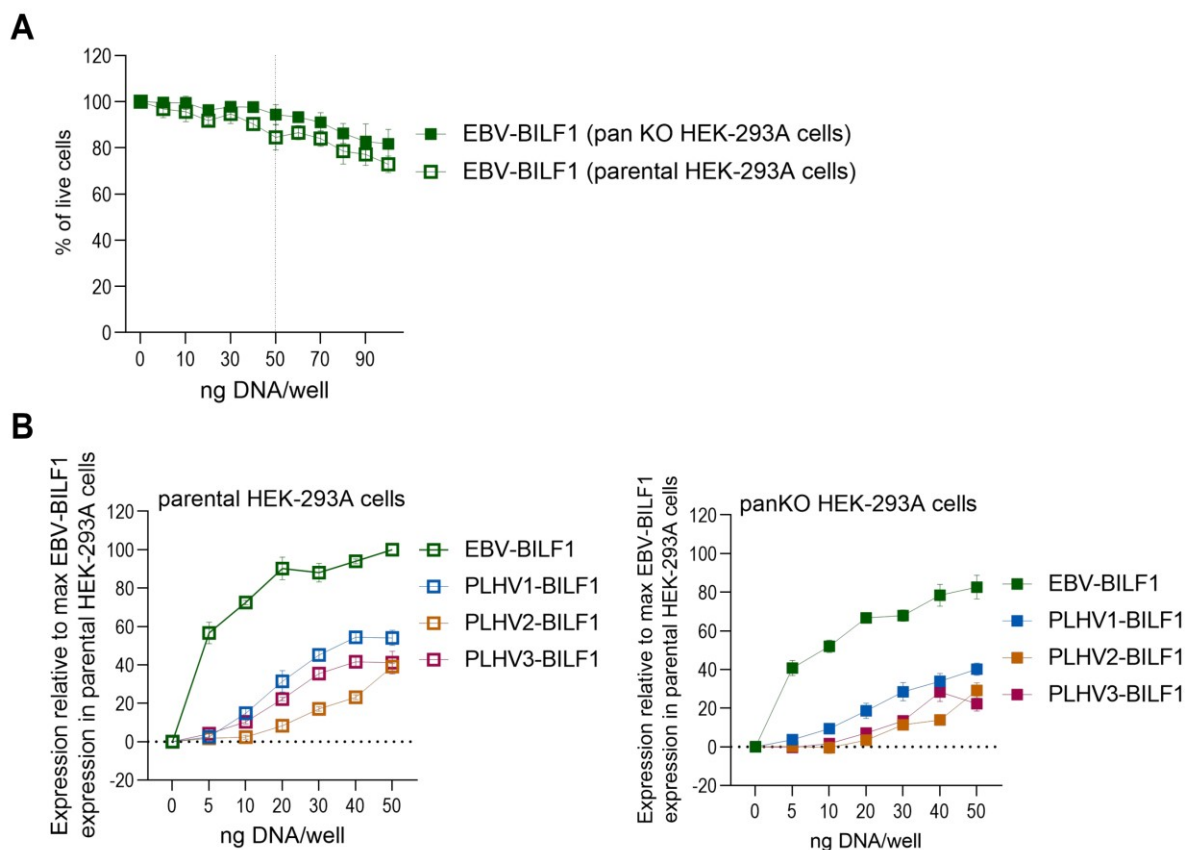


Figure 29: Comparison of viability and BILF1 expression in pan KO HEK-293A and parental HEK-293A cell line.

Slika 29: Primerjava preživetvene sposobnosti in izražanja receptorjev BILF1 v celičnih linijah “pan KO HEK-293A” in “parental HEK-293A”.

A) The difference in parental HEK-293A and pan KO HEK-293 cell viability was tested using a Cell Titer Glo assay. Cells were transfected with increasing concentrations of EBV-BILF1 and 30ng/well of NF- κ B transcription factor. B) Using cell-based ELISA, we determined the difference in BILF1 surface expression in parental HEK-293A and pan KO HEK-293A cells. Cells were seeded and transfected in parallel with the cells used in NFAT transcription factor assay. Values are mean \pm SEM, (n = 3).

Comparing the NF- κ B activity for EBV-BILF1 in pan KO cells with parental cells, only 56% activation was observed (Figure 27), which could account for lower receptor expression observed (Figure 29) or suggests the involvement of additional G proteins in NF- κ B activation. The NFAT activity, in contrast, was comparable in both cell lines (~90%) and confirms G α_i as a primary G protein involved in this pathway (Figure 28). PLHV1-BILF1, PLHV2-BILF1, and PLHV3-BILF1 showed comparable (62%), higher (83%) or no activity for NF- κ B, respectively, compared to EBV-BILF1 in pan KO cells (Figure 27). However, similar to the observation in the parental cell line, PLHV3-BILF1 only induced NFAT activity (100%) comparable to EBV-BILF1 in pan KO, whereas PLHV2-BILF1 again failed to activate this transcription factor (Figure 28). PLHV1-

BILF1 mediated NFAT activity in pan KO cells reached approximately 30% of the maximal EBV-BILF1 activity, which was different to the results in parental cells, in which the NFAT activity was low (Figure 28). Comparing NFAT activity in parental and pan KO cells expressing PLHV3-BILF1 showed minimal differences in activity (Figure 28) indicating that, similar to EBV-BILF1, $G\alpha_i$ plays a main role in mediating downstream signaling although the statistically significant increased levels in parental cells for PLHV3-BILF1 did implicate an additional more minor role for other G proteins that was not apparent for EBV-BILF1. Therefore additional “rescue” studies were performed using co-transfection with $G\alpha_q$ and $G\alpha_{11}$, G proteins typically associated with NFAT activity (Figure 30). Consistent with the main role of $G\alpha_i$ in NFAT activation, no significant effect of $G\alpha_{q/11}$ was observed in pan KO cells for PLHV3-BILF1, (neither for EBV-BILF1 and PLHV1-2-BILF1), supporting that the observed NFAT activity is $G\alpha_i$ dependent. The results above suggest the importance of $G\alpha_i$ for signaling of all studied BILF1 receptors; however, differences were observed in downstream signaling for the activation of the NF- κ B and NFAT transcription factors.

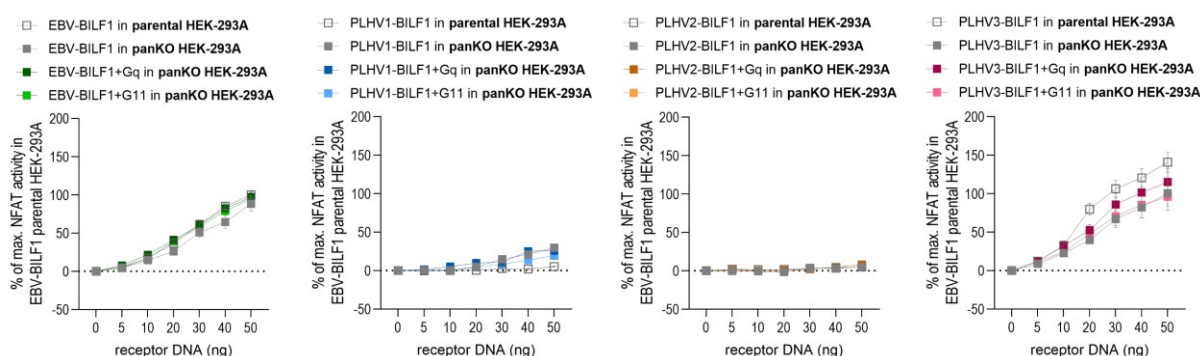


Figure 30: NFAT activity of BILF1 receptors with additional co-transfection of $G\alpha_q$ and $G\alpha_{11}$.

Slika 30: NFAT-aktivnost receptorjev BILF1, kotransfeciranih s proteinoma $G\alpha_q$ in $G\alpha_{11}$.

NFAT activity was measured in parental HEK-293A cells and HEK-293A cells expressing only $G\alpha_i$ (pan KO HEK-293A cells) co-transfected with BILF1 receptors and $G\alpha_q$ and $G\alpha_{11}$ constructs. Graphs represent the receptor-dependent NFAT activity relative to the maximal activity of EBV-BILF1 in parental cells. Values are means \pm SEM, (n = 3).

4.4 BIOLOGICAL ROLE OF BILF1 RECEPTORS

4.4.1 Comparison of immunoevasive properties for BILF1 receptors

One important biological functions of EBV-BILF1 is its ability to downregulate MHC-I molecules at the surface of infected cells, leading to immunoevasion (Zuo et al., 2009, Griffin et al., 2013). This property was suggested to be driven by receptor's ability to internalize constitutively. Observing the constitutive internalization for at least two PLHV-BILF1 receptors, the potential role in downregulating MHC-I at the cell surface was further determined in HEK-293 cells. The use of human HEK-293 cells was supported by the 74% sequence homology and high structure identity between human HLA class I and porcine SLA class I molecules shown in the homology model (Figure 31). Flow cytometry was the method of choice based on previously reported EBV-BILF1-mediated MHC-I downregulation and the specificity of the method. Using antibodies against endogenous MHC-I, its expression at the surface of BILF1 transfected cells was measured and compared to the control (pcDNA) transfected HEK-293 cells. The results presented on Figure 32A show the ratio between MHC-I expression in BILF1 transfected and BILF1 non-transfected cells. As a control, a ratio of MHC-I expression in pcDNA transfected and pcDNA non-transfected cells was calculated (0.91).

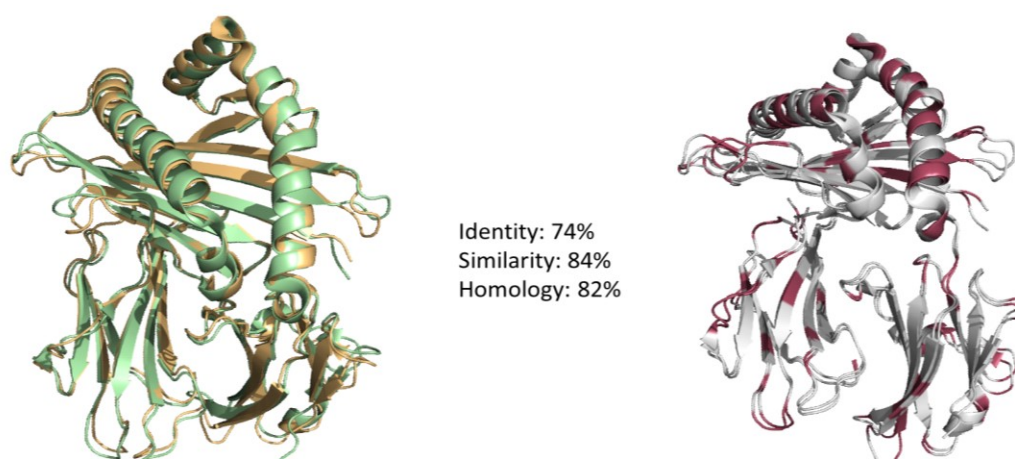


Figure 31: Homology model of human HLA-I and porcine SLA-I molecules.

Slika 31: Primerjava med humano molekulo HLA-I in prašičjo molekulo SLA-I.

Porcine SLA-I molecule (green) and human HLA-I molecule (orange) were compared for their identity, similarity, and homology. The differences are marked in red (right).

For EBV-BILF1, the results were in agreement with previous studies, confirming the MHC-I downregulation property for the receptor in HEK-293 cells, with a 0.61 ratio. Although challenged by a low transfection efficiency observed in the experiment, a significantly lower MHC-I expression was determined for PLHV3-BILF1 comparable to EBV-BILF1 (0.67). With the ratio of 0.84 and 0.83, PLHV1- and PLHV2-BILF1 respectively showed a tendency downregulating MHC-I (Figure 32A). Despite the optimization of transfection protocol, higher DNA concentrations and different vectors used (pcDNA and bicistronic IRES vector), the transfection efficiency remained low for PLHV1-3 BILF1 receptors. Therefore, a new approach was used allowing to visualize and further quantify the MHC-I expression in BILF1-transfected cells using fluorescence microscopy (Figure 33). With this approach, MHC-I expression was determined on transfected (coloured bars) and non-transfected cells (grey bars) in both HEK-293 and PK-15 cells, avoiding the low transfection efficiency.

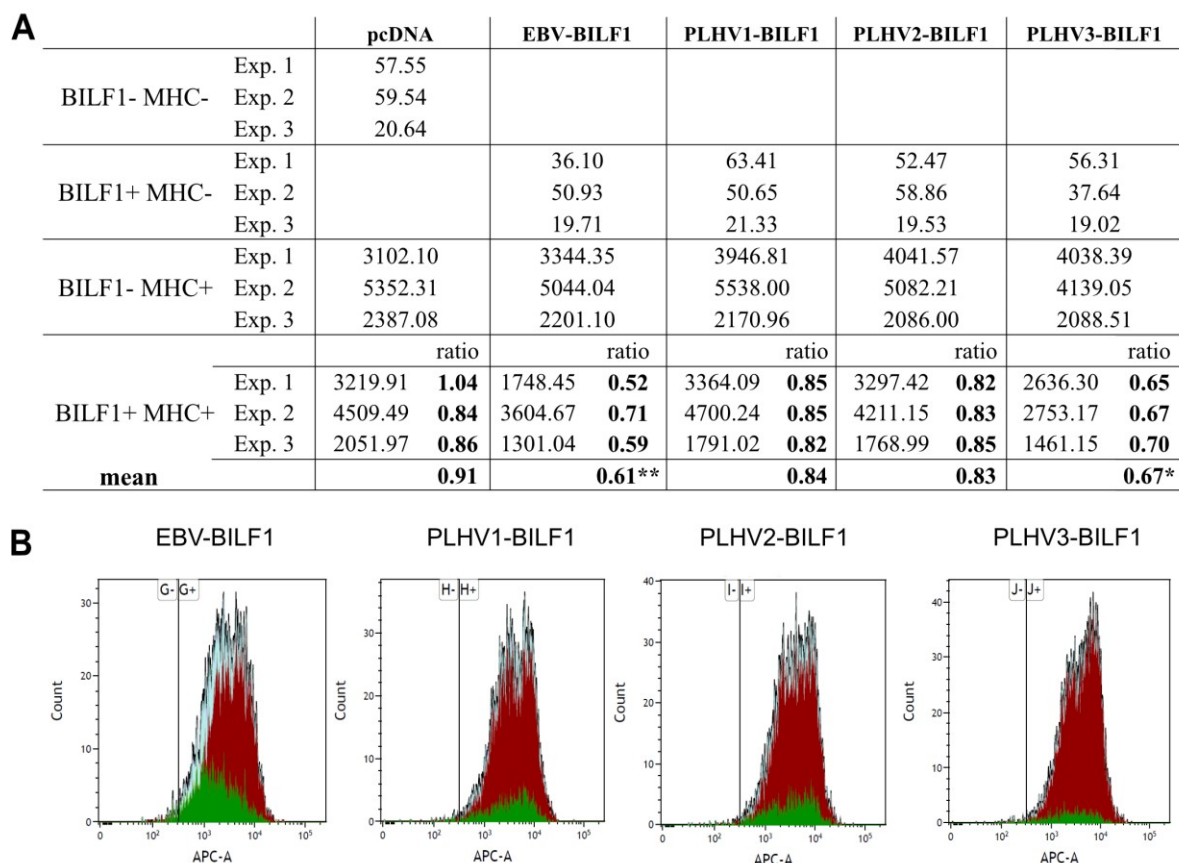


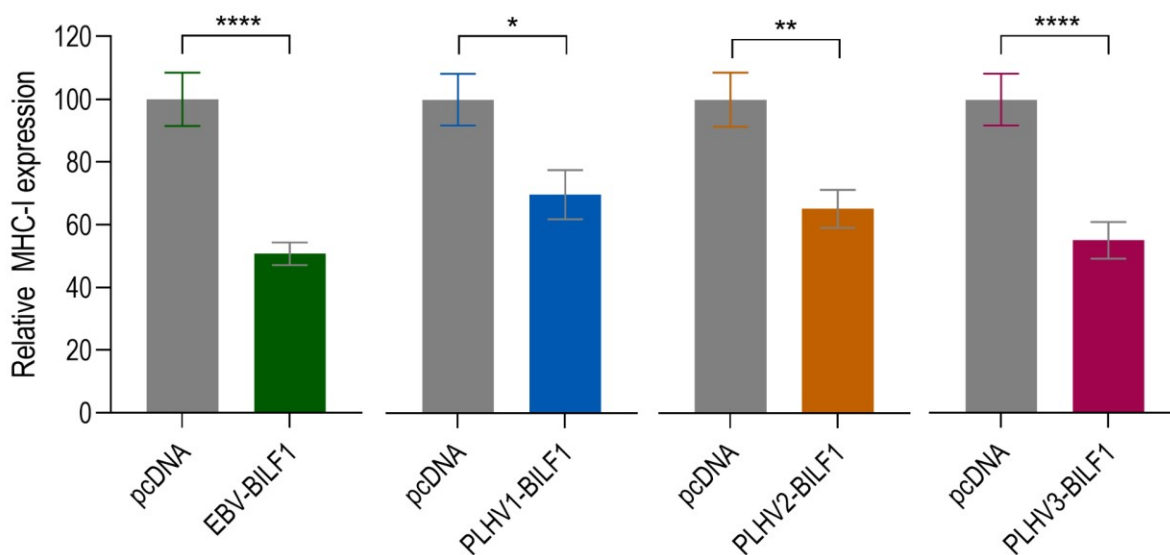
Figure 32: MHC-I downregulation studied by flow cytometry.

Slika 32: Meritve zniževanja površinske izraženosti molekul MHC-I z uporabo pretočne citometrije.

In HEK-293 cells expressing BILF1 receptors, MHC-I downregulation was measured. A) This table represents the MHC-I expression in a population of BILF1 transfected (BILF1+) and non-transfected (BILF1-) cells. Ratios were calculated from values of MHC-I expression in BILF1-expressing cell / MHC-I expression in BILF1 not expressing cells. Statistical analysis was performed using one-way ANOVA analysis. ** $P < 0.005$; * $P < 0.05$. B) Two-colour flow cytometry histograms represent MHC-I expression in BILF1 transfected cells (green) and BILF1 non-transfected cells (red).

Comparable to the findings using flow cytometry, EBV-BILF1, and PLHV3-BILF1 showed the highest (approximately 50%) downregulation of MHC-I and PLHV1-BILF1, and PLHV2-BILF1 showed lower (30–35%) downregulation in transfected, compared to non-transfected cells (Figure 33A). The BILF1-mediated MHC-I downregulation was conserved for all BILF1 receptors in HEK-293 cells. However, MHC-I downregulation in PK-15 cells was not observed for any of BILF1 receptors including EBV-BILF1 (Figure 33B). Instead, an upregulation was observed, which is in contrast to our and previously published observations in HEK-293 cells. Therefore, the immunomodulatory function of BILF1 seems to depend on the cell type.

A HEK-293



B PK-15

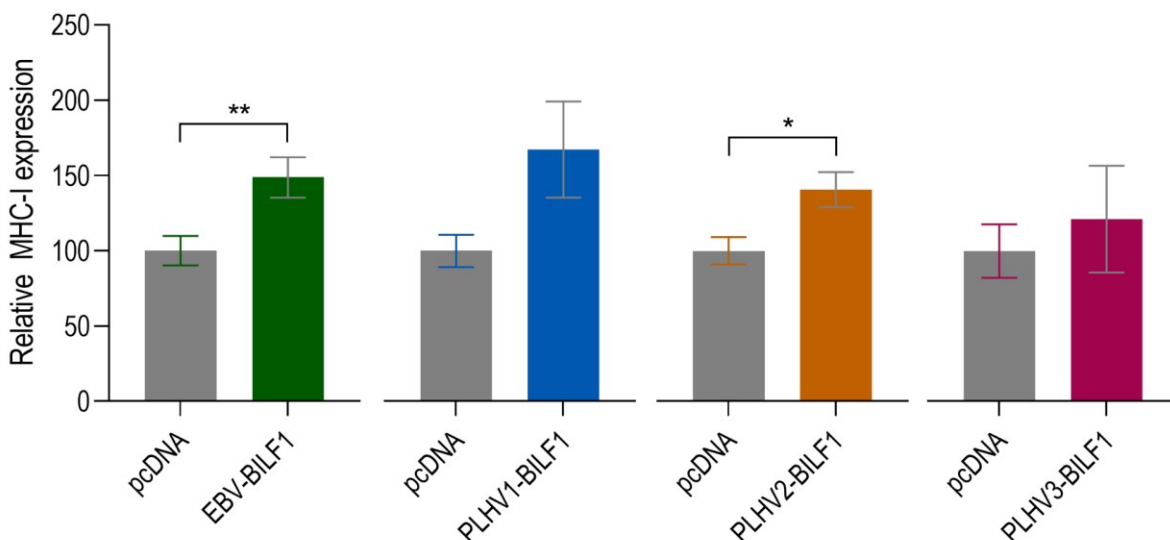


Figure 33: MHC-I downregulation studied by microscopy approach.

Slika 33: Meritve zniževanja površinske izraženosti molekul MHC-I z uporabo mikroskopije.

A novel approach using fluorescent microscopy was applied to measure the MHC-I expression in both A) HEK-293 and B) PK-15 cells expressing the BILF1 receptors. Rabbit anti-FLAG (BILF1 receptors) and mouse anti-human HLA-I antibodies were used to visualize the receptors and MHC-I molecules. Graphs represent the expression of MHC-I molecules at the surface of BILF1-transfected normalized to non-transfected cells (n = 33). Statistics were performed by unpaired Student t-test using GraphPad Prism. * $P < 0.05$; ** $P < 0.01$; **** $P < 0.0001$.

4.4.2 Expression of PLHV1 and PLHV1-BILF1 in samples from PTLD diseased pigs

Huang et al. previously proposed a novel model to study EBV-mediated disease, based on their observation that miniature pigs undergoing SOT or HSCT transplantation and immunosuppression develop EBV-like PTLD disease associated with PLHV1 infection (Huang et al., 2001). The expression of all three PLHVs in tissue samples of PTLD-diseased pigs was examined with Illumina sequencing (Figure 34A, B). Only PLHV1, but not PLHV2 or PLHV3, was detected in these samples, supporting the association of only one virus with PTLD. By RT-qPCR, the expression of PLHV1-3 BILF1 receptors was investigated in five samples (sample numbers: 13318, 13432, 15005, 13813, 14203) and in a control sample from a non-PTLD-diseased pig (noPTLD) (Figure 34C). RT-qPCR confirmed that only the PLHV1-BILF1 receptor was highly expressed in all five samples. Moreover, the expression of PLHV1-3 BILFs was compared in samples from before and after the disease onset (13318, 13432, and 15005) and in the no-PTLD control sample. Importantly, PLHV1-BILF1 was only detected after the disease onset but not in the samples from before the transplant of the same animal nor in a negative control (Figure 34C). Considering the fact that during EBV-mediated PTLD, a latency III program genes are expressed (Tse and Kwong, 2015), this indicates a potential expression of BILF1 during latency. However, a more detailed biological context remains to be studied in future.

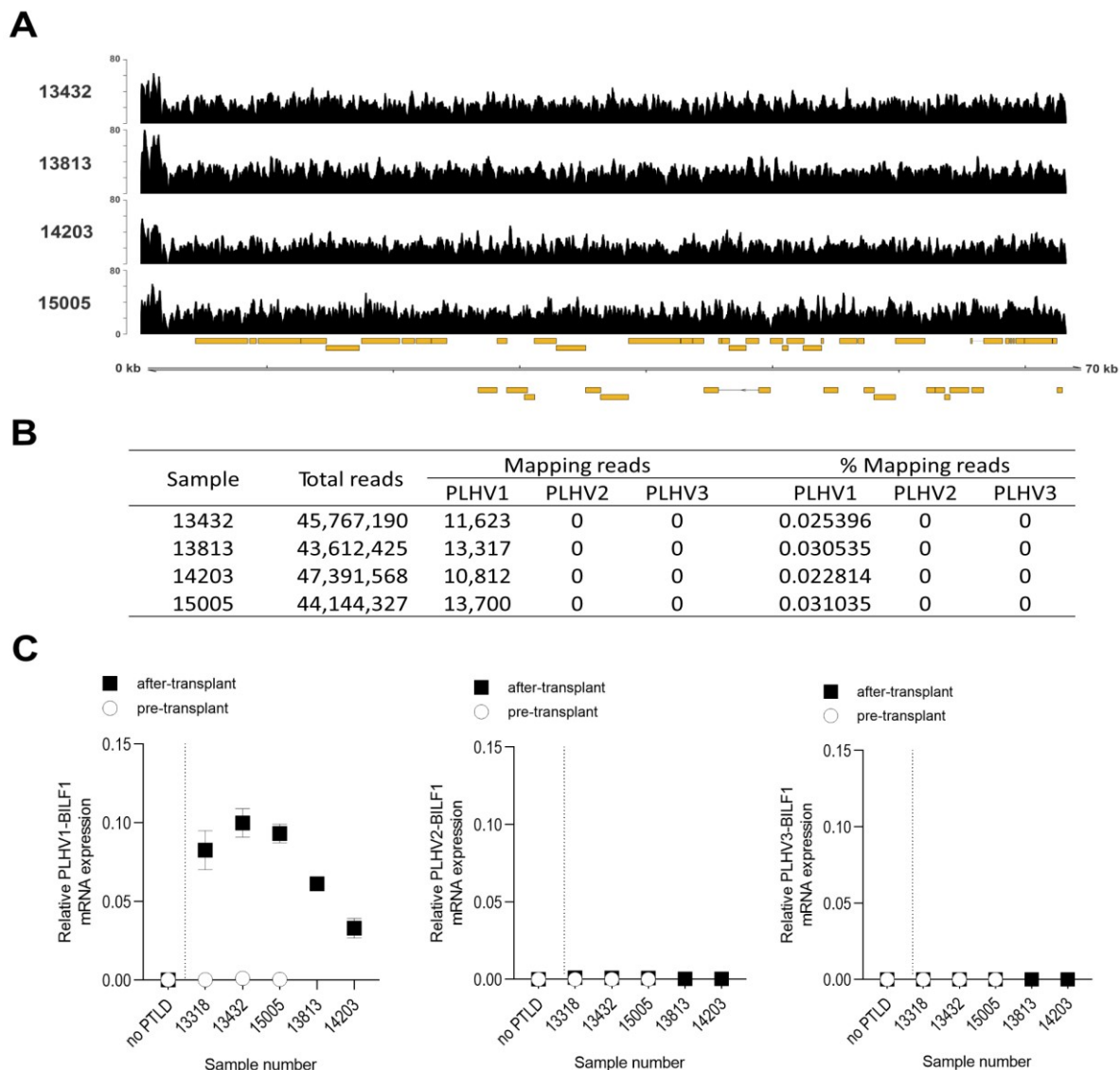


Figure 34: PLHV1 infection and PLHV1-BILF1 expression in PTLD diseased pigs.

Slika 34: Infekcija s PLHV1 in izražanje PLHV1-BILF1 v vzorcih tkiv prašičev, ki so razvili PTLD.

A) Illumina sequencing was used to identify a small number of sequence reads aligning to the PLHV1 UL region. Figure A represents coverage plots for each sample. The y-axis scale shows read depth and the x-axis indicates the genome fragment with annotated ORFs (gold boxes). B) Illumina sequence reads were used for competitive alignment against PLHV1, PLHV2, and PLHV3 genome fragments. C) RT-qPCR was used to determine the expression levels of PLHV1-3 BILF1 from cDNA of lymphoid tissue. Lymphoid tissue samples of PTLD diseased pigs were collected before and after disease onset. Results are mean \pm SEM of raw data and presented as $2^{\Delta Ct}$.

5 DISCUSSION

This thesis provides an in-depth characterization and comparison of the localization, internalization, trafficking, signaling, and immunoevasive properties of PLHV1-3 BILFs in comparison with EBV-BILF1.

Cell surface localization and constitutive endocytosis for all three BILF1 receptors in both human HEK-293 and porcine PK-15 cells were confirmed and described. Using a novel FRET-based real-time internalization assay, the constitutive internalization was measured in live HEK-293 cells and the requirement for functional dynamin and clathrin in their internalization was shown, suggesting the involvement of clathrin-mediated endocytosis. Applying internalization assay, BRET2, and bioinformatics analysis, it was shown that this pathway does not involve β -arrestin-1 and -2 for any of the BILF1 receptors. The observed effect of Cav S80E on BILF1 mediated trafficking and expression further showed the involvement of caveolin-1 in endocytosis for these vGPCRs. Finally, tracking the receptors intracellularly showed marked co-localization of BILF1 receptors with early endosomes (CD71 marker) but not with lysosomes or recycling endosomes. However, additional BRET1 saturation analysis proposed the interaction between EBV-BILF1 and PLHV1-2 BILF1 with marker of late endosomes/lysosomes Rab7. Additionally, comparing receptor expression under different labelling conditions proposed recycling for all BILF1 receptors.

Studies of BILF1 receptor-signaling pathways did not confirm the involvement of a MAPK pathway for any of the studied BILF1 receptors. However, conserved constitutive signaling mediated predominantly through $G\alpha_i$ was observed for all BILF1 receptors. Compared to EBV-BILF1, PLHV1-3 BILF1 activation of $Nf-\kappa B$ and NFAT transcription factors differed.

In a biological context, the ability of BILF1 receptors to downregulate MHC-I molecules from the cell surface was shown in human HEK-293 but not in PK-15 cells. Consistent with the data from previous studies showing the association of PLHV-1 with PTLD

disease, PLHV-1 infection and increased expression of PLHV1-BILF1 was observed in samples from PTLD-diseased pigs.

5.1 CONSTITUTIVE ENDOCYTOSIS AND TRAFFICKING

Constitutive internalization is a term describing the membrane receptor entering the cell independently of extracellular ligand. It has been observed for many vGPCRs (i.e., BILF1 receptors from human EBV (Spiess et al., 2015a, Mavri et al., 2020, Mavri et al., 2022), chimpanzee, orangutan, and siamang lymphocryptoviruses (Spiess et al., 2015a); ORF74 encoded by KSHV (de Munnik et al., 2015); US28 encoded by HCMV (Fraile-Ramos et al., 2001, Fraile-Ramos et al., 2003) and several endogenous GPCRs, such as β 2AR, M3 muscarinic receptor (Scarselli and Donaldson, 2009) and adhesion G protein-coupled receptor A3 (ADGRA3 also named GPR125) (Spiess et al., 2019). Although confirmed in many receptors, the functional role of constitutive internalization remains poorly understood. However, previous studies proposed several different functions for constitutive internalization of vGPCRs and GPCRs.

By constitutive internalization and subsequent recycling back to the plasma membrane, receptor expression at the plasma membrane is increased in the case of prolonged exposure to the agonist (Jacobsen et al., 2017). Constitutive internalization has also been described as a result of basal constitutive receptor activity (Leterrier et al., 2004). Moreover, recent studies are focusing on prolonged signaling, which occurs intracellularly in endosomes after receptor internalization. Furthermore, HCMV-US28 uses fast constitutive internalization to actively remove chemokines from the cell surface (i.e., ligand scavenge) (Bodaghi et al., 1998, Kledal et al., 1998). However, *in vitro* studies on endothelial cells did not report this effect, as US28 failed to prevent leukocyte adhesion; therefore, its scavenging role was questioned (Boomker et al., 2006). Furthermore, fast constitutive internalization of a previously mentioned HCMV-US28 has been exploited for drug-targeting purposes. By targeting the receptor with a selective fusion toxin protein (FTP), US28 constitutively delivered the toxin in the infected cells and induced cell death (Spiess et al., 2015b, Krishna et al., 2017, Spiess et al., 2017). This mechanism shows a targeting strategy for constitutively internalized

vGPCRs as novel drug targets, because their exclusive expression on infected cells provides a selective targeting mechanism. Here, the constitutive internalization for EBV and PLHV1-3 BILF1 receptors was confirmed using an antibody-feeding approach and novel FRET-based real-time internalization assay. The first approach allowed the visualization of the cells and receptors under the microscope, whereas the FRET-based real-time internalization assay allowed studying the endocytic properties in live cells. This novel method allows to perform multiple sequential measurements during the internalization process with no additional manipulation of the cells. In a previous study, Zuo et al. suggested that constitutive internalization of EBV-BILF1 may be the mechanism behind MHC-I downregulation (Zuo et al., 2009). However, to assign the biologic function more specifically for BILFs' constitutive internalization, further studies are warranted. With the recent progress and interest for pharmaceutical targeting of vGPCRs in general and recently reported BILF1 structure (Tsutsumi et al., 2021), the understanding of endocytic properties of these receptors can significantly contribute to designing a mechanism to target BILF1 in infected cells and thereby prevent its influence on infected cells. The results presented in this study show that the endocytic properties of BILF1 receptors require the intact functions of dynamin and clathrin assembly, which indicates the involvement of clathrin-mediated internalization. Previously, DNM Dyn K44A and chemical inhibitor Pitstop2 were used to determine endocytic properties of different GPCRs (Damke et al., 1994, Schmidlin et al., 2001, Kubale et al., 2007, von Kleist et al., 2011, Kroppen et al., 2021, Tazat et al., 2021). These studies reported these inhibitors as tools for the investigation of clathrin-mediated endocytosis. Dyn K44A prevents the scission of newly formed endocytic vesicles at the membrane; therefore, the mutant prevents the entry of the material in the cell through clathrin-coated pits and through caveolae. Pitstop2, in contrast, prevents the assembly between clathrin and amphiphysin, which prevents the formation of clathrin-coated vesicles. In addition to significant changes in BILF1 internalization induced by Dyn K44A and Pitstop2, changes in receptor expression were observed after the addition of Dyn K44A. RT-internalization assay allows measurement of receptor surface expression by measuring the donor emission only. Therefore, a comparison of the donor emission at time point 0 in cells expressing BILF1 receptors only, or BILF1 receptors together with Dyn K44A was performed. The surface

expression of BILF1 receptors (with the exception of PLHV3-BILF1) increased when co-transfected with increasing concentrations of Dyn K44A. This indicates that in the presence of Dyn K44A, BILF1 receptors retain at the cell surface, and the effect depends on the Dyn K44A concentration, which is in line with the effect of Dyn K44A on BILF1 receptor internalization. Noteworthy, PLHV3-BILF1 showed lowest effect in the FRET-based real-time internalization assay, which could be due to its low surface expression observed. The interpretation of the internalization results for this receptor is therefore difficult.

Clathrin-mediated endocytosis has been reported for majority of GPCRs (Weinberg and Puthenveedu, 2019). The pathway has been traditionally described as a consequence of G protein-mediated signaling, which is terminated at the cellular surface by β -arrestin. β -arrestin then further directs the cargo to clathrin-coated pits and promotes their internalization. However, the requirement for β -arrestin in this process depends on the receptor and receptor's mode of internalization (Luttrell and Lefkowitz, 2002). HCMV-US28, for example, can internalize in a constitutive or ligand-induced manner. In β -arrestin KO embryonic fibroblasts transfected with HCMV-US28, Fraile-Ramos et al. reported constitutive internalization as a β -arrestin-independent clathrin-mediated pathway (Fraile-Ramos et al., 2003). Furthermore, an adhesion GPCR ADGRA3 (GPR125) has also been reported to undergo the clathrin-dependent β -arrestin-independent pathway (Spiess et al., 2019). Here, this pathway was described as a characteristic of EBV-BILF1 and PLHV1-3 BILF1-mediated internalization. First, the receptors were expressed in both $\Delta\beta$ -arr1/2 KO HEK-293A cells and parental HEK-293 cells showing comparable internalization curves in both cell lines. Furthermore, these findings were supported by BRET2 assay, showing a non-specific recruitment between BILF1 receptors and β -arr2 and by bioinformatics that did not predict the interaction between these two proteins. BRET2-based β -arrestin recruitment assay has been widely used to determine specific interaction of GPCRs (e.g., NK-1 (Kubale et al., 2007) and D2 dopamine receptor (Kubale et al., 2016)) with β -arr2. A saturation assay was used, which resulted in simple linear regression curve, which indicates a so-called "bystander" or non-specific BRET2, indicating only random interaction between two proteins. BRET2 saturation assay was

also performed previously, describing insulin receptor (IR) homo- and heterodimerization (Mandić et al., 2014) and GLP-1 recruitment to β -arr2 (Jorgensen et al., 2011). Although the evidence for β -arrestin-independent, clathrin-mediated pathways has been reported for several GPCRs, its functional role remains to be defined. One mechanism directing these GPCRs to clathrin-mediated pits in an arrestin-independent way could be the interaction of GPCRs through the μ 2 adaptin subunit of AP2, which has been reported previously (Diviani et al., 2003, Paing et al., 2006). ISM analysis and identification of ELM motifs further confirmed the interaction of all BILF1 receptors with AP2, supporting the pathway proposed above.

In addition to clathrin-mediated pathways, endocytosis through caveolae has been described as a pathway for several GPCRs, viruses, and bacteria (Parton, 2018). However, novel studies report different tissue specific functions for caveolae. Caveolins (caveolin-1, -2 and -3) are characteristic proteins involved in the development of functional caveolae with cell-type and tissue-specific localization. Caveolin-1 and -3, but not caveolin-2, are importantly involved in the formation of caveolae. In HEK-293 cells, low levels of caveolin-1 and high levels of caveolin-2 have been observed; however, the formation of flask-shaped caveolae has not been reported in this cell line (Scherer et al., 1997, Li et al., 1998, Yu et al., 2004). In this study, the blocked function of caveolin-1 was achieved by expressing DNM Cav S80E. The mutant retains in the endoplasmic reticulum together with caveolin-2, and prevents its expression at the cell surface. Thereby, it also prevents the formation of caveolae. Despite low caveolin-1 expression and lack of caveolae in HEK-293 cells, a decreased internalization of BILF1 receptors co-transfected with increasing concentrations of Cav S80E was observed using RT-internalization assay. Similar was observed in previous studies by Lajoie et al; they studied endocytosis of cholera toxin B subunit (CT-B) and used *Mgat5*^{-/-} cell line that express few or no caveolae, similar to HEK-293 cells (Lajoie et al., 2009). They reported dynamin-dependent, raft-mediated endocytosis and suggested the involvement of caveolin-1 in the regulation of endocytosis after observing the effect of caveolin-1 depletion on CT-B mediated internalization. They further suggested the importance of caveolin-1 for internalization even at the expression levels below the threshold for caveolae formation. Moreover, they used the

same cell line to show the caveolin-1 mediated regulation of EGF-R diffusion and signaling (Lajoie et al., 2007). Similarly, the results presented here showed the importance for preserved dynamin and caveolin-1 function in BILF1 mediated internalization. Co-transfection with increasing concentrations of Cav S80E resulted in decreased surface expression for all BILF1 receptors. Presumably, this shows the intracellular retention of the receptor after the caveolin-1 function is impaired. Previously, caveolin has been reported to function as a chaperone for several GPCRs. After inhibiting caveolin function by DNMs, surface expression of GLP-1 receptor, insulin receptor and excitatory amino acid carrier 1 (EAAC1) decreased (Nystrom et al., 1999, Syme et al., 2006, González et al., 2007). To further support this observation, they mutated caveolin binding motifs on GLP-1R and IR and reported lower surface expression. Similar mutations were also performed on type 1 receptor for angiotensin II (AT1), which showed impaired surface expression and thereby suggested the involvement of caveolin in transporting the GPCRs toward the plasma membrane (Leclerc et al., 2002, Chini and Parenti, 2004). This implicates the involvement of multiple endocytic routes for BILF1 mediated endocytosis; however, their biological role remains to be elucidated.

After allowing their initial internalization from the plasma membrane, further investigation of the intracellular fate of the receptors was performed by visualizing the receptors in HEK-293 cells together with markers for intracellular organelles (early endosomes, lysosomes, and recycling endosomes). By measuring the colocalization on microscopy images, the colocalization between all BILF1 receptors and early endosomes was observed. For PLHV2-BILF1 and PLHV3-BILF1, a low colocalization was further observed with lysosomes, whereas for EBV-BILF1 and PLHV1-BILF1 a rather negative correlation was observed. Studying the colocalization on microscopy pictures is a challenging procedure and should ideally be supported with another approach to determine the specificity of interaction for different proteins. Moreover, different markers of recycling endosomes and lysosomes exist. In this study, Rab8 and LAMP1 were chosen based on the endogenous marker expression and antibody detection in HEK-293 cells. Additionally, BRET1 saturation experiments were performed, investigating possible recruitment between BILF1 receptors and Rab7, a

marker of late endosomes/lysosomes. A saturation was observed for EBV, PLHV1, and PLHV2 BILF1 receptors, showing that these receptors localize at these compartments during trafficking. A previously published study reporting MHC-I downregulating properties for EBV-BILF1 also showed that the addition of lysosomal inhibitors enhanced the intracellular pool of MHC-I molecules in EBV-BILF1 transfected cells (Zuo et al., 2009). To specifically determine the role of BILF1 constitutive endocytosis and to see the mechanism behind MHC-I downregulation, further studies are warranted.

Furthermore, comparing the expression of BILF1 receptors after SNAP-Lumi4Tb donor labelling at 4 °C and 37 °C, we have observed a difference in receptor amount that accounts for the receptors recycling back to plasma membrane. From the perspective of viral manipulation mechanisms, recycling of constitutively active BILF1 receptors, would provide adequate receptor expression at the cell surface and therefore the efficient MHC-I downregulation.

5.2 CONSTITUTIVE SIGNALING

Constitutive activity has been described for many vGPCRs with a link to their transforming potential (Rosenkilde et al., 2008, van Senten et al., 2020). HCMV-US28 (Casarosa et al., 2001, Miller et al., 2003) and KSHV-ORF74 (Waldhoer et al., 2003, Azzi et al., 2014) as well as EBV-BILF1 and BILFs of non-human primate Lymphocryptoviruses (Spiess et al., 2015a) have been described to signal and internalize constitutively. The oncogenic potential of EBV-BILF1 has been reported *in vitro* in stably transduced 3T3 cells and in mice, where it induced tumour growth *in vivo* and was linked to the ability of the receptor to signal constitutively through G α_i (Lyngaa et al., 2010). A previously described driver of KSHV-associated malignancies, KSHV-ORF74 induces cellular transformation, angiogenesis, and inflammation (Moore et al., 1996, Yang et al., 2000, Grisotto et al., 2006) as a consequence of ligand dependent (e.g., G α_q , G α_i , G $\alpha_{12/13}$, MAP kinases and transcription factors NF- κ B, NFAT and CRE) or constitutive activation of multiple signaling pathways (Bais et al., 1998, Munshi et al., 1999, Rosenkilde et al., 1999, Sodhi et al., 2000, McLean et al., 2004).

Furthermore, HCMV-US28 has been described as an onco-modulator, but direct oncogenic potential of this receptor remains to be described (Maussang et al., 2006, Heukers et al., 2018).

The ability of BILF1 receptors to activate ERK1/2 signaling pathways was investigated in this thesis for the first time. Biologically, this pathway regulates various processes from cell cycle progression, cell migration and survival, differentiation, metabolism to proliferation (Zou et al., 2019). Moreover, the pathway is upregulated in association with several oncogenic diseases (Marampon et al., 2019). Previous studies have reported a major role for β -arrestins as a scaffold protein of ERK, mediating the GPCRs signaling in a G protein-independent manner (Lefkowitz and Shenoy, 2005). In this study, no proof of the activation of ERK1/2 signaling pathway for any of the BILF1 receptors was shown. This is consistent with the finding that BILF1 receptors do not recruit and interact with β -arrestin, which presumably excludes the biased signaling for these vGPCRs.

In contrast, studying G protein-dependent signaling, the data obtained in this study showed constitutive, $G\alpha_i$ -dependent signaling for PLHV1-3 BILFs by observing inhibited forskolin induced CRE activity and enhanced CRE activity when co-transfected with chimeric $G\alpha_{\Delta 6qj4myr}$ protein. Based on transforming properties induced by $G\alpha_i$ mediated constitutive signaling of EBV-BILF1, a similar biological role could be assigned to PLHV1-3 BILFs, and these receptors may behave as oncogenes.

Activation of two downstream transcription factors NF- κ B and NFAT was previously reported for EBV-BILF1 in HEK-293 and COS-7 cells (Beisser et al., 2005, Zuo et al., 2011, Griffin et al., 2013, Spiess et al., 2015a). The advantage of this study was the use of CRISPR/Cas9 modified cells, which is a novel system to study specific G protein activation mediated by vGPCRs. Using this approach, downstream signaling of EBV-BILF1 and PLHV1-3 BILFs was determined, which allowed studying the involvement of specific G proteins leading to transcription factor activation. Both NF- κ B and NFAT transcription factors are regulating several important functions in the cell. NF- κ B regulates chemokine, cytokine, and growth factor secretion (Baeuerle and Henkel,

1994). NFAT plays an important role in cell proliferation and apoptosis as well as in the immune system function (Macian, 2005). Both transcription factors are regulated by KSHV-ORF74 and HCMV-US28, and their activation has been reported to control other downstream effectors eventually contributing to different cancer hallmarks, such as angiogenesis, production of inflammatory cytokines, and tumour-promoting properties (Soroceanu et al., 2011, Spiess et al., 2015a, van Senten et al., 2020).

EBV-BILF1-mediated NF- κ B activation was previously shown to up-regulate intracellular adhesion molecule-1 (ICAM-1), a factor involved in the progression of malignant cancer (Guo et al., 2020). Testing the activation of NF- κ B in parental HEK-293A cells and pan KO HEK-293A cells, we observed that PLHV1-2 BILF1 receptors activate this transcription factor to comparable levels as EBV-BILF1. PLHV3-BILF1, in contrast, did not activate NF- κ B. A comparison of signaling between cells expressing only G α_i (pan KO) and cells expressing total repertoire of G proteins (parental) showed approximately 50% lower activity for pan KO cells. This could indicate the involvement of other signaling pathways contributing to the activation of this factor (Ye, 2001). Such promiscuous G protein activation has been previously confirmed for HCMV-US28, for which coupling to different G proteins also depend on cell type and ligand binding (Vischer et al., 2006, Vomasse et al., 2009). Furthermore, endogenous receptors are also known for their high signaling promiscuity showing differential signaling properties in different tissues (tissue bias) and with different ligands (ligand bias) (Jørgensen et al., 2018). This is particularly important for drug development, as differential signaling could lead to specific effects associated with different signaling pathways (Jørgensen et al., 2018).

In BILF1 receptor family NFAT activation is conserved by EBV, marmoset and siamang herpesvirus-encoded BILF1 receptors (Spiess et al., 2015a). In contrast to the observed NF- κ B activity, NFAT was only activated by PLHV3-BILF1 to a level comparable to EBV-BILF1. The addition of G $\alpha_{q/11}$ proteins did not enhance NFAT activity in pan KO cells, which shows that NFAT activity of BILF1 receptors is mediated through G α_i . PLHV1-2 BILF1, in contrast, did not show NFAT activity, which suggests differences in PLHV BILF1 receptor downstream signaling. Importantly, the constitutive

signaling through G α_i protein was conserved for all PLHV BILF1 receptors and was comparable with the observed and previously reported EBV-BILF1 activity.

Several studies have reported the detection of all three PLHVs in blood and tissue samples from domestic pigs (Ehlers et al., 1999, Chmielewicz et al., 2003). Co-infections with different viruses occur frequently in pigs, and in the case of co-infection with porcine circovirus 2 (PCV2) and porcine reproductive and respiratory syndrome virus (PRRSV), the clinical outcome is severely worsened. However, in the case of separate infections, the viruses caused only mild or subclinical disease (Dong et al., 2015, Tu et al., 2015). Multiple infection with these viruses can alter the expression pattern of Toll-like receptors (TLRs) and pro-inflammatory cytokines, which may be one mechanism by which co-infection could lead to a more severe pathological outcome. The interplay between PLHV1-3 needs further investigation, but the fact that PLHV1-3 BILFs mediate different transcription factors may indicate differences between PLHV1-3 and their contribution to virus-associated diseases in pigs. Alternatively, all three viruses might be required to regulate the viral replication cycle in pigs, in contrast to EBV, where only one γ -herpesvirus has been reported. However, to conclude on this, studies in a more biological context are warranted.

5.3 BIOLOGICAL ROLE FOR BILF1 RECEPTORS

EBV-BILF1 has been assigned an important immunoregulatory role by showing its ability to downregulate MHC-I molecules at the surface of infected cells (Zuo et al., 2009). We therefore tested the ability of PLHV1-3 BILFs to downregulate MHC-I molecules in HEK-293 cells and PK-15 cells. Initially, flow cytometry studies showed the significant downregulation effect for PLHV3-BILF1, and a tendency for PLHV1-2 BILF1. However, the observed low transfection efficiency for PLHV1-3 BILF1 receptors in HEK-293 cells, both in terms of intensity of expression and percentage of transfected cells, aggravated the analysis. To overcome this limitation, a single-cell microscopy-based approach was applied, which allowed the study of the downregulation in cells with high expression levels of PLHV1-3 BILFs in both HEK-293 and PK-15 cells. This

method has the advantage of measuring the fluorescence intensity of the antibody-labelled MHC-I molecule on an individual single cell basis. Importantly, the experiments performed with the microscopy approach in HEK-293 cells supported and complemented the initial flow cytometry results, suggesting a conserved immunoevasive property for PLHV1-3 BILF1 receptors compared to EBV-BILF1. The homology model showed high sequence identity of human and porcine MHC-I molecules, which may explain the ability of PLHV1-3 BILFs to downregulate human MHC-I (HLA-I) molecules. It is important to add that the microscopy approach is limited by the small number of cells analysed. However, this method allowed reliable investigation of MHC-I downregulation in cells expressing higher levels of PLHV1-3 BILF1. Surprisingly, in PK-15 cells, neither EBV-BILF1 nor any PLHV1-3 BILF were able to downregulate porcine MHC-I molecules as shown by microscopy approach. It is unclear why downregulation, especially for PLHV BILFs, was not observed in porcine cells. However, it shows the importance for the choice of cell type to study this vGPCR property. A more appropriate tissue model to study BILF1-mediated MHC-I downregulation would be the B-cells, in which γ -herpesviruses establish a latent infection. PLHV1-3 frequently naturally occur in pigs. Therefore, the isolation of B-cells from seronegative piglets being bottle feed as negative controls is very work- and cost-intensive. Furthermore, to date, the PLHV1-3 whole genome sequence is not available. Genome sequences would be required for engineering a PLHV1-3- viruses or the deletion viruses, which would be further used for B-cell infection. These experiments are out of scope of this study, although they are highly relevant for future studies to establish the potential porcine *in vivo* model.

PTLD disease in pigs has been associated with PLHV1 infection and resembles the EBV-associated PTLD in humans occurring after HCT and SOT. The disease occurs as a response to either primary infection or reactivation of PLHV1 (Huang et al., 2001, Cho et al., 2004, Doucette et al., 2007). Similar disease aetiology between humans and pigs is further supported by the requirement for immunosuppression. This suggests that pigs represent a potential large animal model to study PTLD. Here, PLHV1 infection in PTLD diseased pigs and enhanced expression of only PLHV1-BILF1 was confirmed after disease onset, supporting the involvement of PLHV1 in

PTLD development. However, the detection of only PLHV1 but not PLHV2 and 3 in PTLD samples could result from the small experimental group size of minipigs. These pigs were also derived from a closed herd that has been bred intentionally over a long period to maintain defined MHC types for transplantation research (Cho et al., 2007, Duran-Struuck et al., 2015a, Duran-Struuck et al., 2015b). The high seroprevalence for all three PLHVs has been previously reported in many different breeds from around the world (Meng, 2012). Data here further support the involvement of PLHV1 infection in PTLD but cannot rule out the possibility that the PLHV2 and 3 infection may, similar to PLHV1, also be associated with this disease in animals infected with these viruses. It is also not possible to conclude whether the enhanced expression of BILF1 encoded by PLHV1 in these samples is a result of viral reactivation or upregulation of BILF1. It would be of interest to know whether PLHV1-BILF1 is upregulated during virus replication or through reactivation, but the whole genome sequence of PLHV1 remains lacking to answer this question. However, identification of the whole genome sequence of PLHV1 will be part of future studies and is out of the scope of this study.

Prior to organ transplantation, the degree of immunosuppression administered to prevent graft rejection is an important risk factor in EBV-PTLD development (Martinez and Krams, 2017) because PTLD results from uncontrolled expansion of EBV positive B cells from either donor or recipient. Previous studies reported that reconstitution of EBV specific cytotoxic T cells in the donor prevented the development of EBV-PTLD. This demonstrates that reconstituting the immunity against EBV is a successful approach against PTLD development (Papadopoulos et al., 1994, Heslop et al., 2010). Given its ability to downregulate MHC-I expression and thereby reduce CD8+ T recognition of infected cells, targeting BILF1 and suppressing its function would allow the immune system (T cells) to recognize and eliminate EBV infected cells. In a wider perspective, to identify EBV-BILF1 as a potential drug target and to study EBV mediated diseases, a reliable *in vivo* model is needed. Several different models exist but all show limitations. In general, mice are considered a valuable model in many different fields, but due to major differences of human and mice genetics, immunologic and physiologic characteristics, direct translation to human diseases, especially cancer, is limited (Duran-Struuck et al., 2019). However, severely immunodeficient

mouse strains (NOG and NSG) reconstituted with human stem cells provide a small animal model to study the development of lymphoma or lymphoproliferative disease (Islas-Ohlmayer et al., 2004, Yajima et al., 2008, Strowig et al., 2009, Fujiwara et al., 2015) and limited features of primary infection (Sato et al., 2011, Chijioke et al., 2013). Large animal models infected with inherent gammaherpesviruses homologous to EBV provide an excellent model to study different aspects of EBV infection and disease. Infection of naïve rhesus macaques with rhesus lymphocryptovirus (RhLCV) causes primary infection mimicking the one observed in EBV (Moghaddam et al., 1997). Further, in NHP models the development of PTLD has been observed following experimental immunosuppression and transplantation, in which cells in tumour tissue showed an infection with inherent Lymphocryptoviruses (Feichtinger et al., 1992, McInnes et al., 2002, Schmidtke et al., 2002, Kamperschroer et al., 2016). Pigs can also mimic the characteristics of human PTLD after both HCT and SOT as a response to either reactivation or primary infection of PLHV1 (Huang et al., 2001, Cho et al., 2004, Doucette et al., 2007) and therefore serve as an excellent large animal model for PTLD disease. The large size and long-life span of pigs allows sample collection (blood, tissue) and monitoring over a long period of time (Dor et al., 2004, Doucette et al., 2007, Duran-Struuck et al., 2015a, Duran-Struuck et al., 2015b, Duran-Struuck et al., 2019). Human PTLD samples are mostly limited to serum samples due to technical challenges to conserve whole blood samples over time. Further, large amounts of organ tissue are not easily available. With serum sample material lacking B-cells, the expression levels of EBV-BILF1 cannot be determined. In contrast, suitable sample material is available in porcine models, where the expression of BILF1 receptor can be determined from tissue material, such as spleen and lymph nodes during PTLD development. Furthermore, such model would allow using recombinant viruses such as PLHV1-3 BILF1 deletion viruses and genetically modified PLHV1-3 BILFs and thus study their importance in PTLD development. Considering the ethical problems and high costs of NHP models, similarities between human and porcine PTLD and the homology between EBV-BILF1 and PLHV1-BILF1 in terms of signaling, internalization, and MHC-I downregulation, PLHV1-infected pigs could contribute to PTLD studies and the development of anti-cancer drugs in pre-clinical trials. Blocking specific functions of EBV-BILF1 by drug targeting has been suggested after engineering this receptor to

contain a binding site for a “tool” compound (Fares et al., 2019). EBV-BILF1 remains an orphan receptor, but new technologies such as phage display and a recently published structure of EBV-BILF1 offer a potential to determine the potential ligand for the vGPCR (Tsutsumi et al., 2021). A future development of a minipig model infected with PLHV1, could provide a suitable *in vivo* model to study the role of BILF1 in PTLD development and its potential use as drug target for the treatment of PTLD.

6 CONCLUSIONS

HYPOTHESIS 1: The BILF1 receptor family undergoes constitutive endocytosis by employing multiple pathways.

- Constitutive internalization was confirmed by antibody-feeding approach and novel real-time internalization method for all BILF1 receptors.
- The effect of DNM Dyn K44A and chemical inhibitor Pitstop2 on BILF1 receptor internalization and BILF1 receptor expression shows the involvement of clathrin-mediated pathways.
- The effect of DNM Cav S80E on BILF1 receptor internalization shows the importance for functional caveolin in receptor trafficking and suggests the involvement of clathrin-independent endocytosis.

HYPOTHESIS 2: Internalization of the BILF1 receptor family is independent of the cell type.

- Constitutive internalization was confirmed by antibody-feeding approach and novel real-time internalization method for all BILF1 receptors in both human HEK-293 cells and porcine PK-15 cells.

HYPOTHESIS 3: Constitutive signaling properties of BILF1 depend on G proteins.

- All BILF1 receptors signal constitutively through $G\alpha_i$ as exemplified by the ability to downregulate forskolin induced cAMP and by increasing the CRE activation when co transfected with chimeric $G\alpha_{\Delta 6q14myr}$ protein.
- None of the BILF1 receptors activate ERK1/2-mediated pathways and do not recruit or interact with β -arrestin.
- Differences were observed in the ability of BILF1 receptors to activate downstream transcription factors NF- κ B and NFAT.

HYPOTHESIS 4: The immune evasion strategy of PLHV1 corresponds to that of EBV.

- The ability to downregulate MHC-I molecules was conserved for all BILF1 receptors in human HEK-293 cells as shown by flow cytometry and microscopy approach.
- None of the BILF1 receptors downregulated the MHC-I molecules in porcine PK-15 cells.

7 SUMMARY

Several herpesviruses (e.g. EBV, HCMV, KSHV) use multiple strategies to infect and persist in the host for lifetime. One such mechanism is the expression of vGPCRs, proteins structurally and functionally similar to endogenous GPCRs that are critically involved in physiological, immunological, and metabolic processes in the cell. vGPCRs were presumably acquired from the host through ancient act of molecular piracy and are now used by the virus to manipulate and evade the host immune response and thereby benefit the viral life cycle. Moreover, GPCRs and, more recently, vGPCRs are recognized as important drug targets for many diseases. A critical step in confirming a receptor as a drug target requires an in-depth characterization and validation of pharmacological properties.

The aim of this thesis was to characterize the pharmacological properties of BILF1 receptors encoded by three porcine gammaherpesviruses (PLHV1-3) and compare them to the well-described EBV-BILF1 receptor. We characterized BILF1 receptor localization, signaling, trafficking and immune evasive properties, as well as their contribution in PTLD disease was described. According to our aims, four hypothesis were tested: i) the BILF1 receptor family undergoes constitutive endocytosis by employing multiple pathways; ii) internalization of the BILF1 receptor family is independent of the cell type; iii) constitutive signaling properties of BILF1 depend on G proteins, and iv) the immune evasion strategy of PLHV1 corresponds to that of EBV.

We first confirmed predominant surface expression in both HEK-293 and PK-15 cells for all BILF1 receptors. Comparing the expression profiles between BILF1 receptors, EBV-BILF1 showed highest expression in both cell lines whereas PLHV3-BILF1 showed lowest expression. The low expression of PLHV3-BILF1 was further observed in other assays described below, and often complicated the analysis of the results.

Internalization occurs at the plasma membrane and allows receptors to enter the cell after ligand-induced activation or in a ligand-independent way (i.e., constitutive internalization). Constitutive internalization was here confirmed for all BILF1 receptors

in both human HEK-293 and porcine PK-15 cells, using an antibody feeding approach, which allows visualization of the internalized receptors and a novel FRET-based real-time internalization assay which allows the measurement of receptor internalization in live cells. Using this novel assay in HEK-293A cells expressing SNAP-tagged BILF1 receptors and DNM Dyn K44A or chemical inhibitor Pitstop2, we determined that internalization occurs through clathrin-coated vesicles. Furthermore, additional internalization studies in $\Delta\beta$ -arr1/2 KO cells, and studies of protein-protein interactions by BRET2 saturation assay and ISM analysis, showed that the internalization occurs in a β -arrestin independent manner. Similar was also observed in other GPCRs, i.e., HCMV-US28 and ADGRA3 (GPR125). In addition, using novel FRET-based real-time internalization assay in combination with DNM Cav S80E, trafficking of BILF1 receptors in association with caveolin has also been shown. Together, these results confirm our hypothesis 1 and 2, showing conserved constitutive internalization in HEK-293 and PK-15 cells which includes multiple pathways.

Furthermore, the fate of BILF1 receptors after their internalization from the plasma membrane was investigated. Initially, using microscopy approach observing the co-localization of BILF1 receptors and markers of intracellular organelles (transferrin receptor or CD71 as a marker of early endosomes, LAMP1 as a marker of lysosomes and Rab8 as a marker of recycling endosomes), the co-localization was only confirmed with early endosomes. Further, to support microscopy studies, BRET1 studies were performed, looking at the interaction between BILF1 receptors and Rab7 (marker of late endosomes/lysosomes). In contrast to microscopy studies, BRET1 confirmed the trafficking of BILF1 receptors to late endosomes/lysosomes and showed that at least a fraction of these receptors gets degraded.

Moreover, novel FRET-based real-time internalization assay allows the measurement of receptor expression by measuring the emission of donor labelled receptors. Observing the expression differences when labelling receptors at 4 °C (internalization is prevented during donor labelling step) or 37 °C (internalization is allowed during donor labelling step) indicated the recycling of BILF1 receptors.

Constitutive activity is a conserved property among vGPCRs. For EBV-BILF1, signaling through G α_i has been described to induce cell transformation *in vitro* and tumour growth *in vivo*. Constitutive, G α_i -dependent signaling was confirmed here for PLHV-BILF1 receptors. This possibly suggests that these receptors, like EBV-BILF1, may have cell-transforming properties and may behave as oncogenes. In contrast, the fact that PLHV1-3-BILFs mediate different transcription factors may indicate differences between PLHV1-3 and their contribution to virus-associated diseases in pigs. Alternatively, all three viruses might be required to regulate the viral replication cycle and establish latency in pigs, in contrast to EBV, for which only one gammaherpesvirus has been reported. Based on the different signaling properties of PLHV1-3 BILFs, multiple infection with all three PLHVs may be required to exhibit what EBV-BILF1 can activate as a single vGPCR. Additionally, we did not show the BILF1-mediated activation of ERK1/2, a pathway usually associated with the recruitment of β -arrestin. This is in line with the observation from BRET2 and ISM analysis where the interaction between BILF1 receptors and β -arrestin2 was not confirmed. This indicates that constitutive activity of EBV and PLHV1-3 BILFs is G protein-dependent, which confirms our hypothesis 3. However, the hypothesis is only partially confirmed because the signaling properties were not conserved for all BILF1 receptors, as shown by differential activation of NF- κ B and NFAT transcription factors.

In a biological context, EBV-BILF1 has an important immunoevasive role through downregulation of surface MHC-I molecules. Significantly, we showed this to be a conserved property for all PLHV1-3 BILFs in HEK-293 cells. However, in porcine PK-15 cells, we did not observe the downregulation of porcine MHC-I molecules but rather upregulation by EBV- and PLHV1-3-BILF1 receptors. This partially confirms our hypothesis 4, as the effect on MHC-I expression is conserved for all receptors, although the effect varies depending on the cell type.

The development of human PTLD is associated with EBV and causes a possibly fatal complications after organ transplant. In pigs, similar disease was reported with a link to the infection with PLHV1. Here, we had an opportunity to examine samples of pigs taken prior and after the disease onset and determine the virus and receptor

expression. We showed the exclusive expression of PLHV1 in these samples, which confirms the findings of the previous studies showing the link between PLHV1 and PTLD. Moreover, we showed that PLHV1-BILF1 expression increased after the disease onset, which points out the importance of the receptor in the development of the disease. In a wider perspective, the requirement for a novel drug target against EBV-associated diseases is high. Reconstituted immunity against EBV has been shown as a successful approach against the PTLD development. Since EBV-BILF1 reduces CD8⁺ T-cell recognition of infected cells by manipulating MHC-I expression, targeting BILF1 and suppressing its function would allow better recognition and elimination of EBV infected cells by T-cell recognition.

Given the high drugability of GPCRs in general and its function as an immunoevasin, BILF1 represent a possible novel drug target against EBV. Recently published structure of EBV-BILF1, showing the specific features of this receptor and a highly conserved constitutive activity, will importantly contribute to the development of BILF1 receptor targeting strategies.

However, pre-clinical models allowing the target validation of BILF1 receptors and the study of EBV-mediated diseases are currently lacking. The data presented in this thesis suggest that pigs infected with PLHV1 could serve as such a model to study BILF1 as potential driver and drug target in EBV-mediated proliferative diseases.

8 POVZETEK

Cilja te raziskave sta opredelitev farmakoloških lastnosti ortologov BILF1, ki so kodirani v treh prašičjih gamaherpesvirusih (PLHV1-3), in primerjava s predhodno proučevanim receptorjem EBV-BILF1. Receptorje BILF1 smo proučevali z vidika njihove lokalizacije, znotrajceličnega prenosa signala, znotrajcelične prerazporeditve ter sposobnosti izogibanja imunskemu sistemu in izražanja virusne RNA v vzorcih prašičev, ki so razvili posttransplantacijsko limfoproliferativno bolezen. V širšem kontekstu je poglobljena študija receptorjev BILF1 na celični in molekularni ravni potrebna za nadaljnje raziskave za opredelitev novega *in vivo* modela, s katerim bi prikazali potencial receptorja BILF1 kot tarče za zdravila.

S proteinom G sklopljeni receptorji (GPCR-ji) so velika skupina transmembranskih proteinov, ki prenašajo signal v celico prek membrane iz zunajceličnega prostora. So tarče za kar 34 % vseh trenutno odobrenih zdravil na tržišču in tako pomembno prispevajo k zdravljenju različnih oblik bolezni. Imajo značilno strukturo, sestavljeno iz sedmih transmembranskih segmentov (od tod tudi alternativno poimenovanje 7-transmembranski receptorji; 7TM), ki so povezani s tremi zunajceličnimi zankami in tremi znotrajceličnimi. Receptorji se v citoplazemskem delu končujejo s karboksilnim koncem (C-terminalni del), na zunajceličnem delu pa z amskim (N-terminalni del). Na osnovi sekvence in strukturne podobnosti so GPCR-ji razdeljeni v pet poddružin: družina receptorjev, podobnih rodopsinu (družina A), sekretinska/glukagonska receptorska družina (družina B), metabotropična/glutamatska družina (družina C) ter družina adhezijskih receptorjev in receptorjev za okus (družina F). GPCR-je aktivirajo različni stimuli: endogeni metaboliti, neurotransmiterji, citokini, hormoni, okoljski ioni, vonjave in svetloba. Najnovejši napredki na področju krio-elektronske mikroskopije (krio-EM) so omogočili vpogled v molekularne mehanizme receptorjev, ki temeljijo na strukturnih lastnostih in so poglobili poznavanje na področju prenosa signala pri GPCR-jih. Ti novi pristopi bodo v prihodnje tudi pomembno vplivali na raziskave s področja neopredeljenih receptorjev in raziskave novih potencialnih zdravil.

Družino herpesvirusov (Herpesviridae) sestavljajo tri poddružine: alfaherpesvirus (Alphaherpesvirinae), betaherpesvirus (Betaherpesvirinae) in gamaherpesvirus

(Gammaherpesvirinae). Poddružina gamaherpesvirusov se naprej deli še na rodove limfokriptovirus, macavirus, patagivirus, percavirus in radinivirus. Gamaherpesvirusi so široko razširjeni DNA-virusi z značilnim dvofaznim življenjskim ciklom: litično (uničujočo) in latentno (prikrito) fazo. Po primarni okužbi, ki je običajno asimptomatska, virusi okužijo dovzetne celice in med litično fazo sprožijo aktivno replikacijo. Imunski sistem se običajno na okužbo odzove in prepreči hujši potek bolezni. Med evolucijo so se herpesvirusi na gostiteljev imunski odziv prilagodili z več mehanizmi: i) z razvojem strategij za izogibanje imunskemu sistemu; ii) s tem da so zmanjšali izražanje genov na omejeno število; iii) z integracijo v gostiteljev genom. Vsi ti mehanizmi jim omogočajo, da učinkovito in neopaženo doživljenjsko preživijo v gostitelju. Čeprav virus med latentno okužbo izraža le omejeno število genov, lahko v tem času povzroči nastanek patoloških sprememb oz. novotvorb, na primer PTLD in Burkittov maligni limfom. Herpesvirusi se lahko občasno reaktivirajo in sprožijo litično fazo ter tako okužijo nove celice ali novega gostitelja. Pri imunsko oslabljenih gostiteljih in otrocih lahko reaktivacija vodi do nastanka hujših patoloških obolenj.

Virus Epstein-Barr (EBV) ali humani herpesvirus 4 (HHV4) spada v rod limfokriptovirusov in je razširjen pri 95 % svetovne populacije. Je onkavirus, ki letno povzroči približno 50.000 novih onkogenih obolenj, in je pogosto povezan z nastankom klasičnega Hodgkinovega limfoma, karcinoma nosnega žrela, Burkittovega malignega limfoma in raka želodca. Poleg tega je bil EBV prepoznan kot vodilni dejavnik pri razvoju PTLD pri imunsko oslabljenih pacientih po presaditvi organov ali kostnega mozga. PTLD je hujša komplikacija, ki se pojavlja po transplantaciji, ter se kaže v obliki različnih vrst tumorjev in ima visoko incidenco umrljivosti. Tako kot drugi gamaherpesvirusi lahko tudi EBV prehaja med litično in latentno okužbo. Po primarni okužbi, ki je običajno asimptomatska, EBV vzpostavi latentno doživljenjsko okužbo v spominskih limfocitih B. Pri EBV poznamo štiri stopnje latentnosti (0, I, II, III), ki se med seboj razlikujejo po tem, kateri specifični proteini so izraženi v določeni fazi. Različne faze so tudi značilne za različna z EBV povezana maligna obolenja. Na drugi strani se litična faza pojavi ob primarni okužbi ali pri ponovni aktivaciji virusa. Za to fazo je značilno uravnavano izražanje genov s takojšnjimi zgodnjimi (iz angl. immediate early; IE), zgodnjimi (iz angl. early; E) in poznimi (iz angl. late; L) geni. Izražanje genov IE

spodbudi začetek litične faze ter hkrati aktivira gene E in L. Geni E imajo pomembno vlogo pri i) podvojevanju virusne DNA z virusno DNA polimerazo (BALF5), ii) metabolizmu in iii) inhibiciji procesiranja antigenov, pri čemer imajo glavno vlogo proteini BNLF2a, BGLF5 in BILF1. Geni L imajo strukturno vlogo in sodelujejo pri sestavljanju ovojničnih glikoproteinov oziroma novih virionov in pri imunoregulaciji.

Pri prašičih poznamo tri gamaherpesviruse – PLHV1, 2 in 3 –, imenovane tudi prašičji herpesvirus 3, 4 in 5 (SuHV-3, SuHV-4 in SuHV-5), ki spadajo v rod macavirusov. Podobni so antilopjemu herpesvirusu 1 (AIHV-1), ovčjemu herpesvirusu 2 (OvHV-2) govejemu limfotropnemu gamaherpesvirusu in humanemu virusu EBV. Aminokislinsko zaporedje PLHV1 in PLHV2 kaže 85–98-odstotno identičnost, medtem ko ima PLHV3 nižjo, 49–89-odstotno identičnost s PLHV1 in PLHV2. Prevalenca okužbe pri prašičih je 29–80-odstotna (PLHV1), 11–41-odstotna (PLHV2) in 5–65-odstotna (PLHV3). Nekateri raziskave opisujejo tudi sočasno okužbo z vsemi tremi virusi pri domačih prašičih. Podobno kot EBV tudi PLHV-ji po primarni okužbi navadno vzpostavijo vseživljenjsko latentno okužbo v limfocitih B. Patološkega potenciala za PLHV1-3 do danes še niso dokazali, vendar je znano, da lahko virusi ob sočasni infekciji z drugimi patogenimi povzročitelji poslabšajo klinično sliko. Poleg tega so pri poskusnih prašičih, ki so bili poskusno imunsko oslabljeni, ob presaditvi kostnega mozga ugotovili, da lahko razvijejo PTLD s podobnimi morfološkimi in histološkimi značilnostmi, kot se kažejo pri humani obliki bolezni PTLD, ki jo povzroča EBV.

Herpesvirusi uporabljajo za okužbo gostitelja in preživetje v njem različne strategije. Ena od teh je izražanje vGPCR-jev, proteinov, ki so strukturno in funkcionalno podobni znotrajceličnim GPCR-jem. Ti so pomembno vpleteni v fiziološke, imunološke in metabolne procese v celici. vGPCR-je so virusi med evolucijo prevzeli od gostitelja ter jih zdaj uporabljajo za manipulacijo in izogibanje gostiteljevemu imunskemu sistemu, kar posledično koristi življenjskemu ciklu virusa. GPCR-ji in v zadnjem času tudi vGPCR-ji so prepoznani kot pomembne tarče za zdravila proti različnim boleznim. Pomembna koraka pri potrjevanju receptorjev kot potencialnih tarč za zdravila sta njihova podrobna opredelitev in potrditev njihovih farmakoloških lastnosti.

Predstavniki vGPCR-jev so US28, kodiran v humanem citomegalovirusu (HCMV, beta herpesvirus); ORF74, kodiran v humanem herpesvirusu 8 (HHV8, gamma herpesvirus; KSHV iz angl. Kaposi's sarcoma herpesvirus) in ekvinem herpesvirusu 2 (EHV2, gamma herpesvirus), ter BILF1, kodiran v 21 različnih gamma herpesvirusih, vključujoč EBV, primatske limfokriptoviruse, PLHV1, 2 in 3, AIHV1, OvHV2 in EHV2. ORF74 in US28 sta strukturna GPCR homologa gostiteljevim kemokinskim receptorjem ter imata visoko afiniteto za vezavo z virusnimi in gostiteljevimi kemokini, kar vodi do aktivacije znotrajceličnega prenosa signala. Nasprotno je EBV-BILF1 uvrščen med receptorje »sirote«, saj še ne poznamo liganda, ki bi se vezal nanj. Vsi trije omenjeni receptorji so bili povezani z nastankom tumorjev ali kot onkogeni (ORF74 in BILF1) ali kot onkomodulatorji (US28).

EBV-BILF1 je do danes najbolje opisan receptor iz družine receptorjev BILF1. Primarno se izraža med litično fazo okužbe z značilno progresivno aktivnostjo med to fazo, vendar so njegovo izražanje zaznali tudi med latentno okužbo v vzorcih tkiv Burkittovega limfoma. EBV-BILF1 se večinoma izraža na površini okuženih celic. Je onkogen z od liganda neodvisno konstitutivno aktivnostjo prek G_{α_i} ; aktivnost, povezana s celično transformacijo, ki je bila dokazana tako *in vitro* kot tudi *in vivo*. EBV-BILF1 konstitutivno aktivira znotrajcelični transkripcijski jedrni faktor kapa B (NF- κ B) in jedrni faktor aktiviranih celic T (NFAT) in znižuje s forskolinom inducirano transkripcijo odzivnega elementa za ciklični adenzin monofosfat (cAMP) (CRE). V limfocitih B, ki izvirajo iz tkiv Burkittovega limfoma, in celicah COS-7 EBV-BILF1 znižuje fosforilacijo od RNA odvisne proteinske kinaze (PKR; iz angl. RNA-dependent protein kinase), encim, ki pomembno vpliva na gostiteljev obrambni mehanizem pred virusno okužbo. Dodatno so pred kratkim odkrili še en mehanizem, ki ga EBV-BILF1 uporablja za izogibanje imunskemu sistemu gostitelja. Na površini okuženih celic znižuje površinsko izraženo molekulo MHC-I in s tem preprečuje prepoznavo okuženih celic s strani limfocitov CD8+. Ta lastnost naj bi bila pogojena s sposobnostjo receptorja EBV-BILF1 za konstitutivno endocitozo. Predvideva se, da je EBV-BILF1 vpleten pri procesiranju nosilcev novosintetiziranih molekul MHC-I na površino celice (eksocitoza) in pri prehajanju molekul MHC-I v celico (endocitoza). Pred kratkim objavljena struktura EBV-BILF1 je pokazala značilne razlike v primerjavi z družino A GPCR-jev. V nasprotju

z do zdaj znanimi strukturami kemokinskih receptorjev in vGPCR-jev je zunajcelična zanka 2 (ECL2; iz angl. extracellular loop 2) pri receptorju EBV-BILF1 oblikovana kot pokrov, ki skupaj z zunajcelično zanko 3 (ECL3; iz angl. extracellular loop 3) zapira vhod v vezavno mesto in tako onemogoča vezavo zunajceličnih ligandov. Glede na ohranjenost sekvenc na območju ECL2 pri drugih predstavnikih družine BILF1 lahko sklepamo, da je ta lastnost ohranjena pri vseh predstavnikih BILF1.

V nasprotju z EBV-BILF1 farmakološke lastnosti BILF1, kodiranih v PLHV1-3, še niso bile opisane. PLHV1-ji so zanimivi z vidika podobnosti z EBV in zaradi dejstva, da lahko prašiči, ki so naravno okuženi z virusom PLHV1, eksperimentalno razvijejo PTLD, primerljiv s humano obliko PTLD, pri kateri je bil EBV prepoznan kot gonilo bolezni. V širšem pogledu bo poglobljeno poznavanje lastnosti ortologov BILF1 postavilo temelj za razvoj novega prašičjega modela *in vivo* in pokazalo ustreznost receptorja BILF1 kot tarče za protivirusna zdravila.

Ortologe BILF1 smo opredelili z vidika lokalizacije, signalizacije, znotrajceličnega razporejanja in izogibanja imunskemu sistemu ter njihove vloge pri razvoju bolezni PTLD. V skladu s cilji smo si zastavili štiri hipoteze: i) konstitutivna endocitoza receptorjev družine BILF1 poteka prek različnih poti; ii) internalizacija receptorjev družine BILF1 ne poteka v odvisnosti od vrste celic; iii) konstitutivno signaliziranje receptorjev BILF1 je odvisno od proteinov G; iv) za izogibanje imunskemu sistemu gostitelja uporablja PLHV1 enako strategijo kot EBV.

Za dosego teh ciljev smo uporabili dve celični liniji (humane celice HEK-293 in prašičje celice PK-15) in z epitopom označen receptor BILF1, vstavljen v različne vektorske sisteme. Oznaka na receptorju BILF1 omogoča prepoznavo receptorjev, saj specifična protitelesa niso na voljo. Standardne metode v molekularni biologiji, kot so transformacija plazmidne DNA, čiščenje plazmidne DNA in kvantifikacija DNA, so omogočile pripravo cDNA visoke kakovosti, ki smo jo pozneje vnesli v evkarionske celice s prehodnimi kemičnimi metodami transfekcije. Različne vektorske sisteme smo uporabili glede na posebne zahteve različnih uporabljenih metod.

Najprej smo s testom ELISA in mikroskopijo potrdili prevladujočo izraženost receptorjev BILF1, označenih z oznako FLAG na N-terminalnem koncu na površini celic HEK-293 in PK-15. Primerjava izraženosti med receptorji BILF1 je pokazala največjo izraženost EBV-BILF1 v obeh celičnih linijah, medtem ko je bil receptor PLHV3-BILF1 najnižje izražen. Nizka izraženost receptorja PLHV3-BILF1 je bila pozneje opažena tudi pri drugih metodah, opisanih v nadaljevanju, in je pogosto otežila analizo rezultatov.

Za vzdrževanje homeostaze v celici se ta odziva na zunanje okolje in se sporazumeva z njim prek celične membrane. Različne molekule iz zunajceličnega okolja prehajajo prek celične membrane s pomočjo različnih mehanizmov endocitoze. Poleg tega endocitoza receptorjev, ki vključuje internalizacijo teh, uravnava znotrajcelični prenos signala na membrane in nadzoruje razpoložljivost receptorjev na membrani za nadaljnjo aktivnost, ki je odvisna ali neodvisna od liganda.

Glede na material se endocitoza deli na dva procesa, na pinocitozo in fagocitozo. Prek pinocitoze celica prevzema majhne delce in tekočino. Fagocitoza poteka v posebej prilagojenih celicah, imenovanih fagociti, ki so specializirane za prevzem večjih molekul (> 500 nm). Pinocitoza se glede na velikost veziklov, ki se oblikujejo na membrani, deli še na makro- in mikropinocitozo. Makropinosomi so večji, raznoliki endocitotski vezikli (200–500 nm), medtem ko so mikropinosomi manjši (50–60 nm) ter jih glede na proteinsko sestavo delimo še na klatrinske vezikle (klatrinsko posredovana endocitoza), kaveole (kaveolinsko posredovana endocitoza) in neobložene mešičke.

Internalizacija je proces, ki receptorjem omogoči prehod iz celične membrane v celico ali po njihovi aktivaciji z ligandom ali od liganda neodvisno (konstitutivna internalizacija). Zadnja je bila pred kratkim opisana kot pomembna lastnost receptorja US28, kodiranega v humanem citomegalovirusu (HCMV), ki so ga uporabili kot tarčo za imunotoksin in nanotelesa, s čimer so celice, okužene z virusom HCMV, uspešno odstranili. Dodatno je bila sposobnost EBV-BILF1 za zniževanje površinske izraženost molekul MHC-I na površini celic opisana kot posledica internalizacije kompleksa

BILF1/MHC-I. Z uporabo testa, ki obravnava od temperature odvisno endocitozo receptorjev v različnih časovnih intervalih (iz angl. antibody-feeding), ki omogoča vizualizacijo receptorjev in novega testa internalizacije v realnem času, ki omogoča meritve internalizacije receptorjev v živih celicah, smo pokazali ohranjenost konstitutivne internalizacije za vse receptorje BILF1 v humanih celicah HEK-293 in prašičjih celicah PK-15. Nova metoda internalizacije v realnem času omogoča spremljanje internalizacije receptorjev, označenih z oznako SNAP, v živih celicah na podlagi prenosa energije med donorjem in prejemnikom. Receptor, označen z oznako SNAP, v prvem delu poskusa označimo z donorsko molekulo, ki se ireverzibilno veže na oznako SNAP. V nadaljevanju poskusa celicam dodamo akceptorsko molekulo, ki ne prehaja med zunaj- in znotrajceličnim prostorom, tako da z donorsko molekulo reagira le, ko je ta prisotna na zunajcelični strani membrane. Tako lahko v realnem času opazujemo spremembe v prenosu energije med molekulama in sklepamo, ali je receptor na površini celice ali v njeni notranjosti.

Z novo metodo internalizacije v realnem času smo v celicah HEK-293A, ki so izražale receptor BILF1, označen z oznako SNAP, in DNM Dyn K44A ali kemični zaviralec Pitstop2, potrdili, da internalizacija poteka prek klatrinskih mešičkov. Dodatne analize internalizacije v modificiranih celicah CRISPR/Cas9 z izbitim genom za β -arrestin 1 in 2 ($\Delta\beta$ -arr1/2 KO celice) ter analize proteinsko-proteinskih interakcij s testom BRET2 in analizo ISM so pokazale, da internalizacija poteka neodvisno od β -arrestina. Podobno so predhodno opazili tudi za druge GPCR-je, na primer za HCMV-US28 in ADGRA3 (GPR152). Dodatno smo z novim testom internalizacije v realnem času v kombinaciji z DNM Cav S80E ugotovili, da je prerazporeditev receptorjev BILF1 v celici odvisna tudi od kaveolina-1. S temi rezultati smo potrdili hipotezi 1 in 2, saj smo dokazali konstitutivno internalizacijo v humanih in prašičjih celičnih linijah in vključenost različnih endocitotskih poti.

Proučili smo tudi, kaj se zgodi z receptorji BILF1 po internalizaciji s plazmatske membrane. V uvodu smo opazovali kolokalizacijo receptorjev BILF1 z markerji znotrajceličnih organel (receptor za transferin ali CD71 kot marker zgodnjih endosomov, LAMP1 kot marker lizosomov in Rab8 kot marker reciklirajočih

endosomov) z uporabo mikroskopije, pri čemer smo potrdili le kolokalizacijo z zgodnjimi endosomi. Da bi podprli rezultate mikroskopije, smo uporabili metodo BRET1, pri kateri smo opazovali interakcijo med receptorjem BILF1 in markerjem poznih endosomov/lizosomov Rab7. V nasprotju z rezultati mikroskopije smo z metodo BRET1 potrdili prerazporeditev receptorjev BILF1 v pozne endosome/lizosome, kar kaže, da gre vsaj del teh receptorjev v razgradnjo.

Nova metoda internalizacije v realnem času omogoča tudi merjenje izražanja receptorjev prek meritev emisije z donorjem označenega receptorja BILF1. Opažena razlika pri izražanju receptorjev, označenih pri 4 °C (prepreči internalizacijo med označevanjem receptorja z donorsko molekulo) ali 37 °C (omogoči internalizacijo med označevanjem z donorsko molekulo), kaže sposobnosti receptorjev BILF1 za recikliranje.

Kot nakazuje njihovo ime, GPCR-ji signal prenašajo prek proteina G. Gre za heterotrimerni protein, ki ga sestavljajo tri podenote: alfa, beta in gama. Pri aktivaciji receptorja z ligandom ali brez (konstitutivno), $G\alpha$ podenota izmenja gvanozin difosfat (GDP) z gvanozin trifosfatom (GTP), pri čemer pride do spremembe v strukturi proteina in posledične odcepitve podenote $G\alpha$ od podenote $G\beta\gamma$. Sproščene podenote proteina G v citoplazmi nato prenašajo signal. Glede na strukturo in funkcijo se podenota $G\alpha$ deli na štiri družine: $G\alpha_s$ (olf in s), $G\alpha_i$ (1, oA, t1, g, z, i2, oB, t2 in i3), $G\alpha_q$ (q, 11, 14, 15 in 16) in $G\alpha_{12}$ (12 in 13). Aktivirana podenota $G\alpha_s$ se veže in aktivira adenilat ciklazo (AC), encim, ki vpliva na sintezo cikličnega adenozinmonofosfata (cAMP). cAMP aktivira proteinsko kinazo A (PKA), ki nato uravnava aktivnost znotrajceličnih signalnih proteinov in efektornih proteinov. Po drugi strani protein $G\alpha_i$ zavre AC in s tem povzroči znižanje produkcije cAMP.

Konstitutivna aktivnost je ohranjena lastnost med vGPCR-ji. Za receptor EBV-BILF1 je bilo dokazano, da konstitutiven znotrajcelični prenos signala prek $G\alpha_i$ privede do transformacije celic *in vitro* in rasti tumorjev *in vivo*. Za raziskavo prenosa signala prek proteinov G smo uporabili luciferazni test. Dodatno smo prenos signala receptorjev BILF1 proučevali v CRISPR/Cas9 modificiranih celicah HEK-293A, ki imajo izbite gene

za večino proteinov G (izražajo samo $G\alpha_i$), in ga primerjali z nemodificiranimi celicami HEK-293A. S tem smo potrdili ohranjeno konstitutivno aktivnost prek proteina $G\alpha_i$. To nakazuje na sposobnost transformacije celic, ki je bila opisana za EBV-BILF1, tudi za ortologe BILF1, kodirane v prašičjih herpesvirusih. Nasprotno pa dejstvo, da receptorji PLHV1-3 BILF1 različno uravnavajo znotrajcelične transkripcijske faktorje, lahko pomeni razlike v delovanju receptorjev PLHV1-3 BILF1 in različno vlogo pri virusnih boleznih prašičev. Mogoče je tudi, da so pri prašičih potrebni vsi trije virusi za regulacijo replikacijskega cikla virusa v nasprotju s človekom, za katerega je do zdaj znan le en gamaherpesvirus. Na podlagi razlik v znotrajceličnem prenosu signala receptorjev PLHV1-3 BILF1 bi lahko bila za aktivacijo signalnih poti, ki jih je receptor EBV-BILF1 sposoben aktivirati sam, potrebna sočasna infekcija z vsemi tremi virusi. Dodatno smo pokazali, da nobeden od receptorjev BILF1 ni sposoben aktivirati zunajcelično signalno uravnavane kinaze (ERK1/2), poti znotrajceličnega prenosa signala, ki navadno poteka prek arestina β . Ti rezultati so v skladu z našimi opažanji pri testu BRET2 in ISM, kjer nismo potrdili interakcije med receptorji BILF1 in arestinom β . To kaže na vključenost proteinov G pri konstitutivnem znotrajceličnem prenosu signala receptorjev BILF1 in potrjuje našo hipotezo 3. Hipotezo bi lahko opredelili tudi kot delno potrjeno, saj smo opazili razlike pri znotrajcelični aktivaciji transkripcijskih faktorjev NF- κ B in NFAT.

V biološkem kontekstu je bil receptor EBV-BILF1 opredeljen kot pomemben protein za izmikanje imunskemu sistemu gostitelja z zniževanjem površinsko izraženih molekul MHC-I. V raziskavi smo pokazali, da se ta lastnost ohranja tudi pri ortologih PLHV1-3 BILF1 v humanih celicah HEK-293. V prašičjih celicah PK-15 te lastnosti nismo potrdili, ker smo opazili površinsko zviševanje molekul MHC-I. S tem smo delno potrdili svojo hipotezo 4, saj je bil učinek zniževanja površinske izraženosti molekul MHC-I sicer opazen za vse receptorje BILF1, vendar samo v eni celični liniji.

Razvoj bolezni PTLD je pri človeku povezan z EBV in povzročča potencialno smrtno komplikacijo po presaditvi organov. Pri prašičih so bolezen s podobnimi znaki in patohistološko sliko potrdili v povezavi z okužbo s PLHV1. V raziskavi smo imeli priložnost proučevati vzorce prašičev, odvzete pred razvojem bolezni in po njem, in

preveriti izražanje ortologov BILF1. Pokazali smo prisotnost virusa PLHV1, medtem ko virusa PLHV2 in PLHV3 v teh vzorcih nista bila prisotna. S tem smo tudi potrdili ugotovitve predhodnih raziskav, ki so dokazale povezavo med boleznijo in virusom PLHV1. Dodatno smo preverili izražanje receptorjev PLHV1-BILF1 v teh vzorcih in pokazali značilno povišanje izražanja receptorja po nastopu bolezni, kar nakazuje pomembnost receptorja pri razvoju PTLD. S širšega vidika je potreba po razvoju zdravila proti EBV in boleznim, povzročenim z njim, velika. Pri razvoju humane oblike PTLD je stopnja imunosupresije, ki jo prejemnik organa prejme pred transplantacijo, pomemben dejavnik, ki omogoča nenadzorovano razmnoževanje virusa EBV. Rekonstitucija specifičnih citotoksičnih celic T proti EBV pri darovalcu je pomembno preprečila razvoj bolezni PTLD, kar kaže, da je krepitev obrambe proti EBV uspešen pristop pri preprečevanju razvoja PTLD. Ker receptor EBV-BILF1 dokazano znižuje prepoznavanje okuženih celic s strani celic T CD8+ prek zniževanja površinske izraženosti molekul MHC-I, bi lahko zaviranje funkcije BILF1 pomembno prispevalo k boljšemu odzivu celic T gostitelja.

Hkrati s splošno uporabnostjo GPCR-jev v farmaciji in vlogo receptorja BILF1 pri imunskem odzivu je receptor BILF1 potencialna nova tarča za zdravljenje EBV. Pred kratkim objavljena struktura EBV-BILF1, ki kaže posebne strukturne lastnosti receptorja in visoko ohranjenost za konstitutivno (to je od liganda neodvisno) aktivacijo, bo pomembno vplivala na razvoj strategij za uporabo BILF1 kot tarče za zdravila. vGPCR HCMV-US28 je bil uspešno uporabljen kot selektivna tarča v celicah, okuženih s HCMV, pri čemer je receptor prek konstitutivne internalizacije uspešno prenesel toksin ali nanotelo v okuženo celico. To strategijo bi lahko potencialno uporabili tudi pri receptorju BILF1, saj smo dokazali ohranjeno konstitutivno internalizacijo receptorja.

Predklinični modeli, uporabni za validacijo receptorja BILF1 kot tarče za zdravila in za raziskavo bolezni, povzročenih z EBV, trenutno niso dostopni. Zaradi striktnega tropizma virusa EBV za okužbo ljudi in pomanjkanja virusov, podobnih EBV pri glodavcih, se mišji in podganji modeli trenutno uporabljajo le za raziskave enega specifičnega vidika bolezni, povzročene z EBV, in ne morejo posnemati celotne patologije virusa. Hkrati je uporaba nečloveških primatov draga in etično

problematična, kar potrjuje veliko potrebo po primernem predkliničnem modelu za testiranje delovanja zdravil na receptor BILF1. Podatki naše raziskave kažejo, da bi lahko prašiče uporabili kot modelni mehanizem za raziskavo receptorja BILF1 kot potencialne tarče za zdravila in njegove vloge pri razvoju bolezni PTLD.

9 ACKNOWLEDGEMENTS

This thesis is a result of a lot of hard work and input from a long list of people. It is impossible for me to adequately thank everyone involved for their guidance, support, and mentorship, but I have to at least try.

I would first of all like to thank my mentor, Assoc. Prof. Valentina Kubale Dvojmoč, not only for affording me the great opportunity to work with her as a young researcher, but also for her guidance and support during the five years of my doctoral studies and for always making sure that everything ran smoothly. It was great to have a mentor who understood and respected not only my professional life but also my personal one. Secondly, I would like to thank my co-mentor, Assist. Prof. Katja Spiess, for all the knowledge and invaluable experience she shared with me. I really appreciate all of the time she spent with me, discussing science, and guiding me on my path of becoming a better scientist.

I would also like to thank Prof. Mette M. Rosenkilde, for hosting me as a guest doctoral student in her lab and for giving me opportunities outside my doctoral project, which gave me a wider perspective in the research field. I am also grateful to the head of the department, Prof. Milka Vrecl Fazarinc, for all the advice and project discussions over the years.

Furthermore, I would like to thank everyone at the Institute for Preclinical Sciences, especially my colleagues at the Department of Anatomy, Histology, and Cellular biology, for their support and help during these five years. Special thanks to Magdalena Dobravec for helping me with the everyday struggles.

Likewise, I would like to thank my dear PhD colleagues at the Veterinary Faculty for their support, non-formal discussions and for sharing their experience with me.

I would further like to thank everyone at the Laboratory for Molecular Pharmacology for advice, discussions and for creating a great working atmosphere. Special thanks to

my dear friends Sofie, Astrid, Sheyma, and Lola for the unforgettable time, motivation, and croissants, and for making me feel at home every day. Thanks to Olav for being the kindest lab mentor, Maibritt, Soren, and Sussi for all the help in the lab, Julius and Dagmar for teaching me more than I taught them and to Mette Trauelsen for being so awesome.

Many thanks also to Jianmin Zuo, who hosted me in Birmingham and taught me FACS method, Toni Petan and Eva Jarc Jovičić from the Josef Stefan Institute for their help with FACS, Samo Hudoklin from Faculty of Medicine for his kindness and advice on microscopy, Thor Christian Moller for helping us setup the RT internalization method, CFIM team – especially Pablo Hernandez-Varas for all the help with microscopy and Frederik Vilhardt for his help and generosity.

I would also like to acknowledge the members of the committee for evaluation of the doctoral dissertation, Biljana Grubišič for all the administrative help and Stanislava Ujc and Gita Grecs–Smole for all the help with the literature and the final look of the thesis. Moreover, I would like to thank Terry Jackson and Nina Novak Kerbler for final language editing of the thesis.

A special thanks goes to the Elbo family and our dear Jan for giving us a home in Denmark and for making us feel we were a part of the family.

Last but definitely not least, I would like to thank my family for their endless support and motivation, my husband for moving across Europe with me, and my little boy for giving my life a new perspective.

10 LITERATURE

Alberts B, Johnson A, Lewis J, et al. Molecular biology of the cell. 6th ed. New York: Garland Science, 2015.

Andrei G, Trompet E, Snoeck R. Novel therapeutics for Epstein–Barr virus. *Molecules* 2019; 24(5): e997(20pp.).
doi: 10.3390/molecules24050997

Arancibia-Cárcamo IL, Fairfax BP, Moss SJ, Kittler JT. Studying the localization, surface stability and endocytosis of neurotransmitter receptors by antibody labeling and biotinylation approaches. In: Kittler JT, Moss SJ, eds. *The Dynamic Synapse: Molecular Methods in Ionotropic Receptor Biology*. (Online) Boca Raton (FL): CRC Press/Taylor & Francis, 2006: chapter 6 (21pp.).
<https://www.ncbi.nlm.nih.gov/books/NBK2552/>

Arfelt KN, Fares S, Rosenkilde MM. EBV, the human host, and the 7TM receptors: defense or offense? *Prog Mol Biol Transl Sci* 2015; 129: 395–427.
doi: 10.1016/bs.pmbts.2014.10.011

Ariotti N, Hall TE, Rae J, et al. Modular detection of GFP-labeled proteins for rapid screening by electron microscopy in cells and organisms. *Dev Cell* 2015; 35(4): 513–25.
doi: 10.1016/j.devcel.2015.10.016

Arvin A, Campadelli-Fiume G, Mocarski E, et al. Human herpesviruses: biology, therapy, and immunoprophylaxis. Cambridge: Cambridge University Press, 2007.
<https://www.ncbi.nlm.nih.gov/books/NBK47376/>

Azzi S, Smith SS, Dwyer J, et al. YGLF motif in the kaposi sarcoma herpes virus G-protein-coupled receptor adjusts NF- κ B activation and paracrine actions. *Oncogene* 2014; 33(49): 5609–18.
doi: 10.1038/onc.2013.503

Babcock GJ, Decker LL, Volk M, Thorley-Lawson DA. EBV persistence in memory B cells *in vivo*. *Immunity* 1998; 9(3): 395–404.
doi: 10.1016/s1074-7613(00)80622-6

Baer R, Bankier AT, Biggin MD, et al. DNA sequence and expression of the B95-8 Epstein-Barr virus genome. *Nature* 1984; 310(5974): 207–11.
doi: 10.1038/310207a0

Baeuerle PA, Henkel T. Function and activation of NF-kappa B in the immune system. *Annu Rev Immunol* 1994; 12: 141–79.
doi: 10.1146/annurev.iy.12.040194.001041

Bais C, Santomasso B, Coso O, et al. G-protein-coupled receptor of kaposi's sarcoma-associated herpesvirus is a viral oncogene and angiogenesis activator. *Nature* 1998; 391(6662): 86–9.
doi: 10.1038/34193

Barbieri E, Di Fiore PP, Sigismund S. Endocytic control of signaling at the plasma membrane. *Curr Opin Cell Biol* 2016; 39: 21–7.
doi: 10.1016/j.ceb.2016.01.012

Bass AJ, Thorsson V, Shmulevich I, et al. Comprehensive molecular characterization of gastric adenocarcinoma. *Nature* 2014; 513(7517): 202–9.
doi: 10.1038/nature13480

Bayguinov PO, Oakley DM, Shih CC, Geanon DJ, Joens MS, Fitzpatrick JAJ. Modern laser scanning confocal microscopy. *Curr Protoc Cytom* 2018; 85(1): e39(17pp.).
doi: 10.1002/cpcy.39

Beck-García K, Beck-García E, Bohler S, et al. Nanoclusters of the resting T cell antigen receptor (TCR) localize to non-raft domains. *Biochim Biophys Acta* 2015; 1853(4): 802–9.
doi: 10.1016/j.bbamcr.2014.12.017

Beisser PS, Laurent L, Virelizier JL, Michelson S. Human cytomegalovirus chemokine receptor gene US28 is transcribed in latently infected THP-1 monocytes. *J Virol* 2001; 75(13): 5949–57.
doi: 10.1128/jvi.75.13.5949-5957.2001

Beisser PS, Verzijl D, Gruijthuisen YK, et al. The Epstein-Barr virus BILF1 gene encodes a G protein-coupled receptor that inhibits phosphorylation of RNA-dependent protein kinase. *J Virol* 2005; 79(1): 441–9.
doi: 10.1128/jvi.79.1.441-449.2005

Birkenbach M, Josefsen K, Yalamanchili R, Lenoir G, Kieff E. Epstein-Barr virus-induced genes: first lymphocyte-specific G protein-coupled peptide receptors. *J Virol* 1993; 67(4): 2209–20.
doi: 10.1128/jvi.67.4.2209-2220.1993

Bodaghi B, Jones TR, Zipeto D, et al. Chemokine sequestration by viral chemoreceptors as a novel viral escape strategy: withdrawal of chemokines from the environment of cytomegalovirus-infected cells. *J Exp Med* 1998; 188(5): 855–66.
doi: 10.1084/jem.188.5.855

Boomker JM, de Jong EK, de Leij LF, Harmsen MC. Chemokine scavenging by the human cytomegalovirus chemokine decoy receptor US28 does not inhibit monocyte adherence to activated endothelium. *Antiviral Res* 2006; 69(2): 124–7.
doi: 10.1016/j.antiviral.2005.11.003

Brock C, Schaefer M, Reusch HP, et al. Roles of G beta gamma in membrane recruitment and activation of p110 gamma/p101 phosphoinositide 3-kinase gamma. *J Cell Biol* 2003; 160(1): 89–99.
doi: 10.1083/jcb.200210115

Brunovskis P, Kung HJ. Retrotransposition and herpesvirus evolution. *Virus Genes* 1995; 11(2-3): 259–70.
doi: 10.1007/bf01728664

Carter M, Shieh J. Biochemical assays and intracellular signaling. In: Carter M, Shieh J, eds. *Guide to Research Techniques in Neuroscience*. 2nd ed. (Online) San Diego: Academic Press, 2015: 311–43.
<https://doi.org/10.1016/B978-0-12-800511-8.00015-0>

Casarosa P, Bakker RA, Verzijl D, et al. Constitutive signaling of the human cytomegalovirus-encoded chemokine receptor US28. *J Biol Chem* 2001; 276(2): 1133–7.
doi: 10.1074/jbc.M008965200

Chang RS, Lewis JP, Reynolds RD, Sullivan MJ, Neuman J. Oropharyngeal excretion of Epstein-Barr virus by patients with lymphoproliferative disorders and by recipients of renal homografts. *Ann Intern Med* 1978; 88(1): 34–40.
doi: 10.7326/0003-4819-88-1-34

Chang Y, Cesarman E, Pessin MS, et al. Identification of herpesvirus-like DNA sequences in AIDS-associated kaposi's sarcoma. *Science* 1994; 266(5192): 1865–9.
doi: 10.1126/science.7997879

Chaudhuri R, Lindwasser OW, Smith WJ, Hurley JH, Bonifacino JS. Downregulation of CD4 by human immunodeficiency virus type 1 NEF is dependent on clathrin and involves direct interaction of nef with the AP2 clathrin adaptor. *J Virol* 2007; 81(8): 3877–90.
doi: 10.1128/jvi.02725-06

Chee MS, Satchwell SC, Preddie E, Weston KM, Barrell BG. Human cytomegalovirus encodes three G protein-coupled receptor homologues. *Nature* 1990; 344(6268): 774–7.
doi: 10.1038/344774a0

Chijioke O, Müller A, Feederle R, et al. Human natural killer cells prevent infectious mononucleosis features by targeting lytic Epstein-Barr virus infection. *Cell Rep* 2013; 5(6): 1489–98.
doi: 10.1016/j.celrep.2013.11.041

Chini B, Parenti M. G-protein coupled receptors in lipid rafts and caveolae: how, when and why do they go there? *J Mol Endocrinol* 2004; 32(2): 325–38.
doi: 10.1677/jme.0.0320325

Chmielewicz B, Goltz M, Franz T, et al. A novel porcine gammaherpesvirus. *Virology* 2003; 308(2): 317–29.
doi: 10.1016/s0042-6822(03)00006-0

Cho PS, Lo DP, Wikiel KJ, et al. Establishment of transplantable porcine tumor cell lines derived from MHC-inbred miniature swine. *Blood* 2007; 110(12): 3996–4004.
doi: 10.1182/blood-2007-02-074450

Cho PS, Mueller NJ, Cameron AM, et al. Risk factors for the development of post-transplant lymphoproliferative disorder in a large animal model. *Am J Transplant* 2004; 4(8): 1274–82.
doi: 10.1111/j.1600-6143.2004.00506.x

Choy BC, Cater RJ, Mancina F, Pryor EE, Jr. A 10-year meta-analysis of membrane protein structural biology: detergents, membrane mimetics, and structure determination techniques. *Biochim Biophys Acta Biomembr* 2021; 1863(3): e183533(9pp.).
doi: 10.1016/j.bbamem.2020.183533

Coen N, Duraffour S, Naesens L, et al. Evaluation of novel acyclic nucleoside phosphonates against human and animal gammaherpesviruses revealed an altered metabolism of cyclic prodrugs upon Epstein-Barr virus reactivation in P3HR-1 cells. *J Virol* 2013; 87(22): 12422–32.
doi: 10.1128/jvi.02231-13

Coen N, Duraffour S, Topalis D, Snoeck R, Andrei G. Spectrum of activity and mechanisms of resistance of various nucleoside derivatives against gammaherpesviruses. *Antimicrob Agents Chemother* 2014; 58(12): 7312–23.
doi: 10.1128/aac.03957-14

Cohen JI. Vaccine development for Epstein-Barr virus. *Adv Exp Med Biol* 2018; 1045: 477–93.
doi: 10.1007/978-981-10-7230-7_22

Conklin BR, Kostenis E. Methods and compositions for identifying modulators of G-protein-coupled receptors. Patent: PCT/US1998/015567.
Geneva: Organization WIP, 1999.
<https://patentscope.wipo.int/search/en/detail.jsf?docId=WO1999005177>

Couet J, Li S, Okamoto T, Ikezu T, Lisanti MP. Identification of peptide and protein ligands for the caveolin-scaffolding domain. Implications for the interaction of caveolin with caveolae-associated proteins. *J Biol Chem* 1997a; 272(10): 6525–33.
doi: 10.1074/jbc.272.10.6525

Couet J, Sargiacomo M, Lisanti MP. Interaction of a receptor tyrosine kinase, EGF-R, with caveolins. Caveolin binding negatively regulates tyrosine and serine/threonine kinase activities. *J Biol Chem* 1997b; 272(48): 30429–38.
doi: 10.1074/jbc.272.48.30429

Damke H, Baba T, Warnock DE, Schmid SL. Induction of mutant dynamin specifically blocks endocytic coated vesicle formation. *J Cell Biol* 1994; 127(4): 915–34.
doi: 10.1083/jcb.127.4.915

Davison AJ. Herpesvirus systematics. *Vet Microbiol* 2010; 143(1): 52–69.
doi: 10.1016/j.vetmic.2010.02.014

De Groof TWM, Elder EG, Lim EY, et al. Targeting the latent human cytomegalovirus reservoir for T-cell-mediated killing with virus-specific nanobodies. *Nat Commun* 2021; 12(1): e4436(11pp.).
doi: 10.1038/s41467-021-24608-5

de Martel C, Georges D, Bray F, Ferlay J, Clifford GM. Global burden of cancer attributable to infections in 2018: a worldwide incidence analysis. *Lancet Glob Health* 2020; 8(2): e180–90.
doi: 10.1016/s2214-109x(19)30488-7

de Munnik SM, Kooistra AJ, van Offenbeek J, et al. The viral G protein-coupled receptor ORF74 hijacks β -arrestins for endocytic trafficking in response to human chemokines. *PLoS One* 2015; 10(4): e0124486(21pp.).
doi: 10.1371/journal.pone.0124486

Dewulf M, Köster DV, Sinha B, et al. Dystrophy-associated caveolin-3 mutations reveal that caveolae couple IL6/STAT3 signaling with mechanosensing in human muscle cells. *Nat Commun* 2019; 10(1): e1974(13pp.).
doi: 10.1038/s41467-019-09405-5

Dierickx D, Habermann TM. Post-transplantation lymphoproliferative disorders in adults. *N Engl J Med* 2018; 378(6): 549–62.
doi: 10.1056/NEJMra1702693

Diviani D, Lattion AL, Abuin L, Staub O, Cotecchia S. The adaptor complex 2 directly interacts with the alpha 1b-adrenergic receptor and plays a role in receptor endocytosis. *J Biol Chem* 2003; 278(21): 19331–40.
doi: 10.1074/jbc.M302110200

Dong VH, Tu PY, Tsai PC, et al. Expression of toll-like receptor signaling-related genes in pigs co-infected with porcine reproductive and respiratory syndrome virus and porcine circovirus type 2. *Res Vet Sci* 2015; 101: 180–6.
doi: 10.1016/j.rvsc.2015.05.006

Dor FJ, Doucette KE, Mueller NJ, et al. Posttransplant lymphoproliferative disease after allogeneic transplantation of the spleen in miniature swine. *Transplantation* 2004; 78(2): 286–91.
doi: 10.1097/01.tp.0000128342.64240.cf

Doray B, Lee I, Knisely J, Bu G, Kornfeld S. The gamma/sigma1 and alpha/sigma2 hemicomplexes of clathrin adaptors AP-1 and AP-2 harbor the dileucine recognition site. *Mol Biol Cell* 2007; 18(5): 1887–96.
doi: 10.1091/mbc.e07-01-0012

Doucette K, Dor FJ, Wilkinson RA, et al. Gene expression of porcine lymphotropic herpesvirus-1 in miniature swine with posttransplant lymphoproliferative disorder. *Transplantation* 2007; 83(1): 87–90.
doi: 10.1097/01.tp.0000228237.32549.16

Drinovec L, Kubale V, Nøhr Larsen J, Vrecl M. Mathematical models for quantitative assessment of bioluminescence resonance energy transfer: application to seven transmembrane receptors oligomerization. *Front Endocrinol* 2012; 3: e104(10pp.).
doi: 10.3389/fendo.2012.00104

Droese J, Mokros T, Hermosilla R, et al. HCMV-encoded chemokine receptor US28 employs multiple routes for internalization. *Biochem Biophys Res Commun* 2004; 322(1): 42–9.
doi: 10.1016/j.bbrc.2004.07.076

Drouet E. The role of the Epstein-Barr virus lytic cycle in tumor progression: consequences in diagnosis and therapy. In: Thomasini RL, eds. *Human Herpesvirus Infection - Biological Features, Transmission, Symptoms, Diagnosis and Treatment*. (Online) London: IntechOpen, 2019: chapter 6 (20pp.).
doi: 10.5772/intechopen.88607

Duran-Struuck R, Huang CA, Matar AJ. Cellular therapies for the treatment of hematological malignancies; swine are an ideal preclinical model. *Front Oncol* 2019; 9: e418(9pp.).
doi: 10.3389/fonc.2019.00418

Duran-Struuck R, Huang CA, Orf K, Bronson RT, Sachs DH, Spitzer TR. Miniature swine as a clinically relevant model of graft-versus-host disease. *Comp Med* 2015a; 65(5)(5): 429–43.
doi:

Duran-Struuck R, Matar AJ, Huang CA. Myeloid leukemias and virally induced lymphomas in miniature inbred swine: development of a large animal tumor model. *Front Genet* 2015b; 6: e332(6pp.).
doi: 10.3389/fgene.2015.00332

Ehlers B, Ulrich S, Goltz M. Detection of two novel porcine herpesviruses with high similarity to gammaherpesviruses. *J Gen Virol* 1999; 80: 971–8.
doi: 10.1099/0022-1317-80-4-971

Ensser A, Pflanz R, Fleckenstein B. Primary structure of the alcelaphine herpesvirus 1 genome. *J Virol* 1997; 71(9): 6517–25.
doi: 10.1128/jvi.71.9.6517-6525.1997

Epstein MA, Achong BG, Barr YM. Virus particles in cultured lymphoblasts from burkitt's lymphoma. *Lancet* 1964; 1(7335): 702–3.
doi: 10.1016/s0140-6736(64)91524-7

Estall JL, Yusta B, Drucker DJ. Lipid raft-dependent glucagon-like peptide-2 receptor trafficking occurs independently of agonist-induced desensitization. *Mol Biol Cell* 2004; 15(8): 3673–87.
doi: 10.1091/mbc.e03-11-0825

Ewers H, Helenius A. Lipid-mediated endocytosis. *Cold Spring Harb Perspect Biol* 2011; 3(8): a004721(14pp.).
doi: 10.1101/cshperspect.a004721

Fares S, Spiess K, Olesen ETB, et al. Distinct roles of extracellular domains in the Epstein-Barr virus-encoded BILF1 receptor for signaling and major histocompatibility complex class I downregulation. *mBio* 2019; 10(1): e01707–18(15pp.).
doi: 10.1128/mBio.01707-18

Fecchi K, Anticoli S, Peruzzi D, et al. Coronavirus interplay with lipid rafts and autophagy unveils promising therapeutic targets. *Front Microbiol* 2020; 11: e1821(9pp.).
doi: 10.3389/fmicb.2020.01821

Feichtinger H, Li SL, Kaaya E, et al. A monkey model for Epstein Barr virus-associated lymphomagenesis in human acquired immunodeficiency syndrome. *J Exp Med* 1992; 176(1): 281–6.
doi: 10.1084/jem.176.1.281

Foster SR, Bräuner-Osborne H. Investigating internalization and intracellular trafficking of GPCRs: new techniques and real-time experimental approaches. *Handb Exp Pharmacol* 2018; 245: 41–61.
doi: 10.1007/164_2017_57

Fraile-Ramos A, Kledal TN, Pelchen-Matthews A, Bowers K, Schwartz TW, Marsh M. The human cytomegalovirus US28 protein is located in endocytic vesicles and undergoes constitutive endocytosis and recycling. *Mol Biol Cell* 2001; 12(6): 1737–49.
doi: 10.1091/mbc.12.6.1737

Fraile-Ramos A, Kohout TA, Waldhoer M, Marsh M. Endocytosis of the viral chemokine receptor US28 does not require beta-arrestins but is dependent on the clathrin-mediated pathway. *Traffic* 2003; 4(4): 243–53.
doi: 10.1034/j.1600-0854.2003.00079.x

Fredriksson R, Lagerström MC, Lundin LG, Schiöth HB. The G-protein-coupled receptors in the human genome form five main families. Phylogenetic analysis, paralogon groups, and fingerprints. *Mol Pharmacol* 2003; 63(6): 1256–72.
doi: 10.1124/mol.63.6.1256

Fujiwara S, Imadome KI, Takei M. Modeling EBV infection and pathogenesis in new-generation humanized mice. *Exp Mol Med* 2015; 47(1): e135(7pp.).
doi: 10.1038/emm.2014.88

Fujiwara S, Nakamura H. Animal models for gammaherpesvirus infections: recent development in the analysis of virus-induced pathogenesis. *Pathogens* 2020; 9(2): e116(19pp.).
doi: 10.3390/pathogens9020116

Fus-Kujawa A, Prus P, Bajdak-Rusinek K, et al. An overview of methods and tools for transfection of eukaryotic cells *in vitro*. *Front Bioeng Biotechnol* 2021; 9: e701031(15pp.).
doi: 10.3389/fbioe.2021.701031

García-Nafria J, Tate CG. Structure determination of GPCRs: cryo-em compared with X-ray crystallography. *Biochem Soc Trans* 2021; 49(5): 2345–55.
doi: 10.1042/bst20210431

Garcia J, Bagwell J, Njaine B, et al. Sheath cell invasion and trans-differentiation repair mechanical damage caused by loss of caveolae in the zebrafish notochord. *Curr Biol* 2017; 27(13): 1982–9.
doi: 10.1016/j.cub.2017.05.035

Goltz M, Ericsson T, Patience C, et al. Sequence analysis of the genome of porcine lymphotropic herpesvirus 1 and gene expression during posttransplant lymphoproliferative disease of pigs. *Virology* 2002; 294(2): 383–93.
doi: 10.1006/viro.2002.1390

González MI, Krizman-Genda E, Robinson MB. Caveolin-1 regulates the delivery and endocytosis of the glutamate transporter, excitatory amino acid carrier 1. *J Biol Chem* 2007; 282(41): 29855–65.
doi: 10.1074/jbc.M704738200

Goodman OB, Jr., Krupnick JG, Santini F, et al. Beta-arrestin acts as a clathrin adaptor in endocytosis of the beta2-adrenergic receptor. *Nature* 1996; 383(6599): 447–50.
doi: 10.1038/383447a0

Griffin BD, Gram AM, Mulder A, et al. EBV BILF1 evolved to downregulate cell surface display of a wide range of HLA class I molecules through their cytoplasmic tail. *J Immunol* 2013; 190(4): 1672–84.
doi: 10.4049/jimmunol.1102462

Grisotto MG, Garin A, Martin AP, et al. The human herpesvirus 8 chemokine receptor vGPCR triggers autonomous proliferation of endothelial cells. *J Clin Invest* 2006; 116(5): 1264–73.
doi: 10.1172/JCI26666

Grundmann M, Kostenis E. Temporal bias: time-encoded dynamic GPCR signaling. *Trends Pharmacol Sci* 2017; 38(12): 1110–24.
doi: 10.1016/j.tips.2017.09.004

Guo Q, Gao J, Cheng L, Yang X, Li F, Jiang G. The Epstein-Barr virus-encoded G protein-coupled receptor BILF1 upregulates ICAM-1 through a mechanism involving the NF- κ B pathway. *Biosci Biotechnol Biochem* 2020; 84(9): 1810–9.
doi: 10.1080/09168451.2020.1777525

Hahne F, Ivanek R. Visualizing genomic data using gviz and bioconductor. *Methods Mol Biol* 2016; 1418: 335–51.
doi: 10.1007/978-1-4939-3578-9_16

Hansen CG, Howard G, Nichols BJ. Pacsin 2 is recruited to caveolae and functions in caveolar biogenesis. *J Cell Sci* 2011; 124(16): 2777–85.
doi: 10.1242/jcs.084319

Hanyaloglu AC, von Zastrow M. Regulation of GPCRs by endocytic membrane trafficking and its potential implications. *Annu Rev Pharmacol Toxicol* 2008; 48: 537–68.
doi: 10.1146/annurev.pharmtox.48.113006.094830

Hartline CB, Conner RL, James SH, et al. Xenotransplantation panel for the detection of infectious agents in pigs. *Xenotransplantation* 2018; 25(4): e12427(15pp.).
doi: 10.1111/xen.12427

Hauser AS, Attwood MM, Rask-Andersen M, Schioth HB, Gloriam DE. Trends in GPCR drug discovery: new agents, targets and indications. *Nat Rev Drug Discov* 2017; 16(12): 829–42.
doi: 10.1038/nrd.2017.178

Hawryluk MJ, Keyel PA, Mishra SK, Watkins SC, Heuser JE, Traub LM. Epsin 1 is a polyubiquitin-selective clathrin-associated sorting protein. *Traffic* 2006; 7(3): 262–81.
doi: 10.1111/j.1600-0854.2006.00383.x

Hayer A, Stoeber M, Bissig C, Helenius A. Biogenesis of caveolae: stepwise assembly of large caveolin and cavin complexes. *Traffic* 2010; 11(3): 361–82.
doi: 10.1111/j.1600-0854.2009.01023.x

Henne WM, Boucrot E, Meinecke M, et al. FCHO proteins are nucleators of clathrin-mediated endocytosis. *Science* 2010; 328(5983): 1281–4.
doi: 10.1126/science.1188462

Heslop HE, Slobod KS, Pule MA, et al. Long-term outcome of EBV-specific T-cell infusions to prevent or treat EBV-related lymphoproliferative disease in transplant recipients. *Blood* 2010; 115(5): 925–35.
doi: 10.1182/blood-2009-08-239186

Hetmanski JHR, de Belly H, Busnelli I, et al. Membrane tension orchestrates rear retraction in matrix-directed cell migration. *Dev Cell* 2019; 51(4): 460–75.
doi: 10.1016/j.devcel.2019.09.006

Heukers R, Fan TS, de Wit RH, et al. The constitutive activity of the virally encoded chemokine receptor US28 accelerates glioblastoma growth. *Oncogene* 2018; 37(30): 4110–21.
doi: 10.1038/s41388-018-0255-7

Hilger D, Masureel M, Kobilka BK. Structure and dynamics of GPCR signaling complexes. *Nat Struct Mol Biol* 2018; 25(1): 4–12.
doi: 10.1038/s41594-017-0011-7

Hill MM, Bastiani M, Luetterforst R, et al. PTRF-cavin, a conserved cytoplasmic protein required for caveola formation and function. *Cell* 2008; 132(1): 113–24.
doi: 10.1016/j.cell.2007.11.042

Hinshaw JE, Schmid SL. Dynamin self-assembles into rings suggesting a mechanism for coated vesicle budding. *Nature* 1995; 374(6518): 190–2.
doi: 10.1038/374190a0

Huang CA, Fuchimoto Y, Gleit ZL, et al. Posttransplantation lymphoproliferative disease in miniature swine after allogeneic hematopoietic cell transplantation: Similarity to human PTLN and association with a porcine gammaherpesvirus. *Blood* 2001; 97(5): 1467–73.
doi: 10.1182/blood.v97.5.1467

Huang CA, Yamada K, Murphy MC, et al. *In vivo* T cell depletion in miniature swine using the swine CD3 immunotoxin, PCD3-CRM9. *Transplantation* 1999; 68(6): 855–60.
doi: 10.1097/00007890-199909270-00019

Huotari J, Helenius A. Endosome maturation. *EMBO J* 2011; 30(17): 3481–500.
doi: 10.1038/emboj.2011.286

Inglese J, Koch WJ, Touhara K, Lefkowitz RJ. G beta gamma interactions with PH domains and RAS-MAPK signaling pathways. *Trends Biochem Sci* 1995; 20(4): 151–6.
doi: 10.1016/s0968-0004(00)88992-6

Irannejad R, Tsvetanova NG, Lobingier BT, von Zastrow M. Effects of endocytosis on receptor-mediated signaling. *Curr Opin Cell Biol* 2015; 35: 137–43.
doi: 10.1016/j.ceb.2015.05.005

Islas-Ohlmayer M, Padgett-Thomas A, Domiati-Saad R, et al. Experimental infection of NOD/SCID mice reconstituted with human CD34+ cells with Epstein-Barr virus. *J Virol* 2004; 78(24): 13891–900.
doi: 10.1128/jvi.78.24.13891-13900.2004

Jackson LP, Kelly BT, McCoy AJ, et al. A large-scale conformational change couples membrane recruitment to cargo binding in the AP2 clathrin adaptor complex. *Cell* 2010; 141(7): 1220–9.
doi: 10.1016/j.cell.2010.05.006

Jacobsen L, Calvin S, Lobenhofer E. Transcriptional effects of transfection: the potential for misinterpretation of gene expression data generated from transiently transfected cells. *Biotechniques* 2009; 47(1): 617–24.
doi: 10.2144/000113132

Jacobsen SE, Ammendrup-Johnsen I, Jansen AM, Gether U, Madsen KL, Bräuner-Osborne H. The GPCR6A receptor displays constitutive internalization and sorting to the slow recycling pathway. *J Biol Chem* 2017; 292(17): 6910–26.
doi: 10.1074/jbc.M116.762385

Janetzko J, Kise R, Barsi-Rhyne B, et al. Membrane phosphoinositides regulate GPCR- β -arrestin complex assembly and dynamics. *Cell* 2022; 185: S0092-8674(22)01360-5(14pp.).
doi: 10.1016/j.cell.2022.10.018

Johannsen E, Luftig M, Chase MR, et al. Proteins of purified Epstein-Barr virus. *Proc Natl Acad Sci U S A* 2004; 101(46): 16286–91.
doi: 10.1073/pnas.0407320101

Jørgensen AS, Rosenkilde MM, Hjortø GM. Biased signaling of G protein-coupled receptors - from a chemokine receptor CCR7 perspective. *Gen Comp Endocrinol* 2018; 258: 4–14.
doi: 10.1016/j.ygcen.2017.07.004

Jørgensen R, Norklit Roed S, Heding A, Elling CE. Beta-arrestin2 as a competitor for GRK2 interaction with the GLP-1 receptor upon receptor activation. *Pharmacology* 2011; 88(3-4): 174–81.
doi: 10.1159/000330742

Joseph JG, Liu AP. Mechanical regulation of endocytosis: new insights and recent advances. *Adv Biosyst* 2020; 4(5): e1900278(15pp.).
doi: 10.1002/adbi.201900278

Jovic M, Sharma M, Rahajeng J, Caplan S. The early endosome: a busy sorting station for proteins at the crossroads. *Histol Histopathol* 2010; 25(1): 99–112.
doi: 10.14670/hh-25.99

Jung W, Sierecki E, Bastiani M, et al. Cell-free formation and interactome analysis of caveolae. *J Cell Biol* 2018; 217(6): 2141–65.
doi: 10.1083/jcb.201707004

Kadlecova Z, Spielman SJ, Loerke D, Mohanakrishnan A, Reed DK, Schmid SL. Regulation of clathrin-mediated endocytosis by hierarchical allosteric activation of AP2. *J Cell Biol* 2017; 216(1): 167–79.
doi: 10.1083/jcb.201608071

Kaksonen M, Roux A. Mechanisms of clathrin-mediated endocytosis. *Nat Rev Mol Cell Biol* 2018; 19(5): 313–26.
doi: 10.1038/nrm.2017.132

Kamperschroer C, Gosink MM, Kumpf SW, O'Donnell LM, Tartaro KR. The genomic sequence of lymphocryptovirus from cynomolgus macaque. *Virology* 2016; 488: 28–36.
doi: 10.1016/j.virol.2015.10.025

Kanda T. Ebv-encoded latent genes. *Adv Exp Med Biol* 2018; 1045: 377–94.
doi: 10.1007/978-981-10-7230-7_17

Kaufman RJ. Stress signaling from the lumen of the endoplasmic reticulum: Coordination of gene transcriptional and translational controls. *Genes Dev* 1999; 13(10): 1211–33.
doi: 10.1101/gad.13.10.1211

Keith KA, Hartline CB, Bowlin TL, Prichard MN. A standardized approach to the evaluation of antivirals against DNA viruses: polyomaviruses and lymphotropic herpesviruses. *Antiviral Res* 2018; 159: 122–9.
doi: 10.1016/j.antiviral.2018.09.016

Kelly BT, Graham SC, Liska N, et al. Clathrin adaptors. AP2 controls clathrin polymerization with a membrane-activated switch. *Science* 2014; 345(6195): 459–63.
doi: 10.1126/science.1254836

Kledal TN, Rosenkilde MM, Schwartz TW. Selective recognition of the membrane-bound CX3C chemokine, fractalkine, by the human cytomegalovirus-encoded broad-spectrum receptor US28. *FEBS Lett* 1998; 441(2): 209–14.
doi: 10.1016/s0014-5793(98)01551-8

Kobayashi H, Picard LP, Schönege AM, Bouvier M. Bioluminescence resonance energy transfer-based imaging of protein-protein interactions in living cells. *Nat Protoc* 2019; 14(4): 1084–107.
doi: 10.1038/s41596-019-0129-7

Kosaka T, Ikeda K. Reversible blockage of membrane retrieval and endocytosis in the garland cell of the temperature-sensitive mutant of *Drosophila melanogaster*, shibirets1. *J Cell Biol* 1983; 97(2): 499–507.
doi: 10.1083/jcb.97.2.499

Kostenis E, Martini L, Ellis J, et al. A highly conserved glycine within linker I and the extreme C terminus of G protein alpha subunits interact cooperatively in switching G protein-coupled receptor-to-effector specificity.
J Pharmacol Exp Ther 2005; 313(1): 78–87.
doi: 10.1124/jpet.104.080424

Kovtun O, Tillu VA, Ariotti N, Parton RG, Collins BM. Cavin family proteins and the assembly of caveolae. *J Cell Sci* 2015; 128(7): 1269–78.
doi: 10.1242/jcs.167866

Kovtun O, Tillu VA, Jung W, et al. Structural insights into the organization of the cavin membrane coat complex. *Dev Cell* 2014; 31(4): 405–19.
doi: 10.1016/j.devcel.2014.10.002

Krishna BA, Spiess K, Poole EL, et al. Targeting the latent cytomegalovirus reservoir with an antiviral fusion toxin protein. *Nat Commun* 2017; 8: e14321(9pp.).
doi: 10.1038/ncomms14321

Kroppen B, Teske N, Yambire KF, et al. Cooperativity of membrane-protein and protein-protein interactions control membrane remodeling by epsin 1 and affects clathrin-mediated endocytosis. *Cell Mol Life Sci* 2021; 78(5): 2355–70.
doi: 10.1007/s00018-020-03647-z

Krupnick JG, Goodman OB, Jr., Keen JH, Benovic JL. Arrestin/clathrin interaction. Localization of the clathrin binding domain of nonvisual arrestins to the carboxy terminus. *J Biol Chem* 1997; 272(23): 15011–6.
doi: 10.1074/jbc.272.23.15011

Kubale V, Abramovic Z, Pogacnik A, Heding A, Sentjurc M, Vrecl M. Evidence for a role of caveolin-1 in neurokinin-1 receptor plasma-membrane localization, efficient signaling, and interaction with beta-arrestin 2. *Cell Tissue Res* 2007; 330(2): 231–45.
doi: 10.1007/s00441-007-0462-y

Kubale V, Blagotinšek K, Nøhr J, Eidne KA, Vrecl M. The conserved arginine cluster in the insert of the third cytoplasmic loop of the long form of the D₂ dopamine receptor (D2L-R) acts as an intracellular retention signal.
Int J Mol Sci 2016; 17(7): e1152(16pp.).
doi: 10.3390/ijms17071152

Kumar M, Michael S, Alvarado-Valverde J, et al. The eukaryotic linear motif resource: 2022 release. *Nucleic Acids Res* 2022; 50(D1): D497–d508.
doi: 10.1093/nar/gkab975

Kumari S, Mg S, Mayor S. Endocytosis unplugged: Multiple ways to enter the cell. *Cell Res* 2010; 20(3): 256–75.
doi: 10.1038/cr.2010.19

Lajoie P, Kojic LD, Nim S, Li L, Dennis JW, Nabi IR. Caveolin-1 regulation of dynamin-dependent, raft-mediated endocytosis of cholera toxin-b sub-unit occurs independently of caveolae. *J Cell Mol Med* 2009; 13(9b): 3218–25.
doi: 10.1111/j.1582-4934.2009.00732.x

Lajoie P, Partridge EA, Guay G, et al. Plasma membrane domain organization regulates EGFR signaling in tumor cells. *J Cell Biol* 2007; 179(2): 341–56.
doi: 10.1083/jcb.200611106

Laporte SA, Oakley RH, Holt JA, Barak LS, Caron MG. The interaction of beta-arrestin with the AP-2 adaptor is required for the clustering of beta 2-adrenergic receptor into clathrin-coated pits. *J Biol Chem* 2000; 275(30): 23120–6.
doi: 10.1074/jbc.M002581200

Laporte SA, Oakley RH, Zhang J, et al. The beta2-adrenergic receptor/betaarrestin complex recruits the clathrin adaptor AP-2 during endocytosis. *Proc Natl Acad Sci U S A* 1999; 96(7): 3712–7.
doi: 10.1073/pnas.96.7.3712

Lawrence M, Huber W, Pagès H, et al. Software for computing and annotating genomic ranges. *PLoS Comput Biol* 2013; 9(8): e1003118.
doi: 10.1371/journal.pcbi.1003118

Leclerc PC, Auger-Messier M, Lanctot PM, Escher E, Leduc R, Guillemette G. A polyaromatic caveolin-binding-like motif in the cytoplasmic tail of the type 1 receptor for angiotensin II plays an important role in receptor trafficking and signaling. *Endocrinology* 2002; 143(12): 4702–10.
doi: 10.1210/en.2002-220679

Lefkowitz RJ, Shenoy SK. Transduction of receptor signals by beta-arrestins. *Science* 2005; 308(5721): 512–7.
doi: 10.1126/science.1109237

Leterrier C, Bonnard D, Carrel D, Rossier J, Lenkei Z. Constitutive endocytic cycle of the CB1 cannabinoid receptor. *J Biol Chem* 2004; 279(34): 36013–21.
doi: 10.1074/jbc.M403990200

Levy SE, Boone BE. Next-generation sequencing strategies. *Cold Spring Harb Perspect Med* 2019; 9(7): e025791(11pp.).
doi: 10.1101/cshperspect.a025791

Li H, Handsaker B, Wysoker A, et al. The sequence alignment/map format and samtools. *Bioinformatics* 2009; 25(16): 2078–9.
doi: 10.1093/bioinformatics/btp352

Li S, Galbiati F, Volonte D, et al. Mutational analysis of caveolin-induced vesicle formation. Expression of caveolin-1 recruits caveolin-2 to caveolae membranes. *FEBS Lett* 1998; 434(1-2): 127–34.
doi: 10.1016/s0014-5793(98)00945-4

Lim YW, Lo HP, Ferguson C, et al. Caveolae protect notochord cells against catastrophic mechanical failure during development. *Curr Biol* 2017; 27(13): 1968–81.
doi: 10.1016/j.cub.2017.05.067

Lindner I, Ehlers B, Noack S, et al. The porcine lymphotropic herpesvirus 1 encodes functional regulators of gene expression. *Virology* 2007; 357(2): 134–48.
doi: 10.1016/j.virol.2006.08.008

Liu L, Pilch PF. PTRF/cavin-1 promotes efficient ribosomal rna transcription in response to metabolic challenges. *Elife* 2016; 5: e17508(20pp.).
doi: 10.7554/eLife.17508

Lo HP, Nixon SJ, Hall TE, et al. The caveolin-cavin system plays a conserved and critical role in mechanoprotection of skeletal muscle. *J Cell Biol* 2015; 210(5): 833–49.
doi: 10.1083/jcb.201501046

Luttrell LM, Lefkowitz RJ. The role of beta-arrestins in the termination and transduction of G-protein-coupled receptor signals. *J Cell Sci* 2002; 115(3): 455–65.
doi: 10.1242/jcs.115.3.455

Lyngaa R, Norregaard K, Kristensen M, Kubale V, Rosenkilde MM, Kledal TN. Cell transformation mediated by the Epstein-Barr virus G protein-coupled receptor BILF1 is dependent on constitutive signaling. *Oncogene* 2010; 29(31): 4388–98.
doi: 10.1038/onc.2010.173

Macian F. Nfat proteins: Key regulators of T-cell development and function. *Nat Rev Immunol* 2005; 5(6): 472–84.
doi: 10.1038/nri1632

Mandić M, Drinovec L, Glisic S, Veljkovic N, Nøhr J, Vrecl M. Demonstration of a direct interaction between β 2-adrenergic receptor and insulin receptor by BRET and bioinformatics. *PLoS One* 2014; 9(11): e112664(15pp.).
doi: 10.1371/journal.pone.0112664

Marampon F, Ciccarelli C, Zani BM. Biological rationale for targeting MEK/ERK pathways in anti-cancer therapy and to potentiate tumour responses to radiation. *Int J Mol Sci* 2019; 20(10): e2530(20pp.).
doi: 10.3390/ijms20102530

Martinez OM, Krams SM. The immune response to Epstein Barr virus and implications for posttransplant lymphoproliferative disorder. *Transplantation* 2017; 101(9): 2009–16.
doi: 10.1097/tp.0000000000001767

Matar AJ, Patil AR, Al-Musa A, et al. Effect of irradiation on incidence of post-transplant lymphoproliferative disorder after hematopoietic cell transplantation in miniature swine. *Biol Blood Marrow Transplant* 2015; 21(10): 1732–8.
doi: 10.1016/j.bbmt.2015.07.017

Mathiasen S, Palmisano T, Perry NA, et al. G12/13 is activated by acute tethered agonist exposure in the adhesion GPCR ADGRL3. *Nat Chem Biol* 2020; 16(12): e1440(21pp.).
doi: 10.1038/s41589-020-0649-z

Matthaeus C, Lahmann I, Kunz S, et al. EHD2-mediated restriction of caveolar dynamics regulates cellular fatty acid uptake. *Proc Natl Acad Sci U S A* 2020; 117(13): 7471–81.
doi: 10.1073/pnas.1918415117

Maurer ME, Cooper JA. The adaptor protein DAB2 sorts LDL receptors into coated pits independently of AP-2 and ARH. *J Cell Sci* 2006; 119(20): 4235–46.
doi: 10.1242/jcs.03217

Maussang D, Verzijl D, van Walsum M, et al. Human cytomegalovirus-encoded chemokine receptor US28 promotes tumorigenesis. *Proc Natl Acad Sci U S A* 2006; 103(35): 13068–73.
doi: 10.1073/pnas.0604433103

Mavri M, Kubale V, Depledge DP, et al. Epstein-Barr virus-encoded BILF1 orthologues from porcine lymphotropic herpesviruses display common molecular functionality. *Front Endocrinol* 2022; 13: e862940(16pp.).
doi: 10.3389/fendo.2022.862940

Mavri M, Spiess K, Rosenkilde MM, Rutland CS, Vrecl M, Kubale V. Methods for studying endocytotic pathways of herpesvirus encoded G protein-coupled receptors. *Molecules* 2020; 25(23): e5710(23pp.).
doi: 10.3390/molecules25235710

McCombie WR, McPherson JD, Mardis ER. Next-generation sequencing technologies. *Cold Spring Harb Perspect Med* 2019; 9(11): e036798(8pp.).
doi: 10.1101/cshperspect.a036798

McInnes EF, Jarrett RF, Langford G, et al. Posttransplant lymphoproliferative disorder associated with primate gamma-herpesvirus in cynomolgus monkeys used in pig-to-primate renal xenotransplantation and primate renal allotransplantation. *Transplantation* 2002; 73(1): 44–52.
doi: 10.1097/00007890-200201150-00008

McLean KA, Holst PJ, Martini L, Schwartz TW, Rosenkilde MM. Similar activation of signal transduction pathways by the herpesvirus-encoded chemokine receptors US28 and ORF74. *Virology* 2004; 325(2): 241–51.
doi: 10.1016/j.virol.2004.04.027

McMahon HT, Boucrot E. Molecular mechanism and physiological functions of clathrin-mediated endocytosis. *Nat Rev Mol Cell Biol* 2011; 12(8): 517–33.
doi: 10.1038/nrm3151

McMahon HT, Gallop JL. Membrane curvature and mechanisms of dynamic cell membrane remodelling. *Nature* 2005; 438(7068): 590–6.
doi: 10.1038/nature04396

McMahon KA, Wu Y, Gambin Y, et al. Identification of intracellular cavin target proteins reveals cavin-pp1alpha interactions regulate apoptosis. *Nat Commun* 2019; 10(1): e3279(17pp.).
doi: 10.1038/s41467-019-11111-1

McMahon KJ, Minihan D, Campion EM, et al. Infection of pigs in Ireland with lymphotropic gamma-herpesviruses and relationship to postweaning multisystemic wasting syndrome. *Vet Microbiol* 2006; 116(1-3): 60–8.
doi: 10.1016/j.vetmic.2006.03.022

McNally KE, Cullen PJ. Endosomal retrieval of cargo: retromer is not alone. *Trends Cell Biol* 2018; 28(10): 807–22.
doi: 10.1016/j.tcb.2018.06.005

Meftahi GH, Bahari Z, Zarei Mahmoudabadi A, Iman M, Jangravi Z. Applications of western blot technique: from bench to bedside. *Biochem Mol Biol Educ* 2021; 49(4): 509–17.
doi: 10.1002/bmb.21516

Mei S, Zhu H. A simple feature construction method for predicting upstream/downstream signal flow in human protein-protein interaction networks. *Sci Rep* 2015; 5: e17983(12pp.).
doi: 10.1038/srep17983

Meier-Trummer CS, Tobler K, Hilbe M, et al. Ovine herpesvirus 2 structural proteins in epithelial cells and M-cells of the appendix in rabbits with malignant catarrhal fever. *Vet Microbiol* 2009; 137(3-4): 235–42.
doi: 10.1016/j.vetmic.2009.01.030

Meng XJ. Emerging and re-emerging swine viruses. *Transbound Emerg Dis* 2012; 59 (suppl 1): 85–102.
doi: 10.1111/j.1865-1682.2011.01291.x

Mettlen M, Chen PH, Srinivasan S, Danuser G, Schmid SL. Regulation of clathrin-mediated endocytosis. *Annu Rev Biochem* 2018; 87: 871–96.
doi: 10.1146/annurev-biochem-062917-012644

Miller WE, Houtz DA, Nelson CD, Kolattukudy PE, Lefkowitz RJ. G-protein-coupled receptor (GPCR) kinase phosphorylation and beta-arrestin recruitment regulate the constitutive signaling activity of the human cytomegalovirus US28 GPCR. *J Biol Chem* 2003; 278(24): 21663–71.
doi: 10.1074/jbc.M303219200

Modica G, Lefrancois S. Post-translational modifications: how to modulate Rab7 functions. *Small GTPases* 2020; 11(3): 167–73.
doi: 10.1080/21541248.2017.1387686

Modica G, Skorobogata O, Sauvageau E, et al. Rab7 palmitoylation is required for efficient endosome-to-TGN trafficking. *J Cell Sci* 2017; 130(15): 2579–90.
doi: 10.1242/jcs.199729

Moghaddam A, Rosenzweig M, Lee-Parritz D, Annis B, Johnson RP, Wang F. An animal model for acute and persistent Epstein-Barr virus infection. *Science* 1997; 276(5321): 2030–3.
doi: 10.1126/science.276.5321.2030

Monier S, Parton RG, Vogel F, Behlke J, Henske A, Kurzchalia TV. VIP21-caveolin, a membrane protein constituent of the caveolar coat, oligomerizes *in vivo* and *in vitro*. *Mol Biol Cell* 1995; 6(7): 911–27.
doi: 10.1091/mbc.6.7.911

Moore PS, Boshoff C, Weiss RA, Chang Y. Molecular mimicry of human cytokine and cytokine response pathway genes by KSHV. *Science* 1996; 274(5293): 1739–44.
doi: 10.1126/science.274.5293.1739

Morén B, Shah C, Howes MT, et al. EHD2 regulates caveolar dynamics via ATP-driven targeting and oligomerization. *Mol Biol Cell* 2012; 23(7): 1316–29.
doi: 10.1091/mbc.E11-09-0787

Mosier DE, Gulizia RJ, Baird SM, Wilson DB. Transfer of a functional human immune system to mice with severe combined immunodeficiency. *Nature* 1988; 335(6187): 256–9.
doi: 10.1038/335256a0

Mueller NJ, Kuwaki K, Knosalla C, et al. Early weaning of piglets fails to exclude porcine lymphotropic herpesvirus. *Xenotransplantation* 2005; 12(1): 59–62.
doi: 10.1111/j.1399-3089.2004.00196.x

Munshi N, Ganju RK, Avraham S, Mesri EA, Groopman JE. Kaposi's sarcoma-associated herpesvirus-encoded G protein-coupled receptor activation of c-jun amino-terminal kinase/stress-activated protein kinase and lyn kinase is mediated by related adhesion focal tyrosine kinase/proline-rich tyrosine kinase 2. *J Biol Chem* 1999; 274(45): 31863–7.

doi: 10.1074/jbc.274.45.31863

Munz C. Humanized mouse models for Epstein Barr virus infection. *Curr Opin Virol* 2017; 25: 113–8.

doi: 10.1016/j.coviro.2017.07.026

Murata T. Encyclopedia of EBV-encoded lytic genes: an update.

Adv Exp Med Biol 2018; 1045: 395–412.

doi: 10.1007/978-981-10-7230-7_18

Naik S, Zheng H, Rakszawski K, Sample C, Sample J, Bayerl M. Clinical and pathological review of post transplant lymphoproliferative disorders. In: Tsoulfas G, eds. *Organ Donation and Transplantation - Current Status and Future Challenges*. (Online) London: IntechOpen, 2018: 395–407.

doi: 10.5772/intechopen.75356

Nygaard AB, Jørgensen CB, Cirera S, Fredholm M. Selection of reference genes for gene expression studies in pig tissues using sybr green qPCR.

BMC Mol Biol 2007; 8: e67(6pp.).

doi: 10.1186/1471-2199-8-67

Nystrom FH, Chen H, Cong LN, Li Y, Quon MJ. Caveolin-1 interacts with the insulin receptor and can differentially modulate insulin signaling in transfected COS-7 cells and rat adipose cells. *Mol Endocrinol* 1999; 13(12): 2013–24.

doi: 10.1210/mend.13.12.0392

O'Sullivan MJ, Lindsay AJ. The endosomal recycling pathway-at the crossroads of the cell. *Int J Mol Sci* 2020; 21(17): e6074(21pp.).

doi: 10.3390/ijms21176074

Ohno H, Stewart J, Fournier MC, et al. Interaction of tyrosine-based sorting signals with clathrin-associated proteins. *Science* 1995; 269(5232): 1872–5.

doi: 10.1126/science.7569928

Owen DJ, Vallis Y, Pearse BM, McMahon HT, Evans PR. The structure and function of the beta 2-adaptin appendage domain. *EMBO J* 2000; 19(16): 4216–27.

doi: 10.1093/emboj/19.16.4216

Paing MM, Johnston CA, Siderovski DP, Trejo J. Clathrin adaptor AP2 regulates thrombin receptor constitutive internalization and endothelial cell resensitization. *Mol Cell Biol* 2006; 26(8): 3231–42.

doi: 10.1128/mcb.26.8.3231-3242.2006

Palade GE. An electron microscope study of the mitochondrial structure.
J Histochem Cytochem 1953; 1(4): 188–211.
doi: 10.1177/1.4.188

Papadopoulos EB, Ladanyi M, Emanuel D, et al. Infusions of donor leukocytes to treat Epstein-Barr virus-associated lymphoproliferative disorders after allogeneic bone marrow transplantation. N Engl J Med 1994; 330(17): 1185–91.
doi: 10.1056/nejm199404283301703

Parton RG. Caveolae: structure, function, and relationship to disease.
Annu Rev Cell Dev Biol 2018; 34: 111–36.
doi: 10.1146/annurev-cellbio-100617-062737

Parton RG, Del Pozo MA, Vassilopoulos S, et al. Caveolae: the faqs.
Traffic 2020; 21(1): 181–5.
doi: 10.1111/tra.12689

Parton RG, Tillu V, McMahon KA, Collins BM. Key phases in the formation of caveolae. Curr Opin Cell Biol 2021; 71: 7–14.
doi: 10.1016/j.ceb.2021.01.009

Patterson LL, Velayutham TS, Byerly CD, et al. *Ehrlichia* SLiM ligand mimetic activates notch signaling in human monocytes. mBio 2022; 13(2): e0007622(19pp.).
doi: 10.1128/mbio.00076-22

Paulsen SJ, Rosenkilde MM, Eugen-Olsen J, Kledal TN. Epstein-Barr virus-encoded BILF1 is a constitutively active G protein-coupled receptor.
J Virol 2005; 79(1): 536–46.
doi: 10.1128/jvi.79.1.536-546.2005

Pelkmans L, Bürli T, Zerial M, Helenius A. Caveolin-stabilized membrane domains as multifunctional transport and sorting devices in endocytic membrane traffic.
Cell 2004; 118(6): 767–80.
doi: 10.1016/j.cell.2004.09.003

Polo S, Sigismund S, Faretta M, et al. A single motif responsible for ubiquitin recognition and monoubiquitination in endocytic proteins.
Nature 2002; 416(6879): 451–5.
doi: 10.1038/416451a

Prior IA, Harding A, Yan J, Sluimer J, Parton RG, Hancock JF. GTP-dependent segregation of H-ras from lipid rafts is required for biological activity.
Nat Cell Biol 2001; 3(4): 368–75.
doi: 10.1038/35070050

Quilliam LA, Rebhun JF, Castro AF. A growing family of guanine nucleotide exchange factors is responsible for activation of ras-family GTPases. *Prog Nucleic Acid Res Mol Biol* 2002; 71: 391–444.
doi: 10.1016/s0079-6603(02)71047-7

Quinlan AR, Hall IM. Bedtools: a flexible suite of utilities for comparing genomic features. *Bioinformatics* 2010; 26(6): 841–2.
doi: 10.1093/bioinformatics/btq033

Quinn LL, Zuo J, Abbott RJ, et al. Cooperation between Epstein-Barr virus immune evasion proteins spreads protection from CD8+ T cell recognition across all three phases of the lytic cycle. *PLoS Pathog* 2014; 10(8): e1004322(14pp.).
doi: 10.1371/journal.ppat.1004322

Rapoport I, Chen YC, Cupers P, Shoelson SE, Kirchhausen T. Dileucine-based sorting signals bind to the beta chain of AP-1 at a site distinct and regulated differently from the tyrosine-based motif-binding site. *EMBO J* 1998; 17(8): 2148–55.
doi: 10.1093/emboj/17.8.2148

Razani B, Rubin CS, Lisanti MP. Regulation of cAMP-mediated signal transduction via interaction of caveolins with the catalytic subunit of protein kinase A. *J Biol Chem* 1999; 274(37): 26353–60.
doi: 10.1074/jbc.274.37.26353

Rosenkilde MM. Virus-encoded chemokine receptors--putative novel antiviral drug targets. *Neuropharmacology* 2005; 48(1): 1–13.
doi: 10.1016/j.neuropharm.2004.09.017

Rosenkilde MM, Kledal TN, Brauner-Osborne H, Schwartz TW. Agonists and inverse agonists for the herpesvirus 8-encoded constitutively active seven-transmembrane oncogene product, ORF74. *J Biol Chem* 1999; 274(2): 956–61.
doi: 10.1074/jbc.274.2.956

Rosenkilde MM, Kledal TN, Schwartz TW. High constitutive activity of a virus-encoded seven transmembrane receptor in the absence of the conserved DRY motif (Asp-Arg-Tyr) in transmembrane helix 3. *Mol Pharmacol* 2005; 68(1): 11–9.
doi: 10.1124/mol.105.011239

Rosenkilde MM, Smit MJ, Waldhoer M. Structure, function and physiological consequences of virally encoded chemokine seven transmembrane receptors. *Br J Pharmacol* 2008; 153 (suppl 1): S154–66.
doi: 10.1038/sj.bjp.0707660

Rosenkilde MM, Tsutsumi N, Knerr JM, Kildedal DF, Garcia KC. Viral G protein-coupled receptors encoded by β - and γ -herpesviruses. *Annu Rev Virol* 2022; 9(1): 329–51.
doi: 10.1146/annurev-virology-100220-113942

Roskoski R, Jr. Erk1/2 MAP kinases: structure, function, and regulation. *Pharmacol Res* 2012; 66(2): 105–43.
doi: 10.1016/j.phrs.2012.04.005

Roy S, Luetterforst R, Harding A, et al. Dominant-negative caveolin inhibits H-ras function by disrupting cholesterol-rich plasma membrane domains. *Nat Cell Biol* 1999; 1(2): 98–105.
doi: 10.1038/10067

Sato K, Misawa N, Nie C, et al. A novel animal model of Epstein-Barr virus-associated hemophagocytic lymphohistiocytosis in humanized mice. *Blood* 2011; 117(21): 5663–73.
doi: 10.1182/blood-2010-09-305979

Scarselli M, Donaldson JG. Constitutive internalization of G protein-coupled receptors and G proteins via clathrin-independent endocytosis. *J Biol Chem* 2009; 284(6): 3577–85.
doi: 10.1074/jbc.M806819200

Scherer PE, Lewis RY, Volonte D, et al. Cell-type and tissue-specific expression of caveolin-2. Caveolins 1 and 2 co-localize and form a stable hetero-oligomeric complex *in vivo*. *J Biol Chem* 1997; 272(46): 29337–46.
doi: 10.1074/jbc.272.46.29337

Schlegel A, Arvan P, Lisanti MP. Caveolin-1 binding to endoplasmic reticulum membranes and entry into the regulated secretory pathway are regulated by serine phosphorylation. Protein sorting at the level of the endoplasmic reticulum. *J Biol Chem* 2001; 276(6): 4398–408.
doi: 10.1074/jbc.M005448200

Schlossman DM, Schmid SL, Braell WA, Rothman JE. An enzyme that removes clathrin coats: purification of an uncoating atpase. *J Cell Biol* 1984; 99(2): 723–33.
doi: 10.1083/jcb.99.2.723

Schmidlin F, Dery O, DeFea KO, et al. Dynamin and Rab5a-dependent trafficking and signaling of the neurokinin 1 receptor. *J Biol Chem* 2001; 276(27): 25427–37.
doi: 10.1074/jbc.M101688200

Schmidtko J, Wang R, Wu CL, et al. Posttransplant lymphoproliferative disorder associated with an Epstein-Barr-related virus in cynomolgus monkeys. *Transplantation* 2002; 73(9): 1431–9.
doi: 10.1097/00007890-200205150-00012

Seemann E, Sun M, Krueger S, et al. Deciphering caveolar functions by syndapin III KO-mediated impairment of caveolar invagination. *Elife* 2017; 6: e29854(37pp.).
doi: 10.7554/eLife.29854

Senju Y, Itoh Y, Takano K, Hamada S, Suetsugu S. Essential role of pacsin2/syndapin-II in caveolae membrane sculpting. *J Cell Sci* 2011; 124(12): 2032–40.
doi: 10.1242/jcs.086264

Sezgin E, Levental I, Mayor S, Eggeling C. The mystery of membrane organization: composition, regulation and roles of lipid rafts. *Nat Rev Mol Cell Biol* 2017; 18(6): 361–74.
doi: 10.1038/nrm.2017.16

Shvets E, Bitsikas V, Howard G, Hansen CG, Nichols BJ. Dynamic caveolae exclude bulk membrane proteins and are required for sorting of excess glycosphingolipids. *Nat Commun* 2015; 6: e6867(16pp.).
doi: 10.1038/ncomms7867

Sigismund S, Confalonieri S, Ciliberto A, Polo S, Scita G, Di Fiore PP. Endocytosis and signaling: cell logistics shape the eukaryotic cell plan. *Physiol Rev* 2012; 92(1): 273–366.
doi: 10.1152/physrev.00005.2011

Sinha B, Köster D, Ruez R, et al. Cells respond to mechanical stress by rapid disassembly of caveolae. *Cell* 2011; 144(3): 402–13.
doi: 10.1016/j.cell.2010.12.031

Smith JS, Lefkowitz RJ, Rajagopal S. Biased signalling: from simple switches to allosteric microprocessors. *Nat Rev Drug Discov* 2018; 17(4): 243–60.
doi: 10.1038/nrd.2017.229

Sobhy H. A comparative review of viral entry and attachment during large and giant dsDNA virus infections. *Arch Virol* 2017; 162(12): 3567–85.
doi: 10.1007/s00705-017-3497-8

Sodhi A, Montaner S, Patel V, et al. The Kaposi's sarcoma-associated herpes virus G protein-coupled receptor up-regulates vascular endothelial growth factor expression and secretion through mitogen-activated protein kinase and p38 pathways acting on hypoxia-inducible factor 1alpha. *Cancer Res* 2000; 60(17): 4873–80.

Sönnichsen B, De Renzis S, Nielsen E, Rietdorf J, Zerial M. Distinct membrane domains on endosomes in the recycling pathway visualized by multicolor imaging of Rab4, Rab5, and Rab11. *J Cell Biol* 2000; 149(4): 901–14.
doi: 10.1083/jcb.149.4.901

Soroceanu L, Matlaf L, Bezrookove V, et al. Human cytomegalovirus US28 found in glioblastoma promotes an invasive and angiogenic phenotype. *Cancer Res* 2011; 71(21): 6643–53.
doi: 10.1158/0008-5472.can-11-0744

Spiess K, Bagger SO, Torz LJ, et al. Arrestin-independent constitutive endocytosis of GPR125/ADGRA3. *Ann N Y Acad Sci* 2019; 1456(1): 186–99.
doi: 10.1111/nyas.14263

Spiess K, Fares S, Sparre-Ulrich AH, et al. Identification and functional comparison of seven-transmembrane G-protein-coupled BILF1 receptors in recently discovered nonhuman primate lymphocryptoviruses. *J Virol* 2015a; 89(4): 2253–67.
doi: 10.1128/jvi.02716-14

Spiess K, Jakobsen MH, Kledal TN, Rosenkilde MM. The future of antiviral immunotoxins. *J Leukoc Biol* 2016; 99(6): 911–25.
doi: 10.1189/jlb.2MR1015-468R

Spiess K, Jeppesen MG, Malmgaard-Clausen M, et al. Rationally designed chemokine-based toxin targeting the viral G protein-coupled receptor US28 potently inhibits cytomegalovirus infection *in vivo*.
Proc Natl Acad Sci U S A 2015b; 112(27): 8427–32.
doi: 10.1073/pnas.1509392112

Spiess K, Jeppesen MG, Malmgaard-Clausen M, Krzywkowski K, Kledal TN, Rosenkilde MM. Novel chemokine-based immunotoxins for potent and selective targeting of cytomegalovirus infected cells.
J Immunol Res 2017; 2017: e4069260(12pp.).
doi: 10.1155/2017/4069260

Sproul TW, Malapati S, Kim J, Pierce SK. Cutting edge: B cell antigen receptor signaling occurs outside lipid rafts in immature B cells.
J Immunol 2000; 165(11): 6020–3.
doi: 10.4049/jimmunol.165.11.6020

Stimpson HE, Toret CP, Cheng AT, Pauly BS, Drubin DG. Early-arriving Syp1p and Ede1p function in endocytic site placement and formation in budding yeast.
Mol Biol Cell 2009; 20(22): 4640–51.
doi: 10.1091/mbc.e09-05-0429

Strowig T, Gurer C, Ploss A, et al. Priming of protective T cell responses against virus-induced tumors in mice with human immune system components.
J Exp Med 2009; 206(6): 1423–34.
doi: 10.1084/jem.20081720

Sundqvist M, Holdfeldt A, Wright SC, et al. Barbadin selectively modulates FPR2-mediated neutrophil functions independent of receptor endocytosis.
Biochim Biophys Acta Mol Cell Res 2020; 1867(12): e118849(13pp.).
doi: 10.1016/j.bbamcr.2020.118849

Sunil-Chandra NP, Arno J, Fazakerley J, Nash AA. Lymphoproliferative disease in mice infected with murine gammaherpesvirus 68. *Am J Pathol* 1994; 145(4): 818–26.

Svendsen AM, Vrecl M, Knudsen L, et al. Dimerization and negative cooperativity in the relaxin family peptide receptors. *Ann N Y Acad Sci* 2009; 1160: 54–9.
doi: 10.1111/j.1749-6632.2009.03835.x

Sweitzer SM, Hinshaw JE. Dynamin undergoes a GTP-dependent conformational change causing vesiculation. *Cell* 1998; 93(6): 1021–9.
doi: 10.1016/s0092-8674(00)81207-6

Syme CA, Zhang L, Bisello A. Caveolin-1 regulates cellular trafficking and function of the glucagon-like peptide 1 receptor. *Mol Endocrinol* 2006; 20(12): 3400–11.
doi: 10.1210/me.2006-0178

Tang WJ, Gilman AG. Type-specific regulation of adenylyl cyclase by G protein beta gamma subunits. *Science* 1991; 254(5037): 1500–3.
doi: 10.1126/science.1962211

Tarakanova VL, Suarez F, Tibbetts SA, et al. Murine gammaherpesvirus 68 infection is associated with lymphoproliferative disease and lymphoma in BALB beta2 microglobulin-deficient mice. *J Virol* 2005; 79(23): 14668–79.
doi: 10.1128/jvi.79.23.14668-14679.2005

Tazat K, Pomeraniec-Abudy L, Hector-Greene M, et al. ALK1 regulates the internalization of endoglin and the type III TGF- β receptor. *Mol Biol Cell* 2021; 32(7): 605–21.
doi: 10.1091/mbc.E20-03-0199

Teissier E, Pécheur EI. Lipids as modulators of membrane fusion mediated by viral fusion proteins. *Eur Biophys J* 2007; 36(8): 887–99.
doi: 10.1007/s00249-007-0201-z

Telford EA, Watson MS, Aird HC, Perry J, Davison AJ. The DNA sequence of equine herpesvirus 2. *J Mol Biol* 1995; 249(3): 520–8.
doi: 10.1006/jmbi.1995.0314

Tierney RJ, Shannon-Lowe CD, Fitzsimmons L, Bell AI, Rowe M. Unexpected patterns of Epstein-Barr virus transcription revealed by a high throughput PCR array for absolute quantification of viral mRNA. *Virology* 2015; 474: 117–30.
doi: 10.1016/j.virol.2014.10.030

Traub LM, Lukacs GL. Decoding ubiquitin sorting signals for clathrin-dependent endocytosis by CLASPs. *J Cell Sci* 2007; 120(4): 543–53.
doi: 10.1242/jcs.03385

Tripp RA, Hamilton-Easton AM, Cardin RD, et al. Pathogenesis of an infectious mononucleosis-like disease induced by a murine gamma-herpesvirus: role for a viral superantigen? *J Exp Med* 1997; 185(9): 1641–50.
doi: 10.1084/jem.185.9.1641

Tse E, Kwong YL. Epstein Barr virus-associated lymphoproliferative diseases: the virus as a therapeutic target. *Exp Mol Med* 2015; 47(1): e136(7pp.).
doi: 10.1038/emm.2014.102

Tsurumi T, Fujita M, Kudoh A. Latent and lytic Epstein-Barr virus replication strategies. *Rev Med Virol* 2005; 15(1): 3–15.
doi: 10.1002/rmv.441

Tsutsumi N, Qu Q, Mavri M, et al. Structural basis for the constitutive activity and immunomodulatory properties of the Epstein-Barr virus-encoded G protein-coupled receptor BILF1. *Immunity* 2021; 54(7): 1405–16.
doi: 10.1016/j.immuni.2021.06.001

Tu PY, Tsai PC, Lin YH, et al. Expression profile of toll-like receptor mRNA in pigs co-infected with porcine reproductive and respiratory syndrome virus and porcine circovirus type 2. *Res Vet Sci* 2015; 98: 134–41.
doi: 10.1016/j.rvsc.2014.12.003

Tucker AW, McNeilly F, Meehan B, et al. Methods for the exclusion of circoviruses and gammaherpesviruses from pigs. *Xenotransplantation* 2003; 10(4): 343–8.
doi: 10.1034/j.1399-3089.2003.02048.x

Ulrich S, Goltz M, Ehlers B. Characterization of the DNA polymerase loci of the novel porcine lymphotropic herpesviruses 1 and 2 in domestic and feral pigs. *J Gen Virol* 1999; 80 (12): 3199–205.
doi: 10.1099/0022-1317-80-12-3199

Ungewickell E, Ungewickell H, Holstein SE, et al. Role of auxilin in uncoating clathrin-coated vesicles. *Nature* 1995; 378(6557): 632–5.
doi: 10.1038/378632a0

van Senten JR, Fan TS, Siderius M, Smit MJ. Viral G protein-coupled receptors as modulators of cancer hallmarks. *Pharmacol Res* 2020; 156: e104804(13pp.).
doi: 10.1016/j.phrs.2020.104804

Veljkovic N, Glisic S, Perovic V, Veljkovic V. The role of long-range intermolecular interactions in discovery of new drugs. *Expert Opin Drug Discov* 2011; 6(12): 1263–70.
doi: 10.1517/17460441.2012.638280

Veljkovic N, Glisic S, Prljic J, Perovic V, Botta M, Veljkovic V. Discovery of new therapeutic targets by the informational spectrum method. *Curr Protein Pept Sci* 2008; 9(5): 493–506.
doi: 10.2174/138920308785915245

Veljkovic V, Niman HL, Glisic S, Veljkovic N, Perovic V, Muller CP. Identification of hemagglutinin structural domain and polymorphisms which may modulate swine H1N1 interactions with human receptor. *BMC Struct Biol* 2009; 9: e62(11pp.).
doi: 10.1186/1472-6807-9-62

Vischer HF, Leurs R, Smit MJ. HCMV-encoded G-protein-coupled receptors as constitutively active modulators of cellular signaling networks. *Trends Pharmacol Sci* 2006; 27(1): 56–63.
doi: 10.1016/j.tips.2005.11.006

Vischer HF, Siderius M, Leurs R, Smit MJ. Herpesvirus-encoded GPCRs: neglected players in inflammatory and proliferative diseases? *Nat Rev Drug Discov* 2014; 13(2): 123–39.
doi: 10.1038/nrd4189

Vomaske J, Nelson JA, Streblov DN. Human cytomegalovirus US28: a functionally selective chemokine binding receptor. *Infect Disord Drug Targets* 2009; 9(5): 548–56.
doi: 10.2174/187152609789105696

von Kleist L, Stahlschmidt W, Bulut H, et al. Role of the clathrin terminal domain in regulating coated pit dynamics revealed by small molecule inhibition. *Cell* 2011; 146(3): 471–84.
doi: 10.1016/j.cell.2011.06.025

Waldhoer M, Casarosa P, Rosenkilde MM, et al. The carboxyl terminus of human cytomegalovirus-encoded 7 transmembrane receptor US28 camouflages agonism by mediating constitutive endocytosis. *J Biol Chem* 2003; 278(21): 19473–82.
doi: 10.1074/jbc.M213179200

Weeratunga S, Paul B, Collins BM. Recognising the signals for endosomal trafficking. *Curr Opin Cell Biol* 2020; 65: 17–27.
doi: 10.1016/j.ceb.2020.02.005

Weinberg ZY, Puthenveedu MA. Regulation of G protein-coupled receptor signaling by plasma membrane organization and endocytosis. *Traffic* 2019; 20(2): 121–9.
doi: 10.1111/tra.12628

Whitley RJ. Herpesviruses. In: Baron S, eds. *Medical Microbiology*. 4th ed. (Online) Galveston: University of Texas Medical Branch at Galveston, 1996: chapter 68 (22pp.).
<https://www.ncbi.nlm.nih.gov/books/NBK8157/>

Wolfe BL, Trejo J. Clathrin-dependent mechanisms of G protein-coupled receptor endocytosis. *Traffic* 2007; 8(5): 462–70.
doi: 10.1111/j.1600-0854.2007.00551.x

Yajima M, Imadome K, Nakagawa A, et al. A new humanized mouse model of Epstein-Barr virus infection that reproduces persistent infection, lymphoproliferative disorder, and cell-mediated and humoral immune responses. *J Infect Dis* 2008; 198(5): 673–82.
doi: 10.1086/590502

Yamada E. The fine structure of the gall bladder epithelium of the mouse. *J Biophys Biochem Cytol* 1955; 1(5): 445–58.
doi: 10.1083/jcb.1.5.445

Yang D, Zhou Q, Labroska V, et al. G protein-coupled receptors: structure- and function-based drug discovery. *Signal Transduct Target Ther* 2021; 6(1): e7(27pp.).
doi: 10.1038/s41392-020-00435-w

Yang TY, Chen SC, Leach MW, et al. Transgenic expression of the chemokine receptor encoded by human herpesvirus 8 induces an angioproliferative disease resembling kaposi's sarcoma. *J Exp Med* 2000; 191(3): 445–54.
doi: 10.1084/jem.191.3.445

Ye RD. Regulation of nuclear factor kappaB activation by G-protein-coupled receptors. *J Leukoc Biol* 2001; 70(6): 839–48.
doi: 10.1189/jlb.70.6.839

Yeow I, Howard G, Chadwick J, et al. EHD proteins cooperate to generate caveolar clusters and to maintain caveolae during repeated mechanical stress. *Curr Biol* 2017; 27(19): 2951–62.
doi: 10.1016/j.cub.2017.07.047

Yu P, Yang Z, Jones JE, et al. D1 dopamine receptor signaling involves caveolin-2 in HEK-293 cells. *Kidney Int* 2004; 66(6): 2167–80.
doi: 10.1111/j.1523-1755.2004.66007.x

Zhang J, Feng H, Xu S, Feng P. Hijacking GPCRs by viral pathogens and tumor. *Biochem Pharmacol* 2016; 114: 69–81.
doi: 10.1016/j.bcp.2016.03.021

Zhu H, Zhang H, Xu Y, Laššáková S, Korabečná M, Neužil P. PCR past, present and future. *Biotechniques* 2020; 69(4): 317–25.
doi: 10.2144/btn-2020-0057

Zhuang Z, Marshansky V, Breton S, Brown D. Is caveolin involved in normal proximal tubule function? Presence in model PT systems but absence *in situ*. *Am J Physiol Renal Physiol* 2011; 300(1): 199–206.
doi: 10.1152/ajprenal.00513.2010

Zou J, Lei T, Guo P, et al. Mechanisms shaping the role of ERK1/2 in cellular senescence (review). *Mol Med Rep* 2019; 19(2): 759–70.
doi: 10.3892/mmr.2018.9712

Zuo J, Currin A, Griffin BD, et al. The Epstein-Barr virus g-protein-coupled receptor contributes to immune evasion by targeting mhc class I molecules for degradation. *PLoS Pathog* 2009; 5(1): e1000255(16pp.).
doi: 10.1371/journal.ppat.1000255

Zuo J, Quinn LL, Tamblyn J, et al. The Epstein-Barr virus-encoded BILF1 protein modulates immune recognition of endogenously processed antigen by targeting major histocompatibility complex class I molecules trafficking on both the exocytic and endocytic pathways. *J Virol* 2011; 85(4): 1604–14.
doi: 10.1128/jvi.01608-10

11 APPENDIXES

APPENDIX I

REAGENT OR RESOURCE	SOURCE	IDENTIFIER
Antibodies		
Mouse monoclonal anti-FLAG [®] M1 antibody	Sigma-Aldrich	Cat# F3040
Mouse monoclonal anti-FLAG [®] M2 antibody	Sigma-Aldrich	Cat# F1804, RRID: AB_262044
Rabbit monoclonal anti-DYKDDDDK Tag (D6W5B) antibody	CellSignaling	Cat# 14793
Goat polyclonal anti-Mouse IgG (H+L), HRP conjugated	Invitrogen [™]	Cat# 62-6520, RRID: AB_2533947
Goat anti-mouse IgG (H+L) cross-adsorbed secondary antibody, Alexa Fluor [™] 594	Invitrogen [™]	Cat# A-11005
Goat anti-mouse IgG (H+L) cross-adsorbed secondary antibody, Alexa Fluor [™] 488	Invitrogen [™]	Cat# A-11001
Goat anti-Rabbit IgG (H+L) cross-adsorbed secondary antibody, Alexa Fluor [™] 594	Invitrogen [™]	Cat# A-11012
Goat anti-Rabbit IgG (H+L) cross-adsorbed secondary antibody, Alexa Fluor [™] 488	Invitrogen [™]	Cat# A-11008
Goat anti-rabbit IgG (H+L) highly cross-adsorbed secondary antibody, Alexa Fluor [™] 647	Invitrogen [™]	Cat# A-21245
Wheat Germ Agglutinin (WGA), Alexa Fluor [™] 488 conjugate	Invitrogen [™]	Cat# W11261
Donkey anti-mouse Alexa Fluor [®] 488 AffiniPure IgG (H+L)	Jackson ImmunoResearch	Cat# 715-545-150

Donkey anti-mouse Alexa Fluor® 594 AffiniPure IgG (H+L)	Jackson ImmunoResearch	Cat# 715-585-150
Rabbit polyclonal phospho-p44/42 MAPK (Erk1/2) (Thr202/Tyr204) antibody	CellSignaling	Cat# 9101
Rabbit monoclonal p44/42 MAPK (Erk1/2) (137F5) antibody	CellSignaling	Cat# 4695
Rabbit monoclonal anti-Rab8A (D22D8) XP®	Cell Signaling	Cat# 6975
Mouse monoclonal anti-CD71/TFRC/Transferrin receptor antibody (b3/25)	Santa Cruz Biotechnology	Cat# sc-65877
Mouse monoclonal anti-LAMP1 (H4A3) antibody	DSHB	UniprotID: P11279
Mouse APC anti-human HLA-A,B,C antibody	BioLegend	Cat# 311410
Mouse APC IgG2a, κ Isotype Ctrl antibody	BioLegend	Cat# 400220
Mouse monoclonal anti-MHC class I antibody (W6/32)	Santa Cruz Biotechnology	Cat# sc-32235
Mouse monoclonal anti pig SLA class I antibody	Bio-Rad	Cat# MCA2261GA
Mouse monoclonal anti-DYKDDDDK Tag antibody [FITC]	GenScript	Cat# A01632
Chemicals, Peptides, and Recombinant Proteins		
FuGENE HD transfection reagent	Promega	Cat# E2312
FuGENE® 6 Transfection Reagent	Promega	Cat# E2691
Lipofectamine 2000 transfection reagent	Invitrogen™	Cat# 11668019
Lipofectamine™ LTX Reagent with PLUS™ Reagent	Invitrogen™	Cat# 15338100

Dulbecco's Modified Eagle Medium (DMEM), low glucose, GlutaMAX(TM), pyruvate	Gibco™	Cat# 21885
Minimum Essential Media (MEM) alpha, GlutaMAX™ no nucleosides	Gibco™	Cat# 32561029
Opti-MEM I Reduced Serum Medium, GlutaMAX Supplement	Gibco™	Cat# 51985026
Gibco™ Fetal Bovine Serum, qualified, heat inactivated	Gibco™	Cat# 10500064
Penicillin-Streptomycin	Sigma-Aldrich	Cat# P4333
Forskolin	Sigma-Aldrich	Cat# F6886
Formaldehyde solution	Sigma-Aldrich	Cat# 252549
Saponin from quillaja bark	Sigma-Aldrich	Cat# S7900
3, 3', 5, 5'-tetramethylbenzidine (TMB) substrate	Sigma	Cat# T0440
Fibronectin human plasma	Sigma-Aldrich	Cat# F2006
Hoechst 33342, Trihydrochloride, Trihydrate	Invitrogen™	Cat# H3570
Fluorescence Mounting Medium	Agilent DAKO	Cat# S3023
SteadyLite plus reporter gene assay system	Perkin Elmer	Cat# 6066759
CellTiter-Glo® Luminescent Cell Viability Assay	Promega	Cat# G7570
Cell Lines		
<i>Homo Sapiens</i> : HEK-293 cells	ATCC	CRL-1573
<i>Homo Sapiens</i> : parental HEK-293A cells	kindly provided by Asuka Inoue (Tohoku University, Japan)	N/A
<i>Homo Sapiens</i> : Δβ-arr1/2 KO cells: CRISPR/Cas9 modified β-arrestin 1/2 knock out (β-arr KO) HEK-293A	kindly provided by Asuka Inoue (Tohoku University, Japan)	N/A

<i>Homo Sapiens</i> : pan KO HEK-293A cells: modified HEK-293A pan knock-out (KO) cells (Δ Gs/olf/q/11/12/13/z)		kindly provided by Asuka Inoue (Tohoku University, Japan)	N/A
<i>Sus scrofa</i> : PK-15 cells		ATCC	CCL-33
Constructs			
CONSTRUCT	VECTOR	SOURCE	IDENTIFIER
Empty vector	pcDNA3.1+	Genscript	Cat# SC1317
EBV-BILF1: N-terminally FLAG tagged	pcDNA3.1+	Paulsen, S. <i>et al.</i> <i>J Virol</i> (2005). 79, 536-46.	N/A
PLHV1-BILF1: N-terminally FLAG tagged	pcDNA3.1+		N/A
PLHV2-BILF1: N-terminally FLAG tagged	pcDNA3.1+		N/A
PLHV3-BILF1: N-terminally FLAG tagged	pcDNA3.1+		N/A
RLuc8-EBV-BILF1: EBV-BILF1, N-terminally FLAG tagged and C-terminally RLuc8 tagged	pcDNA3.1+	Genscript	N/A
RLuc8-PLHV1-BILF1: PLHV1-BILF1, N-terminally FLAG tagged and C-terminally RLuc8 tagged	pcDNA3.1+	Genscript	N/A
RLuc8-PLHV2-BILF1: PLHV2-BILF1, N-terminally FLAG tagged and C-terminally RLuc8 tagged	pcDNA3.1+	Genscript	N/A

RLuc8-PLHV3-BILF1: PLHV3-BILF1, N-terminally FLAG tagged and C- terminally	pcDNA3.1+	Genscript	N/A
SNAP-EBV-BILF1: EBV-BILF1, N-terminally FLAG and SNAP tagged	pcDNA5/FRT/ TO-FLAG- SNAP	Genscript	N/A
SNAP-PLHV1-BILF1: PLHV1-BILF1, N-terminally FLAG and SNAP tagged	pcDNA5/FRT/ TO-FLAG- SNAP	Genscript	N/A
SNAP-PLHV2-BILF1: PLHV2-BILF1, N-terminally FLAG and SNAP tagged	pcDNA5/FRT/ TO-FLAG- SNAP	Genscript	N/A
SNAP-PLHV3-BILF1: PLHV3-BILF1, N-terminally FLAG and SNAP tagged	pcDNA5/FRT/ TO-FLAG- SNAP	Genscript	N/A
GFP2/ β -arr2	pcDNA3.1+	BioSignal Packard Inc. (Montreal, Canada)	N/A
GFP2/17aa	pcDNA3.1+	kindly provided by Dr. Rasmus Jørgensen (7TM Pharma A/S, Hørsholm, Denmark)	N/A

Cav S80E		kindly provided by Prof. J.E. Pessin (Department of Physiology and Biophysics, University of Iowa, Iowa, USA)	N/A
Dyn K44A		kindly provided by prof. M.G. Caron (Duke University Medical Center, N.C., USA), respectively	N/A
GαΔ6qi4myr	pcDNA3.1+	Kostenis, E. <i>et al.</i> <i>J Pharmacol Exp Ther.</i> (2005). 313, 78-87.	N/A

APPENDIX II

ARTICLES

1. MAVRI, Maša, ČANDEK-POTOKAR, Marjeta, FAZARINC, Gregor, ŠKRLEP, Martin, RUTLAND, Catrin, POTOČNIK, Božidar, BATOREK LUKAČ, Nina, KUBALE, Valentina. Salivary gland adaptation to dietary inclusion of hydrolysable tannins in boars. *Animals*. 2022, vol. 12, no. 17, art. 2171, str. 1-15.
2. MAVRI, Maša, KUBALE, Valentina, DEPLEDGE, Daniel P., ZUO, Jianmin, HUANG, Christene A., BREUER, Judith, VRECL, Milka, JARVIS, Michael A., JARC JOVIČIĆ, Eva, PETAN, Toni, EHLERS, Bernhard, ROSENKILDE, Mette Marie, SPIESS, Katja. Epstein-Barr virus-encoded BILF1 orthologues from porcine lymphotropic herpesviruses display common molecular functionality. *Frontiers in endocrinology*. 2022, vol. 13, art. 862940, str. 1-16.
3. LARSEN, Olav, VELDEN, Wijnand J. C. van der, MAVRI, Maša, SCHUERMANS, Sara, RUMMEL, Pia C., KARLSHØJ, Stefanie, GUSTAVSSON, Martin, PROOST, Paul, VÅBENØ, Jon, ROSENKILDE, Mette Marie. Identification of a conserved chemokine receptor motif that enables ligand discrimination. *Science signaling*. 2022, vol. 15, no. 724, art. 7042, str. 1-13.
4. JØRGENSEN, Astrid S., DAUGVILAITE, Viktorija, DE FILIPPO, Katia, BERG, Christian, MAVRI, Maša, BENNED-JENSEN, Tau, JUZENAITE, Goda, HJORTØ, Gertrud Malene, RANKIN, Sara, VÅBENØ, Jon, ROSENKILDE, Mette Marie. Biased action of the CXCR4-targeting drug plerixafor is essential for its superior hematopoietic stem cell mobilization. *Communications biology*. 2021, vol. 4, art. no. 569, str. 1-12.

5. TSUTSUMI, Naotaka, QU, Qianhui, MAVRI, Maša, BAGGESEN, Maibritt S., MAEDA, Shoji, WAGHRAY, Deepa, BERG, Christian, KOBILKA, Brian K., ROSENKILDE, Mette Marie, SKINIOTIS, Georgios, GARCIA, K. Christopher. Structural basis for the constitutive activity and immunomodulatory properties of the Epstein-Barr virus-encoded G protein-coupled receptor BILF1. *Immunity*. [Online ed.]. 2021, vol. 54, no. 7, str. 1405-1416.
6. BLAGOTINŠEK COKAN, Kaja, MAVRI, Maša, RUTLAND, Catrin, GLISIC, Sanja, SENCANSKI, Milan, VRECL, Milka, KUBALE, Valentina. Critical impact of different conserved endoplasmic retention motifs and dopamine receptor interacting proteins (DRIPs) on intracellular localization and trafficking of the D2 dopamine receptor (D2-R) isoforms. *Biomolecules*. 2020, vol. 10, no. 10, str. 1-18.
7. MAVRI, Maša, SPIESS, Katja, ROSENKILDE, Mette Marie, RUTLAND, Catrin, VRECL, Milka, KUBALE, Valentina. Methods for studying endocytotic pathways of herpesvirus encoded G protein-coupled receptors. *Molecules*. 2020, vol. 25, no. 23, str. 1-23.
8. MAVRI, Maša, KUBALE, Valentina. Zakaj so pomembni herpesvirusni, s proteinom G sklopljeni receptorji (VGPCR), in kakšne poti endocitoze uporabljajo?. *Vestnik Veterinarske zbornice Slovenije*. marec 2021, letn. 16, št. 3, str. 167-175.
9. MAVRI, Maša, GLIŠIĆ, Sanja, SENCANSKI, Milan, VRECL, Milka, ROSENKILDE, Mette Marie, SPIESS, Katja, KUBALE, Valentina. Patterns of human and porcine gammaherpesvirus encoded BILF1 receptor endocytosis. *Cellular & Molecular biology letters* (in submission).

PRESENTATIONS AT SCIENTIFIC MEETINGS

1. MAVRI, Maša, VRECL, Milka, SENCANSKI, Milan, GLISIC, Sanja, ROSENKILDE, Mette Marie, SPIESS, Katja, KUBALE, Valentina. Endocytic properties of BILF1 orthologues encoded by human and porcine gammaherpesviruses. V: *Understanding function of G-protein coupled receptors by atomistic and multiscale simulations : flagship workshop : September 12 - 14, 2022, Lugano*. Lugano: CECAM.
2. MAVRI, Maša, KUBALE, Valentina, DEPLEDGE, Daniel P., ZUO, Jianmin, HUANG, Christene A., BREUER, Judith, JARVIS, Michael A., ROSENKILDE, Mette Marie, SPIESS, Katja. Characterization of BILF1 encoded by porcine lymphotropic herpesviruses as a step towards to establish a novel porcine PTLD model. V: 19th International Symposium on Epstein-Barr Virus and associated diseases : recent advance in basic and clinical research about EBV and EBV-associated disease all over the world : july 29th - 30th, 2011 [and] august 2nd - 15th, 2021, Asahikawa, Japan. Asahikawa: Asahikawa Medical University, 2021. Str. 186.
3. MAVRI, Maša, VRECL, Milka, ROSENKILDE, Mette Marie, SPIESS, Katja, KUBALE, Valentina. Trafficking properties of BILF1 orthologs from Epstein-Barr virus (EBV) and porcine lymphotropic herpesvirus 1 (PLHV1) : [Predstavitev postra preko spletne aplikacije Zoom na: 4th Ernest Conference].
4. MAVRI, Maša, ZUO, Jianmin, EHLERS, Bernhard, KLEDAL, Thomas N., VRECL, Milka, ROSENKILDE, Mette Marie, SPIESS, Katja, KUBALE, Valentina. Characterization of the Bilf1 receptors from Epstein-barr virus (Ebv) and porcine lymphotropic herpesviruses (Plhv1 - 3). V: *Abstract book*. 44th Annual International Herpesvirus Workshop, July 20 - 24, 2019, Knoxville, Tennessee, USA. Knoxville: The University of Tennessee, 2019. Str. 140.

5. MAVRI, Maša, ZUO, Jian-Min, EHLERS, Bernhard, KLEDAL, Thomas N., VRECL, Milka, ROSENKILDE, Mette Marie, SPIESS, Katja, KUBALE, Valentina. Internalization and signaling properties of BILF1 receptors encoded in Epstein-Barr virus and porcine lymphotropic herpesviruses. V: KISOVEC, Matic (ur.). *Book of abstracts = Knjiga povzetkov*. 13th Meeting of the Slovenian Biochemical Society with International Participation = 13. srečanje Slovenskega biokemijskega društva z mednarodno udeležbo, Dobrna, 24 - 27 September 2019. Ljubljana: Slovenian Biochemical Society, 2019. Str. 41.
6. MAVRI, Maša, ZUO, Jianmin, EHLERS, Bernhard, KLEDAL, Thomas N., VRECL, Milka, ROSENKILDE, Mette Marie, SPIESS, Katja, KUBALE, Valentina. Characterization of BILF1 receptors encoded in Epstein-Barr virus and porcine lymphotropic herpesviruses. V: *GPCR Pharmacology: activation, signalling and drug design : programme and abstract booklet*. The inaugural meeting of the European Research Network in Signal Transduction, October 28-30, 2019, Belfast, Northern Ireland. Belfast: European research network on signal transduction, 2019. Str. 40.
7. MAVRI, Maša, SPIESS, Katja, ROSENKILDE, Mette Marie, KUBALE, Valentina. Primerjava lastnosti internalizacije GPCR receptorjev BILF, kodiranih v prašičjih in humanem herpesvirusnem genomu = Comparison of human and porcine herpesvirus encoded GPCR BILF1 receptors internalization properties. V: MAJDIČ, Gregor (ur.). *Slovenski veterinarski kongres : [Portorož, Slovenia, 3 - 6 April 2019]*. 7. slovenski veterinarski kongres, Portorož, 3 - 6 April, 2019. Ljubljana: Veterinarska fakulteta, 2019. Str. 116-117. Slovenian veterinary research, Vol. 56, suppl. 23, 2019.

8. MAVRI, Maša, SPIESS, Katja, ROSENKILDE, Mette Marie, KUBALE, Valentina. Internalization properties of the BILF1 receptors from Epstein-Barr virus (EBV) and porcine lymphotropic herpesvirus (PLHV). V: *Early career scientist forum on GPCR signal transduction (ECSF - GPCR) : a scientific and social network promoting young researchers : Charité - Universitätsmedizin Berlin, Germany, July 11th - 14th, 2018*. Berlin: Charité - Universitätsmedizin, 2018. Str. 110.
9. MAVRI, Maša, SPIESS, Katja, ROSENKILDE, Mette Marie, KUBALE, Valentina. Endocytosis and localization of G protein coupled receptor BILF1, encoded by Epstein Barr virus and porcine lymphotropic herpesviruses. V: *Ligand-binding theory and practice : program & abstracts, 2018*. Nové Hradky: [S. n.], 2018. Str. [25-26].
10. MAVRI, Maša, VRECL, Milka, FAZARINC, Gregor, ŽUŽEK, Monika C., FRANGEŽ, Robert, KUBALE, Valentina. Uporaba konfokalne mikroskopije in metode bioluminiscenčnega prenosa resonančne energije (bret2) na Veterinarski fakulteti v Ljubljani. V: KRANJIC BREZAR, Simona (ur.), MAJDIČ, Gregor (ur.). *Zbornik prispevkov. 4.kongres Slovenskega društva za laboratorijske živali, Domžale, 2018*. Ljubljana: Veterinarska fakulteta, 2018. Vol. 55, suppl. 19, str. 41. Slovenian veterinary research, Vol. 55, suppl. 19, 2018.
11. MAVRI, Maša, VRECL, Milka, FAZARINC, Gregor, ŽUŽEK, Monika C., FRANGEŽ, Robert, KUBALE, Valentina. Examples of the use of confocal microscopy and bioluminescence resonance energy transfer (BRET2). V: ERHARDT, Julija (ur.). *Pokusne živalinje u znanstvenim istraživanjima = Laboratory animals in scientific research. 3. znanstveno-stručni simpozij Hrvatskog društva za znanost o laboratorijskim životinjama i 2. zajednički skup CroLASA-e i SLAS-a s međunarodnim sudjelovanjem., Zagreb: Hrvatsko društvo za znanost o laboratorijskim životinjama, 2018*. Str. 40-41.

MONOGRAPHS

1. MAVRI, Maša. Vpliv različnih koncentracij taninov na žleze slinavke pri merjaških = Influence of different concentrations of hydrolysable tannins on salivary glands in boars. Ljubljana: [M. Rutar], 2017.